

DIELECTRIC STUDIES OF
MOLECULAR MOTIONS IN SOME SOLIDS

A Thesis Submitted By:

© MD. SOHRAB HOSSAIN

*In Partial Fulfillment of
the Requirements of the Degree of
MASTER OF SCIENCE*

TO

Lakehead University
Thunder Bay,
Ontario, Canada

AUGUST 1982.

ProQuest Number: 10611691

All rights reserved

INFORMATION TO ALL USERS

The quality of this reproduction is dependent upon the quality of the copy submitted.

In the unlikely event that the author did not send a complete manuscript and there are missing pages, these will be noted. Also, if material had to be removed, a note will indicate the deletion.



ProQuest 10611691

Published by ProQuest LLC (2017). Copyright of the Dissertation is held by the Author.

All rights reserved.

This work is protected against unauthorized copying under Title 17, United States Code
Microform Edition © ProQuest LLC.

ProQuest LLC.
789 East Eisenhower Parkway
P.O. Box 1346
Ann Arbor, MI 48106 - 1346

SUMMARY

Dielectric absorption of a number of non-polar, weakly polar and fairly polar molecules in the pure solid state are studied. Measurements of these solids using either a General Radio 1621 Precision Capacitance Measurement System or a General Radio 1615-A Capacitance bridge with appropriate temperature-controllable cells are described. The glass transition (T_g) measurements using the Glass Transition Measurement Apparatus are also described. The experimental data as a function of frequency at different temperatures are subjected to analysis by a series of computer programmes written in the APL language. The activation energy barriers for the dielectric relaxation processes were obtained by the application of the Eyring rate equation.

The dielectric absorption of some spherically-shaped nonpolar molecules are observed, the energy barrier values of which agree well with those found from other measurements. It is suggested that this absorption might be due to the interaction of the radiofrequency radiation with an induced moment which results from multiple interaction.

Of the spherically-shaped polar molecules examined, both molecular and co-operative relaxations are detected in all the alkylhalides. Dielectric data for molecular relaxations are described by the Cole-Cole plots, whereas those for co-operative motion, in most of the cases, cannot be accurately represented by the Davidson-Cole skewed-arc function.

Low temperature molecular relaxations are detected in some nonpolar and weakly polar aromatic hydrocarbons. The results of these molecules are used to suggest a possible correlation between enthalpy and entropy of activation and ionization potential and enthalpy of activation. The dielectric absorption of apparently nonpolar aromatic hydrocarbons are explained on the basis of quadrupole or octupole induced moment which may be of significant magnitude when the internuclear distances are small as in the solid state.

Co-operative relaxations of some of the non-polar and weakly polar hydrocarbons are found above the glass transition temperature (T_g). The variation in the energy barrier values for these relaxations are explained in terms of molecular interaction which is measured either

by ionization potential or by the stretching frequency of a suitable solute molecule such as pyrrole (e.g. N-H with which the aromatic hydrocarbon can form hydrogen bond.

The molecular relaxation processes of a number of rigid arylhalides in the pure solid state are found almost in the same temperature and frequency regions as those found in different viscous media. A similar enthalpy of activation values are also observed. For some rigid heterocyclic molecules, except N-methylpyrrole, no molecular relaxation is observed and this could be accounted for by the crystal structure and the lack of free volume for these molecules to relax.

ACKNOWLEDGEMENTS

The work described in this thesis was carried out at Lakehead University, Canada, from September 1980 to May 1982. I would like to express my sincere gratitude to my research supervisor, Professor S. Walker, for his encouragement and invaluable guidance throughout this work.

I am grateful to Dr. M.A. Saleh, Dr. M. Desando and Mr. D.L. Gourlay for many helpful discussions. I greatly acknowledge the co-operation and indispensable technical assistance of Mr. B.K. Morgan. Finally, I would like to thank Mrs. J. Parnell for her work in typing this thesis.

TABLE OF CONTENTS

	<u>PAGE</u>
TITLE PAGE.....	i
SUMMARY.....	ii
ACKNOWLEDGEMENTS.....	v
TABLE OF CONTENTS.....	vi
LIST OF TABLES.....	viii
LIST OF FIGURES.....	x
CHAPTER I.....	1
Introduction and Theory.....	2
References.....	17
CHAPTER II.....	19
Apparatus and Experimental	
Procedure.....	20
References.....	38
CHAPTER III.....	39
Dielectric Absorption of Some Nonpolar	
Spherical molecules in the Solid State..	
Introduction.....	40
Experimental Results.....	42
Discussion.....	46
References.....	59
CHAPTER IV.....	75
Some Polar Fairly Spherical Molecules	
Introduction.....	76
Experimental Results.....	78
Discussion.....	80
References.....	102
CHAPTER V.....	130
Molecular Relaxation of Some Aromatic	
Hydrocarbons	
Introduction.....	131
Experimental Results.....	132
Discussion.....	136
References.....	151

TABLE OF CONTENTS continued...

	<u>PAGE</u>
CHAPTER VI.....	175
Co-operative Relaxation Processes of Some Hydrocarbons	
Introduction.....	176
Experimental Results.....	180
Discussion.....	183
References.....	199
CHAPTER VII.....	228
Some Rigid Dipolar Molecules	
Introduction.....	229
Experimental Results.....	231
Discussion.....	233
References.....	249

LIST OF TABLES

		<u>PAGE</u>
TABLE 3.1	Experimental and literature values of refractive indices and boiling points of some nonpolar compounds	43
TABLE 3.2	Fuoss-Kirkwood Analysis parameters for some nonpolar spherical molecules	61
TABLE 3.3	Relaxation times and Eyring analysis results for some nonpolar spherical molecules	63
TABLE 4.1	Fuoss-Kirkwood analysis parameters, Cole-Cole ϵ_{∞} and experimental dipole moments for some polar, fairly spherical molecules	105
TABLE 4.2	Relaxation times and Eyring analysis results for some polar fairly spherical molecules	109
TABLE 5.1	Fuoss-Kirkwood analysis parameters, Cole-Cole ϵ_{∞} and experimental dipole moments for some aromatic hydrocarbons	153
TABLE 5.2	Relaxation times and Eyring analysis results for some aromatic hydrocarbons	156

LIST OF TABLES continued...

		<u>PAGE</u>
TABLE 6.1	Stretching frequency of N-H bond of pyrrole with some hydrocarbons	197 .
TABLE 6.2	Eyring analysis parameters, maximum loss factor, ϵ''_{\max} , and glass transition temperature for some hydrocarbons	202
TABLE 6.3	Davidson-Cole and Fuoss-Kirkwood analysis parameters and dipole moments for some hydrocarbons in the solid state	203
TABLE 7.1	Eyring Analysis Results for some rigid polar molecules	252
TABLE 7.2	Fuoss-Kirkwood analysis parameters, Cole-Cole ϵ_{∞} and apparent dipole moment for some rigid molecules	254

LIST OF FIGURES

	<u>PAGE</u>
FIGURE 1.1 Relation between ϵ' , ϵ'' , and $\tan\delta$ in the complex quantity of diel- ectric constant (ϵ^*)	6
FIGURE 1.2 Frequency dependance of real (ϵ') and imaginary (ϵ'') parts of the permittivity in a relaxation region.	6
FIGURE 1.3(a) Free energy diagram for dipole- rotating in a crystal lattice	14
FIGURE 1.3(b) Free energy diagram for unequal free energy minima.	14
FIGURE 2.1 Three terminal coaxial cell	22
FIGURE 2.2 Parallel plate Capacitor cell	22
FIGURE 2.3 Precision Capacitance Measurement System	26
FIGURE 2.4 Elementary diagram, 1621 Precision Capacitance Measurement System. Conductance Circuitry is omitted.	26
FIGURE 2.5 Glass Transition Measurement Device	31
FIGURE 2.6 Cole-Cole plot for the Davidson- Cole equation.	34

LIST OF FIGURES continued...

		<u>PAGE</u>
FIGURE 3.1	Dielectric loss factor ϵ'' versus log frequency for neopentane	64
FIGURE 3.2	Cole-Cole plot for neopentane	65
FIGURE 3.3	Eyring plot of $\log(\tau T)$ versus $\frac{1}{T}$ for neopentane	66
FIGURE 3.4	Dielectric loss factor ϵ'' versus log frequency for carbon tetrachloride (lower temperature process)	67
FIGURE 3.5	Eyring plot of $\log(\tau T)$ versus $\frac{1}{T}$ for carbon tetrachloride (lower temperature process)	68
FIGURE 3.6	Dielectric loss factor ϵ'' versus log frequency for carbon tetrachloride (higher temperature process)	69
FIGURE 3.7	Eyring plot of $\log(\tau T)$ versus $\frac{1}{T}$ for carbon tetrachloride (higher temperature process).	70
FIGURE 3.8	Dielectric loss factor ϵ'' versus log frequency for tetramethylsilane (lower temperature process)	71

LIST OF FIGURES continued...

		<u>PAGE</u>
FIGURE 3.9	Eyring plot of $\log(\tau T)$ versus $\frac{1}{T}$ for tetramethylsilane (lower temperature process)	72
FIGURE 3.10	Dielectric loss factor ϵ'' versus log frequency for tetramethylsilane (higher temperature process)	73
FIGURE 3.11	Eyring plot of $\log(\tau T)$ versus $\frac{1}{T}$ for tetramethylsilane (higher temperature process)	74
FIGURE 4.1	Dielectric loss factor ϵ'' versus log frequency for methyl bromide	110
FIGURE 4.2	Cole-Cole plot for methyl bromide at 90.0 K	111
FIGURE 4.3	Eyring plot of $\log(\tau T)$ versus $\frac{1}{T}$ for methyl bromide	112
FIGURE 4.4	Dielectric loss factor ϵ'' versus log frequency for methyl iodide	113
FIGURE 4.5	Complex plane diagram for methyl iodide at 106.1 K	114
FIGURE 4.6	Dielectric loss factor ϵ'' versus log frequency for 2,2-dichloropropane	115

LIST OF FIGURES continued...

		PAGE
FIGURE 4.7	Dielectric loss factor ϵ'' versus log frequency for 1,1,1-trichloroethane	116
FIGURE 4.8	Complex plane diagram for 1,1,1-trichloroethane at 116.4 K	117
FIGURE 4.9	Eyring plot of $\log(\tau T)$ versus $\frac{1}{T}$ for 1,1,1-trichloroethane	118
FIGURE 4.10	Dielectric loss factor ϵ'' versus log frequency for methyltrichlorosilane	119
FIGURE 4.11	Complex plane diagram for methyltrichlorosilane at 120.4 K	120
FIGURE 4.12	Eyring plot of $\log(\tau T)$ versus $\frac{1}{T}$ for methyltrichlorosilane	121
FIGURE 4.13	Dielectric loss factor ϵ'' versus log frequency for t-butylchloride	122
FIGURE 4.14	Complex plane diagram for t-butylchloride at 145.6 K	123
FIGURE 4.15	Eyring plot of $\log(\tau T)$ versus $\frac{1}{T}$ for t-butylchloride	124
FIGURE 4.16	Dielectric loss factor ϵ'' versus temperature for t-butylbromide	125

LIST OF FIGURES continued...

		<u>PAGE</u>
FIGURE 4.17	Dielectric loss factor ϵ'' versus log frequency for t-butylbromide	126
FIGURE 4.18	Complex plane diagram for t-butylbromide at 131.9 K	127
FIGURE 4.19	Cole-Cole plot for 2-methyl-2-nitropropane	128
FIGURE 4.20	Eyring plot of $\log(\tau T)$ versus $\frac{1}{T}$ for 2-methyl-2-nitropropane	129
FIGURE 5.1	Dielectric loss factor ϵ'' versus log frequency for o-xylene	157
FIGURE 5.2	Eyring plot of $\log(\tau T)$ versus $\frac{1}{T}$ for o-xylene	158
FIGURE 5.3	Dielectric loss factor ϵ'' versus temperature for mesitylene	159
FIGURE 5.4	Eyring plot of $\log(\tau T)$ versus $\frac{1}{T}$ for p-diethylbenzene	160
FIGURE 5.5	Dielectric loss factor ϵ'' versus log frequency for isopropylbenzene	161
FIGURE 5.6	Cole-Cole plot for isopropylbenzene at 117.2 K	162
FIGURE 5.7	Eyring plot of $\log(\tau T)$ versus $\frac{1}{T}$ for isopropylbenzene	163

LIST OF FIGURES continued...

		<u>PAGE</u>
FIGURE 5.8	Dielectric loss factor ϵ'' versus log frequency for p-cymene	164
FIGURE 5.9	Cole-Cole plot for p-cymene at 107.2 K	165
FIGURE 5.10	Eyring plot of $\log(\tau T)$ versus $\frac{1}{T}$ for p-cymene	166
FIGURE 5.11	Dielectric loss factor ϵ'' versus temperature for (a) 1-methylnaphthalene, and (b) 1-chloronaphthalene, at 102 Hz	167
FIGURE 5.12	Eyring plot of $\log(\tau T)$ versus $\frac{1}{T}$ for 1-methylnaphthalene	168
FIGURE 5.13	Cole-Cole plot for 1,5-dimethylnaphthalene at 115.6 K	169
FIGURE 5.14	Eyring plot of $\log(\tau T)$ versus $\frac{1}{T}$ for 1,5-dimethylnaphthalene	170
FIGURE 5.15	Dielectric loss factor ϵ'' versus log frequency for 2-methylnaphthalene	171
FIGURE 5.16	Cole-Cole plot for 2-methylnaphthalene at 118.4 K	172
FIGURE 5.17	Eyring plot of $\log(\tau T)$ versus $\frac{1}{T}$ for 2-methylnaphthalene	173

LIST OF FIGURES continued...

	<u>PAGE</u>	
FIGURE 5.18	Plot of Eyring enthalpy of activation versus ionization potential for some aromatic hydrocarbons	174
FIGURE 6.1	Eyring plot of $\log(\tau_0 T)$ versus $\frac{1}{T}$ for n-propylbenzene	207
FIGURE 6.2	Complex plane diagram for n-propylbenzene	208
FIGURE 6.3	Complex plane diagram for 2-methylpentane at 91.2 K	209
FIGURE 6.4	Complex plane diagram for methylcyclohexane at 94.9 K	210
FIGURE 6.5	Complex plane diagram for 4-methylcyclohexene-1 at 109.8 K	211
FIGURE 6.6	Dielectric loss factor ϵ'' versus log frequency for cis-decalin	212
FIGURE 6.7	Complex plane loci of the normalized dielectric constant $(\epsilon^* - \epsilon') / (\epsilon_0 - \epsilon_1)$ for n-propylbenzene at 138.9 and 142.8 K	213
FIGURE 6.8	Dielectric loss factor ϵ'' versus log frequency for 2-methylpentane	214
FIGURE 6.9	Dielectric loss factor ϵ'' versus log frequency for methylcyclohexane	215

LIST OF FIGURES continued...

		<u>PAGE</u>
FIGURE 6.10	Eyring plot of $\log(\tau_0 T)$ versus $\frac{1}{T}$ for methylcyclohexane	216
FIGURE 6.11	Eyring plot $\log(\tau T)$ versus $\frac{1}{T}$ for cis-decalin	217
FIGURE 6.12	Dielectric loss factor ϵ'' versus log frequency for p-xylene	218
FIGURE 6.13	Dielectric loss factor ϵ'' versus log frequency for p-ethyltoluene	219
FIGURE 6.14	Dielectric loss factor ϵ'' versus log frequency for mesitylene	220
FIGURE 6.15	Complex plane diagram for p-ethyltoluene at 133.8 K	221
FIGURE 6.16	Complex plane diagram for mesitylene at 142.1 K	222
FIGURE 6.17	Dielectric loss factor ϵ'' versus log frequency for p-diethylbenzene	223
FIGURE 6.18	Eyring plot of $\log(\tau_0 T)$ versus $\frac{1}{T}$ for p-ethyltoluene	224
FIGURE 6.19	Plot of ΔH_E versus ΔS_E for some hydrocarbons	225
FIGURE 6.20	Stretching frequency, $\Delta\nu$, versus ΔH_E for some hydrocarbons	226

LIST OF FIGURES continued...

		<u>PAGE</u>
FIGURE 6.21	Eyring enthalpy of activation versus ionization potential for some hydrocarbons	227
FIGURE 7.1	Dielectric loss factor ϵ'' versus temperature for fluoro- benzene at 1 kHz	260
FIGURE 7.2	Eyring plot of $\log(\tau T)$ versus $\frac{1}{T}$ for fluorobenzene (lower temperature process)	261
FIGURE 7.3	Cole-Cole plot for fluorobenzene at 108.1 K	262
FIGURE 7.4	Complex plane diagram for fluoro- benzene at 163.2 K	263
FIGURE 7.5	Dielectric loss factor ϵ'' versus log frequency for fluorobenzene	264
FIGURE 7.6	Eyring plot of $\log(\tau T)$ versus $\frac{1}{T}$ for fluorobenzene (higher temperature process)	265
FIGURE 7.7	Dielectric loss factor ϵ'' versus temperature for chlorobenzene at 102 Hz	266
FIGURE 7.8	Dielectric loss factor ϵ'' versus temperature for bromobenzene at 1 kHz	267
FIGURE 7.9	Complex plane diagram for bromo- benzene at 141.8 K	268

LIST OF FIGURES continued...

		<u>PAGE</u>
FIGURE 7.10	Dielectric loss factor ϵ'' versus temperature for o-dichlorobenzene at 1 kHz	269
FIGURE 7.11	Dielectric loss factor ϵ'' versus temperature for 1-chloronaphthalene at 1 kHz	270
FIGURE 7.12	Eyring plot of $\log(\tau T)$ versus $\frac{1}{T}$ for N-methylpyrrole	271
FIGURE 7.13	Cole-Cole plot for N-methylpyrrole at 110.3 K	272
FIGURE 7.14	Dielectric loss factor ϵ'' versus log frequency for pyridine	273
FIGURE 7.15	Complex plane diagram for pyridine at 167.3 K	274
FIGURE 7.16	Eyring plot of $\log(\tau T)$ versus $\frac{1}{T}$ for pyridine	275
FIGURE 7.17	Complex plane diagram for 4-methylpyridine at 181.4 K	276
FIGURE 7.18	Dielectric loss factor ϵ'' versus log frequency for quinoline	277
FIGURE 7.19	Eyring plot of $\log(\tau T)$ versus $\frac{1}{T}$ for quinoline and isoquinoline	278

LIST OF FIGURES continued...

	<u>PAGE</u>
FIGURE 7.20 Complex plane diagram for quinoline at 198.6 K	279
FIGURE 7.21 Complex plane diagram for isoquinoline at 203.9 K	280

TO MY PARENTS

CHAPTER I

I N T R O D U C T I O N A N D T H E O R Y

INTRODUCTION AND THEORY

There are two ways of approaching the subject of dielectrics in relation to chemistry: (i) contributions of chemistry to the theory of dielectrics and (ii) contributions of dielectric study to chemistry. The present thesis is concerned with the second type of study.

Dielectric techniques have been widely utilized in physico-chemical studies (1), particularly of structure and molecular motions present in different types of systems. Microwave measurements have been found an effective means of studying molecular structure in liquids and solutions (2,3). Early studies (4,5) of different types of liquids in the solid state were confined to dielectric constant or permittivity measurement which, in many cases, particularly in the case of non polar and weakly polar compounds, is not sensitive enough to detect the molecular motions and to determine their energy barriers. Later, dielectric absorption techniques were utilized by Meakins, Dryden and coworkers (6-8) who have been concerned mainly with the long-chain compounds. Recently, dielectric studies of a variety of compounds in supercooled liquids have been done by many workers (9-13). In our present

study we have chosen some non polar, weakly polar and fairly polar compounds of different size and shape and studied their dielectric behaviour in the solid state.

The fundamental theories and basic equations for dielectric absorption techniques are well established. This is concerned mainly with the polarization and dielectric absorption due to dipole orientation (14).

An insulating material, when placed in an electric field, becomes polarized due to the relative displacement of positive and negative electric charges. The ratio between the field strength without any dielectric to that in the presence of the dielectric is called the dielectric constant or permittivity, ϵ' , of the material. It may also be defined as the ratio of capacitance, C , of a condenser filled with the material to the capacitance C_0 of the empty condenser.

$$\epsilon' = \frac{C}{C_0} \quad (1.1)$$

The total polarization in any material is made up of different components, according to the nature

of the charges displaced. The electronic polarization component, P_E , is due to the relative displacement of the electrons and nuclei of the atoms and requires about 10^{-15} s corresponding to ultraviolet region. The atomic polarization, P_A , is due to the relative displacement of the atoms in a molecule, involving the stretching, twisting, or bending of chemical bonds. In an ionic solid the corresponding effect is the relative displacement of the ions. This polarization requires 10^{-12} s to 10^{-14} s and corresponds to frequencies in the infrared region. Orientation polarization, P_O , occurs only in dipolar materials and is due to a perturbation of the thermal motion of the dipoles which tend to rotate into positions more favourable to the electric field. The time required for the orientation polarization process depends on the frictional resistance of the medium to the change in molecular orientation. For small molecules in liquids of low viscosity, it is about 10^{-11} s to 10^{-12} s, corresponding to the micro-wave region.

Another type of polarization, called interfacial, or Maxwell-Wagner type polarization (15), occurs in heterogeneous dielectrics when one component has a

higher electrical conductivity than the other. It is most commonly associated with the presence of impurities which form a separate and slightly conducting phase, in which dipoles can be induced by an electric field. This type of polarization is important because it can lead to dielectric absorption at any part of the radio frequency spectrum and is sometimes mistaken for dipole orientation polarization.

The dielectric constant or permittivity, ϵ' , is a frequency dependent quantity. When the dielectric constant is measured at fields of low alternating frequency it has its maximum value which is termed the static dielectric constant, ϵ_0 . As the frequency is increased from a static field up to the microwave region, the reorientation of dipoles in the field will, at some stage, lag behind the voltage oscillations. The resulting phase displacement (δ) leads to a dissipation of energy known as Joule heating which is measured by the dielectric loss (ϵ'') defined by:

$$\epsilon'' = \epsilon' \tan \delta \quad (1.2)$$

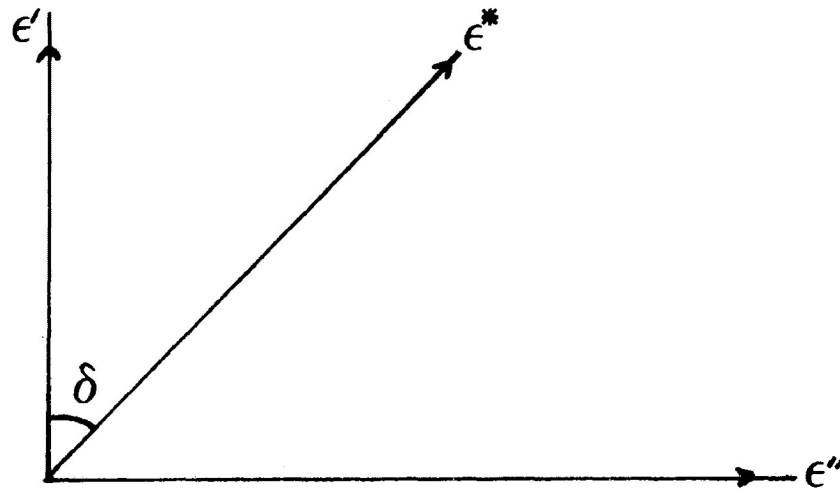


FIGURE 1.1:- Relation between ϵ' , ϵ'' and $\tan \delta$ in the complex quantity of dielectric constant (ϵ^*)

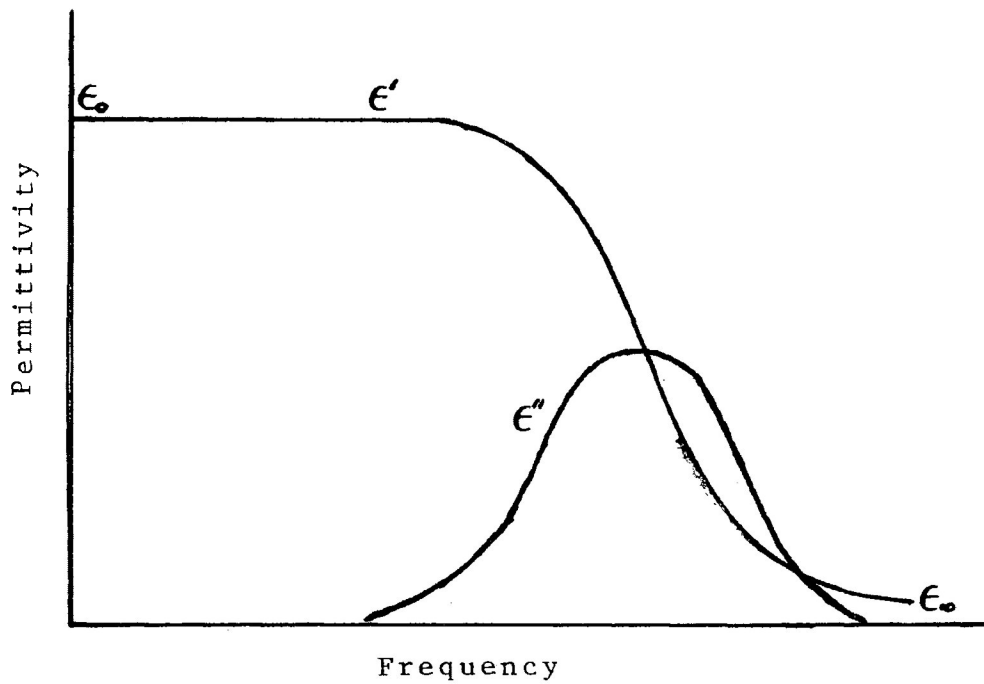


FIGURE 1.2:- Frequency dependence of real (ϵ') and Imaginary (ϵ'') parts of the permittivity in a relaxation region

where ϵ' is the real part of the dielectric constant and $\tan\delta$ is the loss tangent or the energy dissipation factor. In this high frequency region the dielectric constant becomes a complex quantity (ϵ^*) where:

$$\epsilon^* = \epsilon' - i\epsilon'' \quad (1.3)$$

$$i = \sqrt{-1}$$

Figure I.2 shows the frequency dependence of the permittivity for an anomalous dispersion (when the permittivity is a complex quantity). As the frequency of the applied field approaches zero, ϵ'' approaches zero, and ϵ' approaches the static permittivity, ϵ_0 ; and, as the frequency approaches infinity, ϵ'' again approaches zero, and ϵ' approaches ϵ_∞ , the very high frequency or optical permittivity.

At low frequencies, providing that the molecule is sufficiently small and the retarding force is not great, the dipoles respond instantaneously to the field variation with time, but, as the frequency is increased the motion of the molecules is not sufficiently rapid to maintain equilibrium with the field variation. Hence, there is

a time lag in the response of the molecules with respect to the field and the polarization P_t at any time t is less than the equilibrium value P_0 , as described by the equation:

$$P_t = P_0 e^{-t/\tau} \quad (\text{I.4})$$

where τ is known as relaxation time of the dielectric. When $\tau = t$, Eqn. (I.4) becomes:

$$P_t = P_0 \cdot \frac{1}{e} \quad (\text{I.5})$$

So, relaxation time may also be defined as the time required, when the field is switched off, for the polarization (P_t) to decay to $\frac{1}{e}$ of its initial value (P_0) where e is the natural logarithmic base.

The frequency dependence of permittivity ϵ' and loss factor ϵ'' for single relaxation process τ are described by the Debye equation (16,17):

$$\epsilon^* = \epsilon' - i\epsilon'' = \epsilon_\infty + \frac{\epsilon_0 - \epsilon_\infty}{1 + i\omega\tau} \quad (\text{I.6})$$

where $\omega = 2\pi f$ and f is the measuring frequency.

Separating the real and imaginary parts:

$$\epsilon' = \epsilon_{\infty} + \frac{\epsilon_0 - \epsilon_{\infty}}{1 + \omega^2 \tau^2} \quad (\text{I.7})$$

and

$$\epsilon'' = \frac{(\epsilon_0 - \epsilon_{\infty}) \omega \tau}{1 + \omega^2 \tau^2} \quad (\text{I.8})$$

From Equation (I.8) it is evident that ϵ'' is a maximum for $\omega \tau = 1$ and

$$\epsilon''_{\max} = \frac{\epsilon_0 - \epsilon_{\infty}}{2} \quad (\text{I.9})$$

Elimination of $\omega \tau$ between Equations (I.7) and (I.8) gives the equation of a circle:

$$\left(\epsilon' - \frac{\epsilon_0 + \epsilon_{\infty}}{2}\right)^2 + \epsilon''^2 = \left(\frac{\epsilon_0 - \epsilon_{\infty}}{2}\right)^2 \quad (\text{I.10})$$

Hence, a graph of ϵ'' against ϵ' in the complex plane is a semicircle, the so-called Cole-Cole plot (18).

So far the discussion has been limited to the case of a single discrete relaxation time. Many solids (14) give dielectric absorption which is wider than a Debye curve, due to the presence of a range of relaxation times. Cole and Cole (18) assumed a continuous distribution of relaxation times about a most probable value τ_0 and their general dispersion equation for the complex dielectric constant is:

$$\epsilon^* = \epsilon' - i\epsilon'' = \epsilon_\infty + \frac{\epsilon_0 - \epsilon_\infty}{1 + (i\omega\tau_0)^{1-\alpha}} \quad (\text{I.11})$$

α is the distribution parameter which may have values between 0 and 1. When $\alpha = 0$, the Debye equation is obtained.

Similarly, Equation (I.11) can be separated into real and imaginary parts to yield analogous Cole-Cole plot where the centre of the semicircle lies below abscissa:

$$\epsilon' = \epsilon_\infty + \frac{(\epsilon_0 - \epsilon_\infty)(1 + (\omega\tau_0)^{1-\alpha} \sin(\alpha\pi/2))}{1 + 2(\omega\tau_0)^{1-\alpha} \sin(\alpha\pi/2) + (\omega\tau_0)^{2(1-\alpha)}} \quad (\text{I.12})$$

$$\epsilon'' = \frac{(\epsilon_0 - \epsilon_\infty) (\omega \tau_0)^{1-\alpha} \cos(\alpha \pi/2)}{1 + 2 (\omega \tau_0)^{1-\alpha} \sin(\alpha \pi/2) + (\omega \tau_0)^{2(1-\alpha)}} \quad (\text{I.13})$$

The mean relaxation time τ_0 may be obtained from:

$$\tau_0 = \frac{1}{2\pi f_{\max}} \quad (\text{I.14})$$

where f_{\max} is the frequency at which maximum absorption occurs. The values of ϵ_∞ and ϵ_0 may be estimated from the high and low frequency intercepts, respectively, of the Cole-Cole plot. The better value of ϵ_0 may be obtained from heterodyne beat technique.

The most frequently used empirical expression for non-Debye types of relaxation is the Fuoss-Kirkwood relation (19) given by:

$$\epsilon'' = \epsilon''_{\max} \operatorname{sech}(\beta \ln(f/f_{\max})) \quad (\text{I.15})$$

where f is the frequency in Hz and f_{\max} is the frequency of maximum absorption. β value varies between unity for a single relaxation time and zero for an infinite range.

The relation between Fuoss-Kirkwood β -value

and the Cole-Cole α -value was considered by Poley (20):

$$\beta\sqrt{2} = (1-\alpha)/\cos(1-\alpha)\pi/4 \quad (\text{I.16})$$

The Cole-Davidson function (21) also describes expression of non-Debye types of absorption:

$$\epsilon^* = \epsilon' - i\epsilon'' = \epsilon_\infty + \frac{\epsilon_0 - \epsilon_\infty}{(1+i\omega\tau_0)^h} \quad (\text{I.17})$$

h is again a constant having values between 0 and 1, with $h = 1$ corresponding to the Debye equation. Equation (I.17) gives:

$$\epsilon' = \epsilon_\infty + (\epsilon_0 - \epsilon_\infty)(\cos^h\theta \cos(h\theta)) \quad (\text{I.18})$$

and

$$\epsilon'' = (\epsilon_0 - \epsilon_\infty)(\cos^h\theta \sin(h\theta)) \quad (\text{I.19})$$

where $\theta = \arctan(\omega\tau_0)$. Cole-Davidson Equation results a skewed arc from the plot of ϵ' versus ϵ'' at various frequencies. This equation seems to be very successful in representing behaviour of substances at low temperatures.

It is also often employed to interpret the dielectric absorption for a relaxation mechanism involving co-operative motion (22,23).

It is generally assumed that in liquids the dipoles can point in any direction and are continually changing direction as a result of thermal agitation. In solids the dipoles would be more hindered, and to account for the presence of dielectric losses, Debye (16) suggested the following simple mechanism:

Each dipole possesses two positions of equilibrium, equal in energy and opposite in direction, separated by an energy barrier, ΔG_E . This is illustrated by the free energy diagram shown in Figure I.3(a). The dipoles oscillate with a frequency, f_0 , about the equilibrium positions and occasionally acquire enough energy to rotate from one equilibrium position to the other, but at any instant there are equal numbers of dipoles occupying each position. If an electric field is applied, a small excess of dipoles will rotate into more favourable positions, thus giving rise to polarization.

The energy barrier between the equilibrium positions of the dipoles can be obtained from the tempera-

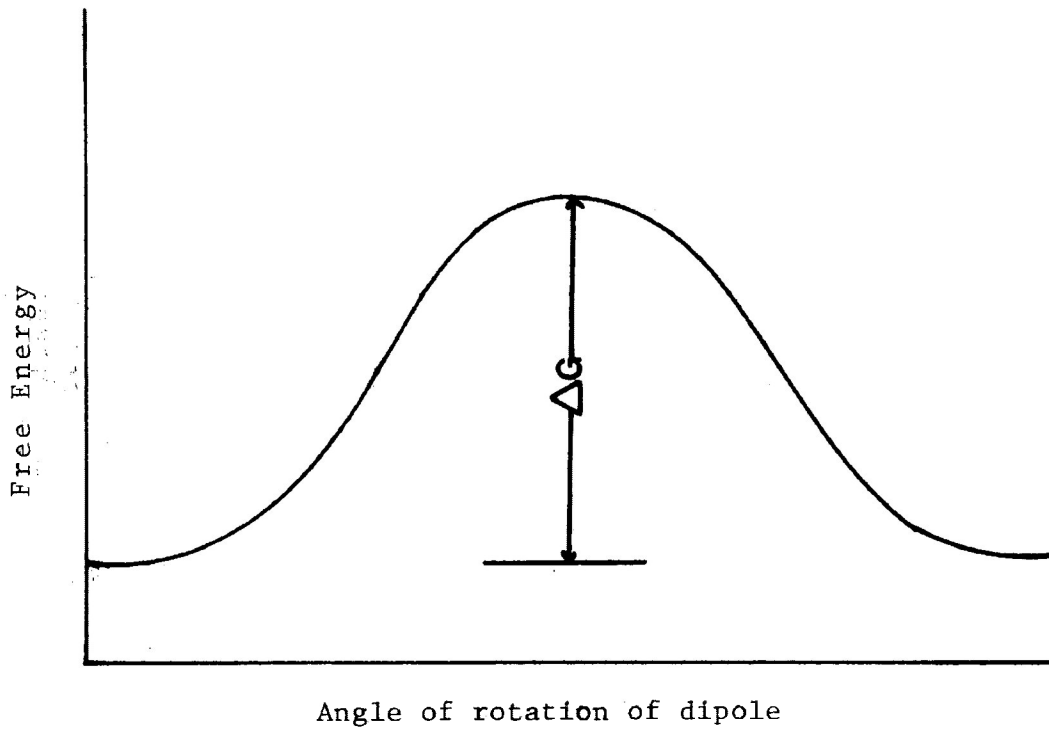


FIGURE 1.3(a):- Free Energy Diagram for dipole rotating in a crystal lattice

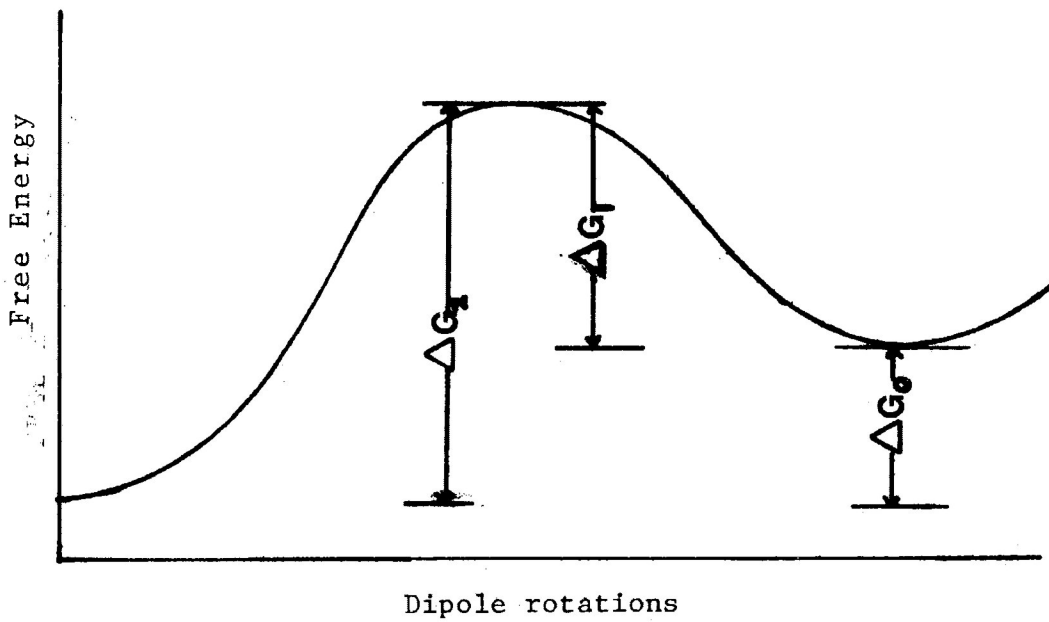


FIGURE 1.3(b):- Free Energy Diagram for unequal free energy minima

ture dependence of the frequency of maximum absorption f_{\max} by means of the equation (24):

$$f_{\max} = \frac{1}{2\pi\tau} = \frac{f_0}{\pi} \exp(-\Delta G_E/RT) \quad (\text{I.20})$$

where R is the universal gas constant and T the absolute temperature.

In most solids the equilibrium positions of the dipoles are unequal, as illustrated in Figure I.3(b). It can be shown (17) that in this case the molecular relaxation time is given approximately by the expression:

$$f_{\max} = \frac{1}{2\pi\tau} = \frac{f_0}{\pi} \exp(-\Delta G_{E(1)}/RT) \quad (\text{I.21})$$

where $\Delta G_{E(1)}$ is approximately equal to the smaller energy barrier.

The more commonly used equation is that of Eyring (24) given by:

$$\frac{1}{\tau} = \frac{kTK}{h} \exp(-\Delta G_E/RT) \quad (\text{I.22})$$

where h is Planck's constant, k is Boltzmann's constant, and K is the transmission coefficient normally taken to be 1. Now:

$$\Delta G_E = \Delta H_E - T\Delta S \quad (I.23)$$

where ΔH_E is the enthalpy of activation and ΔS_E is the entropy of activation. Thus:

$$\tau = \frac{h}{kT} \exp(\Delta H_E/RT) \exp(-\Delta S_E/RT) \quad (I.24)$$

From equation (1.24), it appears that a plot of $\log(\tau T)$ versus $1/T$ should give a straight line. The values of ΔH_E and ΔS_E may be obtained from the slope and intercept respectively. There is a lack of significance in ΔS_E values obtained in this way. However, it is widely quoted and used in the dielectric relaxation studies.

REFERENCES

1. C.P. Smyth, Ann. Rev. Phys. Chem., 17(1966)433.
2. C.P. Smyth, "Dielectric Behaviour and Structure", McGraw-Hill, London, 1955.
3. N.E. Hill, W.E. Vaughan, A.H. Price, and M. Davies "Dielectric Properties and Molecular Behaviour", Van Nostrand-Reinhold, London, 1969.
4. A. Turkevich and C.P. Smyth, J. Am. Chem. Soc., 62(1940)2468.
5. R.W. Crowe and C.P. Smyth, J. Am. Chem. Soc., 72(1950)4009.
6. R.J. Meakins, Trans. Faraday Soc., 51(1955)953; 55(1959)1694.
7. J.S. Dryden, J. Chem. Phys., 26(1957)604.
8. J.S. Dryden and S. Dasgupta, Trans. Faraday Soc., 51(1955)1661.
9. H.A. Khwaja and S. Walker, Adv. Mol. Relax. Int. Processes, 27(1982)22.
10. J. Crossley, D. Gourlay, M. Rujimethabas, S.P. Tay and S. Walker, J. Chem. Phys., 71(1979)4095
11. L. Hayler and M. Goldstein, J. Chem. Phys., 66(1977)736.
12. P.J. Hains and G. Williams, Polymer, 16(1975)725.
13. G.P. Johari, J. Chem. Phys., 58(1973)1766.
14. R.J. Meakins, "Progress in Dielectrics", 3(1961)151.
15. K.W. Wagner, Arch. Elektrotech., 2(1914)371.
16. P. Debye, "Polar Molecules", Chemical Catalog, New York, 1929.

17. H. Fröhlich, "Theory of Dielectrics", Clarendon, Oxford, 1949.
18. K.S. Cole and R.H. Cole, J. Chem. Phys., 9(1941)341.
19. R.M. Fuoss and J.G. Kirkwood, J. Am. Chem. Soc., 63(1941)385.
20. Ref. 3, p. 292.
21. D.W. Davidson and R.H. Cole, J. Chem. Phys., 19(1951)1484.
22. M. Nakamura, H. Takahashi and K. Higasi, Bull. Chem. Soc. Jpn., 47(1974)1593.
23. T.G. Copeland and D.J. Denney, J. Phys. Chem., 80(1976)210.
24. S. Glasstone, K.J. Laidler and H. Eyring, "The Theory of Rate Processes", McGraw-Hill, New York, 1941.

CHAPTER II

A P P A R A T U S A N D
E X P E R I M E N T A L P R O C E D U R E

APPARATUS AND EXPERIMENTAL PROCEDURE

Most of the compounds studied for this thesis were either nonpolar or polar liquids at room temperature. The majority of the nonpolar liquids were of highest available commercial purity (>99%) and were used as received without further purification. Purification, if at all needed, of different samples have been described in each of the following chapters. Two solid samples (m.p. >90°C) were studied as compressed solid disks. The solid disks were prepared by grinding the solid with a mortar and a pestle, placing the powder in the die and pressing it at room temperature with a pressure of 10 tons. Solids which had comparatively low melting points (m.p. <90°C) were first heated to 5°C above their melting points and then poured into the preheated (5°C above the melting point of the sample) coaxial cell. Liquids were measured in a three terminal coaxial cell and the compressed solid disks in a parallel plate capacitor cell. As some of our systems were nonpolar, the dielectric measurement of which is still not well established, we find it necessary to describe in details the three terminal coaxial cell in which most of the measurements were made.

Three Terminal Coaxial Cell

This cell, designed by Mr. B. K. Morgan of this laboratory, shown in cross-section in Figure 2.1 (reproduced by the courtesy of D.L. Gourlay (1) of this laboratory), measures the dielectric properties of liquids over a wide temperature range. The cell is circular and has concentric stainless steel electrodes, A and B. Their shape permits the rapid transfer of heat to or from the solid aluminium case C. The undersides of the electrodes are insulated from the case by a 0.25 cm thick Teflon disk. A 0.50 cm thick Teflon sleeve insulated the outer circumference of electrode B. The fringe field is practically eliminated by the presence of the grounded case below and a grounded guard ring E, above. The circular Teflon cap F fits closely into the top of electrode B to prevent the escape of liquid vapours.

The sample can conveniently be introduced into the 0.50 cm gap between electrodes A and B by a disposable pipette which should first be pushed to the bottom of the semicircular hole cut vertically in the edge of electrode A. Tests have shown that if the gap between the electrodes is filled from the bottom all the air will be expelled.

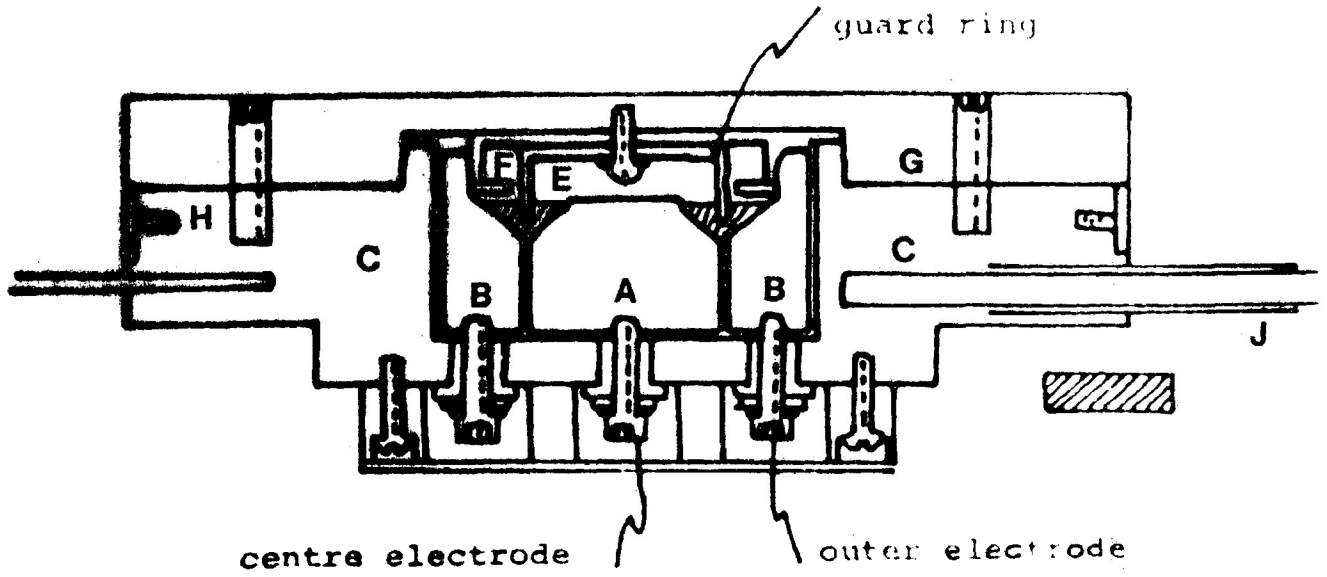


FIGURE:- 2.1 Three terminal coaxial cell

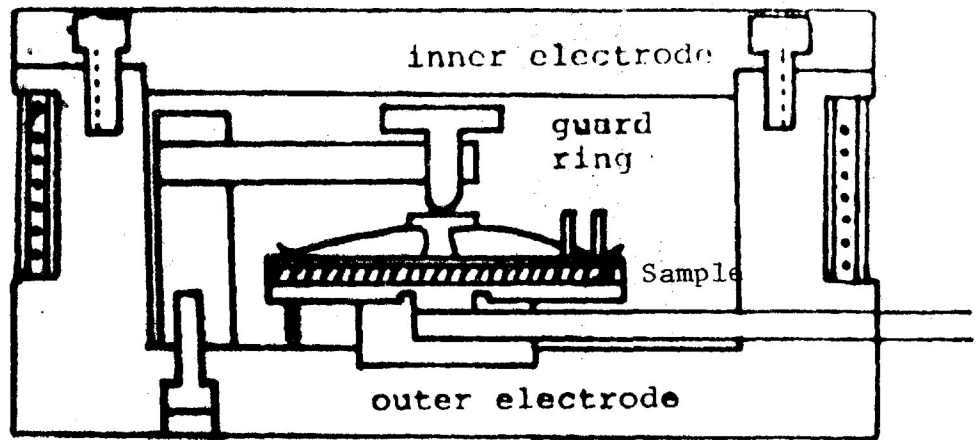


FIGURE:- 2.2 Parallel plate capacitor cell

One and a half millilitres of sample is sufficient to fill the cell. To empty it the sample is sucked up with a dropper and the electrodes are flushed with solvents (first with acetone and then with cyclohexane) several times. To dry the electrodes a cotton swab is pushed down the filling hole. Any remaining liquid is removed by wiping around the electrode gap with 2.50 cm wide strips post card. Hot air is also blown to dry the cell completely.

The lid of the cell G is secured to the case by four recessed bolts. The surface between G and C is coated with heat conductive grease of the type used with semiconductor heat-sinks.

The outer cell wall is insulated by a ring of microcellular polystyrene foam which is flush with the top of G. The insulation has a wall thickness of 5 cm. The cell's underside is also insulated with a 23 cm diameter and 5 cm thick disc of polystyrene.

The cell can be rapidly cooled by placing a 3 litre flat bottomed aluminium container of liquid nitrogen to cover the lid G. The vertical sides of the

nitrogen container are also insulated with polystyrene foam. When the desired temperature is reached an appropriate number of sheets of paper is placed between the nitrogen container and the lid to reduce the rate of cooling. Equilibrium is maintained by a Thermo Electric thermo-regulator model 3814021133 connected via a variac transformer to heater H. This heater is a 300 watt 110 V ARI Industries heater, model number BXA-06F-40-4K, but we run it at about 60 V. The temperature is measured by a Newport 264-3 digital platinum resistance pyrometer. Its probe J is partly insulated from the heater by a Teflon sleeve. The upper temperature limit of the cell is about 368 K, just below the temperature at which the polystyrene deforms.

Connections are made to electrodes A and B through screws insulated by Teflon sleeves and mica washers. The heads of the screws are screened by a 2.5 cm wide aluminium block with three 1.25 cm diameter holes cut into it. The screw from electrode A is connected to a miniature coaxial cable which enters through the side of the block. The cable has Teflon insulation, its type number is RG-316/U. A similar coaxial connection is made to one of the screws from electrode B. The cables are connected to the GR Bridges via extension cables if required.

The principal merits of this cell are its thermal characteristics, which allow the sample to reach equilibrium temperature quickly. The rigidly fixed coaxial electrode design gives a very stable cell constant with very small stray capacitance. Finally, the cell uses only a small volume of liquid and is easy to clean.

Another type of cell, parallel plate capacitor cell, used for solid disks, also designed by Mr. Morgan, is shown in Figure 2.2.

The General Radio Bridges

Dielectric measurements were made either with a GR 1621 Precision Capacitance Measurement System or with a GR 1615-A Bridge in conjunction with their model 1310-B sine-wave signal generator and model 1232-A tuneable amplifier/null detector. The 1621 Precision Capacitance Measurement System consists of a GR 1316 Precision Capacitance Bridge with a GR 1316 Oscillator and GR 1238 Detector, a complete system for the precise measurement of capacitance and conductance. This system is particularly suitable for very low-loss materials.

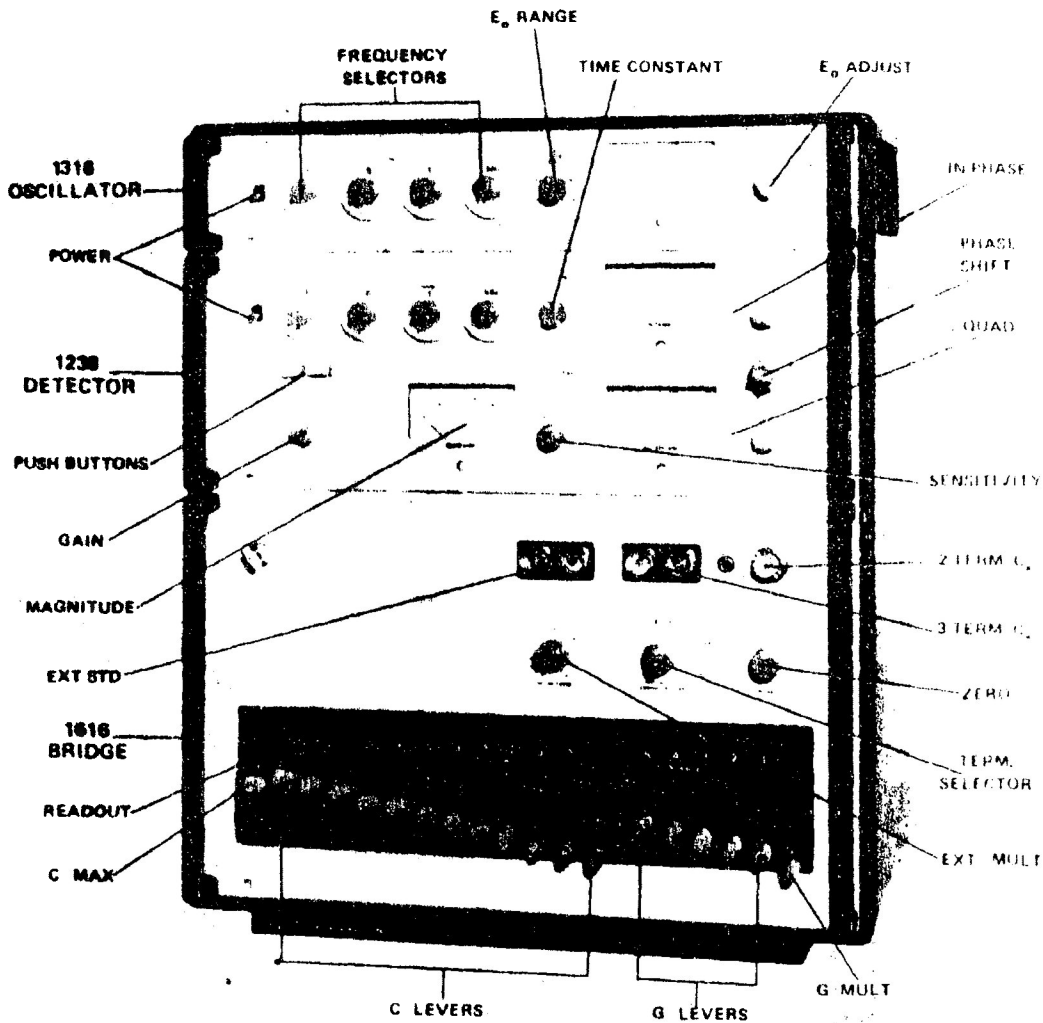


FIGURE:- 2.3 1621 Precision capacitance-measurement system

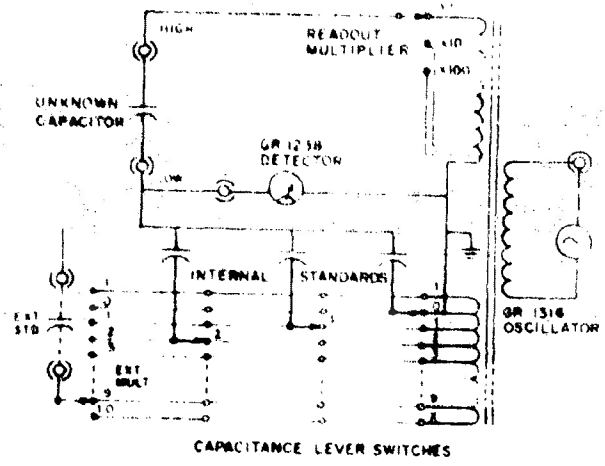


FIGURE:- 2.4 Elementary diagram, 1621 Precision capacitance-measurement system. Conductance circuitry is omitted

The oscillator and detector are mounted above the bridge, in a pedestal cabinet, as shown in Figure 2.3 (Reproduced from GenRad Instruction Manual). An elementary system diagram is given in Figure 2.4.

The ratio arms of the bridge are transformer windings, tapped on the standard side in decimal steps (-1, 0, 1, 2...9, X) and on the unknown side in decade steps (x100, x10, x1). Separate, fixed-capacitance standards are used, whose values range in decade steps from 1 aF to 100 nF. This combination of internal standards and transformer ratios makes possible the wide measurement range of 1 to 10^4 .

Loss in the measured capacitor is expressed as parallel conductance from the resolution limit of 0.1 f~~v~~ to a maximum of 1 M~~v~~; a measurement range of 1 to 10^{13} . The values of the set of 5 conductance standards are effectively extended by series resistance standards, in 6 decade steps (x1...x 10^{-6}).

Measurements made with the General Radio bridges were of conductivity (G) or dissipation (D) factors and capacitance (C) of a sample. These are re-

lated to the components of the complex permittivity by the following relations (2):

$$\epsilon' = \frac{C}{C_0} \quad (1.1)$$

$$\epsilon'' = \frac{G}{\omega C_0} \quad (2.1)$$

and $\epsilon'' = (Dxf)\epsilon' = \epsilon' \tan \delta \quad (1.2)$

where C_0 is the capacitance of the empty condenser, $\omega = 2\pi f$ is the angular frequency of the applied field in radians s^{-1} and f the frequency in kHz, $\tan \delta$ is the loss tangent.

Since it is difficult to obtain C_0 through measurement in the case of parallel plate capacitance cell, C_0 may be calculated from the relation (3).

$$C_0 = \frac{0.08842A}{d}$$

where A is the effective area in square centimeters, and d is the spacing of the plates in centimeters. Elimination

of C_0 from these equations gives:

$$\epsilon' = \frac{C_d}{0.08842A} \quad (2.2)$$

and

$$\epsilon'' = \frac{\epsilon'G}{\omega c} \quad (2.3)$$

ϵ'' may be determined either from equation (2.1) or from a combination of equations (2.2) and (2.3), if the values of C_0 and A are known.

In order to determine the relevant constants (C_0 for coaxial and A for parallel plate cells), both systems were calibrated by studying samples of precisely known ϵ' at a given temperature. The coaxial cell was calibrated with purified cyclohexane at room temperature. A quartz disk, supplied by Rutherford Research Products Co., of 0.1318 cm thickness and a claimed diameter of 3.819 cm was used for calibration of parallel-plate capacitor cell. Calibration studies were initially carried out down to liquid nitrogen temperatures to see if there was any variation between values of ϵ' determined at room temperature and those at lower temperatures. Variation was considered negligible.

Most of the samples showed co-operative like

motion in the solid state. This type of motion is usually observed in supercooled liquids near the glass transition temperature (T_g). For this reason, each of our samples was checked for T_g with the help of the glass transition apparatus, shown in Figure 2.5.

Glass Transition Apparatus

This apparatus was also constructed by Mr. B.K. Morgan of this laboratory having an idea from Dr. N. Koizumi of Koyoto University, Japan. It detects linear expansion of solid or frozen liquid samples. Heating the Sample A causes the inner pyrex tube to move upwards relative to the outer pyrex tube. This movement is transmitted from the cap of the inner tube to the core of transducer B. Movement of the core causes a change in the electromagnetic coupling between the input and output coils of the transducer. The output coil is connected to a strip chart recorder which displaces a rising trace as the sample is heated towards the glass transition temperature. Near the glass transition temperature the trace levels off and then begins to fall as the sample softens.

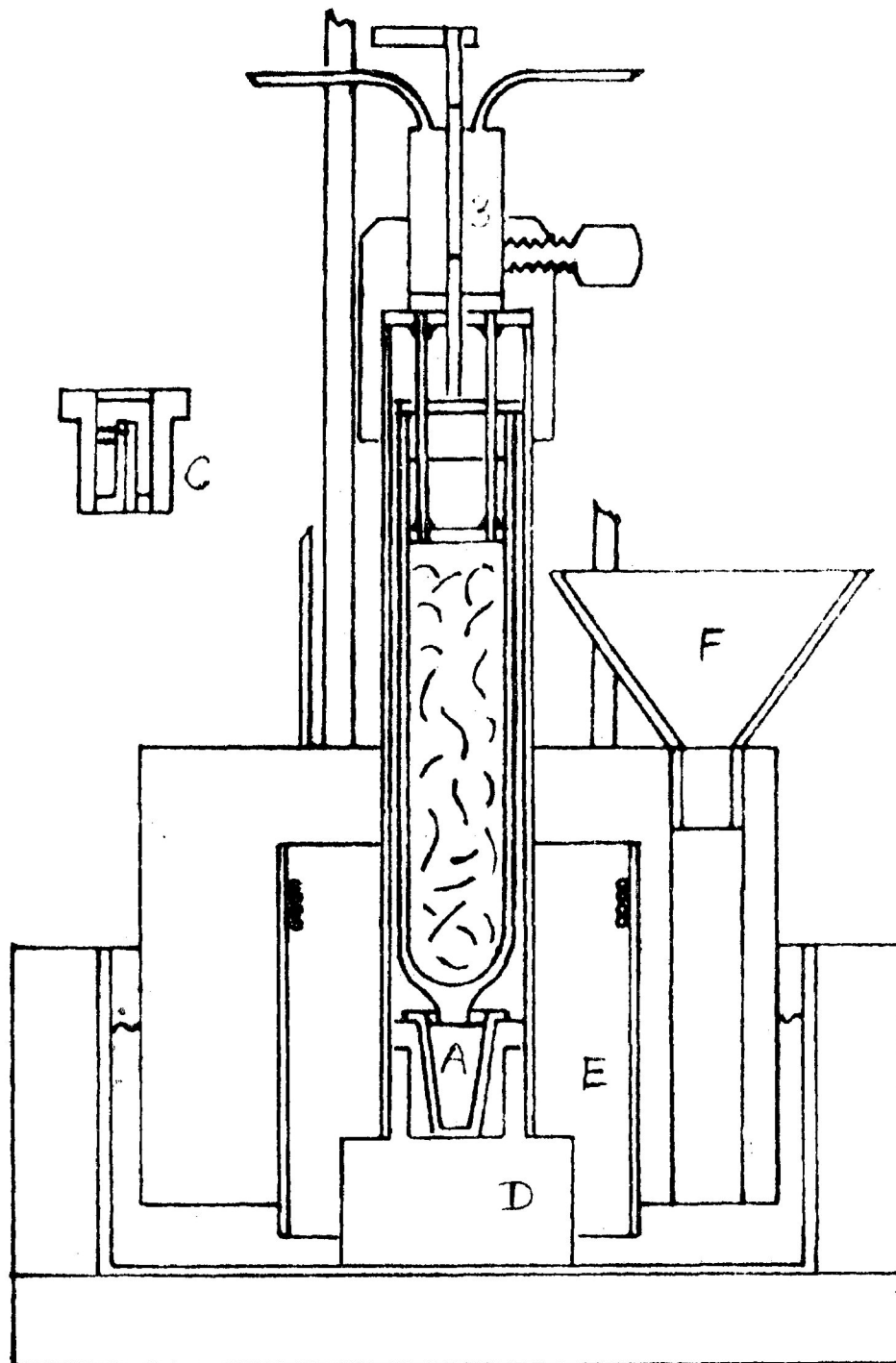


FIGURE:- 2.5 Glass transition measurement device

- A - liquid sample holder
- B - transducer
- C - solid sample holder
- D,E - interlocking circular blocks
- F - funnel

Analysis of Experimental Data

The analysis of experimental data was made by a series of computer programmes written in the APL Language. For each temperature, the dielectric loss values at different frequencies were subjected to analysis by the Fuoss-Kirkwood equation, Eqn. (1.15), the linear form of which is:

$$\cosh^{-1} \frac{\epsilon''_{\max}}{\epsilon''} = 2.303\beta(\log f_{\max} - \log f) \quad (2.4)$$

By iteration the programme (titled FUOSSK) finds that value of ϵ''_{\max} which provides the best straight line fit to the plot of $\cosh^{-1}(\frac{\epsilon''_{\max}}{\epsilon''})$ versus $\log f$; the slope of this straight line gives β -value and f_{\max} is obtained from the slope and intercept.

The Fuoss-Kirkwood equation does not deal with the real part of the complex permittivity nor does it with the limiting values at low and high frequencies, ϵ_0 and ϵ_∞ , respectively, except that the total dispersion is given by the expression:

$$\Delta\epsilon = \epsilon_0 - \epsilon_\infty = \frac{2\epsilon''_{\max}}{\beta} \quad (2.5)$$

In a system involving a distribution of relaxation times, the frequency dependence of permittivity is commonly described by the Cole-Cole distribution given by Eqns., (1.11), (1.12), and (1.13).

The Cole-Cole distribution parameter, α , may be obtained from the Fuoss-Kirkwood distribution parameter, β , by Eqn. (1.16).

The programme titled EINF was used to find the value of ϵ_0 at various temperatures. Equations (1.12) and (1.13), with the experimental values of ϵ' of various frequencies at each temperature, were fed into the computer; ϵ_∞ then came out as an output with an estimate of error involved.

Fuoss-Kirkwood analysis and EINF programmes are based on the fact that $\omega\tau=1$ at the frequency of maximum absorption (f_{\max}). In the case of co-operative motion, $\omega\tau \neq 1$ (5) at the frequency of maximum absorption (f_{\max}) and so the important parameters, e.g. distribution parameter β and relaxation time τ from Fuoss-Kirkwood analysis and ϵ_0 and ϵ_∞ from EINF Programme, are not the true values. In this case Cole-Davidson analysis has been done. Figure 2.6, a typical Cole-Davidson plot, shows

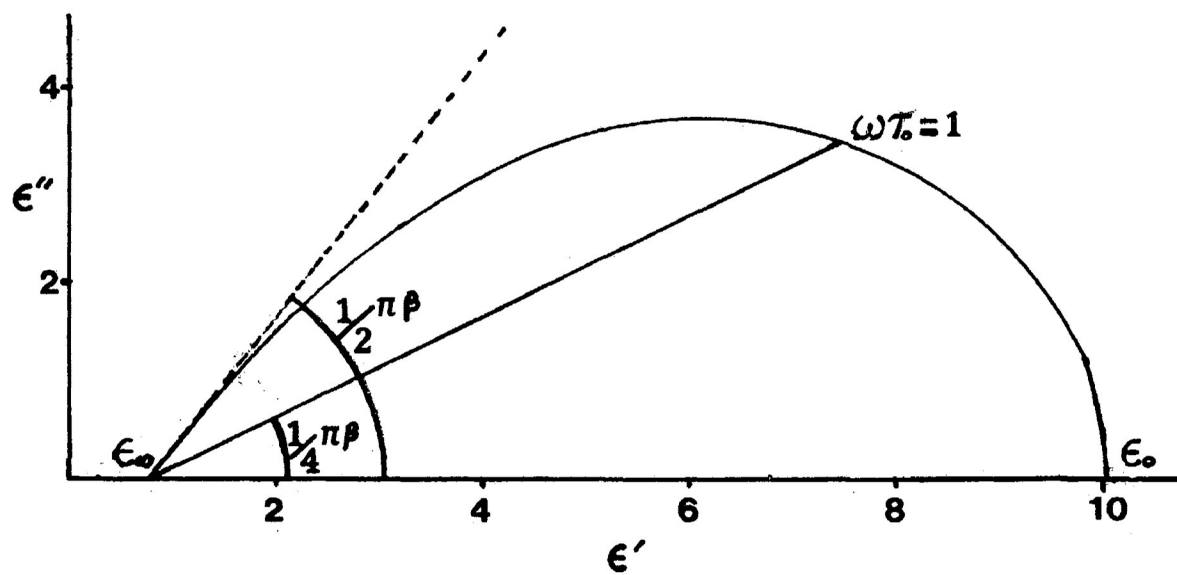


FIGURE 2.6: Cole-Cole plot for the Davidson-Cole Equation

how to find out the above parameters.

The results from the foregoing analysis were used for the calculation of the effective dipole moments involved in the relaxation process from both the Debye (4) equation (2.6) and the Onsagar (5) equation (2.7):

$$\mu^2 = \frac{27000kT(\epsilon_0 - \epsilon_\infty)}{4\pi NC(\epsilon' + 2)^2} \quad (2.6)$$

$$\mu^2 = \frac{9000kT(2\epsilon_0 + \epsilon_\infty)(\epsilon_0 - \epsilon_\infty)}{4\pi NC\epsilon_0(\epsilon_\infty + 2)} \quad (2.7)$$

where: $\epsilon_0 - \epsilon_\infty = \frac{2\epsilon''_{\max}}{\beta}$ (Eqn. (1.9))

ϵ' is the value of ϵ' at f_{\max} , that is $(\epsilon_\infty + \epsilon_0)/2$

ϵ_0 is the static dielectric constant derived from ϵ_∞ and Eqn. (1.9)

N is the Avogadro Number, 6.023×10^{23} molecules mol^{-1}

C is the concentration in mol l^{-1}

k is the Boltzmann constant, 1.38×10^{-16} erg K^{-1}

and T is the temperature in K.

In the present study, dipole reorientation was

considered as rate process and the energy barrier opposing the dielectric relaxation process was obtained by use of Eyring rate equation (1.21), a procedure commonly adapted in dielectric works (4,6,7). Expressing Eqn. (1.21) in a linear form, one obtains:

$$\ln(\tau T) = \frac{\Delta H_E}{RT} - \frac{\Delta S_E}{R} - \ln\left(\frac{h}{k}\right) \quad (2.8)$$

Plots of $\log(\tau T)$ against $\frac{1}{T}$ yielded straight lines for simple molecular processes. Co-operative processes usually yielded curves from such plots. The values of enthalpies of activation, ΔH_E and the entropies of activation, ΔS_E , were obtained from the slope and intercept, respectively, of such graphs by a computer programme based on Eqn. (2.8). The programme also calculated the relaxation times, τ , and the free energies of activation, ΔG_E , at different temperatures according to the equation, $\Delta G_E = \Delta H_E - T\Delta S_E$.

Standard statistical techniques (8) have been employed in the fitting and analysis of the data with the various computer programmes, and the important parameters, viz., $\text{loss}(f_{\max})$ and β values from the Fuoss-Kirkwood analysis, as well as the enthalpies and entropies of

activation from the Eyring analyses, were obtained with different confidence interval widths. In the present study, 95% confidence interval was chosen as a good representation of experimental errors. Any experimental point which deviated from the calculated line by more than its allowed confidence interval was deleted from a repeat run of the Eyring programme.

REFERENCES

1. D.L. Gourlay, M.Sc. Thesis, Lakehead University, Thunder Bay, Canada, 1982.
2. C.P. Smyth, "Dielectric Behaviour and Structure", McGraw-Hill Book Co., New York, 1955.
3. F.E. Terman, "Radio Engineers' Handbook", McGraw-Hill Publishing Co. Ltd., London, 1950.
4. N.E. Hill, W.E. Vaughan, A.H. Price and M. Davies, "Dielectric Properties and Molecular Structure", Van Nostrand-Reinhold Co., London, 1969.
5. C.J.F. Böttcher and P. Bordewijk, "Theory of Electric Polarization", Vol. II, Elsevier Publishing Co., Amsterdam, Netherlands, 1977.
6. M. Davies and A. Edwards, Trans. Faraday Soc., 63(1967)3163.
7. S.P. Tay and S. Walker, J. Chem. Phys., 63(1975) 1634.
8. B. Ostle, "Statistics in Research", (2nd ed.), Iowa State Univ. Press, Ames, Iowa, U.S.A., 1963.
9. M.A. Mazid, M.Sc. Thesis, Lakehead University, Thunder Bay, Canada, 1977.
10. J.C.N. Chao, M.Sc. Thesis, Lakehead University, Thunder Bay, Canada, 1978.

C H A P T E R I I I

DIELECTRIC ABSORPTION OF SOME NONPOLAR SPHERICAL MOLECULES
IN THE SOLID STATE

DIELECTRIC ABSORPTION OF SOME NONPOLAR SPHERICAL MOLECULES
IN THE SOLID STATE

INTRODUCTION

The existence of very low dielectric losses in non-polar liquids was noted by Whiffen (1) in 1950 and confirmed by Heston and Smyth (2) in the same year. Whiffen found that the losses of benzene, carbon tetrachloride, cyclohexane and decalin, all of which have no permanent electric dipole moment, were proportional to the frequency in the range 0.3 to 1.2 cm^{-1} . The plots of loss tangent against frequency suggested Debye behaviour and relaxation times ($\approx 1 \times 10^{-12}$ s) of the order of the time between molecular collisions. The author suggested that the absorptions result from dipole moments induced in molecular collisions. The induced dipole was regarded as changing direction not by molecular rotation, but because of a new collision at another instant with another neighbour.

Similar results have been reported for nonpolar molecules in both liquid (3) and gaseous (4) states. The gaseous measurements have shown that the absorption is proportional to the square of the gas density and is a

consequence of temporary dipole moments induced during molecular collisions.

Gabelnick and Strauss (5) have examined the far infrared spectrum of liquid carbon tetrachloride down to a frequency of 33 cm^{-1} , and of the vapour with comparable amounts of material in the spectrometer. They found no absorption in the gas below that due to an allowed vibration at 315 cm^{-1} , but, in the liquid they observed weak vibrational bands at 220, 145 and possibly at 97 cm^{-1} in addition to a much stronger vibrational band at 315 cm^{-1} . They follow Whiffen in suggesting that the absorption in the liquid may be due to the bending of a C-Cl bond in the molecule, a bending of 10° being sufficient to produce a dipole moment of 0.1-0.2 D.

There are other dielectric measurements of non-polar liquids in the microwave region (6-9) which serve to support these findings and to show that the absorptions are not the result of impurities such as water (8,9) or salts (9).

Radio frequency absorption of a few nonpolar supercooled liquids, e.g. o-terphenyl (10), Santovac (11)

and 3-methylpentane (12) in the glassy state are known. All these liquids show dielectric absorptions above their glass transition temperatures. No dielectric measurements of nonpolar liquids in the solid state appear to have been reported. This lack of information led to the present study on a few nonpolar compounds in the solid state. Here the results of five spherically-shaped molecules are presented.

EXPERIMENTAL RESULTS

The compounds studied in this chapter are listed below along with their sources and claimed purity:

	<u>Compounds</u>	<u>Sources</u>	<u>Purity</u>
1.	Neopentane	Matheson of Canada,	-
2.	Carbon tetra- chloride	Aldrich Chemical Co.	99+%
3.	Tetramethyl- silane	Aldrich Chemical Co.	99.98%
4.	Silicon tetra- chloride	Alfa Products	Ultrapure
5.	Tetramethyl- germanium	Alfa Products	99.5%

All of these chemicals were dried over activated molecular sieves prior to use. Purity of these compounds

(except neopentane) was checked by measuring the refractive indices and boiling points and comparing the experimental values with the literature values (Table 3.1).

Table 3.1: Experimental and literature values of refractive indices and boiling points of the nonpolar compounds

Compounds	Refractive index		Boiling Points	
	n_D^{20}		(K)	
	Experi- mental	Litera- ture	Experi- mental	Litera- ture
Carbon tetra- chloride	1.4606	1.4607 ^(a)	349.5	249.7 ^(a)
Tetramethyl- silane	1.3508	-	299.5	299.64 ^(b)
Silicon tetrachloride	-	-	330.7	332 ^(a)
Tetramethyl- germanium	1.3862	-	316.6	316-317 ^(c)

(a) The Merck Index, Merck and Co., Inc., N.J., 1968;

(b) J. Timmermans, "Physico-chemical constants of pure organic compounds", Elsevier Publishing Company, Inc., Amsterdam, 1950;

(c) D.F. Van de Vondel, J. Organometal Chem., 3(1965)400.

Since all these chemicals (except neopentane) were of very high-grade purity, they were used as received without further purification. Measurements were done on GR 1621 Precision Capacitance Measurement System using a three terminal coaxial cell. The empty cell was tested from room temperature to 83 K and it showed no observable loss at any frequencies though there was a little variation of capacitance. This shows that the cell has got no contribution to the dielectric loss factor.

Each of the samples (except neopentane) was measured twice and each time the dielectric relaxation behaviour was observed almost at the same temperature region suggesting that the absorptions were not the consequence of cracks in the sample. Special precautions were taken for neopentane, tetramethylsilane and silicon tetrachloride as described below:

Neopentane

Neopentane is a gas at ordinary temperature. The following steps were taken for the measurements of this compound:

(i) The gas cylinder was cooled down to about 265 K so that it became liquid.

(ii) The cell was also cooled to about 265 K.

(iii) Both were quickly placed in a box of nitrogen atmosphere.

(iv) The liquid was introduced into the cell and then cooled down to about 80 K by placing a liquid nitrogen container on the lid of the cell.

(v) The cell was then taken outside, connections were made as described in Chapter II and measurements were carried out after an hour making sure that equilibrium has been established.

Tetramethylsilane and Silicon tetrachloride

As both liquids are moisture sensitive their introduction into the cell was carried out in an inert nitrogen atmosphere box. Tetramethylsilane was measured in both ways, by cooling and by warming. In both cases, dielectric

absorption processes were observed almost in the same temperature region.

Figures 3.1-3.11 show the dielectric absorption curves, Cole-Cole plot and Eyring rate plots for some of the compounds. Table 3.2 lists the results from Fuoss-Kirkwood analysis. Eyring analysis results are summarized in Table 3.3.

DISCUSSION

Neopentane

Previous studies of neopentane by n.m.r. techniques (13) have yielded an activation enthalpy of about 5 kJ mol^{-1} for molecular rotation. The present low temperature dielectric absorption studies yield an activation enthalpy of $8.3 \pm 0.6 \text{ kJ mol}^{-1}$ and an activation entropy of $-48 \pm 7 \text{ J K}^{-1} \text{ mol}^{-1}$ which may be attributed to a molecular relaxation process in comparison with the corresponding parameters of 5.1 kJ mol^{-1} and $-95 \text{ J K}^{-1} \text{ mol}^{-1}$ for a polar molecule of fairly similar shape, methyl bromide (see Chapter IV). Both neopentane and methyl bromide show dielectric relaxation

in the same temperature range (82 - 104 K). The Cole-Cole plot (Figure 3.2), a circular arc, indicates a wide range of relaxation behaviour.

Carbon tetrachloride

Figures 3.4 and 3.6 show two sets of absorption curves for carbon tetrachloride in the temperature range 111 to 127 K and 170 to 199 K. The low temperature process yields an activation enthalpy of $26.3 \pm 1.3 \text{ kJ mol}^{-1}$ and an activation entropy of $42 \pm 11 \text{ J K}^{-1} \text{ mol}^{-1}$. N.m.r. studies (13) of a molecule of fairly similar shape, e.g. 1,1,1-trichloroethane, has yielded an energy barrier of $\sim 20 \text{ kJ mol}^{-1}$ for molecular tumbling. Dielectric study of tert-nitrobutane, a polar molecule of fairly similar shape to carbon tetrachloride, also shows molecular rotation almost in the same temperature range (101 to 136 K) (see Chapter IV) with an activation enthalpy of 21 kJ mol^{-1} and an activation entropy of $10 \text{ J K}^{-1} \text{ mol}^{-1}$. The β -value of unity and the symmetry of the loss curves (Figure 3.4) suggests Debye behaviour.

The high temperature process which yields an

Eyring enthalpy of activation $36.5 \pm 2 \text{ kJ mol}^{-1}$ and entropy of activation $16 \pm 11 \text{ J K}^{-1} \text{ mol}^{-1}$ may be attributed to either co-operative motion as indicated by the nature of the Eyring plot (Fig. 3.7) or molecular rotation in different solid phase.

Tetramethylsilane

The activation enthalpy of $23.7 \pm 0.8 \text{ kJ mol}^{-1}$ for tetramethylsilane obtained for a high temperature absorption from the present dielectric study agrees well with a study by n.m.r. spectroscopy (14) which has yielded a value of $30.2 \pm 1.8 \text{ kJ mol}^{-1}$ for molecular rotation. The energy barrier value also agrees well with that for other spherical shaped molecules mentioned above. The high β -values of 0.4-1 suggests predominantly Debye behaviour.

A low temperature dielectric absorption is observed (see Table 3.2) with an activation enthalpy of $81 \pm 17 \text{ kJ mol}^{-1}$ and an activation entropy of $587 \pm 158 \text{ J K}^{-1} \text{ mol}^{-1}$ and may be attributed to a co-operative relaxation process in comparison with the corresponding parameters 96 kJ mol^{-1} and $700 \text{ J K}^{-1} \text{ mol}^{-1}$ for isobutyl

bromide (15) and 81 kJ mol^{-1} and $484 \text{ J K}^{-1} \text{ mol}^{-1}$ for methyltrichlorosilane (see Chapter IV). The $\log \tau T$ versus T^{-1} plot (Figure 3.11) shows non-Arrhenius behaviour.

Silicon tetrachloride

A dielectric relaxation process has been indicated around 110 K, but the approach of melting point rendered the compound difficult to study, and therefore, a complete study of the process could not be made (see Table 3.2).

Tetramethylgermanium

A dielectric relaxation process seems to be present near the liquid nitrogen temperature. At 81 K the free energy of activation, ΔG_E , was found to be 12.8 kJ mol^{-1} .

The high temperature process, which was observed near 107 K, could not be studied through the whole range of frequency again due to the influence presumably arising from the melting effect of the compound. Measurements were

made only in three temperatures which yielded an enthalpy of activation 43.3 kJ mol^{-1} . N.m.r. study (14) yielded an energy barrier of $41 \pm 10 \text{ kJ mol}^{-1}$ for molecular rotation.

From the above discussion, it is evident that a dielectric study of five nonpolar molecules show molecular rotation, the energy barrier values of which agree well with those found from other measurements. This agreement with results suggests by other methods that the observed absorption is not due to impurities. Moreover, the present results, being of smaller loss (except neopentane) are less likely to be influenced by impurities.

The n.m.r. method can study the molecular rotation of these molecules in the solid state and does not depend on the molecule having a permanent electric dipole moment. But the dielectric method depends on the molecule having either a permanent or an induced dipole moment.

The compounds under study are nonpolar in the liquid or gaseous states, that is, they do not have a

permanent dipole moment. Presuming this to be true in the solid state under the experimental conditions, dielectric absorption cannot be expected. The fact that these compounds show definite dielectric absorption, must have been the result of some kind of dipole moment, probably of the induced type.

Induced Moments

The interaction of a nonpolar molecule with an electric field results in a charge separation of the negative symmetrical electronic cloud and the positive localized atomic centre of symmetry, and thus an "induced dipole moment" is produced. This induced electric moment m is proportional to the electric field strength F so that:

$$m = \alpha . F$$

where α , called polarizability, is a measure of the extent to which the symmetrical charge distribution of a molecule is distorted by interaction with the external electric field.

When the intermolecular distance is of the same

order as the molecular dimension, as the approximate case in liquids and solids, the molecule cannot be treated as point charge and so dipole moment induced by this mechanism in our present study seems unlikely.

With molecular radius a , the polarizability α is given by:

$$\alpha = \frac{n^2 - 1}{n^2 + 2} \cdot a^3$$

where n is an "internal refractive index". For a non-polar liquid, $n^2 = \epsilon_0$, static dielectric constant and, for a polar liquid, n^2 is equal to the dielectric constant ϵ_∞ measured at frequencies so high that the permanent dipoles are unable to contribute.

A molecule may have zero total charge but still have a dipole moment if its equal and opposite charges are centred at different places.

Let us consider a system of point charges e_i at distances $r_i (x_i, y_i, z_i)$ from an origin of 0, chosen

somewhere in between the charges. We need to calculate the potential due to this system at a point P (at a distance r from O), with co-ordinates x, y, z (Figure 3.12). Assuming $r > r_i$ for all values of i , we can calculate the potential outside a sphere containing all the charges. Let the distance of a charge e_i

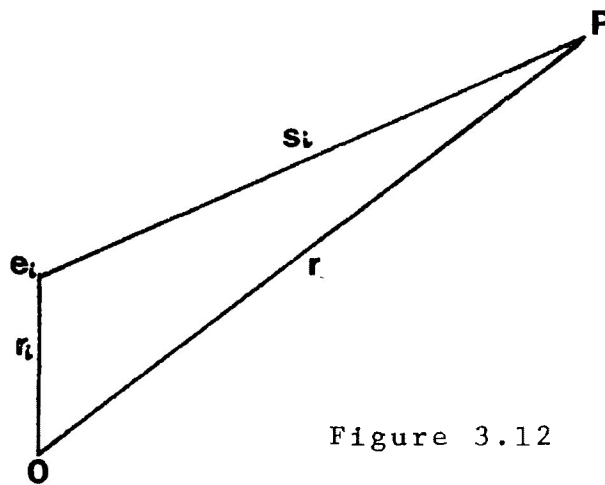


Figure 3.12

to P be s_i . The potential at P due to this system of charges is then given by:

$$V = \sum_i \frac{e_i}{s_i} \quad \dots (3.1)$$

From mathematical treatment involving Taylor's series:

$$\frac{1}{S_i} = \frac{1}{r} + x_i \frac{\delta}{\delta x} \left(\frac{1}{r}\right) + y_i \frac{\delta}{\delta y} \left(\frac{1}{r}\right) + z_i \frac{\delta}{\delta z} \left(\frac{1}{r}\right) +$$

$$\frac{1}{2} \left[x_i^2 \frac{\delta^2}{\delta x^2} \left(\frac{1}{r}\right) + 2x_i y_i \frac{\delta^2}{\delta x \delta y} \left(\frac{1}{r}\right) + \dots \right] + \dots$$

Thus we have:

$$V = \sum_i \frac{e_i}{r} - \sum_i \left[e_i x_i \frac{\delta}{\delta x} \left(\frac{1}{r}\right) + e_i y_i \frac{\delta}{\delta y} \left(\frac{1}{r}\right) + e_i z_i \frac{\delta}{\delta z} \left(\frac{1}{r}\right) \right]$$

$$+ \frac{1}{2} \sum_i \left[e_i x_i^2 \frac{\delta^2}{\delta x^2} \left(\frac{1}{r}\right) + 2e_i x_i y_i \frac{\delta^2}{\delta x \delta y} \left(\frac{1}{r}\right) + \dots \right] - \dots (3.2)$$

The first term of this series is the potential that would be caused at P by a charge $e = \sum_i e_i$, placed at the origin.

The electric moment m of the system is given

by

$$m = \sum_i e_i r_i$$

so we can write the second term of the series in (3.2) as

$$-m \cdot \text{grad} \frac{1}{r}$$

Similarly we can describe the third and subsequent terms of (3.2) by introducing the concepts quadrupole, octupole and multiples of higher order.

Analogously to the definition of the vectorial dipole moment m the quadrupole moment q is defined as a tensor:

$$q = \frac{1}{2!} \sum_i e_i r_i r_i$$

In the same way, the octupole moment u is defined as a tensor of the third degree:

$$u = \frac{1}{3!} \sum_i e_i r_i r_i r_i$$

Similarly the hexadecapole moment and higher multiple moments are defined as tensors of the fourth degree, of the fifth degree, etc. Using these multiple moments, Equation (3.2) can be written as:

$$v = e \cdot \frac{1}{r} - m \cdot \nabla \frac{1}{r} + q : \nabla \nabla \frac{1}{r} - u : \nabla \nabla \nabla \frac{1}{r} + \dots$$

...(3.3)

The electric quadrupole is obtained from a dipole in the same way as the dipole is obtained from a single charge: to construct the quadrupole from a dipole, let us imagine a second dipole, parallel to the original one, that is obtained by displacing the latter over a certain distance in a direction arbitrary to that of the dipole vector. Then we interchange the charges of the original dipole.

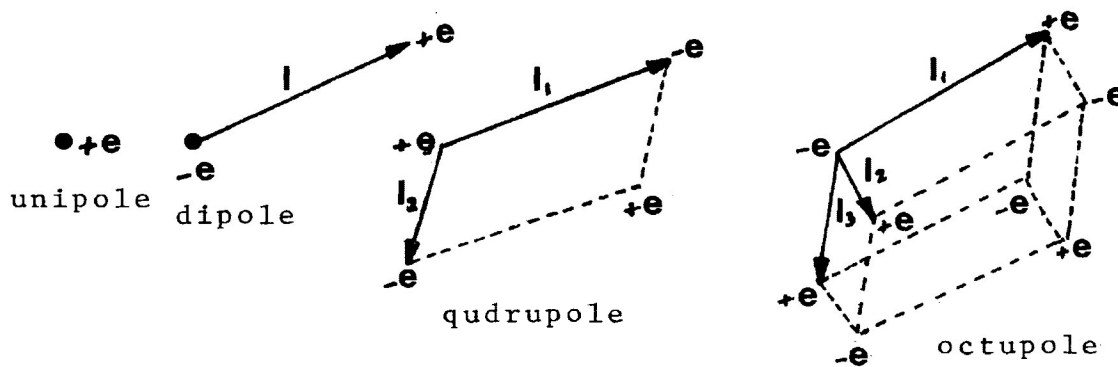


Figure 3.13: Multipoles

The combination of two anti-parallel dipoles thus obtained is a quadrupole (Figure 3.13). The higher multipoles are similarly defined, e.g. an octupole is obtained by dis-

placing a quadrupole over a certain distance in an arbitrary direction and changing the sign of all the charges of the original quadrupole (Figure 3.13).

It is seen from Equation (3.2) that:

(a) the electric potential falls off by $\frac{1}{r}$ due to the total charge,

(b) that due to a dipole moment falls off by $\frac{1}{r^2}$,

(c) that due to a quadrupole moment falls off by $\frac{1}{r^3}$,

(d) that due to an octupole moment falls off by $\frac{1}{r^7}$,

so that at large distances from the distribution the higher moments have negligible effects. However, for liquids and solids the intramolecular distances are not large compared with the molecular dimensions, so a quite strong electromagnetic interaction may arise as a result of the presence of the higher moments.

For most nonpolar molecules the quadrupole term dominates the potential development as given in Equation (3.2). Considering the axial quadrupole to be built up from two dipoles, these quadrupole strengths correspond to dipole strengths of 0.5-5 D and mutual distances of the order of 2 \AA (16).

For molecules such as CH_4 and CCl_4 , the quadrupole moment vanishes after reduction. For these molecules, the potential is dominated by the octupole term.

Constantino and Daniels (17) measured the dielectric constant of solid methane and observed that the molar polarization increases with the decrease of temperature. This was explained by the presence of octupole induced dipoles. These authors also found a dipole moment up to 0.05 D from octupole induced dipoles.

It would seem that the dielectric absorption with the low ΔH_E value observed for the five nonpolar substances may be accounted for in terms of molecular rotation where the dielectric absorption has been detected by interaction of the radiofrequency radiation with an induced moment which results from multipole interaction.

It would have been highly desirable to evaluate the effective dipole moment associated with the dielectric absorption in the non-polar molecules. Unfortunately, this was not feasible as we have no apparatus to determine densities at the low temperature of the absorption. Further, the error in the dispersion is sufficient to make the derived moments too much in error to be of much use.

REFERENCES:

1. D.H. Whiffen, Trans. Faraday Soc., 46(1950)124.
2. W.M. Heston, Jr., and C.P. Smyth, J. Am. Chem. Soc., 72(1950)99.
3. I.R. Dagg and G.E. Reesor, Can. J. Phys., 43(1965)1552.
4. A.A. Maryott and G. Birnbaum, J. Chem. Phys., 39(1961)189.
5. H.S. Gabelnick and H.L. Strauss, J. Chem. Phys., 46(1967)396.
6. E.N. DiCarlo and C.P. Smyth, J. Am. Chem. Soc., 84(1962)1128.
7. J. Crossley and S. Walker, Can. J. Chem., 46(1968)847.
8. S.K. Garg, J.E. Berties, H. Kilp and C.P. Smyth, J. Chem. Phys., 49(1968)2551.
9. N.A. Hermiz, J.B. Hasted and C. Rosenberg, J. Chem. Soc., Faraday Trans. II, 78(1982)147.
10. G.P. Johari and M. Goldstein, J. Chem. Phys., 53(1970)2372.
11. M.A. Kashem, Private Communication, this laboratory.
12. G.P. Johari and M. Goldstein, J. Chem. Phys., 55(1971)4245.
13. E.O. Stejskal, D.E. Woessner, T.C. Farrar and H.S. Gutowsky, J. Chem. Phys., 31(1959)55.
14. G.W. Smith, J. Chem. Phys., 42(1965)4229.
15. W.O. Baker and C.P. Smyth, J. Chem. Phys., 7(1939)574.
16. C.J.F. Bottcher, "Theory of Electric Polarization", 2nd Edition, Vol. 1, Elsevier Scientific Publishing Company, Amsterdam, 1973.
17. M.S. Constantino and W.B. Daniels, J. Chem. Phys., 62(1975)764.

TABLE 3.2: Fuoss-Kirkwood Analysis Parameters for Some Non-polar Spherical Molecules at Various Temperatures

T(K)	$10^6 \tau$ (s)	$\log f_{\max}$	β	$10^3 \epsilon''_{\max}$
<u>Neopentane</u>				
81.5	45.66	3.542	0.39	4.59
83.3	29.47	3.733	0.38	4.55
85.3	23.80	3.825	0.40	4.40
87.3	17.79	3.952	0.42	4.21
89.1	13.36	4.076	0.43	4.08
90.3	11.72	4.133	0.44	3.98
92.6	9.42	4.228	0.45	3.76
94.6	6.48	4.390	0.44	3.55
<u>Carbon tetrachloride</u> <u>Lower Temperature Process</u>				
110.8	6440.5	1.393	1	0.031
113.1	4214.1	1.577	1	0.031
115.9	1843.7	1.936	1	0.031
118.7	1039.8	2.185	1	0.031
120.7	571.5	2.445	1	0.030
124.0	313.0	2.706	1	0.030
126.5	170.2	2.971	1	0.027
<u>Carbon tetrachloride</u> <u>Higher Temperature Process</u>				
169.9	8597.1	1.268	0.44	0.041
173.2	4074.0	1.592	0.72	0.049
176.3	2302.3	1.840	0.72	0.049
179.2	1743.0	1.961	0.56	0.040
181.9	1087.7	2.165	0.59	0.041
184.8	684.2	2.367	0.57	0.041
187.7	490.1	2.512	0.62	0.042
190.6	368.0	2.636	0.64	0.043
194.0	233.0	2.835	0.64	0.041
196.7	185.9	2.933	0.71	0.040
198.7	166.4	2.981	0.72	0.039

TABLE 3.2: Fuoss-Kirkwood Analysis Parameters for Some Non-polar Spherical Molecules at Various Temperatures

T(K)	$10^6 \tau$ (s)	$\log f_{\max}$	β	$10^3 \epsilon''_{\max}$
<u>Tetramethylsilane</u>				
<u>Lower Temperature Process</u>				
104.3	5078.2	1.496	0.40	0.086
105.1	896.2	2.249	0.46	0.088
105.6	441.1	2.557	0.59	0.085
106.2	276.6	2.760	0.60	0.087
106.8	206.8	2.886	0.84	0.092
107.6	91.0	3.243	0.87	0.072
108.2	57.4	3.443	0.92	0.053
108.8	48.9	3.513	0.95	0.040
<u>Tetramethylsilane</u>				
<u>Higher Temperature Process</u>				
129.8	8149.6	1.291	0.92	0.091
131.9	5145.5	1.490	0.91	0.096
134.2	3975.7	1.602	0.96	0.093
136.0	2643.0	1.780	0.89	0.090
138.1	2180.3	1.863	0.88	0.085
140.4	1408.9	2.053	0.72	0.069
142.3	1066.5	2.174	0.74	0.068
144.3	764.9	2.318	0.70	0.063
146.5	573.7	2.443	0.65	0.058
148.5	442.0	2.557	0.70	0.058
<u>Tetramethylgermayium</u>				
107.3	8570.1	1.269	0.73	0.017
108.4	4890.7	1.512	0.72	0.016
110.1	2414	1.819	0.58	0.014
<u>Silicon tetrachloride</u>				
109.1	9953.2	1.204	0.59	0.069
111.0	4431.8	1.555	0.75	0.078
112.9	2348.7	1.831	0.67	0.072

TABLE 3.3:

RELAXATION TIMES AND EYRING ANALYSIS RESULTS FOR SOME NONPOLAR SPHERICAL MOLECULES

MOLECULE	T(K)	τ (s)		ΔG_E (kJ mol ⁻¹)		ΔH_E	ΔS_E
		100 K	200 K	100 K	200 K	(kJ mol ⁻¹)	(J K ⁻¹ mol ⁻¹)
Neopentane	82-95	3.6×10^{-6}		13.2		8.3 ± 0.6	-48 ± 7
Carbon tetra- chloride	111-127	1.7×10^{-1}		22.1		26.3 ± 1.3	42 ± 11
	170-199		1.2×10^{-4}		33.3	36.5 ± 2.1	
Tetramethyl- silane	104-110	1.2×10^{-1}		21.8		80.5 ± 17.0	587 ± 158
	130-149	7.2	2.3×10^{-6}	25.2	26.8	23.7 ± 0.8	-15 ± 6
Silicon tetrachloride	109-113	4.8×10^{-1}		23.0		38.0 ± 14.6	150 ± 132
Tetramethyl- germanium	107-110	3.1×10^{-1}		22.6		43.3 ± 30.8	207 ± 128

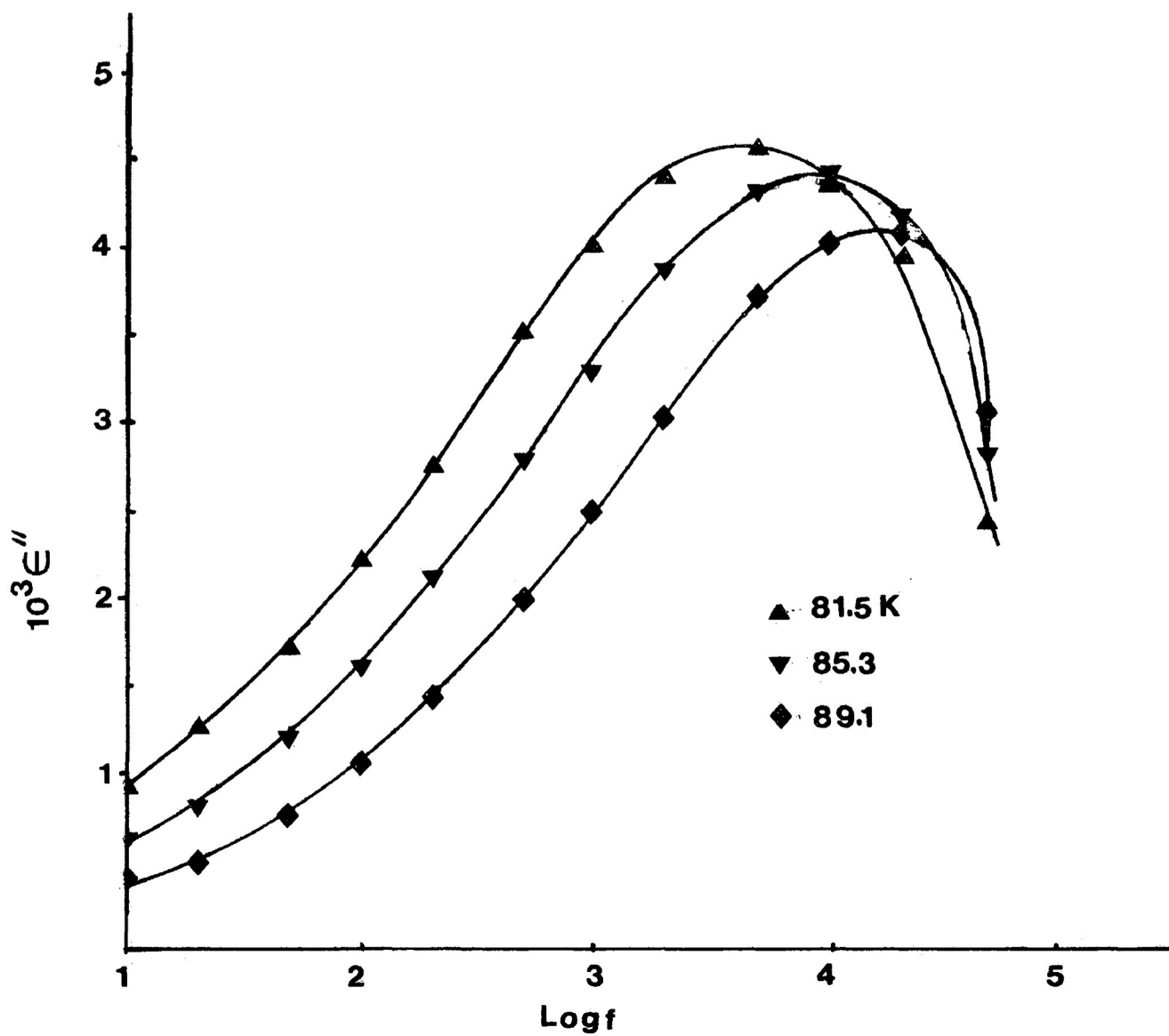


FIGURE 3.1: Dielectric loss factor ϵ'' versus log frequency for neopentane

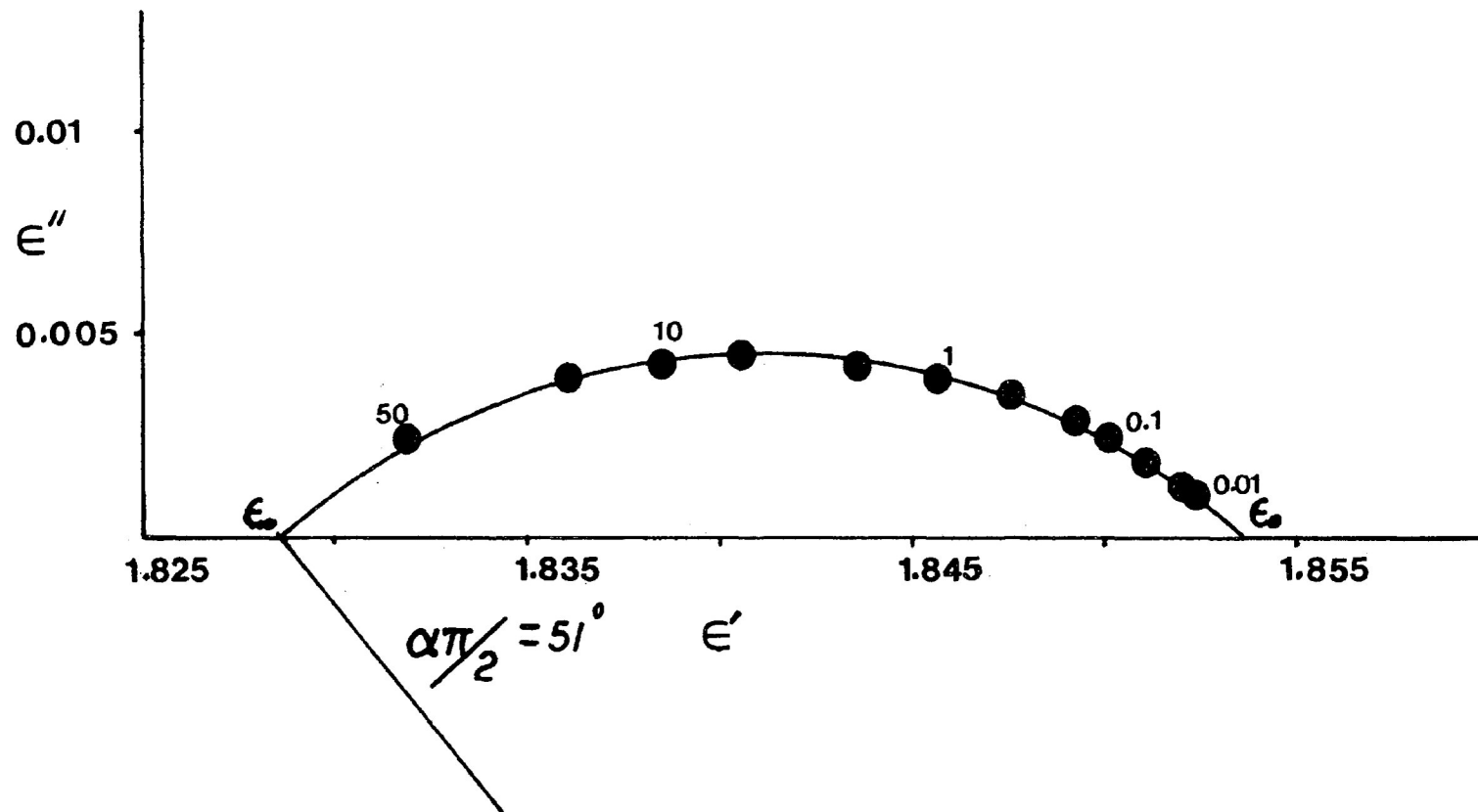


FIGURE 3.2: Cole-Cole Plot for Neopentane at 81.5 K
 Numbers beside points are frequencies in kHz

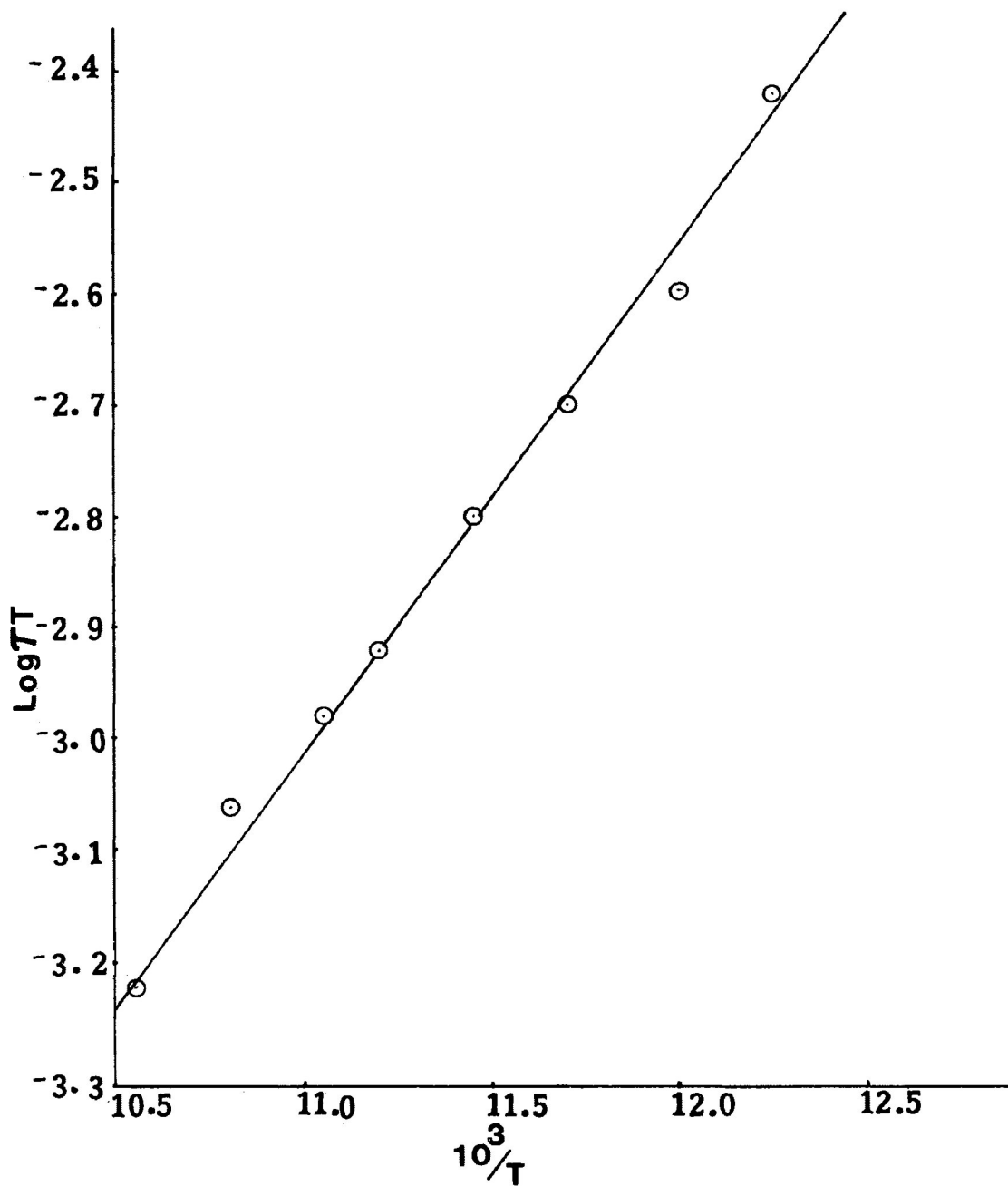


FIGURE 3.3: Eyring plot of $\log(\tau T)$ versus $\frac{1}{T}$ for neopentane

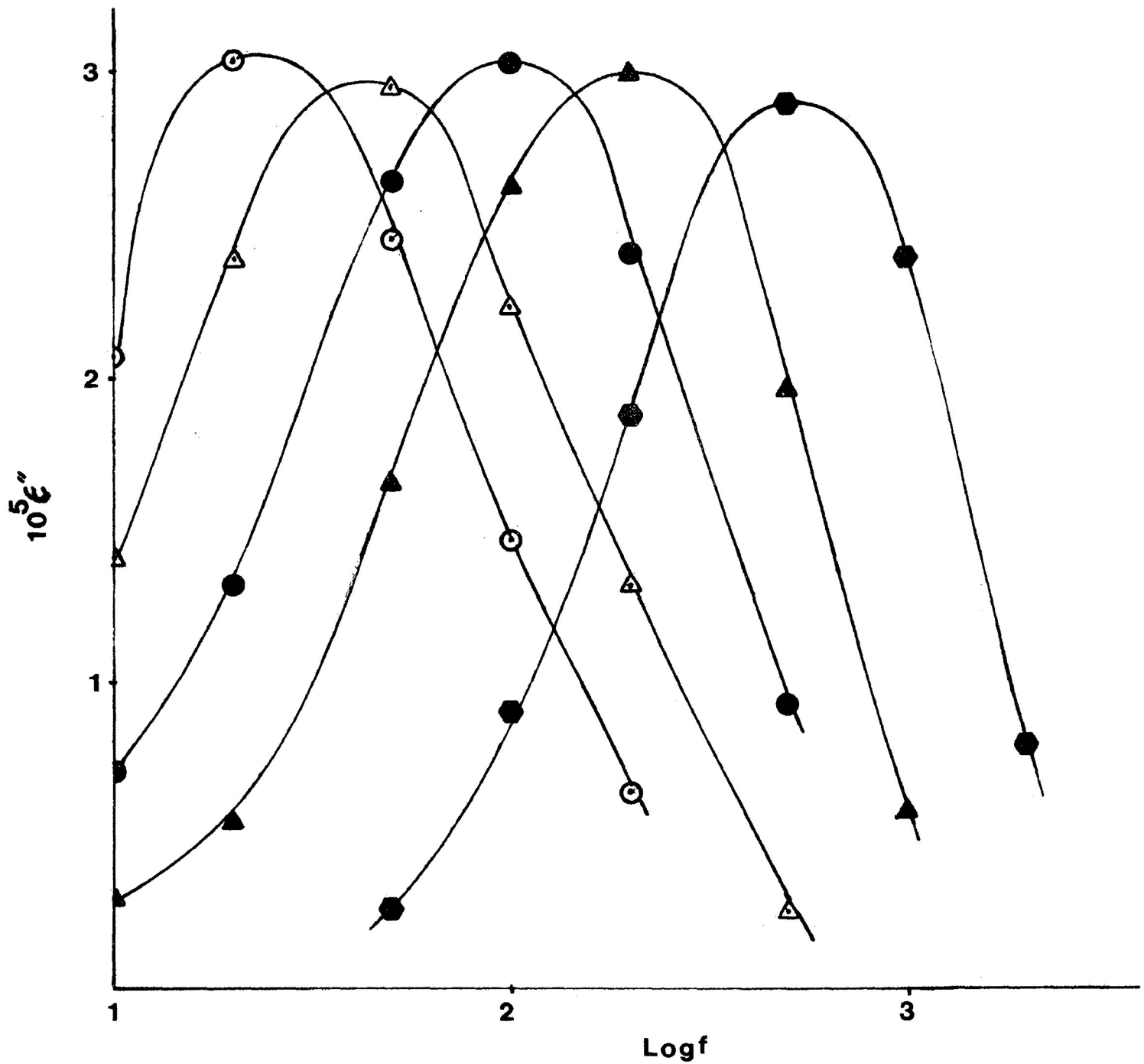


FIGURE 3.4: Dielectric loss factor ϵ'' versus log frequency for carbon tetrachloride

○, 110.8 K; △, 113.1 K; ●, 115.9 K;

▲, 118.7 K; ●, 124.0 K.

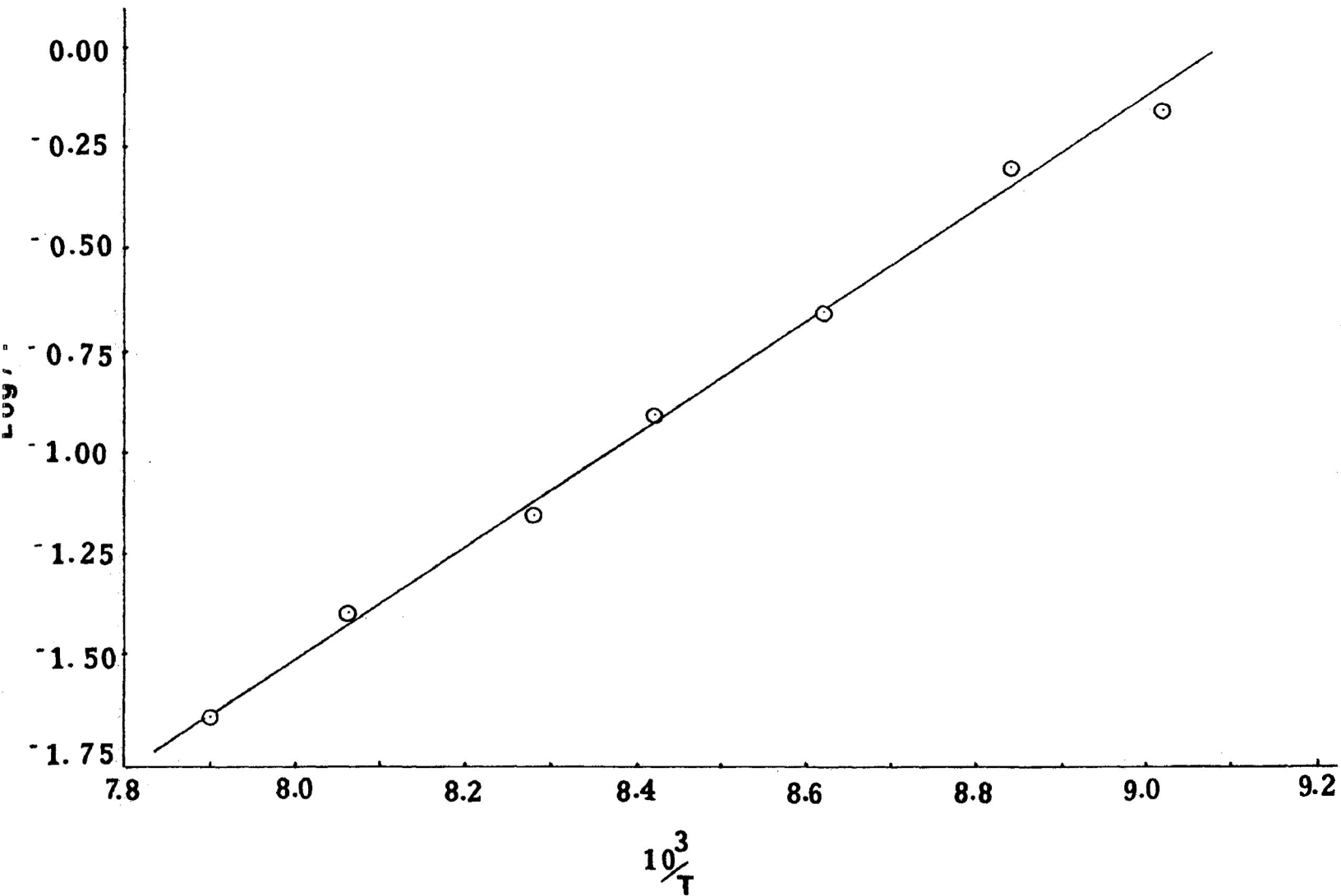


FIGURE 3.5: Eyring plot of $\log(\tau T)$ versus $\frac{1}{T}$ for carbon tetrachloride

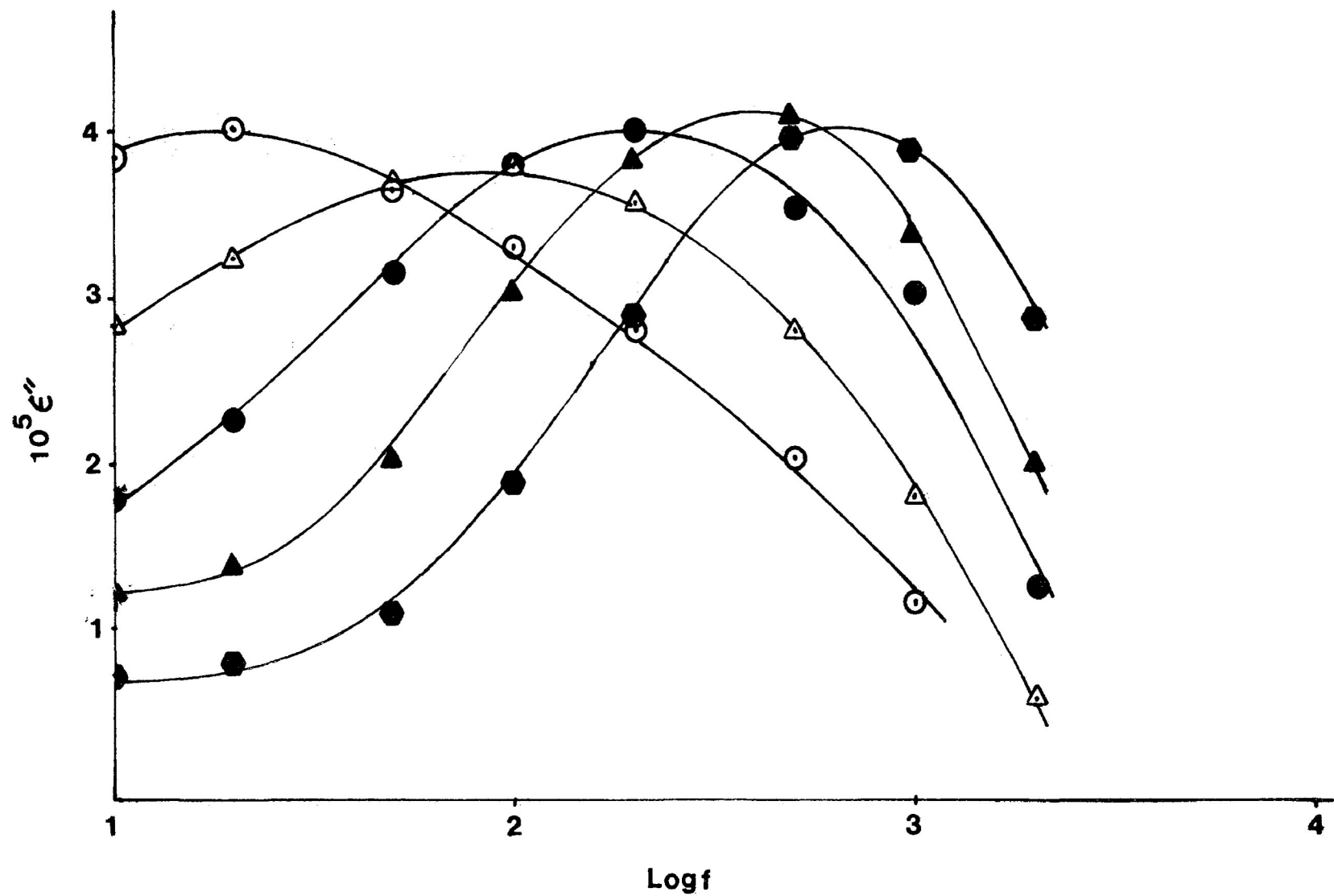


FIGURE 3.6: Dielectric loss factor ϵ'' versus log frequency for carbon tetrachloride

○, 169.9 K; △, 176.3 K; ●, 181.9 K; ▲, 187.7 K; ●, 194.0 K.

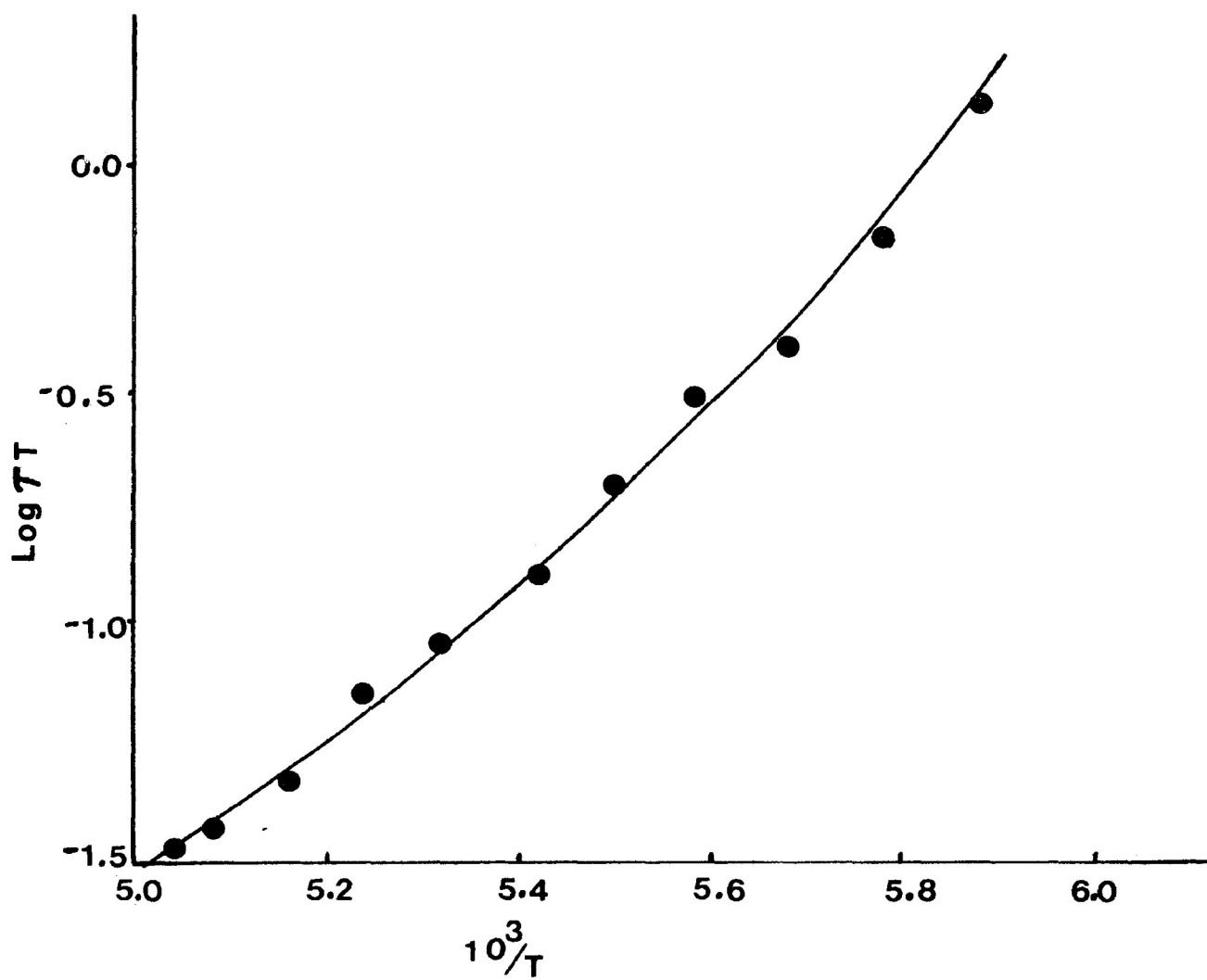


FIGURE 3.7: Eyring plot of $\log(\tau T)$ versus $\frac{1}{T}$ for carbon tetrachloride

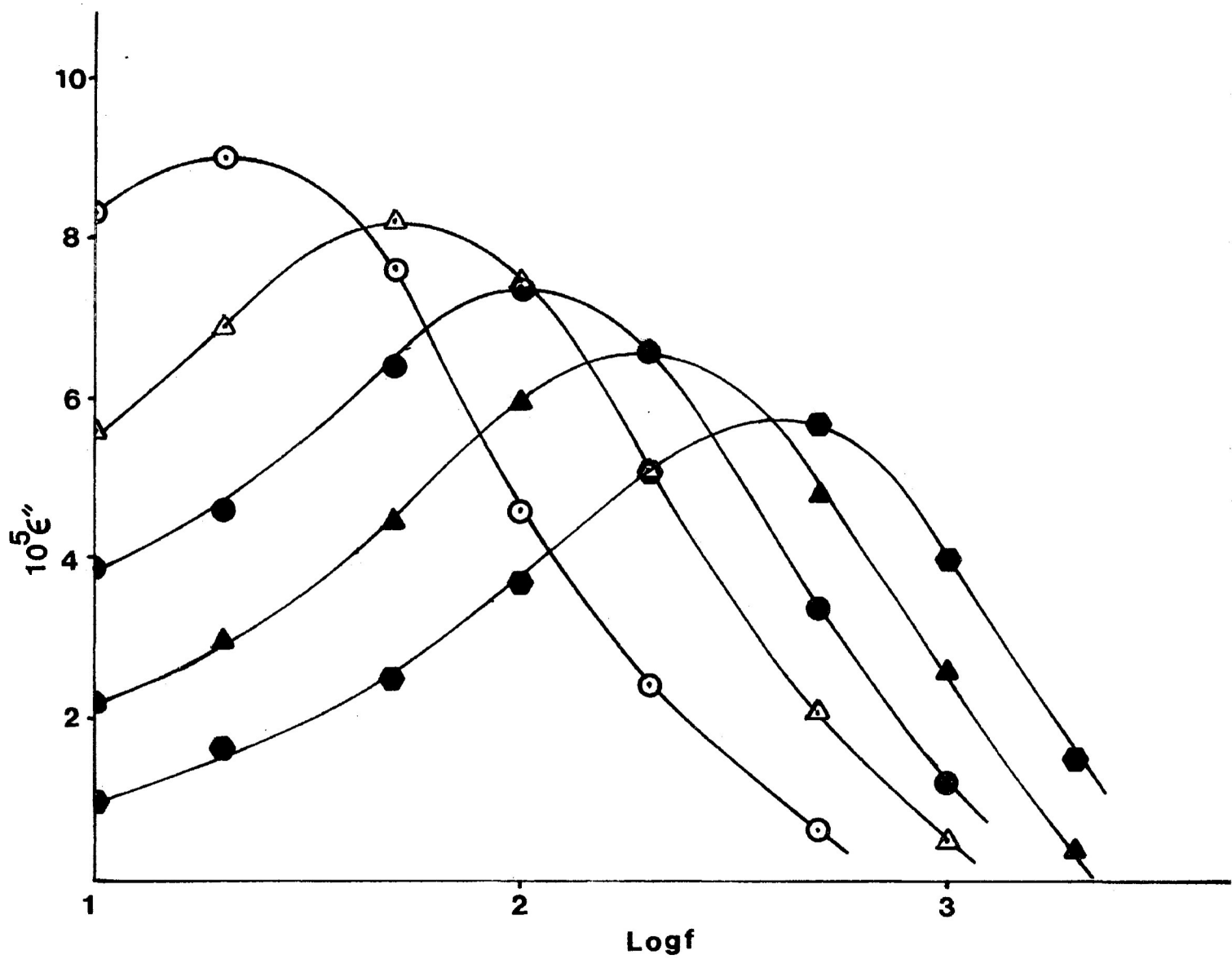


FIGURE 3.8: Dielectric loss factor ϵ'' versus log frequency for tetramethylsilane

○, 129.8 K; △, 134.2 K; ●, 138.1 K;

▲, 142.3 K; ◆, 148.5 K.

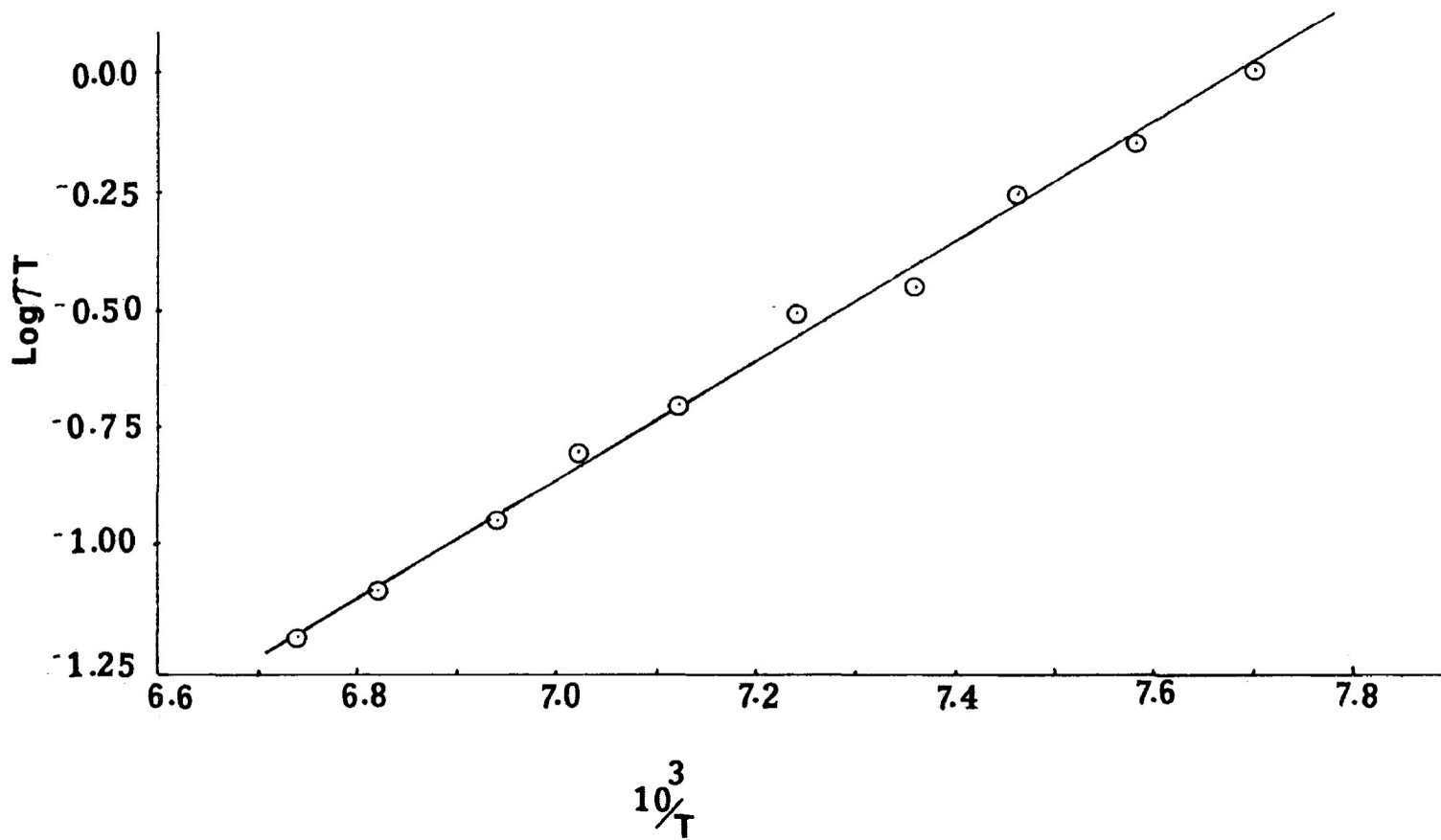


FIGURE 3.9: Eyring plot of $\log(\tau T)$ versus $\frac{1}{T}$ for tetramethylsilane

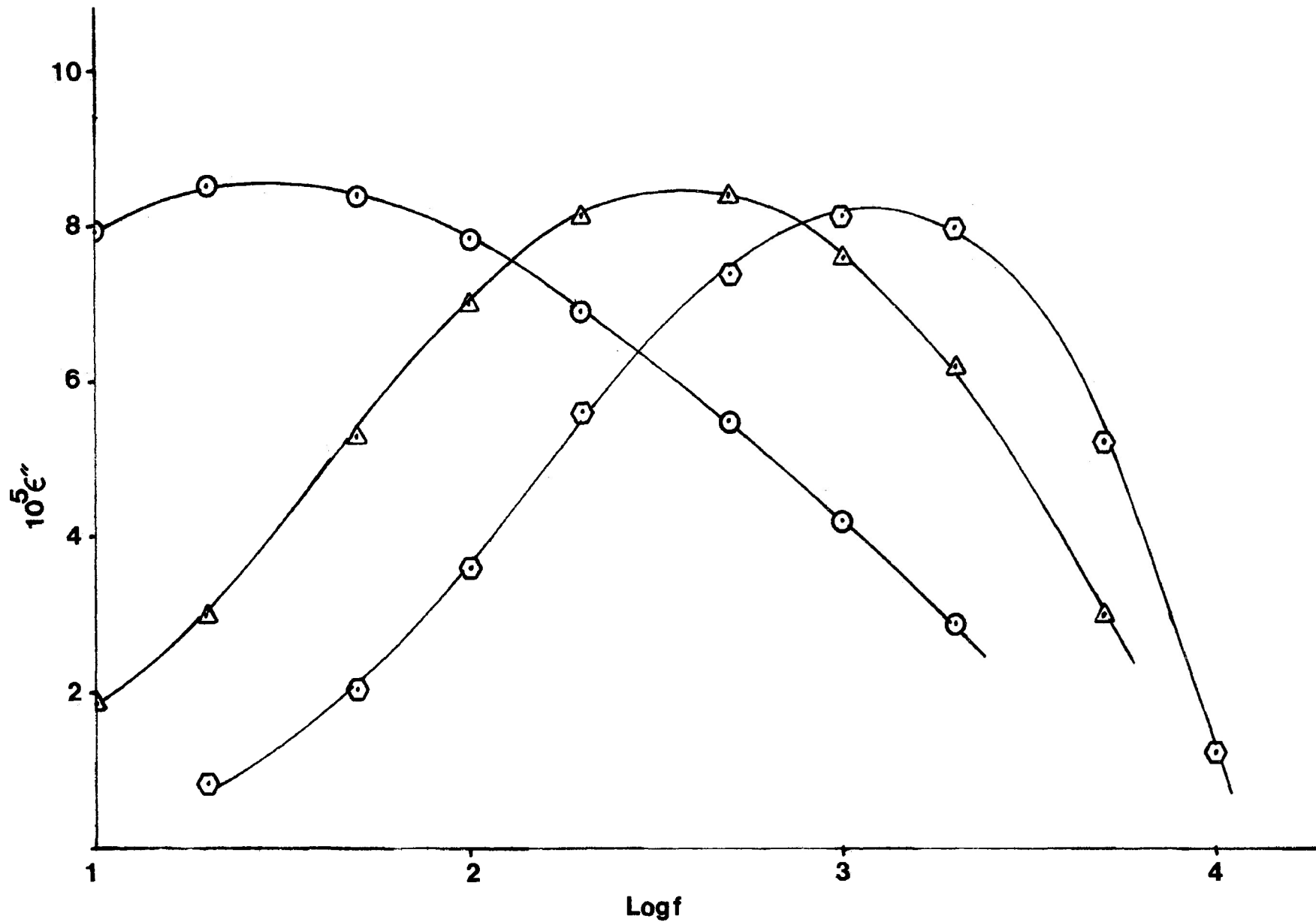


FIGURE 3.10: Dielectric loss factor ϵ'' versus log frequency for tetramethylsilane

○, 104.3 K; △, 105.6 K; ⊙, 106.8 K.

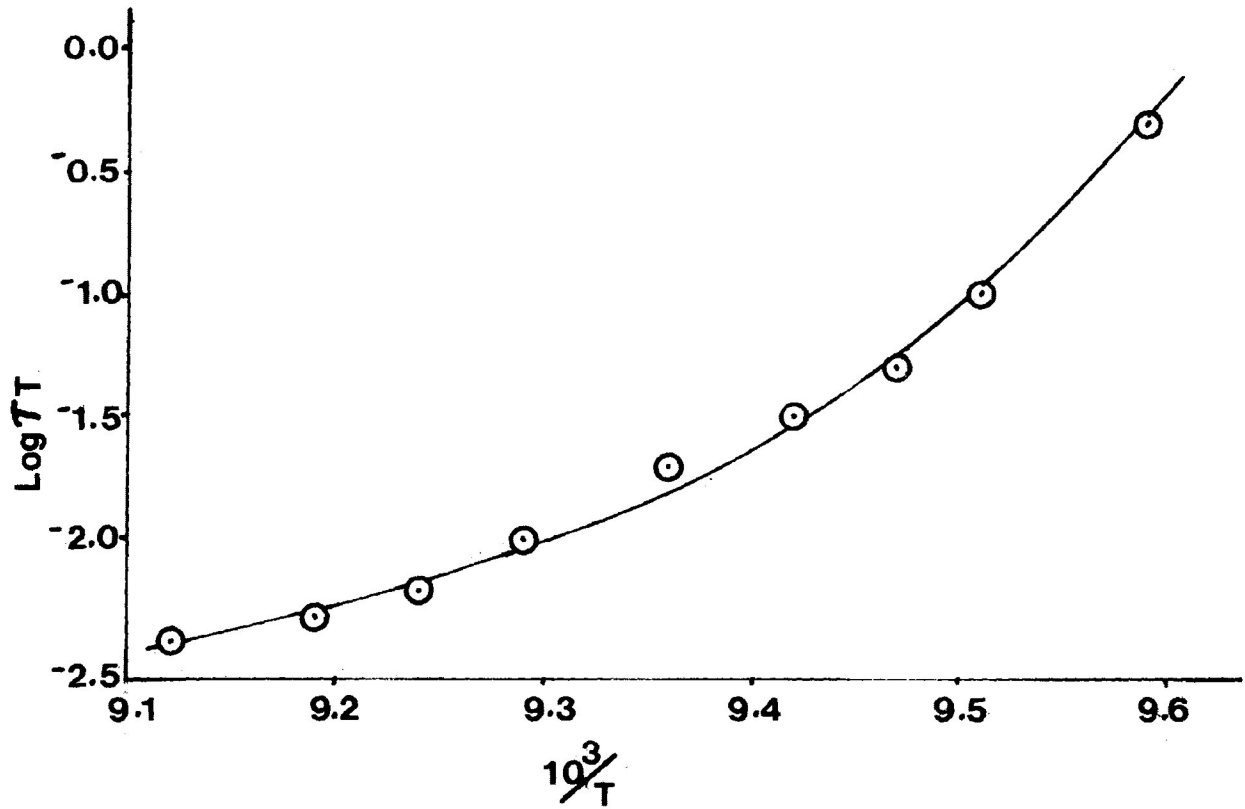


FIGURE 3.11: Eyring plot of $\log(\tau T)$ versus $\frac{1}{T}$ for tetramethylsilane.

CHAPTER IV

S O M E P O L A R F A I R L Y
S P H E R I C A L M O L E C U L E S

INTRODUCTION

Dielectric properties of a number of spherically shaped methane derivatives have been investigated in the solid state by Smyth and his coworkers (1) and by Clemett and Davies (2). The study of 2-chloro-2-methylpropane (t-butylchloride), 2,2-dichloropropane, 1,1,1-trichloroethane, 2-bromo-2-methylpropane (t-butylbromide), 2-chloro-2-nitropropane and 2,2-dinitropropane by Smyth and coworkers was based on dielectric constant and/or heat capacity measurements which were confined to a limited range of temperature (minimum 135 K). These molecules, due to their symmetrical shape, are found to possess rotational freedom in the solid state, as well as polymorphic transitions at temperatures below which such freedom is generally lost.

Dielectric measurements of 2,2-dichloropropane, 1,1,1-trichloroethane, 2-nitro-2-methylpropane, 2-chloro-2-nitropropane and 2-cyano-2-methylpropane have been made by Clemett and Davies (2) at frequencies up

to the GHz region and over a range of temperature in the liquid and rotator solid phases. These authors have shown, through the relaxation times and corresponding activation energies, that molecular rotation is generally as complete and as little hindered in the rotator phase as in the liquid.

Considerable interest has been shown on alkyl halides (3-8), the measurements of which were carried out at room temperature in the microwave region and at low temperatures in the audio-frequency region. Denney (3) has examined the dielectric relaxation of several supercooled, branched alkyl halides. He found that the frequency dependence of the complex dielectric constant ϵ^* was adequately described by the Davidson-Cole skewed-arc function. The appearance of this asymmetric distribution in the supercooled alkyl halides was originally surprising, for previously, similar behaviour had been encountered with only supercooled polyhydroxy compounds (9,10). More recent work (11) has revealed a similar dielectric behaviour and consequently it appears that the skewed-arc function is not specifically a characteristic of associated liquids.

EXPERIMENTAL RESULTS

The present study includes the investigation of:

<u>Number</u>	<u>Name</u>	<u>Molecular Formula</u>
1.	Methyl bromide	CH_3Br
2.	Methyl iodide	CH_3I
3.	2,2-Dichloropropane	$(\text{CH}_3)_2\text{-C-Cl}_2$
4.	1,1,1-Trichloroethane	$\text{CH}_3\text{-C-Cl}_3$
5.	Methyltrichlorosilane	$\text{CH}_3\text{-Si-Cl}_3$
6.	tert -Butylchloride	$(\text{CH}_3)_3\text{-C-Cl}$
7.	tert -Butylbromide	$(\text{CH}_3)_3\text{-C-Br}$
8.	2-Methyl-2-nitropropane	$(\text{CH}_3)_3\text{-C-NO}_2$

All of these chemicals are commercially

available and were dried (except methylbromide) over activated molecular sieve prior to use.

Methyl bromide is a gas at ordinary temperature. For the measurements of this compound, special precautions, as described in Chapter III for neopentane, were taken.

Experimental values of τ , $\log f_{\max}$, β , ϵ''_{\max} , ϵ_{∞} and μ at various temperatures obtained for these compounds are listed in Table 4.1.

Table 4.2 collects the values of ΔH_E , ΔS_E , along with ΔG_E and τ values at 100 K and 150 K for each system where appropriate.

DISCUSSIONMethyl bromide

A single dielectric absorption was found in methyl bromide near the liquid nitrogen temperature. This relaxation gives an enthalpy of activation, ΔH_E , $5.1 \pm 0.2 \text{ kJ mol}^{-1}$ and entropy of activation, ΔS_E , $-95 \pm 3 \text{ J K}^{-1} \text{ mol}^{-1}$. Dielectric (see Chapter III) and n.m.r. (12) studies of neopentane show ΔH_E values of 8 kJ mol^{-1} and 5 kJ mol^{-1} respectively, for molecular rotation. Since these molecules are quite similar in size, and also the temperature range is similar, it is reasonable to assign this lower temperature absorption of methylbromide to a molecular process. When the points of $\log \tau T$ versus $\frac{1}{T}$ were plotted as shown in Figure 4.3, they were on a straight line. This suggests that there is no overlap with other processes. The relaxation time (τ) and the free energy of activation at 100 K are $2.1 \times 10^{-5} \text{ s}$ and 14.6 kJ mol^{-1} . The τ and ΔG_E at 100 K for neopentane are $3.6 \times 10^{-6} \text{ s}$ and 13.2 kJ mol^{-1} respectively. The τ and ΔG_E values of methyl bromide correspond extremely well with this pattern which are typical of the molecular process. The β -range found for methyl

bromide is 0.31-0.47 which is also in the same range as that of neopentane (0.38-0.45). Since the molecule is not a large molecule, the volume swept out by this molecule is not large and thus the energy barrier for this molecular rotation is not great, which is expected. This phenomenon is confirmed by Cooke (13) that the barrier to rotation of a rigid molecule is influenced by the surrounding molecules in the vicinity of the rigid molecule concerned. Hence, the larger the molecule, the more resistance will be experienced by the molecule to reorientation.

It is to be noted that our result for this molecule is in contrast to the interpretation made by Morgan and Lowry (14), which was based on dielectric constant measurements, that below the transition point there was no molecular rotation.

Methyl iodide

Methyl iodide shows a dielectric absorption over a short range of temperature 104-109 K covering $\log f_m$ 2.45-4.06. The Eyring rate plot of $\log \tau T$ versus $\frac{1}{T}$ shows a reasonably straight line over the temperature and

frequency region which gives ΔH_E and ΔS_E values of $71 \pm 5 \text{ kJ mol}^{-1}$ and $509 \pm 46 \text{ J K}^{-1} \text{ mol}^{-1}$ respectively. The longer relaxation time ($\tau = 1 \times 10^{-2} \text{ s}$ at 100 K) and the corresponding higher energy barrier for this relaxation cannot be accounted for by molecular rotation (since the molecule is rigid, no question of intramolecular motion arises).

Baker and Smyth (15) studied *i*-butyl bromide and *i*-amyl bromide in the glassy states and found enthalpy of activation for these molecules 96 kJ mol^{-1} and 74 kJ mol^{-1} , respectively with the corresponding entropy of activation values $700 \text{ J K}^{-1} \text{ mol}^{-1}$ and $440 \text{ J K}^{-1} \text{ mol}^{-1}$. The authors suggested that the relaxation process involved a co-operative process similar to those observed for liquid glucose (16) and glycerol (17).

The characteristic features (18) of a co-operative process include (i) absorption at low frequency which means absorption at high temperature; (ii) rapid variation of f_{max} with temperature; (iii) broad asymmetric nature of the loss curves; (iv) a large apparent enthalpy of activation; (v) a large

apparent entropy of activation and (vi) a curved Eyring plot.

For the dielectric relaxation of methyl iodide, the absorption curves changed rapidly with slight variation of temperature and also the ΔH_E and ΔS_E values fit well into this pattern. But the nature of loss curves (Figure 4.4) differs significantly.

In relation to the distribution of relaxation times, Denney (3) observed an increase of β -values with the increase of temperature for the co-operative motion of some supercooled liquids, e.g. 1-chloro-2-methylpropane (-171°C : $\beta = 0.50$; -160°C $\beta = 0.60$) and 1-bromo-2-methylpropane (-152°C : $\beta = 0.57$; -144°C : $\beta = 0.61$). No such trend of β -values was observed in methyl iodide. The β -range (0.28-0.36) is more of the order of a typical molecular relaxation.

Davies and Edwards (19) suggested that the dipole component responsible for the co-operative absorption decreases markedly with increase of temperature. Chao (18) also observed similar trends for a number of compounds in polystyrene matrices. For the present study

of methyl iodide, no definite trend of dipole moment values was observed.

Co-operative relaxation is usually described by a Davidson-Cole skewed-arc function. Higasi et al (20) made dielectric studies of a number of molecules in supercooled o-terphenyl over the temperature range 283-303 K. Their dielectric data were represented by the asymmetric Davidson-Cole function. Copeland and Denney (11) observed dielectric absorption of n-propylbenzene as a supercooled liquid in the temperature range 138.3-149.4 K with an Eyring activation enthalpy of about 80 kJ mol^{-1} . This absorption was also adequately described by a Davidson-Cole skewed-arc function.

Where the Davidson-Cole function was applied, deviations were sometimes noted, e.g. for 1-chloro-2-methylpropane (3) and 1-bromo-2-methylbutane (7) at high frequency region and these deviations were suspected due to the internal rearrangements of neighbouring bonds.

In the case of methyl iodide no such deviation

at higher frequencies was observed but the overall pattern of Davidson-Cole plot is different (Figure 4.5). The plot can neither be accurately described by Davidson-Cole skewed-arc function nor by Cole-Cole function. Considering all the factors, it may, therefore, be thought that two relaxation processes, probably molecular and co-operative, were overlapped in this investigation region.

2,2-Dichloropropane

Figure 4.6 shows the absorption curves for 2,2-dichloropropane which clearly indicates the overlapping of two relaxation processes. The Eyring plot of these curves (first peaks) gives an enthalpy of activation $65 \pm 2 \text{ kJ mol}^{-1}$ and entropy of activation $507 \pm 20 \text{ J K}^{-1} \text{ mol}^{-1}$. This high ΔH_E and ΔS_E values cannot be accounted for these relaxations solely to be a molecular or intramolecular process. An n.m.r. study (12) of this molecule in the solid state indicates $E_a = 17.1 \text{ kJ mol}^{-1}$ for methyl group reorientation and $E_a \sim 12.5 \text{ kJ mol}^{-1}$ for molecular tumbling.

The high ΔH_E and ΔS_E values as well as the

rapid change of absorption maxima with slight variation of temperature suggests one of the relaxation processes to be a microBrowian co-operative motion. But the β -range (0.14 - 0.20), relaxation time ($\tau = 2 \times 10^{-5}$ s at 100 K) and the free energy of activation ($\Delta G_E = 14.6$ kJ mol⁻¹ at 100 K) all are in favour of molecular relaxation. Hence the molecular process associated with the co-operative motion may be overlapped in this investigation region.

Chao (18) examined the co-operative relaxation behaviour of a number of rigid molecules in polystyrene as well as in polyvinyltoluene. She observed inconsistent results in β , τ and ΔH_E for 4-bromobiphenyl in polyvinyltoluene and 4-phenylpyridine and 4-fluorobiphenyl in polystyrene, which were interpreted as the overlapping of molecular and co-operative processes.

1,1,1-Trichloroethane and Methyltrichlorosilane

Two absorption processes were found for 1,1,1-trichloroethane; one around 100 K and the other in the 115-123 K region. The lower temperature absorption gives a ΔH_E value of 16.6 ± 1.4 kJ mol⁻¹ and a ΔS_E value of -15 ± 14

$\text{J K}^{-1} \text{ mol}^{-1}$.

Previous n.m.r. measurements (12) of this molecule in the solid state show $E_a = 17.1 \text{ kJ mol}^{-1}$ for methyl group reorientation and $E_a \sim 18.8 \text{ kJ mol}^{-1}$ for molecular tumbling. The energy barrier of internal rotation of 1,1,1-trichloroethane has also been determined by neutron incoherent inelastic scattering method (NIIS) (21) and the V_3 value is $25.1 \pm 2.5 \text{ kJ mol}^{-1}$.

Since 1,1,1-trichloroethane is unsymmetrically substituted with three chlorine atoms at one carbon atom and three hydrogen atoms at the other carbon atom, there is no perpendicular dipole moment component and the only dipole moment is along the perpendicular axis. Thus, the intramolecular process along the C-C bond should not be detected by the dielectric relaxation method. Clearly, the low temperature absorption process detected for 1,1,1-trichloroethane is a molecular process. The β -values (0.3-0.4), which are also in the same range as that observed for molecular rotation in methyl bromide, also support this argument.

The high temperature relaxation process

observed over the temperature region 115-123 K in the frequency range $10^1 - 10^5$ Hz gives broad asymmetric loss curves (Figure 4.7) which change rapidly with slight variation of temperatures. The Eyring plot of $\log \tau T$ versus $\frac{1}{T}$ (Figure 4.9) for this relaxation shows non-Arrhenius behaviour (curve ~~is~~ convex toward the abscissa) which gives the apparent enthalpy of activation, $\Delta H_E = 81 \pm 6 \text{ kJ mol}^{-1}$ and entropy of activation, $\Delta S_E = 524 \pm 49 \text{ J K}^{-1} \text{ mol}^{-1}$. Dielectric relaxation data can be accurately represented by the Davidson-Cole skewed-arc function (Figure 4.8). The distribution parameter β -value increases whereas the apparent dipole moment, μ , decreases with the increase of temperature.

All of the characteristic features observed, such as the high temperature at which the process occurred, asymmetric loss curves which varied rapidly with temperature changes, apparent large activation energy, accurate representation of relaxation data by Davidson-Cole plot, non-Arrhenius behaviour of Eyring plot...etc., strongly indicates the evidence of co-operative process in 1,1,1-trichloroethane.

No low temperature (near liquid nitrogen)

dielectric absorption was found for methyltrichlorosilane. This molecule is similar in shape to that of 1,1,1-trichloroethane (both are almost spherical) but slightly bigger in size due to the central silicon atom. The dielectric absorption was observed for this molecule at slightly higher temperature region (120 - 131 K) in comparison to that observed in 1,1,1-trichloroethane for co-operative motion. The pattern of loss curves (Figure 4.10) for methyltrichlorosilane differ from those observed for 1,1,1-trichloroethane though the maxima changed rapidly with slight variation of temperature. The Eyring plot of $\log \tau T$ versus $\frac{1}{T}$ (Figure 4.12) shows a non-Arrhenius behaviour with an apparent enthalpy of activation $81 \pm 9 \text{ kJ mol}^{-1}$ and entropy of activation $484 \pm 74 \text{ J K}^{-1} \text{ mol}^{-1}$. These observations indicate that a co-operative motion might be involved in this relaxation.

Since methyltrichlorosilane is slightly larger in size than 1,1,1-trichloroethane, one would expect a higher energy barrier for the former molecule for absolute co-operative motion. This and inadequate representation of dielectric data by Davidson-Cole skewed-arc function (Figure 4.11) suggest that in

addition to co-operative motion another process might be present in this region of investigation. The trend of β -values (increases with the increase of temperature) and apparent dipole moment component (decreases with the increase of temperature) is in favour of co-operative motion, though the β -range (0.23-0.33) is of the order of a typical molecular process.

Considering all the factors, it is reasonable to assign this relaxation to be an overlapping of co-operative and molecular motion (since dielectric relaxation method cannot detect the intramolecular motion in this molecule, as mentioned above for 1,1,1-trichloroethane).

t-Butylchloride and t-Butylbromide

A dielectric relaxation process seems to be present in t-butylchloride near the liquid nitrogen temperature. At 80 K the free energy of activation was found to be 11.5 kJ mol^{-1} . The higher temperature process (144 - 159 K) gives a curved Eyring plot (Figure 4.15) with an apparent enthalpy of activation

$75 \pm 8 \text{ kJ mol}^{-1}$ and entropy of activation $331 \pm 53 \text{ J K}^{-1} \text{ mol}^{-1}$. This high energy barrier cannot be accounted for a molecular or an intramolecular relaxation. co-operative motion might be suspected from the observed characteristic features, such as (i) high temperature (i.e. low frequency), relaxation; (ii) rapid change of loss curves with slight variation of temperature (Figure 4.13), (iii) large apparent activation energy, (iv) non-Arrhenius behaviour of Eyring plot, and (v) increment of β -values and decrement of dipole moment with the increase of temperature. But absence of other characteristic features, such as (i) adequate representation of dielectric data by Davidson-Cole plot (Figure 4.14) and (ii) broad asymmetry nature of loss curves suggest that another process might be involved in association with the co-operative motion.

Two absorption processes (Figure 4.16) were found for t-butylbromide. One family of peaks in our frequency range 10^1 - 10^5 Hz lies in the temperature region of 79-95 K, and the other process was found in the range of 129-142 K. The dielectric absorption in the lower temperature range gives a ΔH_E value of $13.8 \pm 0.9 \text{ kJ mol}^{-1}$. Bromobenzene in polystyrene (22)

has a ΔH_E value of 16 kJ mol^{-1} for molecular rotation. Since these molecules are quite similar in size, it is reasonable to assign this lower temperature absorption of t-butylbromide to a molecular process. The $\tau_{100 \text{ K}}$ and $\Delta G_{E100 \text{ K}}$ for bromobenzene are $5.5 \times 10^{-4} \text{ s}$ and 17.3 kJ mol^{-1} , respectively, which are slightly bigger than those observed for t-butylbromide ($\tau = 4 \times 10^{-6} \text{ s}$ and $\Delta G_E = 13.2 \text{ kJ mol}^{-1}$). t-Butylbromide is a fairly spherical-shaped molecule; its rotation is much easier than bromobenzene. This is reflected in the low values of τ , ΔG_E and ΔH_E for t-butylbromide. The β -values are also in support of this argument. The high β -value (0.34-0.86), though observed for a molecular process for this molecule, would not seem unreasonable, since the shape of the molecule is spherical and the dielectric absorption of this molecule would tend to show Debye behaviour.

The β -values of t-butylbromide are of the same order as those observed by Davies and Swain (23) for the intramolecular ring inversion of cyclohexyl derivatives. These authors commented that "the increase in β would be expected for an intramolecular dipolar

motion as this would be appreciably less dependent upon the co-operative movement of the adjacent polystyrene units than is the whole molecular rotation". A wide range of local environments are generally encountered by the polar solutes dispersed in polymer matrices or in a supercooled liquid as is reflected in typically low β values. Since this parameter is a measure of the width of the absorption relative to the simplest Debye process for which β equals unity, the high β values obtained for t-butylbromide appears to indicate that the dielectric relaxation of this molecule in solid state occurs by a similar mechanism.

The lower temperature relaxation of t-butylchloride yields $\Delta G_{E80\text{ K}} = 11.5 \text{ kJ mol}^{-1}$ which is slightly lower than that observed for t-butylbromide ($\Delta G_E = 13.2 \text{ kJ mol}^{-1}$) at 100 K. t-Butylchloride is more spherical than t-butylbromide and so the rotation of the former molecule will be less hindered. Moreover, the measured ΔG_E value of t-butylchloride is at lower temperature (80 K). Since the lower temperature absorption of t-butylbromide may be attributed to a molecular relaxation, it seems reasonable to assign the lower temperature relaxation of t-butylchloride to a molecular process.

The high temperature relaxation of t-butylbromide yields an enthalpy of activation $85 \pm 3 \text{ kJ mol}^{-1}$ and entropy of activation $460 \pm 25 \text{ J K}^{-1} \text{ mol}^{-1}$ which may be attributed to a co-operative relaxation process in comparison to the corresponding parameters of 80 kJ mol^{-1} and $411 \text{ J K}^{-1} \text{ mol}^{-1}$ for n-propylbenzene, a supercooled liquid, in the temperature region 138 - 149 K (11). This view is also supported by other observed characteristic features, such as (i) high temperature relaxation and (ii) rapid change of loss curves by slight variation of temperature (Figure 4.17). In this case, deviation was also observed in representation of dielectric data by Davidson-Cole skewed-arc function (Figure 4.18) particularly at high frequencies.

As mentioned earlier, deviation from representation of dielectric data by Davidson-Cole equation was observed for 1-chloro-2-methylpropane (3) and 1-bromo-2-methylbutane (7) at high frequencies and this was presumably due to 'internal rearrangements of neighbouring bonds'.

Since low temperature absorptions for t-butylchloride and t-butylbromide were assigned.

to molecular relaxation, the observed relaxation behaviour at high temperature region for these molecules may be explained by the fact that intramolecular process (methyl group reorientation) associated with the co-operative motion may be overlapped in this investigation region.

2-Methyl-2-nitropropane

In 2-methyl-2-nitropropane only one dielectric absorption measured from 101-136 K was found. It was characterized by a β -range of 0.24 - 0.42 and by an activation enthalpy of $\Delta H_E = 20.7 \text{ kJ mol}^{-1}$. This value of energy barrier is significantly greater than those for molecular relaxation of other similarly sized spherical molecules, the dielectric relaxation of which were found near liquid nitrogen temperature. Dielectric data can be accurately described by a Cole-Cole plot (Figure 4.19) which suggests that the observed relaxation might not be co-operative in nature. When the points of $\log T$ versus $\frac{1}{T}$ were plotted as shown in Figure 4.20, they were on a straight line. This suggests that there is no overlap with other processes.

Khwaja (24) studied some halobenzenes and some halotoluenes in polystyrene and he found that there was a slight increase in the enthalpy of activation from fluorobenzene ($\Delta H_E = 9 \text{ kJ mol}^{-1}$) to iodobenzene ($\Delta H_E = 16 \text{ kJ mol}^{-1}$). The situation is not the same when the halotoluenes are examined. The increase in energy barrier of the molecular relaxation process is quite significant from p-fluorotoluene ($\Delta H_E = 13 \text{ kJ mol}^{-1}$) to p-iodotoluene ($\Delta H_E = 42 \text{ kJ mol}^{-1}$). It can be seen that the higher the molecular energy barrier, the higher is the temperature range for molecular absorption to occur. It can be observed that p-iodotoluene has its molecular absorption process well above liquid nitrogen temperature while fluorobenzene, having the lowest energy barrier of all the halobenzenes and halotoluenes has a lowest temperature range near liquid nitrogen temperature.

Considering the above observations, it is not unreasonable to assign the relaxation behaviour of 2-methyl-2-nitropropane, which occurred well above the liquid nitrogen temperature, to a molecular process.

From the above discussions, it is seen that all the molecules under present study show molecular rotation. Clemett and Davies (2) investigated 2,2-dichloropropane, 1,1,1-trichloroethane, 2-methyl-2-nitropropane and 2-chloro-2-nitropropane in the liquid state as well as at the freezing points of these molecules (solid rotator phases). They reported that the molecular rotation is a complete and as little hindered in the rotator phase as in the liquid state. We have examined the first three molecules well below the rotator phase and found molecular rotation which is not so much hindered as is evident from the values of relaxation times and the corresponding activation energies. Our results for these molecules and *t*-butylchloride and *t*-butylbromide are in contrast to the interpretation made by Smyth and his coworkers (1) that below transitions (e.g. 183 K for *t*-butylchloride) these molecules did not have freedom for molecular rotation.

The most interesting observation in the present study is that all of the halogen containing

compounds show microBrownian co-operative motion (higher temperature region of methyl bromide was not investigated), whereas the only single compound, 2-methyl-2-nitropropane, in which there is no halogen atom, no co-operative motion was detected. Co-operative motion is usually observed immediately above the glass transition temperature of supercooled liquids or amorphous polymers.

Many alkyl halides are known as supercooled liquids and co-operative relaxation behaviour of many of these have already been investigated (25). Since the present study of the halogen containing compounds show co-operative motion, these molecules might have glass-forming ability. But no glass transition temperature was found for these molecules. This may suggest that either our measuring device for glass transition temperatures is not sensitive enough to detect it or that the molecules might not be sufficiently supercooled. Inadequate representation of dielectric data by Davidson-Cole plot may also be the consequence of insufficient undercooling.

Clemett and Davies (2) examined four similarly

sized spherical molecules both in the liquid and in the solid rotator phases. Their results for dielectric relaxation parameters are shown in Table 4.3.

TABLE 4.3: Dielectric Relaxation Parameters for Spherically-shaped methane derivatives in liquid and solid states

	$\Delta H(\text{liq})$ in kJ mol^{-1}	$\Delta H(\text{solid})$	$\Delta S(\text{liq})$ in $\text{J K}^{-1} \text{mol}^{-1}$	$\Delta S(\text{solid})$
$(\text{CH}_3)_2\text{CCl}_2$	5.2	5.8	-12.5	-11.3
$\text{CCl}_3 \cdot \text{CH}_3$	4.7	4.6	-13.8	-15.5
$(\text{CH}_3)_2\text{CClNO}_2$	6.1	5.4	-15.0	-17.6
$(\text{CH}_3)_3\text{CNO}_2$	3.4	2.1	-20.1	-26.8

It is seen that the first three compounds containing chlorine atom(s) (5) have almost the same energy barrier in the liquid as well as in the solid rotator phases, whereas the last compound, 2-methyl-2-nitropropane, which does not have any halogen atom, has a ΔH value much lower than those three compounds. In the solid rotator phase the difference is significant. Since all these molecules are fairly spherical, one would expect a similar energy barrier for molecular process. But

the observed experimental facts suggest that the mechanism involved in the first three molecules might differ from that involved in the last molecule.

Johari and Goldstein (26) studied the dielectric microBrownian relaxation with the activation energy in the range 230 to 293 kJ mol^{-1} in a large number of supercooled systems involving molecules small in size. An apparent activation energy near 260 kJ mol^{-1} was found for some small molecules in the supercooled, o-terphenyl (27). The activation energy of around 300 kJ mol^{-1} was observed for the co-operative process of di-n-butylphthalate in polystyrene (28) which is close to that commonly found for the glass-transition process in amorphous polymers and for polystyrene in particular (29). But an activation energy of 98 kJ mol^{-1} was found for co-operative motion of pure di-n-butylphthalate (30). Similar magnitude of energy barriers have also been observed for other low viscous supercooled liquids (11,15,31). The co-operative relaxation of a molecule when dispersed in either a viscous super-cooled liquid (e.g. o-terphenyl) or in an amorphous polymer (e.g. polystyrene) primarily depends upon the viscous solvent molecules and little

on the solute. Since the solvent molecules are highly viscous, co-operative motions of these molecules yield a higher energy barrier as is evident from the above mentioned results. In this light, the observed activation energy for the co-operative movement of the low viscous molecules under present study would seem reasonable.

REFERENCES

1. W.O. Baker and C.P. Smyth, J. Am. Chem. Soc., 61(1939)2798.
A. Turkevich and C.P. Smyth, *ibid.*, 62(1940)2468.
W.P. Conner and C.P. Smyth, *ibid.*, 63(1941)3424.
R.W. Crowe and C.P. Smyth, *ibid.*, 72(1950)4009.
L.M. Kushner, R.W. Crowe and C.P. Smyth, *ibid.*, 72(1950)1091.
J.G. Poweles, D.E. Williams and C.P. Smyth, J. Chem. Phys., 21(1953)136.
2. C. Clemett and M. Davies, Trans. Faraday Soc., 58(1962)1705.
3. D.J. Denney, J. Chem. Phys., 27(1957)259.
4. D.W. Davidson, Can. J. Chem., 39(1961)571.
5. S.H. Glarum, J. Chem. Phys., 33(1960)639.
6. D.J. Denney and J.W. Ring, J. Chem. Phys., 44(1966)4621.
7. J.G. Berberian and R.H. Cole, J. Am. Chem. Soc., 90(1968)3100.
8. F.I. Mopsik and R.H. Cole, J. Chem. Phys., 44(1966)1015.
9. D.W. Davidson and R.H. Cole, J. Chem. Phys., 19(1951)1484.
10. N. Koizumi and T. Hanai, J. Phys. Chem., 60(1956)1496.
11. T.G. Copeland and D.J. Denney, J. Phys. Chem., 80(1976)210.

12. E.O. Stejskal, D.E. Woessner, T.C. Farrar and H.S. Gutowsky, J. Chem. Phys., 31(1959)55.
13. B.J. Cooke, M.Sc. Thesis, Lakehead University, Thunder Bay, Ontario, Canada, 1969.
14. S.O. Morgan and H.H. Lowry, J. Phys. Chem., 34(1930)2385.
15. W.O. Baker and C.P. Smyth, J. Chem. Phys., 7(1939)574; J. Am. Chem. Soc., 61(1939)2063.
16. S.B. Thomas, J. Phys. Chem., 35(1931)2103.
17. P.P. Kobeko and Co-workers, J. Techn. Phys., (USSR), 8(1938)715.
18. J.C.N. Chao, M.Sc. Thesis, Lakehead University, Thunder Bay, Ontario, Canada, 1978.
19. M. Davies and D.A. Edwards, Trans. Faraday Soc., 63(1967)2163.
20. M. Nakamura, H. Takahashi and K. Higasi, Bull. Chem. Soc. Jpn., 47(1974)1593.
21. P.N. Brier, J.S. Higgins and R.H. Bradley, Mol. Phys., 21(1971)72.
22. M.A. Mazid, M.Sc. Thesis, Lakehead University, Thunder Bay, Ontario, Canada, 1977.
23. M. Davies and J. Swain, Trans. Faraday Soc., 67(1971)1637.
24. H.A. Khwaja, M.Sc. Thesis, Lakehead University, Thunder Bay, Ontario, Canada, 1977.
25. C.J.F. Böttcher and P. Bordewijk, "Theory of Electric Polarization, Vol. 2, Elsevier Scientific Publishing Company, Amsterdam, 1978.
26. G.P. Johari and M. Goldstein, J. Chem. Phys., 53(1970)2372.

27. G. Williams and P.J. Hains, J.C.S. Faraday Symp., 6(1972)14.
28. P.J. Hains and G. Williams, Polymer, 16(1975) 725.
29. N.G. McCrum, B.E. Read, and G. Williams, "Anelastic and Dielectric Effects in Polymer Solids", John Wiley, N.Y., 1967.
30. M.F. Shears and G. Williams, J.C.S. Faraday II, 69(1973)608.
31. L. Hayler and M. Goldstein, J. Chem. Phys., 66(1977)736.

TABLE 4.1: Fuoss-Kirkwood Analysis Parameters, Cole-Cole ϵ_{∞} and Apparent dipole moments for some polar, fairly spherical molecules

T(K)	$10^6 \tau$ (s)	$\log f_{\max}$	β	$10^3 \epsilon''_{\max}$	ϵ_{∞}	μ (D)
<u>Methyl bromide</u>						
82.2	96.92	3.215	0.47	2.35	2.50	-
84.2	77.23	3.314	0.45	2.35	2.35	-
87.3	58.94	3.431	0.44	2.40	2.53	-
90.0	47.83	3.522	0.44	2.48	2.53	-
9.29	35.46	3.652	0.40	2.48	2.54	0.039
95.5	28.93	3.740	0.38	2.49	2.54	0.041
98.1	22.73	3.845	0.36	2.56	2.54	0.043
100.6	19.58	3.910	0.33	2.63	2.54	0.047
104.2	16.70	3.979	0.31	2.71	2.54	0.050
<u>Methyl iodide</u>						
103.6	562.12	2.452	0.35	2.86	2.79	0.048
104.6	245.97	2.811	0.34	2.79	2.79	0.048
105.2	133.19	3.077	0.35	2.81	2.79	0.047
106.1	64.17	3.395	0.32	2.76	2.79	0.049
106.9	40.95	3.590	0.29	2.64	2.79	0.051
107.5	23.36	3.833	0.28	2.59	2.79	0.051
108.5	13.77	4.063	0.30	2.48	2.79	0.049
109.8	11.94	4.125	0.30	2.14	2.79	0.046
<u>2,2-Dichloropropane</u>						
95.0	1352.2	2.071	0.14	2.97	2.50	0.086
95.8	703.7	2.354	0.15	3.07	2.495	0.087
96.5	368.5	2.635	0.17	3.18	2.49	0.089
97.7	138.8	3.059	0.20	3.34	2.49	0.090
98.5	73.6	3.335	0.19	3.43	2.49	0.094
99.8	23.7	3.827	0.18	3.67	2.49	0.100

TABLE 4.1: continued...

T(K)	$10^6 \tau$ (s)	$\log f_{\max}$	β	$10^3 \epsilon''_{\max}$	ϵ_{∞}	μ (D)
<u>1,1,1-Trichloroethane</u>						
<u>Lower Temperature</u>						
94.7	4759.9	1.524	0.33	1.69	2.41	0.049
97.0	2464.1	1.810	0.35	1.79	2.41	0.050
99.9	1342.6	2.074	0.33	1.98	2.41	0.055
104.5	514.22	2.491	0.30	2.29	2.41	0.063
109.6	230.9	2.838	0.40	3.47	2.42	0.069
<u>1,1,1-trichloroethane</u>						
<u>Higher Temperature</u>						
115.1	2191.2	1.861	0.38	21.23	2.42	0.178
116.4	567.07	2.448	0.45	21.98	2.42	0.168
117.3	267.53	2.775	0.49	22.30	2.43	0.162
118.1	138.05	3.062	0.55	23.10	2.43	0.156
119.1	72.05	3.344	0.58	23.59	2.44	0.155
120.0	45.84	3.541	0.62	24.00	2.44	0.151
121.0	23.73	3.827	0.61	24.16	2.44	0.154
122.1	13.01	4.088	0.61	24.18	2.44	0.154
122.7	8.28	4.284	0.59	24.18	2.44	0.158
<u>Methyltrichlorosilane</u>						
120.4	3484.2	1.660	0.23	16.38	2.60	0.215
121.3	1821.7	1.941	0.23	16.35	2.60	0.215
122.8	371.26	2.632	0.25	16.15	2.60	0.207
123.8	189.32	2.925	0.25	15.93	2.60	0.206
125.1	86.12	3.267	0.29	15.94	2.61	0.192
126.2	43.83	3.560	0.31	16.00	2.61	0.187
127.0	25.39	3.797	0.33	15.83	2.61	0.181
128.8	12.05	4.121	0.30	15.43	2.61	0.189
130.7	6.47	4.391	0.30	14.55	2.62	0.184

TABLE 4.1: continued...

T(K)	$10^6 \tau$ (s)	$\log f_{\max}$	β	$10^3 \epsilon''_{\max}$	ϵ_{∞}	μ (D)
<u>t-Butylchloride</u>						
143.7	5209.7	1.485	0.22	12.94	2.29	0.221
144.8	1828.4	1.940	0.24	12.94	2.29	0.212
145.6	1105.8	2.158	0.26	12.93	2.29	0.204
146.6	572.43	2.444	0.28	12.90	2.29	0.197
147.6	328.03	2.686	0.29	12.72	2.29	0.193
149.4	142.10	3.049	0.32	12.46	2.30	0.183
151.4	70.37	3.354	0.34	12.10	2.30	0.176
153.4	36.83	3.636	0.37	11.72	2.30	0.167
155.3	22.59	3.848	0.40	11.34	2.30	0.159
157.2	12.90	4.091	0.41	10.99	2.31	0.156
159.2	7.71	4.315	0.42	10.70	2.31	0.153
<u>t-Butylbromide</u>						
<u>Lower Temperature Process</u>						
78.6	491.5	2.510	0.34	2.15	2.29	0.055
80.5	287.5	2.743	0.38	2.30	2.29	0.054
83.9	93.7	3.230	0.86	3.56	2.29	0.046
87.4	52.1	3.485	0.43	3.34	2.30	0.064
90.3	29.2	3.737	0.62	3.67	2.30	0.057
92.9	14.5	4.039	0.49	4.04	2.30	0.068
95.3	9.5	4.225	0.54	4.53	2.30	0.070
<u>t-Butylbromide</u>						
<u>Higher Temperature Process</u>						
128.8	8728.2	1.261	0.20	11.45	2.49	0.201
129.3	5171.9	1.488	0.22	11.59	2.49	0.193
130.8	1685.9	1.975	0.24	11.83	2.49	0.188
131.9	863.76	2.265	0.25	11.89	2.50	0.185
134.2	237.83	2.826	0.28	11.89	2.51	0.176
136.2	77.15	3.314	0.27	11.60	2.51	0.179
138.4	27.87	3.757	0.28	11.27	2.52	0.174
140.5	7.99	4.299	0.23	10.79	2.52	0.189
142.3	3.92	4.609	0.22	9.98	2.53	0.187

TABLE 4.1: continued...

T (K)	$10^6 \tau$ (s)	$\log f_{\max}$	β	$10^3 \epsilon''_{\max}$	ϵ_{∞}	μ (D)
<u>2-Methyl-2-nitropropane</u>						
100.6	11493.0	1.141	0.24	0.94	2.36	0.047
104.5	2919.1	1.737	0.28	1.01	2.36	0.046
108.6	1049.4	2.181	0.32	1.08	2.36	0.045
111.7	535.6	2.473	0.35	1.15	2.37	0.045
116.3	228.3	2.843	0.38	1.23	2.37	0.046
121.4	87.9	3.258	0.40	1.33	2.38	0.047
125.9	44.9	3.549	0.42	1.43	2.38	0.049
130.5	22.4	3.852	0.41	1.48	2.38	0.051
135.5	12.4	4.108	0.41	1.49	2.38	0.052

TABLE 4.2: RELAXATION TIMES AND EYRING ANALYSIS RESULTS FOR SOME POLAR FAIRLY SPHERICAL MOLECULES

Molecule	T(K)	$\log f_{\max}$	β -Range	Relaxation times τ (s)		ΔG_E in kJ mol ⁻¹		ΔH_E in	ΔS_E in
				100 K	150 K	100 K	150 K	kJ mol ⁻¹	J K ⁻¹ mol ⁻¹
Methyl bromide	82-104	3.215-3.979	0.31-0.47	2.1×10^{-5}		14.6		5.1 ± 0.2	-95 ± 3
Methyl bromide	103.6-108.5	2.452-4.063	0.28-0.36	1.0×10^{-2}		19.8		71 ± 5	509 ± 46
2,2-Dichloro- propane	95.0-99.8	2.071-3.827	0.14-0.20	2.1×10^{-5}		14.6		65 ± 2	507 ± 20
1,1,1-Trichloro- ethane	95-110	1.524-2.838	0.30-0.40	1.4×10^{-3}		18.1		16.6 ± 1.4	-15 ± 14
	115.1-122.7	1.861-4.284	0.38-0.62	6.7×10^{-2}	3.1×10^{-12}	29.0	2.8	81 ± 6	524 ± 49
Methyltri- chlorosilane	120.4-130.7	1.660-4.391	0.23-0.33	4.0×10^{-4}	2.3×10^{-10}	32.4	8.2	81 ± 9	484 ± 74
t-Butyl chloride	143.7-159.2	1.485-4.315	0.22-0.42	2.6×10^{-9}	1.7×10^{-4}	41.6	25.1	75 ± 8	331 ± 53
t-Butyl bromide	78.6-95.3	2.510-4.225	0.34-0.86	4×10^{-6}		13.2		13.2 ± 0.9	6 ± 10
	128.8-142.3	1.261-4.609	0.20-0.28	6.5×10^{-7}	8.1×10^{-8}	38.5	15.5	85 ± 3	460 ± 25
2-Methyl-2- nitropropane	101-136	1.141-4.108	0.24-0.42	9.6×10^{-3}	1.6×10^{-6}	19.7	19.2	20.7 ± 1.4	10 ± 10

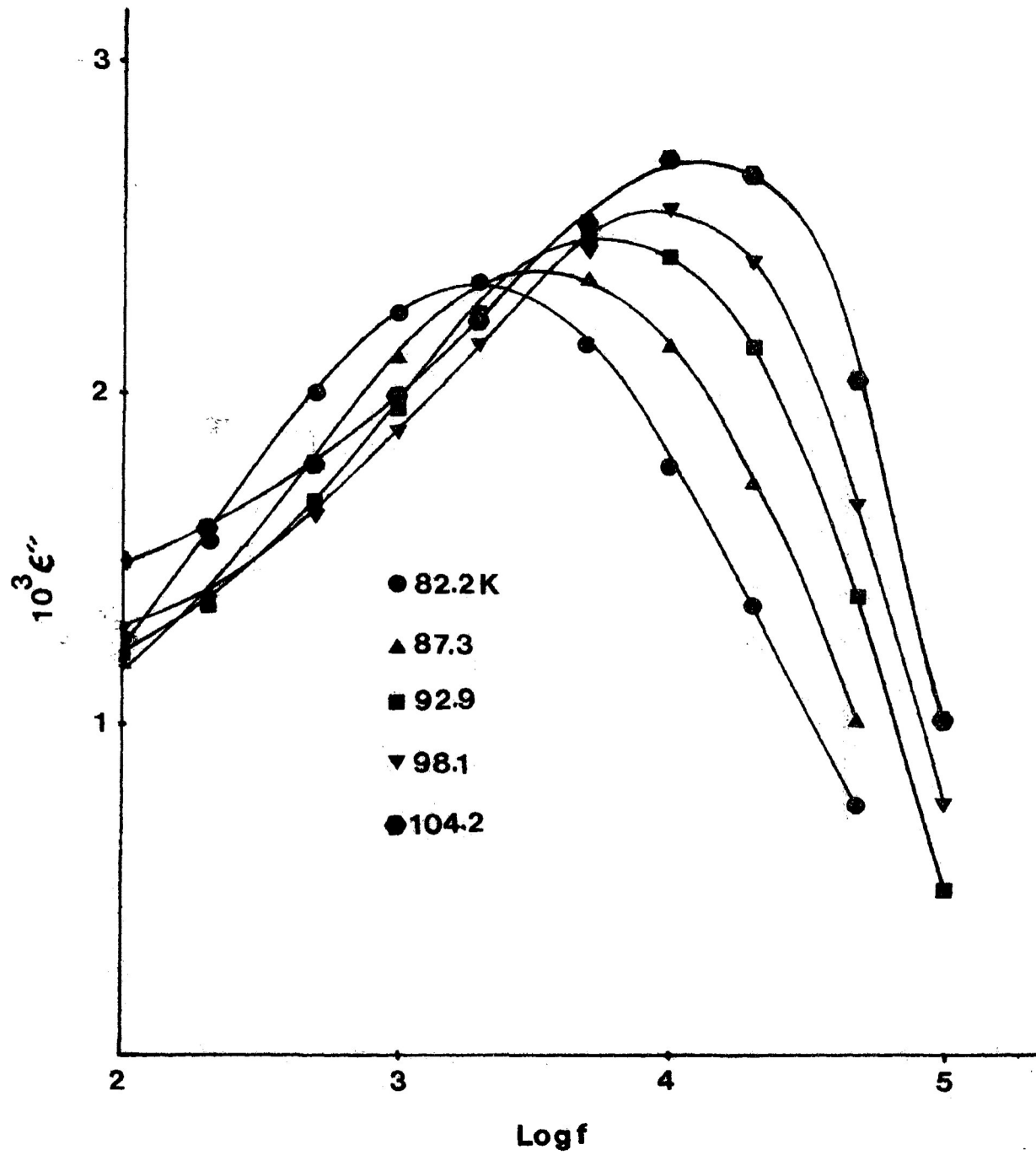


FIGURE 4.1: Dielectric loss factor ϵ'' versus log frequency for methyl bromide

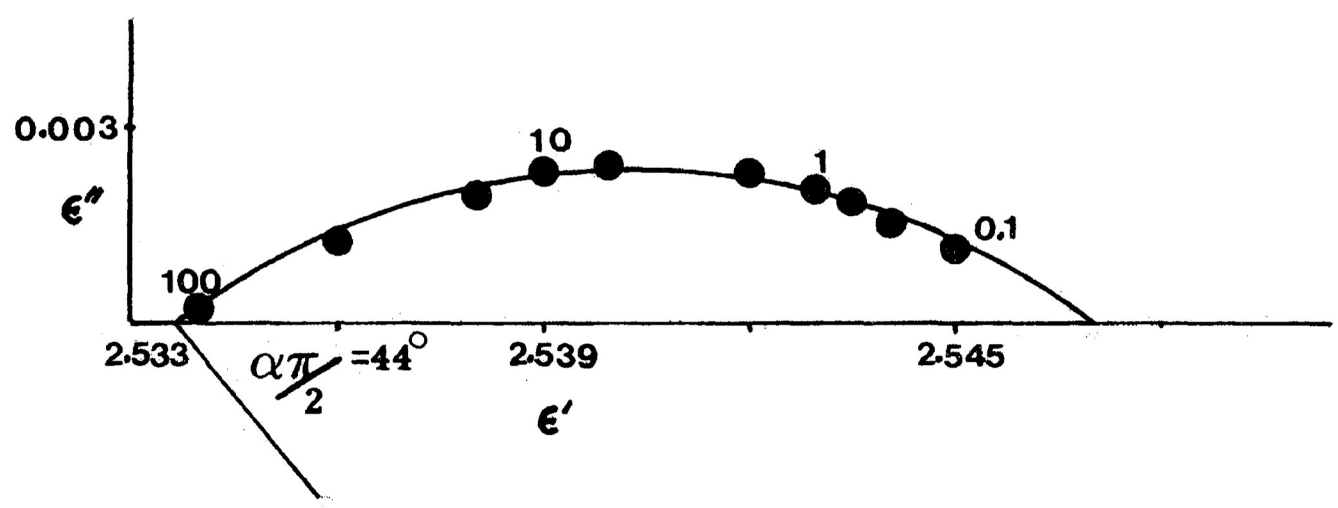


FIGURE 4.2: Cole-Cole plot for methyl bromide at 90.0 K
Numbers beside points are frequencies in kHz

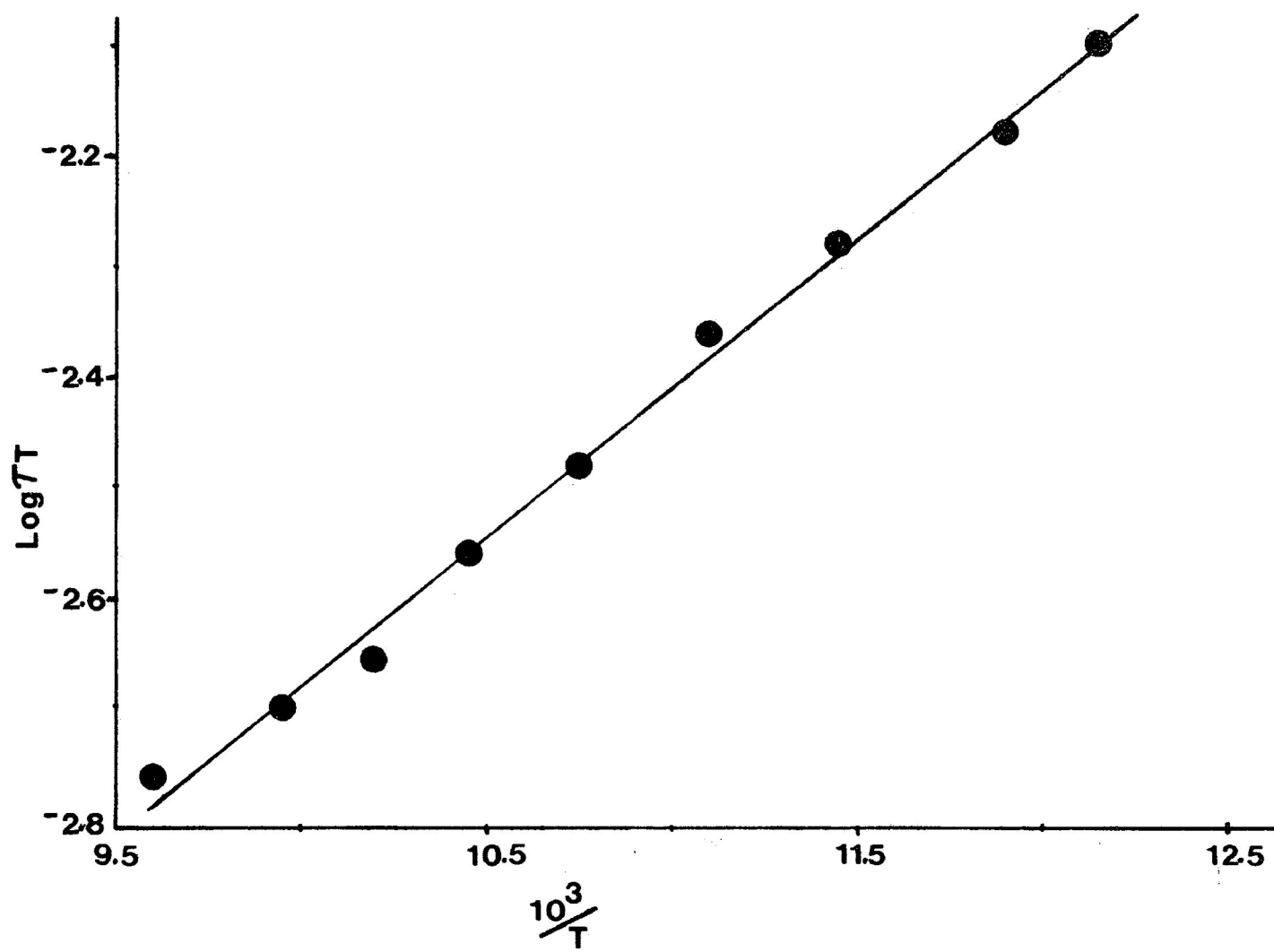


FIGURE 4.3: Eyring plot of $\log(\tau T)$ versus $\frac{1}{T}$ for methyl bromide.

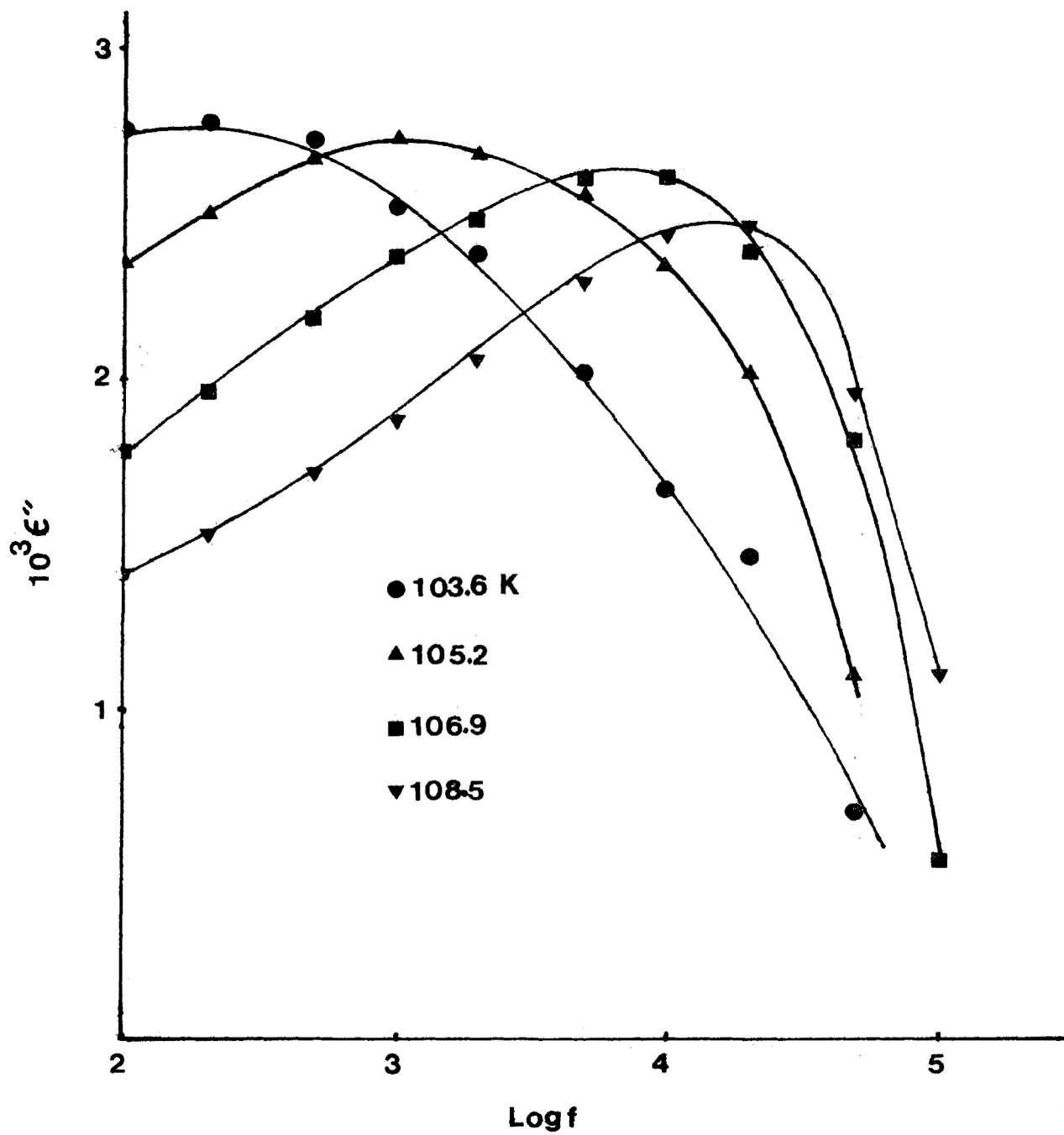


FIGURE 4.4: Dielectric loss factor ϵ'' versus log frequency for methyl iodide

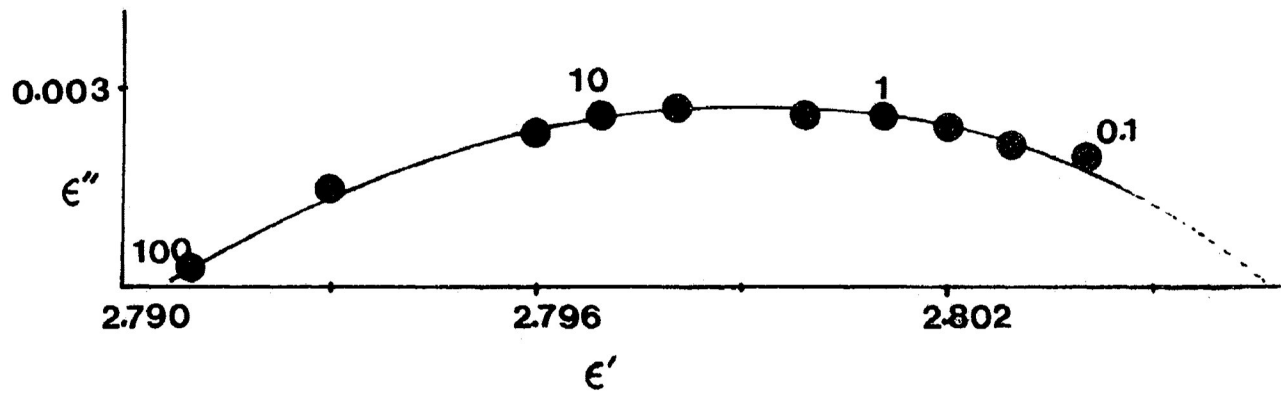


FIGURE 4.5: Complex plane diagram for methyl iodide at 106.1 K
Numbers beside points are frequencies in kHz

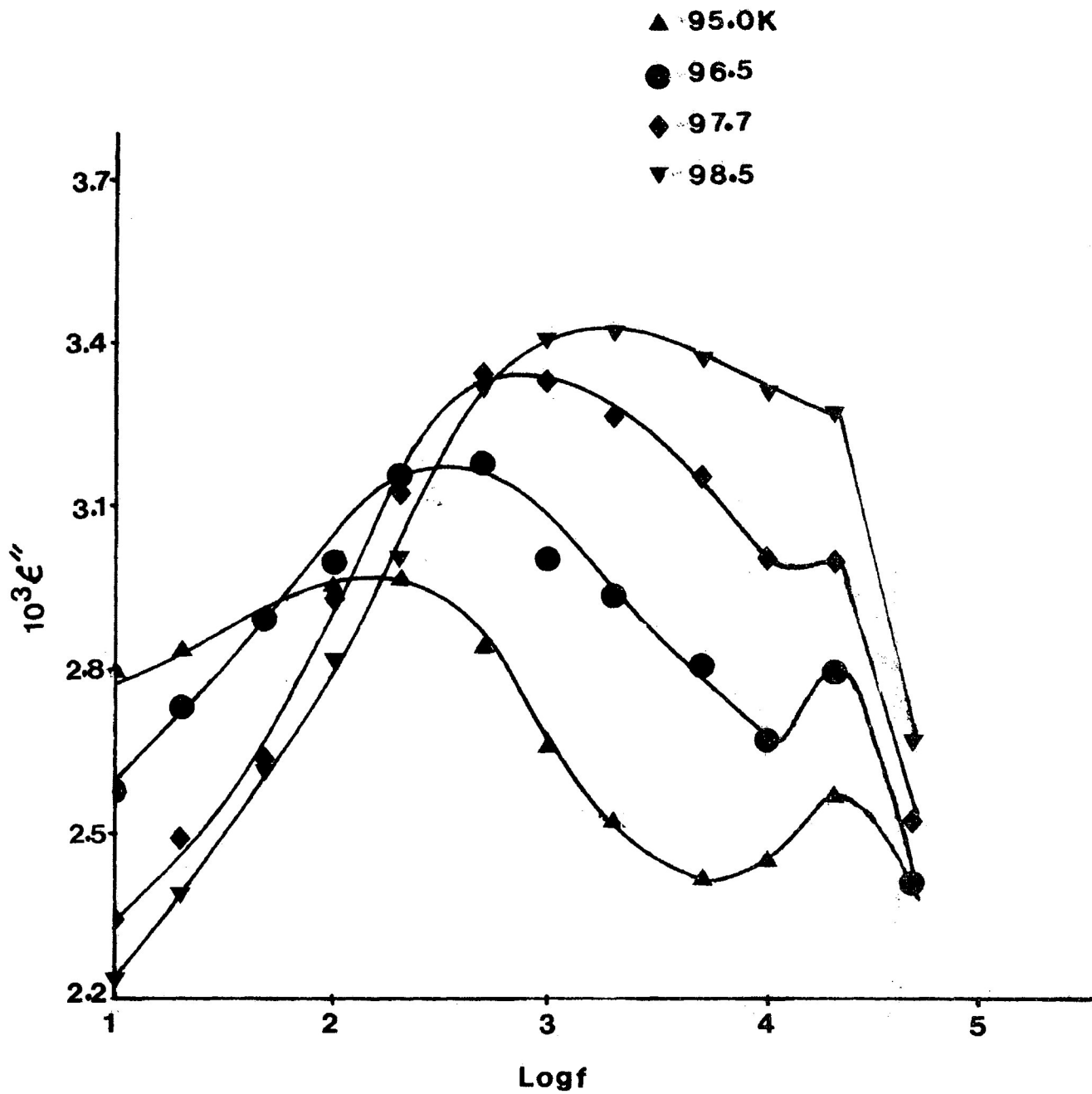


FIGURE 4.6: Dielectric loss factor ϵ'' versus log frequency for 2,2-dichloropropane

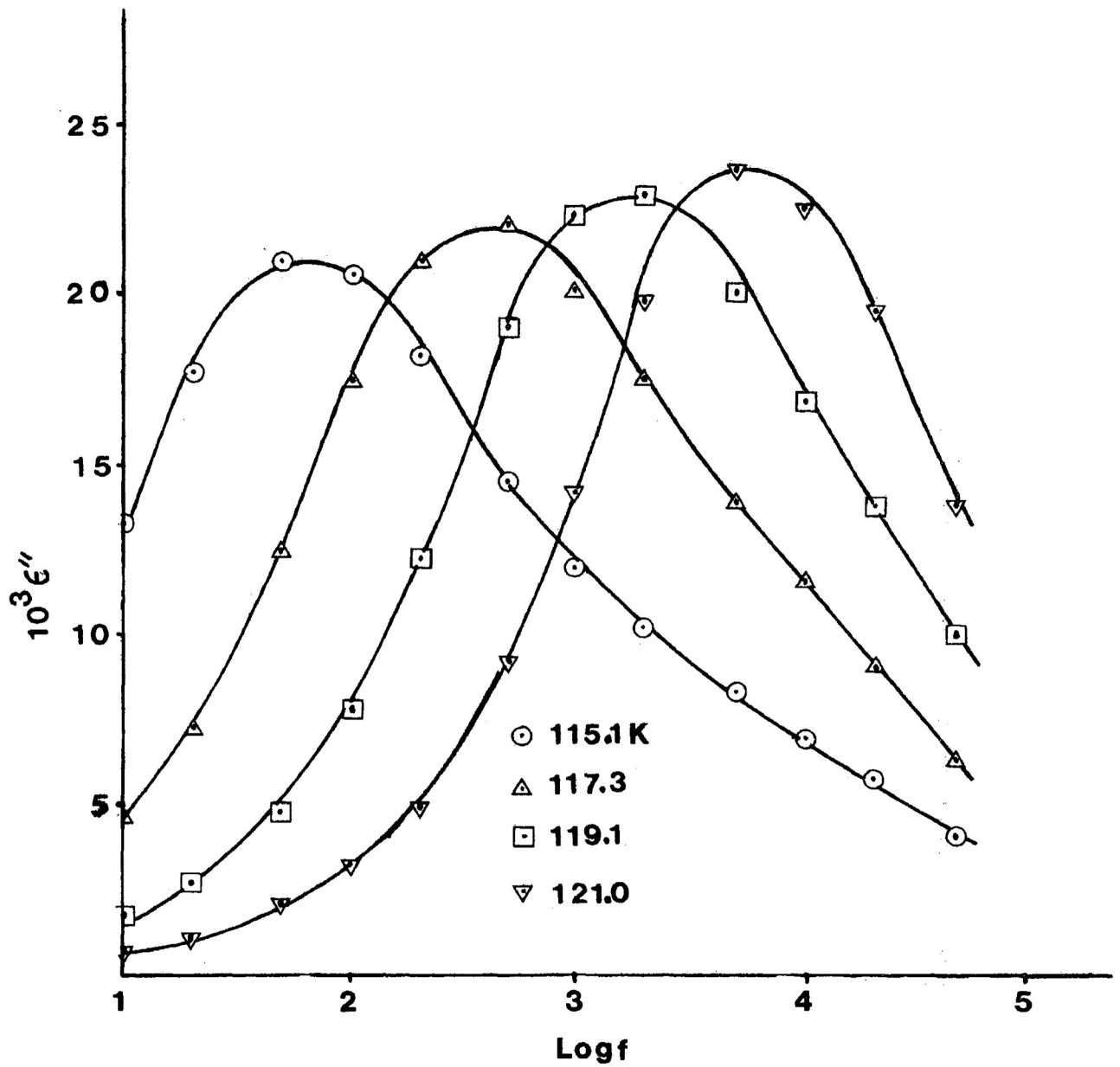


FIGURE 4.7: Dielectric loss factor ϵ'' versus log frequency for 1,1,1-trichloroethane

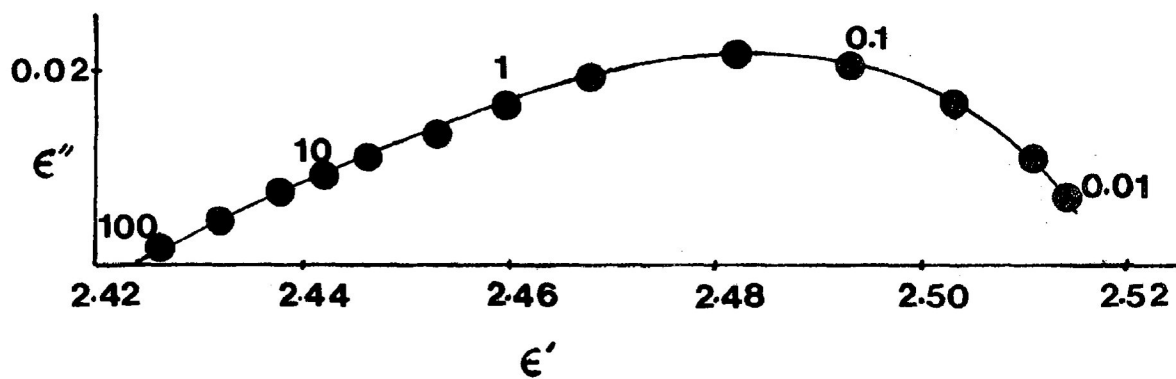


FIGURE 4.8: Complex plane diagram for 1,1,1-trichloroethane at 116.4 K
Numbers beside points are frequencies in kHz

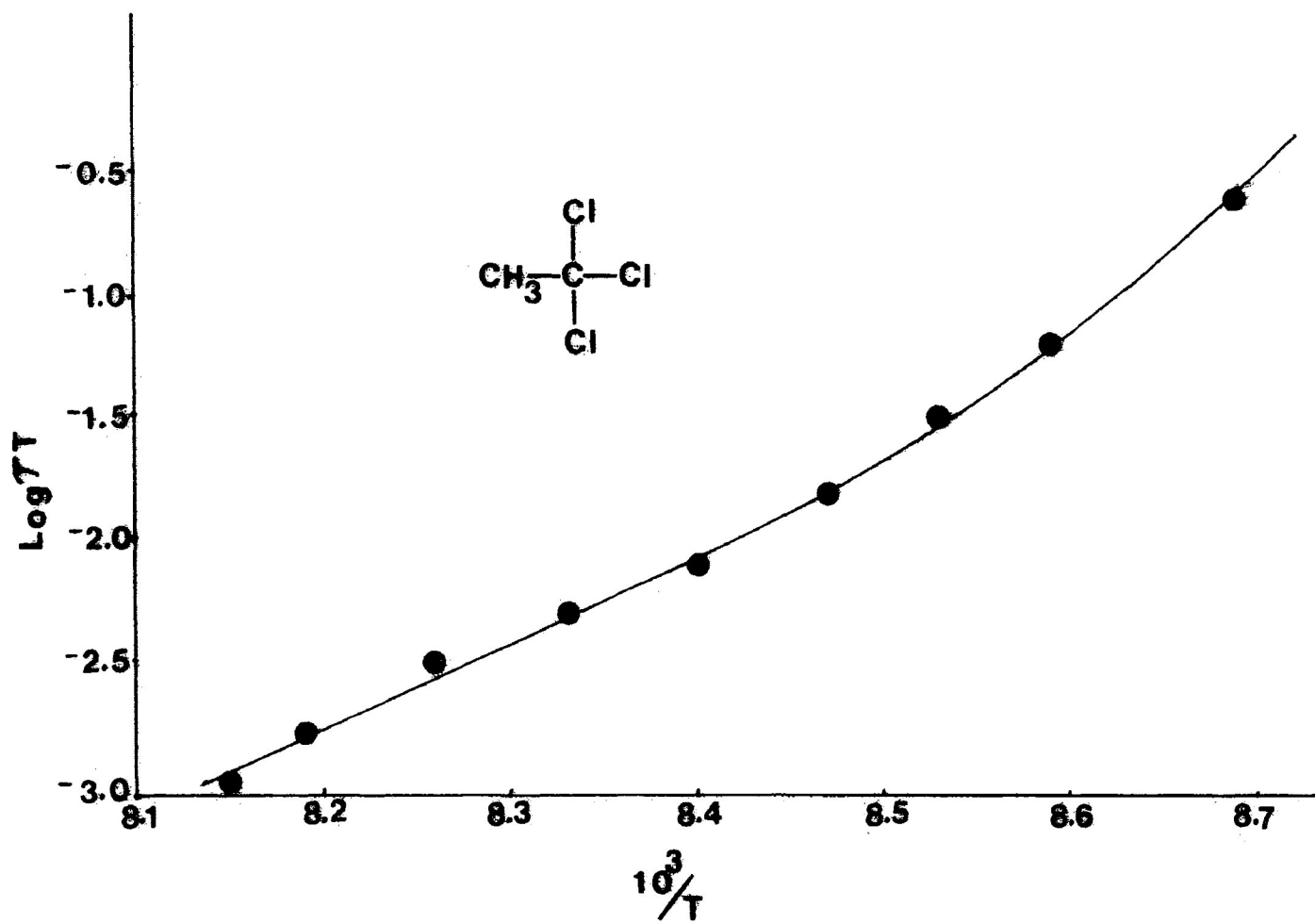


FIGURE 4.9: Eyring plot of $\log(\tau T)$ versus $\frac{1}{T}$ for 1,1,1-trichloroethane

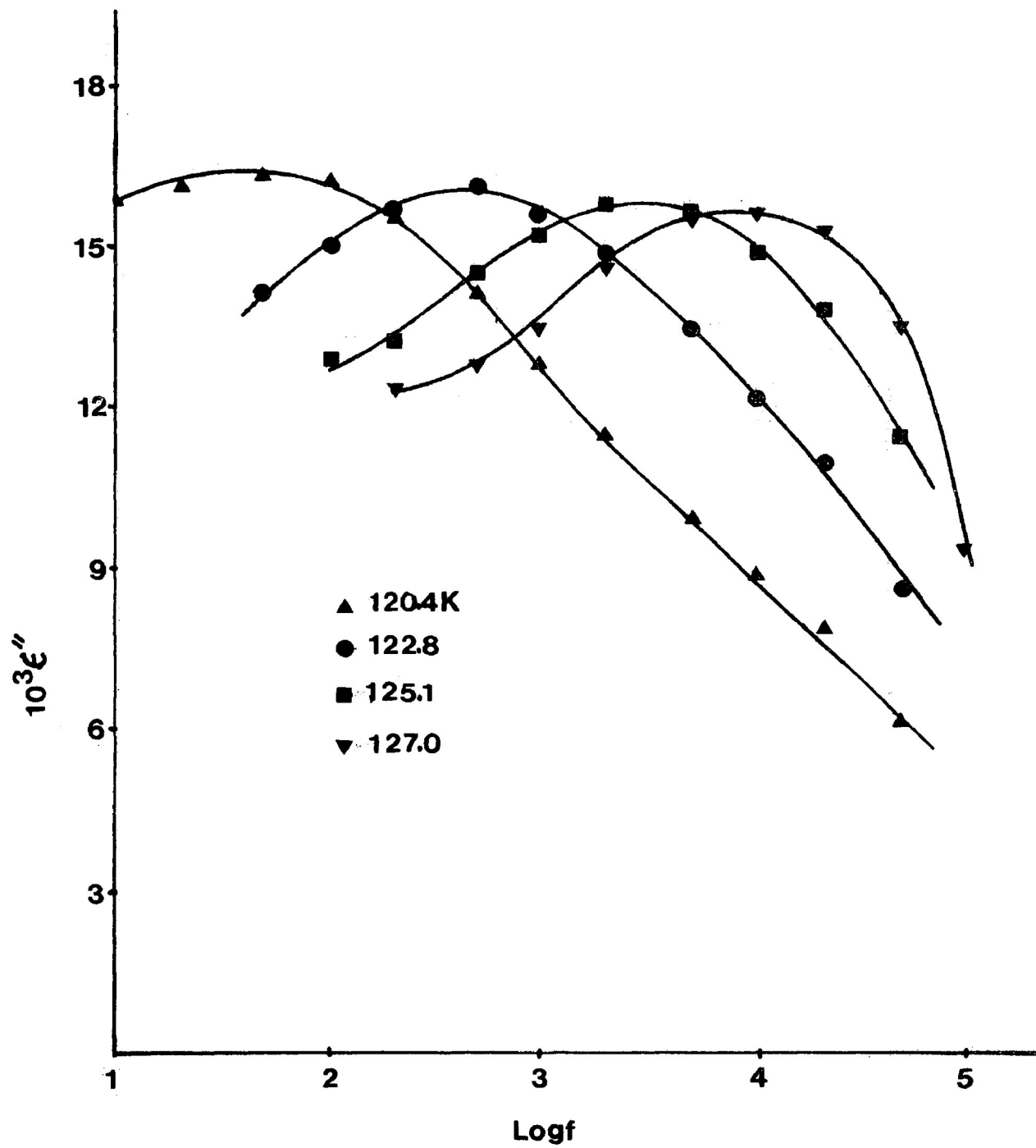


FIGURE 4.10: Dielectric loss factor ϵ'' versus log frequency for methyltrichlorosilane

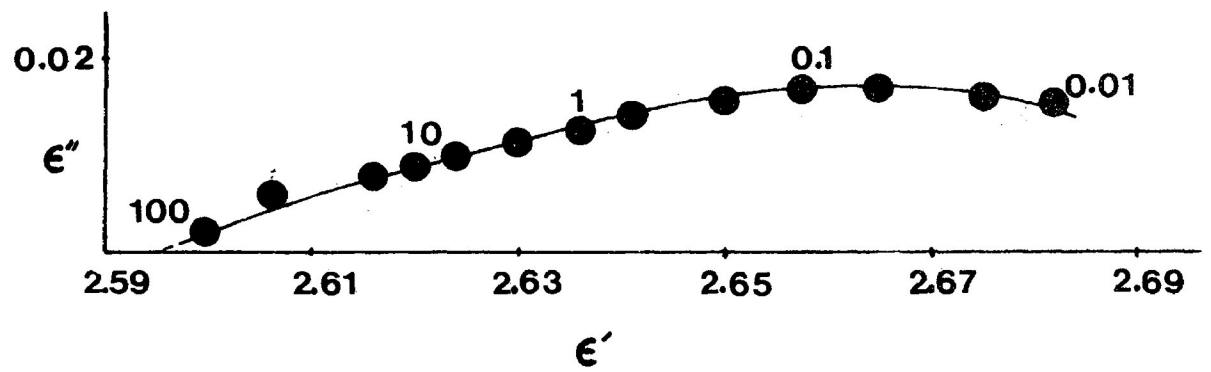


FIGURE 4.11: Complex plane diagram for methyltrichlorosilane at 120.4 K
Numbers beside points are frequencies in kHz

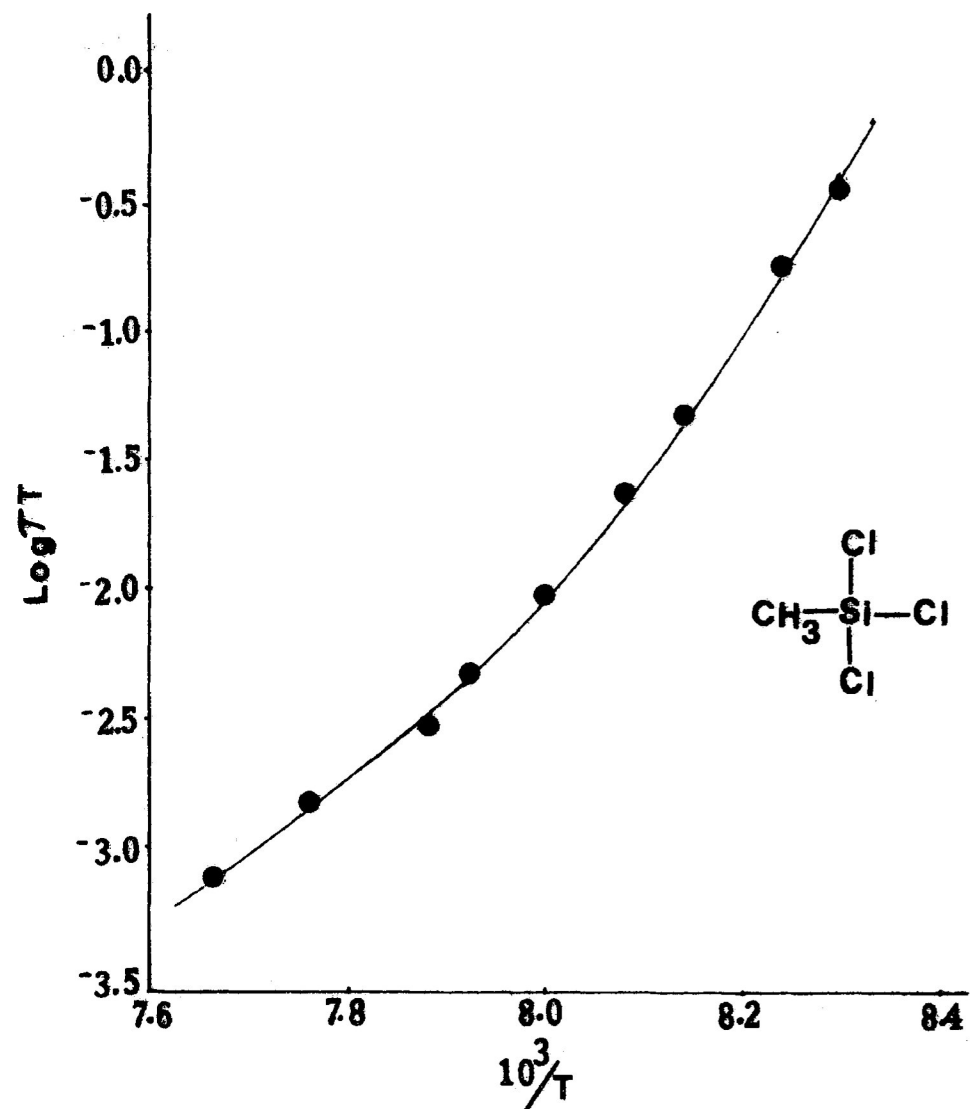
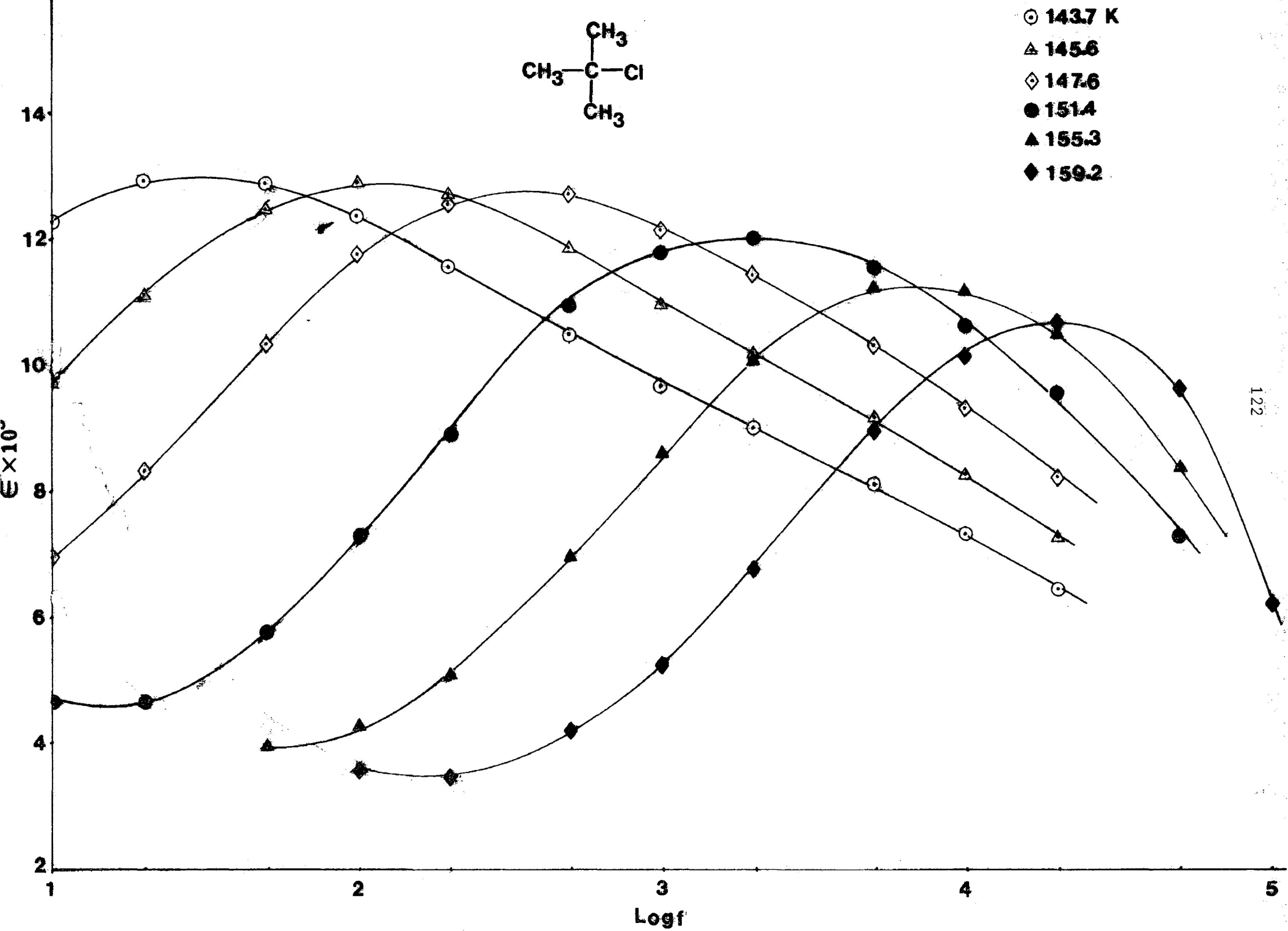


FIGURE 4.12: Eyring plot of $\log(\tau T)$ versus $\frac{1}{T}$ for methyltrichlorosilane

FIGURE 4.13: Dielectric loss factor ϵ'' versus $\log f$ for *t*-butylchloride



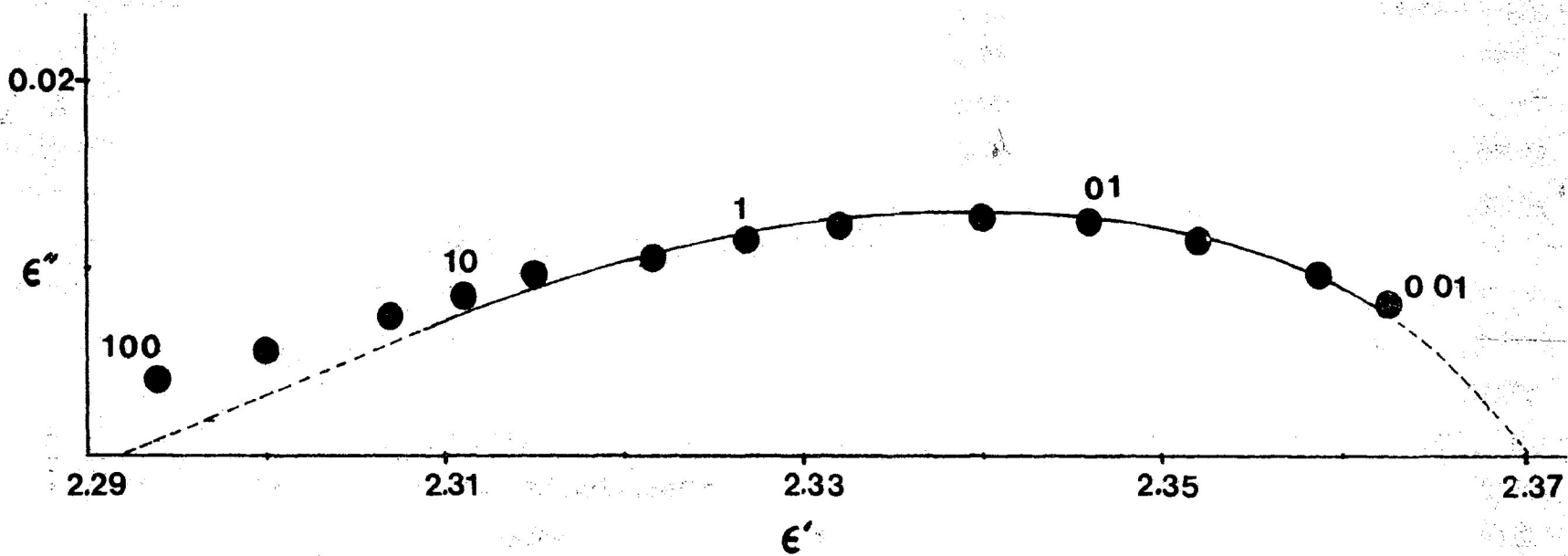


FIGURE 4.14: Complex plane diagram for t-butylchloride at 145.6 K
 Numbers beside points are frequencies in kHz

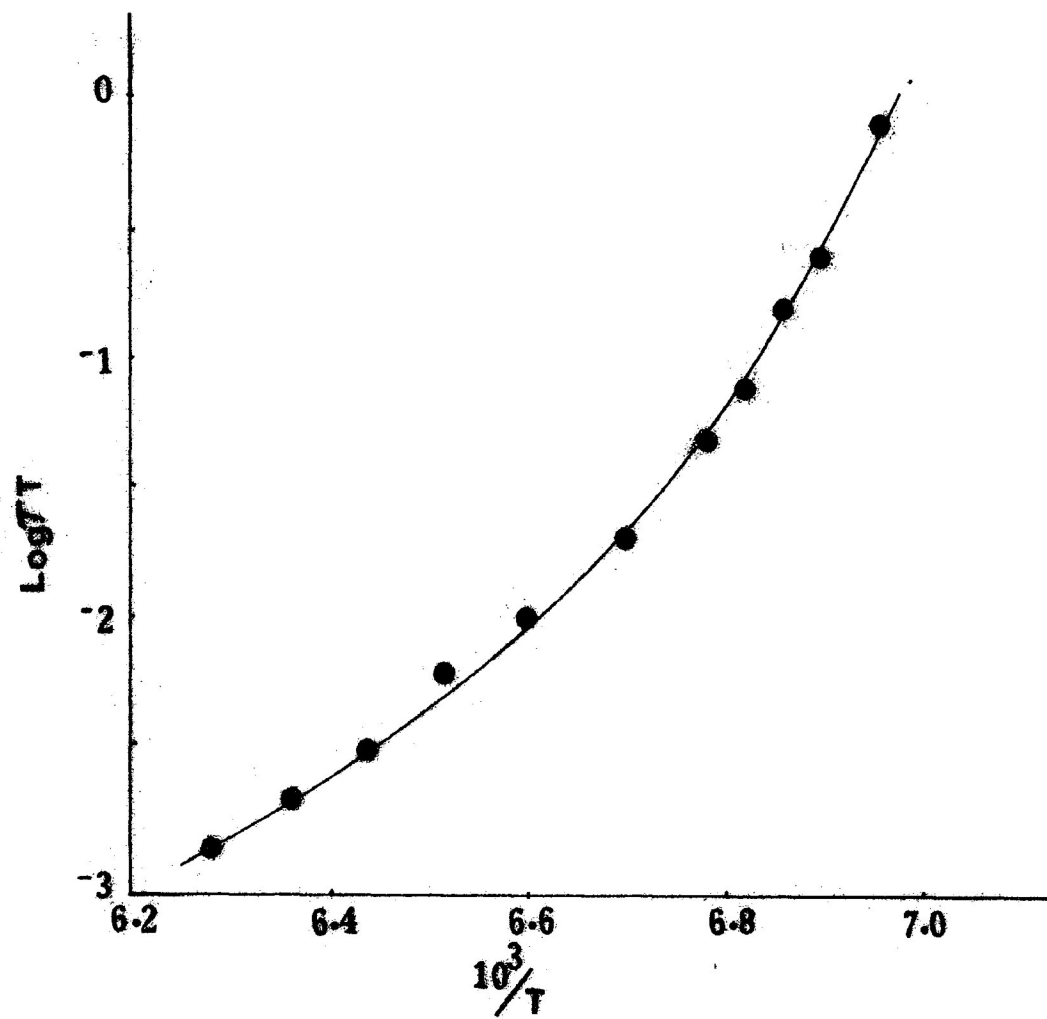


FIGURE 4.15: Eyring plot of $\log(\tau T)$ versus $\frac{1}{T}$ for t-butylchloride

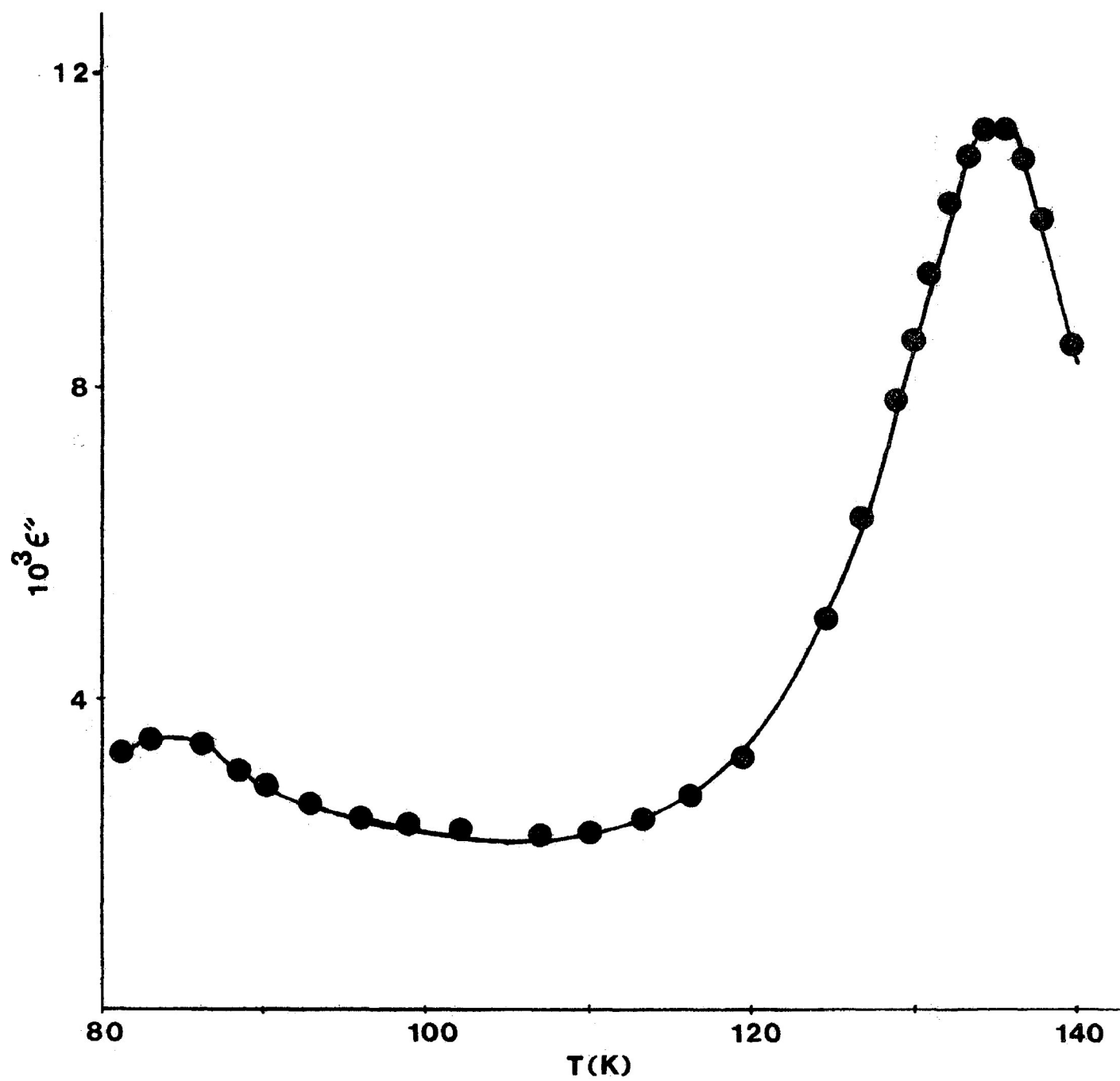


FIGURE 4.16: Dielectric loss factor ϵ'' versus temperature for t-butylbromide

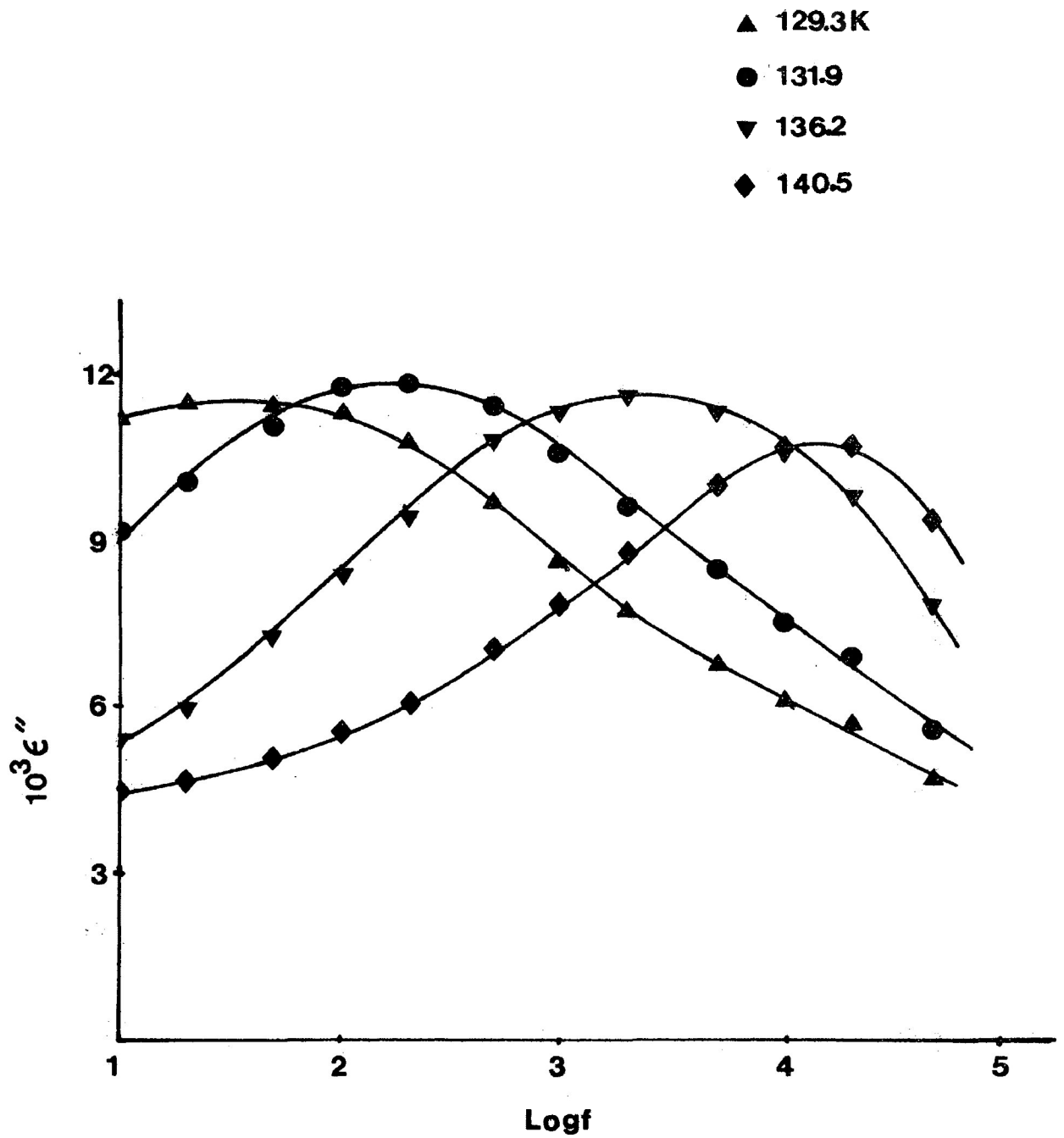


FIGURE 4.17: Dielectric loss factor ϵ'' versus log frequency for t-butylbromide

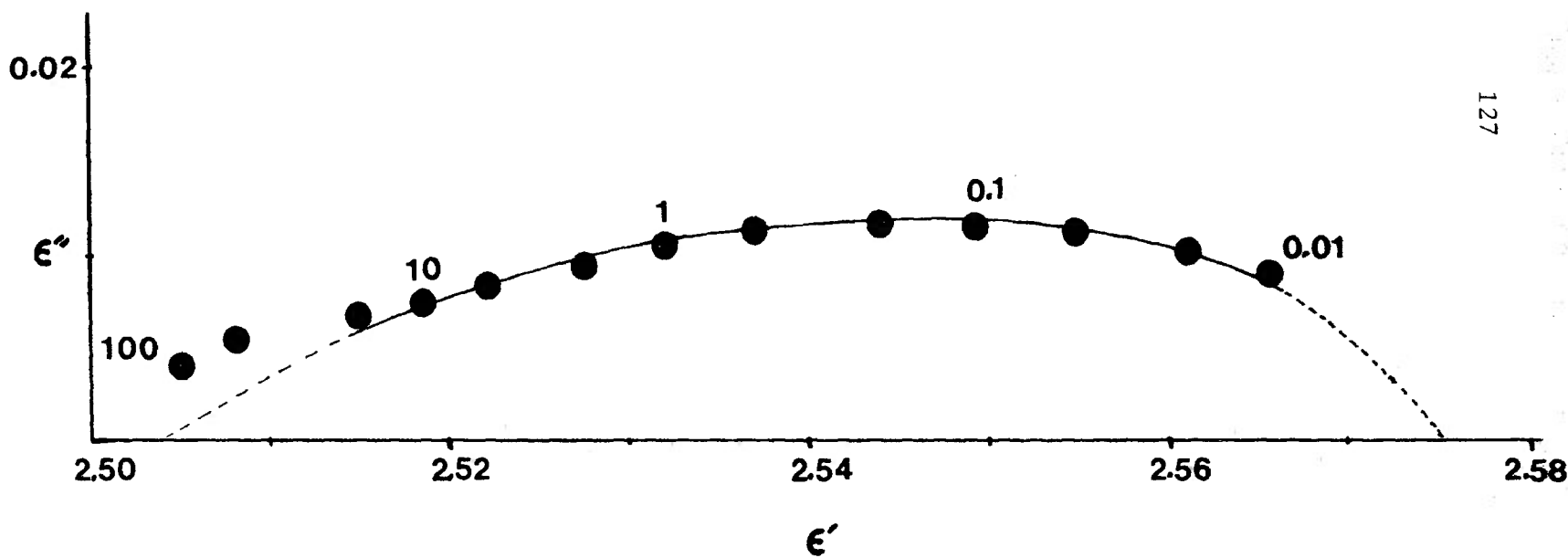


FIGURE 4.18: Complex plane diagram for t-butylbromide at 131.9 K
 Numbers beside points are frequencies in kHz

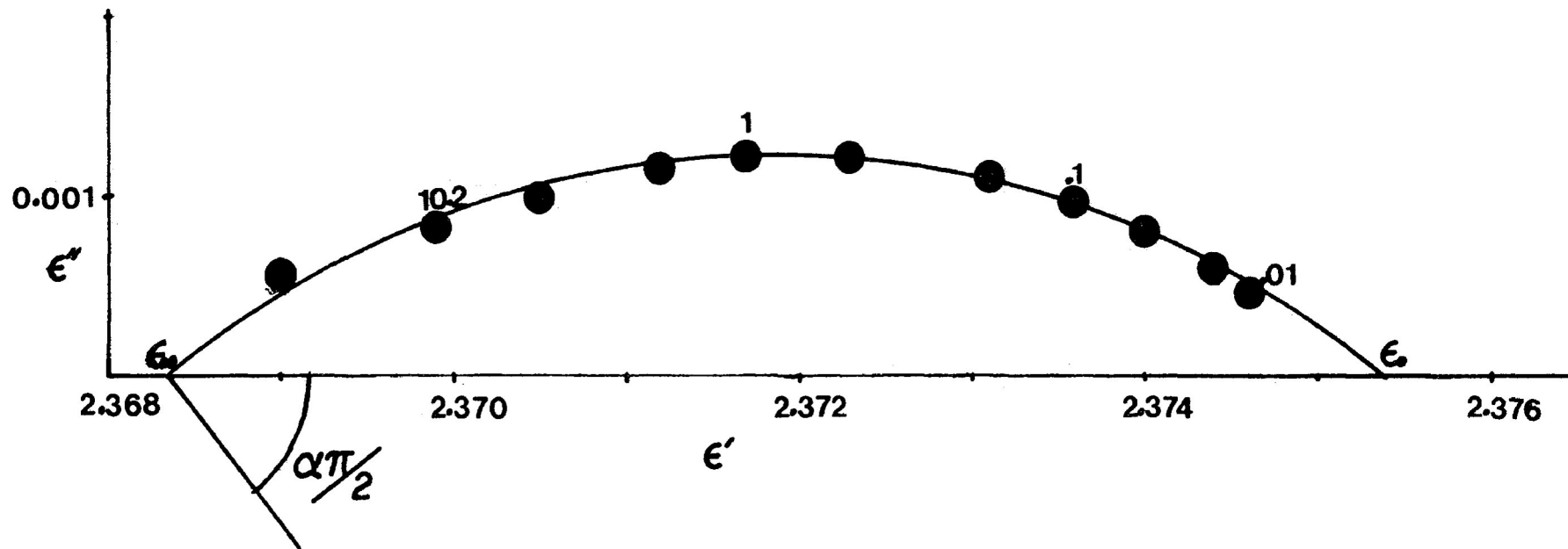


FIGURE 4.19: Complex plane diagram (Cole-Cole plot) for 2-methyl-2-nitropropane at 116.3 K
 Numbers beside points are frequencies in kHz

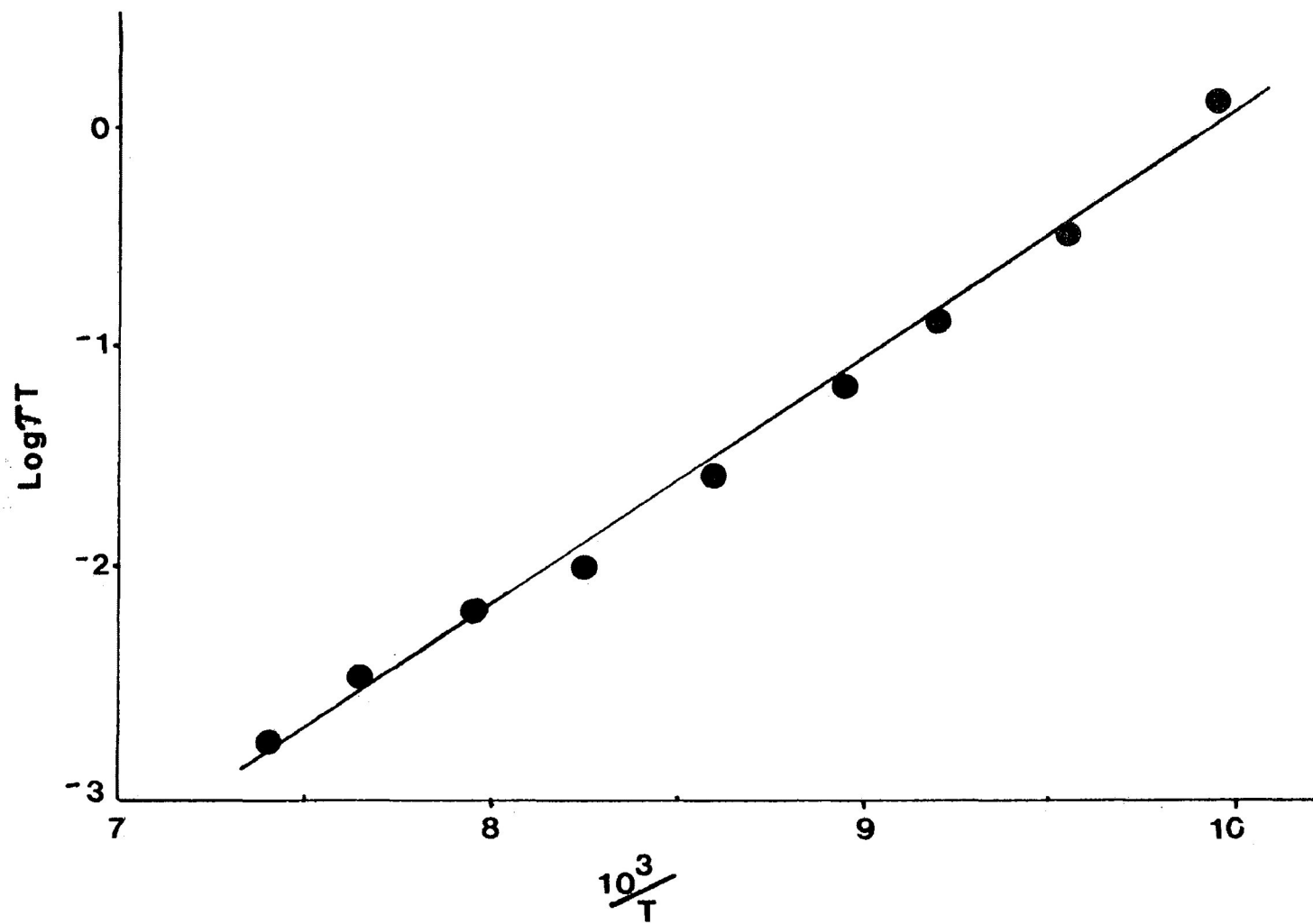


FIGURE 4.20: Eyring plot of $\log(\tau T)$ versus $\frac{1}{T}$ for 2-methyl-2-nitropropane

CHAPTER V

M O L E C U L A R R E L A X A T I O N
O F S O M E A R O M A T I C
H Y D R O C A R B O N S

INTRODUCTION

Around room temperature pure alkylbenzenes, in the liquid state, exhibit dielectric absorption in the microwave region (1-6). The mean relaxation times of o-xylene, m-xylene, toluene, ethyl-, isopropyl-, and t-butylbenzene were short in comparison with those of rigid molecules of similar shape and size (3). The dielectric absorption of these alkylbenzenes was analyzed in terms of molecular orientation and also a short relaxation time process. Crossley and Walker (6) reported small dielectric losses for some so-called nonpolar alkylbenzenes, e.g. p-xylene, p-cymene, mesitylene, durene and hexamethylbenzene. They interpreted their results on the basis of the mechanism proposed by Whiffen (7), which essentially assumes that dipole moments are induced by molecular collisions.



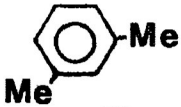
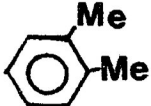
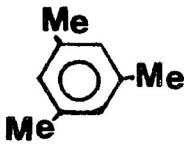
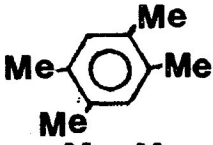
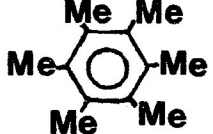
For nonpolar solids, creation of induced dipole moment by such mechanism seems quite unlikely since in this case there is little scope for molecular collisions to be occurred.

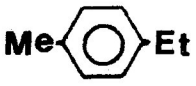
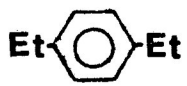
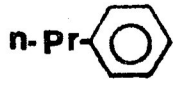
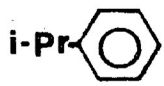
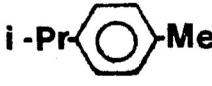
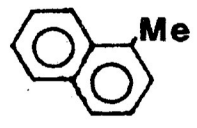
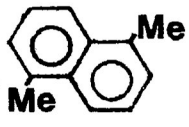
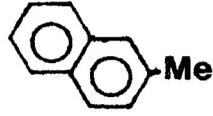
No dielectric measurements of nonpolar aromatic

hydrocarbons in the solid state appear to have been reported. It seemed worthwhile, therefore, to examine a few nonpolar and weakly polar aromatic hydrocarbons in the solid state.

EXPERIMENTAL RESULTS

The following aromatic hydrocarbons were included in the present study:

<u>Number</u>	<u>Name</u>	<u>Structure</u>
1	benzene	
2	p-xylene	
3	m-xylene	
4	o-xylene	
5	mesitylene	
6	durene	
7	hexamethylbenzene	

<u>Number</u>	<u>Name</u>	<u>Structure</u>
8	p-ethyltoluene	
9	p-diethylbenzene	
10	n-propylbenzene	
11	isopropylbenzene	
12	p-cymene	
13	1-methylnaphthalene	
14	1,5-dimethylnaphthalene	
15	2-methylnaphthalene	

All of these compounds were commercially available. p-Xylene, p-cymene, 1-methylnaphthalene and p-diethylbenzene were redistilled from either sodium or activated molecular sieve, using a 30 theoretical plate spinning band column. Purity of these compounds

was confirmed by agreement of the dipole moment values with the literature values. All the liquids were dried over either sodium or activated molecular sieve at least 48 hours prior to use.

Alkylbenzenes are not known as hygroscopic and the solubility of water in these compounds is almost nil (8). Benzene can absorb the highest amount (0.07 in 100 parts) of water (8). However, worst cases check were made with benzene and p-xylene both saturated with water. In either case no dielectric loss was observed below 110 K in our frequency range (10^1 to 10^5 Hz). Recently Haylor and Goldstein (9) also observed no significant loss below 120 K when they filled their cell with distilled water. Thus it appears that most of our low temperature peaks for nonpolar compounds are below this region, and we assume that they would probably show no effect even if we had not made efforts to avoid introduction of water in sample handling.

Hexamethylbenzene was measured as compressed solid disk in a parallel plate capacitor cell. All other compounds were measured in a three-terminal coaxial cell.

Most of the samples were measured twice and in each time the dielectric relaxation behaviour was observed at the same temperature region suggesting that the absorptions were not the consequence of cracks in the sample.

The errors involved in the dielectric constants for low-loss compounds (e.g. o-xylene, mesitylene and durene) are such that Cole-Cole plots are difficult to formulate, and it is more realistic to examine the absorption in terms of the dielectric losses.

Figures 5.1 to 5.7 show the dielectric absorption curves, Cole-Cole plots, Eyring rate plots and temperature versus loss factor plots of some of the aromatic hydrocarbons here. Table 5.1 lists the results from Fuoss-Kirkwood analyses, the ϵ_{∞} and the experimental dipole moments. Eyring analysis results are summarized in Table 5.2.

DISCUSSION

Among the fifteen aromatic hydrocarbons studied here, eleven of which exhibit low temperature dielectric absorption. The five compounds in which low temperature relaxation could not be detected are benzene, p-xylene, m-xylene and p-ethyltoluene, all of which are so-called nonpolar compounds except m-xylene which has a dipole moment of 0.31 D (10).

The low temperature relaxation of o-xylene (Fig. 5.1) yields an enthalpy of activation, $\Delta H_E = 16 \pm 1 \text{ kJ mol}^{-1}$ and entropy of activation, $\Delta S_E = -35 \pm 6 \text{ J K}^{-1} \text{ mol}^{-1}$ from a good straight line of Eyring plot (Fig. 5.2). o-Dichlorobenzene, a fairly polar molecule (2.56 D)(10) is similar in size and shape to o-xylene. This molecule was examined as pure solid (see Chapter VII) as well as in different media (11,12) and observed in each case the dielectric absorption near liquid nitrogen temperature. The ΔH_E values for this compound were found to be 11 kJ mol^{-1} as pure solid, 11 kJ mol^{-1} in o-terphenyl (12), 13 kJ mol^{-1} in Santovac (12) and 11 kJ mol^{-1} (12) and 16 kJ mol^{-1} (11) in polystyrene with the corresponding ΔS_E values, -42, -34, -17, and -21 and $1 \text{ J K}^{-1} \text{ mol}^{-1}$ for molecular rotation. Since o-xylene

shows relaxation at higher temperature region (102-118 K), higher energy barrier would be expected for molecular rotation of this molecule, which was actually observed.

A complete study of low temperature relaxation for mesitylene could not be made due to the influence of co-operative motion (Figure 5.3). The results reported here are for a short temperature range (113-121 K) and hence are subject to considerable error

The enthalpy of activation of $41 \pm 2 \text{ kJ mol}^{-1}$ and entropy of activation of $35 \pm 13 \text{ J K}^{-1} \text{ mol}^{-1}$ for hexamethylbenzene are to be compared with the corresponding values of 48 kJ mol^{-1} and $40 \text{ J K}^{-1} \text{ mol}^{-1}$ and 43 kJ mol^{-1} and $50 \text{ J K}^{-1} \text{ mol}^{-1}$ obtained for molecular relaxation in fairly similar sized and shaped pentachlorotoluene and 1,2,4-trimethyl-3,5,6-trichlorobenzene molecules (13).

It is also to be noted that the temperature and frequency ranges for molecular relaxation in pentachlorotoluene and 1,2,4-trimethyl-3,5,6-trichlorobenzene are very close to the corresponding values in the hexamethylbenzene.

From Table 5.2 it is notable that in the temperature range of maximum absorption, the enthalpy of activation increases on passing from o-xylene to hexamethylbenzene. The increasing sequence of ΔH_E values of 16, 19, 24 and 41 kJ mol^{-1} for o-xylene, p-diethylbenzene, durene and hexamethylbenzene, respectively, can be interpreted in terms of the increasing size of the molecule.

It can be seen that for o-xylene, mesitylene, p-diethylbenzene and durene, negative ΔS_E values are associated with small ΔH_E values. This finding is supported by Higasi's (14) earlier investigation, in which he examined 120 substances for which ΔH_E and ΔS_E are available for molecular relaxation processes, and tentatively postulated that, "the entropy change ΔS_E is zero or has a small negative value, if ΔH_E is below 13.4 kJ mol^{-1} ." In addition, negative entropies of activation for a molecular relaxation process are also found in the literature. For example, Davies et al (11, 15) reported for cyclohexylchloride ($-12.6 \text{ J K}^{-1} \text{ mol}^{-1}$); cyclohexylbromide ($-20.0 \text{ J K}^{-1} \text{ mol}^{-1}$); anthrone ($-33.5 \text{ J K}^{-1} \text{ mol}^{-1}$) and camphor ($-31.4 \text{ J K}^{-1} \text{ mol}^{-1}$)

in a polystyrene matrix. Moreover, Tay and Walker (16) reported that the ΔS_E values for molecular relaxation of 2-fluoronaphthalene, 2-chloronaphthalene and 1-bromo-naphthalene in a polystyrene matrix are -8.4 , -10.5 and -3.8 $\text{J K}^{-1} \text{mol}^{-1}$, respectively.

Examination of the relaxation times in Table 5.2 in the sequence o-xylene, mesitylene, p-diethylbenzene, durene and hexamethylbenzene shows increasing lengthening of the relaxation time at 100 K, their respective values being 7.1×10^{-3} , 4.9×10^{-2} , 7.9×10^{-2} , 8.1 and 3.2×10^7 s. The increment in the relaxation time with increasing size of the molecules is quite significant and more obvious than is the case for ΔH_E along the same sequence. This is what would be expected for a molecular process where τ , in particular, increases appreciably with increasing size for a given shape (16).

n-Propylbenzene and isopropylbenzene, having fairly similar shape and size, exhibit low temperature dielectric absorption in a similar range of temperature. These two compounds are well known as being able to exist as supercooled liquids. The glass transition temperature

(T_g) of n-propylbenzene is 123 K (see next Chapter) and for isopropylbenzene it is 127 K (9,17). So, one would expect a β -relaxation near $0.75 T_g$ at 1 kHz (9). This is what we observed in both the compounds. Energy barrier of 15 kJ mol^{-1} has been observed for both the compounds in these low temperature relaxations which may be attributed to molecular relaxation processes.

Our result for isopropylbenzene is in contrast to that observed by Johari and Goldstein (17). These authors also indicated the presence of β -relaxation over the temperature region 109-138 K but with an Arrhenius energy barrier of 33 kJ mol^{-1} which they interpreted as the hindered rotation of the isopropyl group about the C-C bond.

Petro and Smyth (18) and Crossley and Walker (5) have also studied isopropylbenzene at microwave region. Their results showed an energy barrier of $\sim 10.5 \text{ kJ mol}^{-1}$ for molecular rotation. However, our results differ from this because of the difference of macroscopic viscosity at the different temperatures.

The support of our result for isopropylbenzene

can also be found from the result of p-cymene, a compound having a methyl group in the para position of isopropylbenzene (see Table 5.2). Moreover, a significant variation in τ and ΔG_E values in the low temperature range (~ 100 K), is evident (Table 5.6) between n-propylbenzene, isopropylbenzene and p-cymene. This is what one would expect for a molecular relaxation process where both the parameters increase with increasing size for a given shape (16).

The support of low temperature absorption for n-propylbenzene, isopropylbenzene and p-cymene as molecular relaxation process can also be found from the negative ΔS_E values; as mentioned earlier, negative ΔS_E values are observed for molecular rotation of a number of rigid molecules.

Figure 5.11(a) shows the loss factor versus temperature plot for 1-methylnaphthalene which clearly indicates the overlapping of two relaxation processes. The Eyring plot of these relaxations yields an enthalpy of activation, $\Delta H_E = 33 \pm 5 \text{ kJ mol}^{-1}$ and entropy of activation $22 \pm 32 \text{ J K}^{-1} \text{ mol}^{-1}$ with a clear indication of

two processes (Figure 5.12). Separating the lower and higher temperature region of the Eyring plot, yields ΔH_E and ΔS_E values of 33 kJ mol^{-1} and $22 \text{ J K}^{-1} \text{ mol}^{-1}$ for lower temperature process and 49 kJ mol^{-1} and $114 \text{ J K}^{-1} \text{ mol}^{-1}$ for higher temperature process, respectively.

A similar dielectric relaxation behaviour (Figure 5.11(b)) was observed in 1-chloronaphthalene, a fairly similar sized and shaped molecule (see Chapter VII). Two processes, one being overlapped with the other, were found in the temperature range of 91 - 139 K and 128 - 158 K, with the enthalpy of activation 16 and 25 kJ mol^{-1} , respectively. Since 1-chloronaphthalene is a rigid molecule, these two relaxations could be accounted for molecular processes in two different solid phases.

Dielectric relaxation of 1-methylnaphthalene seeks a similar explanation. The evidence of phase change is found from the high dielectric loss factor ($\epsilon'' \approx 40 \times 10^{-3}$) which cannot be expected from such a weakly polar compound (0.35 D). Near phase transition random movement of dipoles occurs which could give rise to high dielectric loss factor.

Since the relaxation behaviour was observed at higher temperatures (152 - 190 K), higher enthalpy of activation for molecular relaxation would not seem unreasonable for this molecule.

1,5-Dimethylnaphthalene shows low temperature (103 - 131 K) relaxation with an Eyring enthalpy of activation of $17 \pm 2 \text{ kJ mol}^{-1}$ and an entropy of activation of $-24 \pm 13 \text{ J K}^{-1} \text{ mol}^{-1}$. A similar value of enthalpy of activation ($\Delta H_E = 16 \text{ kJ mol}^{-1}$) was found for the low temperatures (91 - 139 K) molecular relaxation of 1-chloronaphthalene. The volume swept-out by 1,5-dimethylnaphthalene and by 1-chloronaphthalene for molecular reorientation will almost be the same. So, for molecular rotation for these two molecules one would expect a similar ΔH_E value, which is actually observed. The observed low temperature relaxation of 1,5-dimethylnaphthalene may, therefore, be assigned to molecular rotation; the support of this view can also be found from negative ΔS_E values.

Figure 5.17 shows an Eyring rate plot of 2-methylnaphthalene, which yields an energy barrier of 16 kJ mol^{-1} . This value is in agreement with the

previous microwave measurement of 2-methylnaphthalene in Nujol ($\Delta H_E = 14.2 \text{ kJ mol}^{-1}$) for molecular rotation (19).

A linear relation between ΔH_E and ΔS_E for dipole relaxation processes in polymers was indicated by Davies (20) and has been supported by much further data (11,15). Davies and Swain (11) reported the following equation for intramolecular dipole relaxations:

$$\Delta S_E \text{ (J K}^{-1} \text{ mol}^{-1}\text{)} = -173 + 4.2 \Delta H_E \text{ (kJ mol}^{-1}\text{)} \quad \dots(5.1)$$

Higasi (14) examined 120 compounds for which dielectric relaxation had been observed in dilute solutions and found:

$$\Delta S_E \text{ (J K}^{-1} \text{ mol}^{-1}\text{)} = -42 + 2.4 \Delta H_E \text{ (kJ mol}^{-1}\text{)} \quad \dots(5.2)$$

for molecular rotation. Khwaja (21) examined 15 rigid molecules in polystyrene matrices and found to fit ΔH_E and ΔS_E values with the equation:

$$\Delta S_E \text{ (J K}^{-1} \text{ mol}^{-1}\text{)} = -72 + 2.2 \Delta H_E \text{ (kJ mol}^{-1}\text{)} \quad \dots(5.3)$$

A linear regression analysis of nine hydrocarbons (except mesitylene and 1-methylnaphthalene) recorded here yields an equation of:

$$\Delta S_E \text{ (J K}^{-1} \text{ mol}^{-1}\text{)} = -69 + 2.4 \Delta H_E \text{ (kJ mol}^{-1}\text{)} \quad \dots(5.4)$$

for molecular relaxation. This equation is closely similar to Khwaja's equation (5.3) and must be considered strong support for a molecular relaxation process of these rigid molecules. There is no definite theoretical grounds for this correlation. Nevertheless, it could be understood that the larger the activation energy is required for displacing adjacent molecules or groups the larger the local disorder would be.

The distribution parameter, β , of some of the alkylbenzenes (e.g. o-xylene, p-diethylbenzene and durene) are very high which suggest predominantly single relaxation behaviour. Microwave measurement of o-dichlorobenzene (22), a molecule having fairly similar shape and size to o-xylene, shows a single relaxation time or very narrow Cole-Cole distribution parameter ($\alpha \leq 0.03$). High β -value (0.45-0.71) was also found in solid o-dichlorobenzene (see Chapter VII). In this context, the high β -value for o-xylene, p-diethylbenzene and durene,

though observed for a molecular process, would not seem unreasonable. But comparatively low β -values (0.34 - 0.49) for a symmetrical molecule like hexamethylbenzene is unexpected. This may be explained by the fact that a molecule when examined as a solid disc yields a different β -value than when it is examined as powder (23). It is to be noted that hexamethylbenzene was measured as compressed solid disc.

A most interesting correlation between the ionization potential and the values of energy barriers has been found for a number of aromatic hydrocarbons studied here. The relative values of the ionization potential of the different aromatic hydrocarbons may be taken as a measure of the capacity of the molecule to interact where the lower the value the greater the capacity of the molecule to interact. Figure 5.18 shows the plot of ionization potential (24) against the enthalpy of activation for the relaxation process of the hydrocarbons studied here in addition with the n.m.r. result of benzene (25,26) and pyrene (27).

Some of the nonpolar aromatic hydrocarbons show low temperature dielectric absorption. Dielectric absorptions of nonpolar liquids were explained on the

basis of collision-induced dipole (7) which would seem unreasonable in the case of solids where there is little scope for molecular collisions to occur. The fact that these nonpolar compounds show definite dielectric absorption in the solid state, must have resulted from some kind of induced moment, probably quadrupole or octupole induced moment as described in Chapter III which may be of a significant magnitude when the internuclear distances are close as in the solid state.

Depending on this induced moment, we could think of a probable explanation for why some of the non-polar aromatic hydrocarbons exhibit low temperature dielectric absorption whereas the others do not.

The benzene molecule is known to be a plane hexagon of carbon atoms each with a side-bond hydrogen atom in the plane. Re-orientation of benzene molecules in the solid state around their 'hexad axes' was initially discovered by Andrew (28) from solid state n.m.r. studies. This and subsequent studies (25,26) have yielded values for activation energy for the motion in the range 14.6-17.6 kJ mol⁻¹.

Dielectric measurements were not able to detect the presence of low temperature relaxation of the benzene molecule. The dielectric absorptions, which result from dipole orientation, in the case of nonpolar aromatic hydrocarbons, may only arise from the moment induced through π -electron cloud of the aromatic ring systems. In the case of benzene molecule, the induced moment at such a low temperature (at higher temperature co-operative motion has been detected, see next Chapter), at which the molecular motion is supposed to be present, is not sufficient enough which our measuring device could detect. The higher the electron density in the aromatic ring the higher is the possibility of creation of induced dipole moment, and hence the dielectric absorption. The support of this view can be found from the results of all aromatic hydrocarbons studied here.

p-Xylene, a nonpolar compound, having two methyl groups at the 1- and 4-positions in the benzene ring, does not show low temperature secondary relaxation, though in this case the electron density is higher than that of the π -electrons of the benzene ring itself. Dielectric study of p-chlorotoluene, a polar molecule of fairly similar shape and size, indicates the presence

of molecular rotation at low temperatures (29).

Low temperature molecular relaxation was also not found in m-xylene (0.31 D), which has a slightly lower dipole moment than o-xylene (0.50 D)(10). The dielectric loss factor of about 3.5×10^{-5} was found for the molecular relaxation of o-xylene. For m-xylene one would expect a lower loss factor which, perhaps, our measuring device could not detect.

When a methyl group of p-xylene is replaced by an ethyl group, which has a slightly higher electron donating capacity than the methyl group, p-ethyltoluene results. This compound still does not show low temperature molecular relaxation. But when one of the methyl group of p-xylene is replaced by an isopropyl group or the methyl group of p-ethyltoluene by another ethyl group, p-cymene and p-diethylbenzene result, both of which show molecular relaxation.

Mesitylene, a so-called nonpolar liquid, having an extra methyl group in the 5-position of m-xylene and thereby increases the electron density in the aromatic ring, shows a low temperature molecular relaxation.

Hexamethylbenzene shows a considerably high dielectric loss factor ($\sim 2.4 \times 10^{-3}$) than durene and mesitylene which might be related to the presence of a higher number of methyl groups in the ring and the enhanced π -electron density.

REFERENCES

1. W.F. Hassell and S. Walker, Trans. Faraday Soc., 62(1966)861.
2. J. Crossley, A.Holt and S. Walker, Tetrahedron, 21(1965)3141.
3. W.F. Hassell and S. Walker, Trans. Faraday Soc., 62(1966)2695.
4. E.N. DiCarlo and C.P. Smyth, J. Am. Chem. Soc., 84(1962)1128.
5. J. Crossley and S. Walker, Can. J. Chem., 46(1968)841.
6. J. Crossley and S. Walker, Can. J. Chem., 46(1968)848.
7. D.H. Whiffen, Trans. Faraday Soc., 46(1950)124.
8. "Lange's Handbook of Chemistry", edited by J.A. Dean, 12th edition, McGraw-Hill Book Company, N.Y., 1979.
9. L. Hayler and M. Goldstein, J. Chem. Phys., 66(1977)736.
10. A.L. McClellan, "Tables of Experimental Dipole Moments", Vol. 2, Rahara Enterprises, Calif., USA, 1974.
11. M. Davies and J. Swain, Trans. Faraday Soc., 67(1971)1637.
12. M.A. Kashem, Private Communication, This Laboratory.
13. A. Turney, Proc. Instn. elect. Engrs., 11A, 100, 46, 1953.
14. K. Higasi, "Dielectric Relaxation and Molecular Structure", Research Institute of Applied Electricity, Sapporo, Japan, 12, 1961.

15. M. Davies and A. Edwards, *Trans. Faraday Soc.*, 63(1967)2163.
16. S.P. Tay and S. Walker, *J. Chem. Phys.*, 63(1975)1634.
17. G.P. Johari and M. Goldstein, *J. Chem. Phys.*, 53(1970)2372.
18. A.J. Petro and C.P. Smyth, *J. Am. Chem. Soc.*, 79(1957)6142.
19. E.L. Grubb and C.P. Smyth, *J. Am. Chem. Soc.*, 83(1961)4122.
20. M. Davies, *Quart. Rev.*, 8(1954)250.
21. H.A. Khwaja, M.Sc. Thesis, Lakehead University, Thunder Bay, Ontario, Canada, 1977.
22. A. Mansingh and D.B. McLay, *J. Chem. Phys.*, 54(1971)3322.
23. P.G. Hall and G.S. Horsfall, *J. Chem. Soc. Faraday II*, 69(1973)1071.
24. V.I. Vedeneyev, L.V. Gurvich, V.N. Kondrat'yev, V.A. Medvedev and Ye.L. Frankevich, "Bond Energies, Ionization Potentials and Electron Affinities", St. Martin's Press, New York, 1966.
25. J.E. Anderson, *J. Chem. Phys.*, 43(1956)3575.
26. Y.I. Rosenberg and N.E. Ainbinder, *Soviet Phys. Solid State*, 12(1970)641.
27. C.A. Fyfe, D.F.R. Gilson and K.H. Thompson, *Chem. Phys. Lett.*, 5(1970)215.
28. E.R. Andrew, *J. Chem. Phys.*, 18(1950)607.
29. S.P. Tay, Ph.D. Thesis, University of Salford, England, 1977.

TABLE 5.1: Fuoss-Kirkwood Analysis Parameters, Cole-Cole ϵ_∞ and apparent dipole moments for some aromatic hydrocarbons

T(K)	$10^6 \tau$ (s)	$\log f_{\max}$	β	$10^3 \epsilon''_{\max}$	ϵ_∞	μ (D)
<u>o-Xylene</u>						
101.5	5496.6	1.462	1.00	0.030	-	-
103.9	3337.6	1.678	1.00	0.032	-	-
106.3	1981.7	1.905	1.00	0.032	-	-
110.7	1024.3	2.191	1.00	0.037	-	-
114.8	519.2	2.486	0.97	0.034	-	-
118.4	304.4	2.718	0.92	0.038	-	-
<u>Mesitylene</u>						
113.3	5077.8	1.496	0.57	0.083	-	-
115.4	4175.9	1.581	0.46	0.075	-	-
117.9	2490.1	1.806	0.45	0.078	-	-
120.8	1877.5	1.928	0.66	0.094	-	-
<u>p-Diethylbenzene</u>						
110.5	9064.5	1.245	0.96	0.19	-	-
113.5	4464.8	1.552	1.00	0.18	-	-
117.5	2187.9	1.862	0.96	0.21	-	-
120.1	1372.3	2.064	1.00	0.22	-	-
124.5	707.4	2.352	0.81	0.23	-	-
128.7	421.1	2.577	1.00	0.34	-	-
<u>Durene</u>						
146.7	664.9	2.379	1.00	0.13	-	-
151.0	348.1	2.660	1.00	0.12	-	-
155.4	189.1	2.925	1.00	0.14	-	-
158.4	182.8	2.940	1.00	0.15	-	-
160.8	103.4	3.187	0.91	0.16	-	-
164.2	72.8	3.339	0.75	0.17	-	-
169.2	42.4	3.574	0.77	0.15	-	-

TABLE 5.1: continued....

T(K)	$10^6 \tau$ (s)	$\log f_{\max}$	β	$10^3 \epsilon''_{\max}$	ϵ_{∞}	μ (D)
<u>Hexamethylbenzene</u>						
180.1	4843.6	1.517	0.34	2.43	2.659	0.096
185.3	2039.6	1.892	0.34	2.17	2.656	0.092
189.6	894.7	2.250	0.35	1.91	2.654	0.087
194.5	420.9	2.578	0.36	1.68	2.652	0.081
199.0	247.5	2.808	0.42	1.64	2.651	0.075
204.5	126.6	3.099	0.43	1.56	2.649	0.073
210.4	71.3	3.348	0.44	1.47	2.644	0.071
214.9	45.7	3.541	0.49	1.42	2.641	0.067
<u>n-Propylbenzene</u>						
94.3	533.8	2.474	0.30	0.87	2.491	0.043
97.3	376.9	2.626	0.26	0.88	2.492	0.047
102.6	119.2	3.126	0.29	0.95	2.492	0.048
104.7	74.2	3.331	0.31	0.94	2.493	0.046
106.8	53.5	3.473	0.31	0.97	2.492	0.048
111.6	24.0	3.821	0.34	0.99	2.493	0.047
113.6	19.7	3.906	0.37	0.99	2.494	0.045
115.8	15.2	4.018	0.38	1.0	2.494	0.046
117.6	10.4	4.183	0.36	1.00	2.494	0.047
<u>iso-Propylbenzene</u>						
102.1	644.4	2.393	0.23	1.57	2.464	0.069
104.0	504.3	2.499	0.24	1.62	2.464	0.070
106.3	304.3	2.718	0.25	1.67	2.464	0.070
109.5	216.7	2.866	0.24	1.73	2.464	0.074
112.2	121.6	3.117	0.25	1.77	2.465	0.074
114.2	95.3	3.222	0.24	1.80	2.465	0.077
117.2	55.2	3.460	0.25	1.88	2.465	0.078
119.8	40.9	3.590	0.25	1.90	2.465	0.079
122.8	26.2	3.782	0.24	1.97	2.465	0.083
125.9	22.7	3.845	0.24	2.07	2.466	0.086
<u>p-Cymene</u>						
99.2	2172.1	1.865	0.22	0.54	2.426	0.044
103.5	1051.8	2.180	0.23	0.56	2.424	0.045
107.2	521.8	2.484	0.24	0.58	2.424	0.045
111.4	263.8	2.781	0.22	0.59	2.424	0.049
115.4	134.8	3.072	0.22	0.61	2.424	0.050
119.8	73.0	3.338	0.22	0.63	2.425	0.052
123.8	53.2	3.475	0.23	0.65	2.425	0.053

TABLE 5.1: continued...

T (K)	$10^6 \tau$ (s)	$\log f_{\max}$	β	$10^3 \epsilon''_{\max}$	ϵ_{∞}	μ (D)
<u>1-Methylnaphthalene</u>						
151.6	3946.2	1.606	0.29	26.75	2.725	0.29
156.4	1659.5	1.982	0.29	28.46	2.722	0.30
162.0	651.5	2.388	0.31	30.52	2.724	0.31
167.9	292.2	2.736	0.32	33.06	2.727	0.32
173.2	217.7	2.864	0.28	36.59	2.718	0.37
176.7	151.1	3.023	0.30	40.27	2.725	0.38
180.1	81.8	3.289	0.40	46.86	2.749	0.35
185.1	27.0	3.770	0.49	52.48	2.762	0.34
190.2	10.2	4.192	0.50	53.00	2.766	0.34
<u>1,5-Dimethylnaphthalene</u>						
102.6	6187.9	1.410	0.54	0.28	-	-
106.9	1920.9	1.918	0.67	0.28	-	-
111.8	936.5	2.230	0.65	0.28	-	-
115.6	441.1	2.557	0.56	0.28	-	-
119.2	308.7	2.712	0.56	0.28	-	-
125.6	100.5	3.200	0.52	0.26	-	-
131.2	53.4	3.475	0.76	0.23	-	-
<u>2-Methylnaphthalene</u>						
110.1	3772.0	1.625	0.31	0.61	-	-
115.0	1804.8	1.945	0.29	0.64	2.680	0.040
118.4	1070.9	2.172	0.29	0.66	2.680	0.041
122.2	610.1	2.416	0.28	0.68	2.680	0.043
126.9	355.5	2.651	0.27	0.70	2.680	0.046
130.4	221.1	2.857	0.26	0.71	2.681	0.047
135.2	113.7	3.146	0.26	0.72	2.687	0.049
139.2	74.8	3.328	0.25	0.72	2.682	0.050
145.1	47.0	3.529	0.26	0.71	2.683	0.050

TABLE 5.2:

RELAXATION TIMES AND EYRING ANALYSIS RESULTS FOR SOME AROMATIC HYDROCARBONS

MOLECULE	T(K)	τ (s)			ΔG_E (kJ mol ⁻¹)			ΔH_E (kJ mol ⁻¹)	ΔS_E (J K ⁻¹ mol ⁻¹)
		100 K	150 K	200 K	100 K	150 K	200 K		
o-Xylene	102-118	7.1×10^{-3}	7.7×10^{-6}		19.5	21.2		16.0 ± 0.7	-35 ± 6
Mesitylene	113-121	4.9×10^{-2}	8.1×10^{-5}		21.1	24.1		15.0 ± 5.1	-61 ± 44
p-Diethylbenzene	111-129	7.9×10^{-2}	2.7×10^{-5}		21.5	22.8		18.9 ± 17	-26 ± 14
Durene	147-169	8.1	4.0×10^{-4}	2.6×10^{-6}	25.3	26.1	27.0	23.7 ± 10	-16 ± 7
Hexamethylbenzene	180-215	3.2×10^7	1.3	2.4×10^{-4}	38.0	36.2	34.5	41.4 ± 2.6	+35 ± 13
n-propylbenzene	94-118	1.9×10^{-4}	3.1×10^{-7}		16.4	17.2		15.0 ± 0.7	-15 ± 7
isopropylbenzene	102-126	9.9×10^{-4}	1.7×10^{-6}		17.8	19.3		15.0 ± 0.5	-29 ± 0.7
p-cymene	99-120	1.9×10^{-3}	2.5×10^{-6}		18.4	19.8		15.6 ± 0.5	-28 ± 5
1-Methylnaphthalene	152-190		5.7×10^{-3}	6.1×10^{-6}		29.4	28.4	32.7 ± 5.4	+22 ± 32
1,5-Dimethyl-naphthalene	103-131	9.3×10^{-3}	6.1×10^{-6}		19.7	20.9		17.3 ± 1.5	-24 ± 13
2-Methylnaphthalene	110-145	2.5×10^{-2}	2.7×10^{-5}		20.5	22.8		16.0 ± 0.4	-45 ± 3

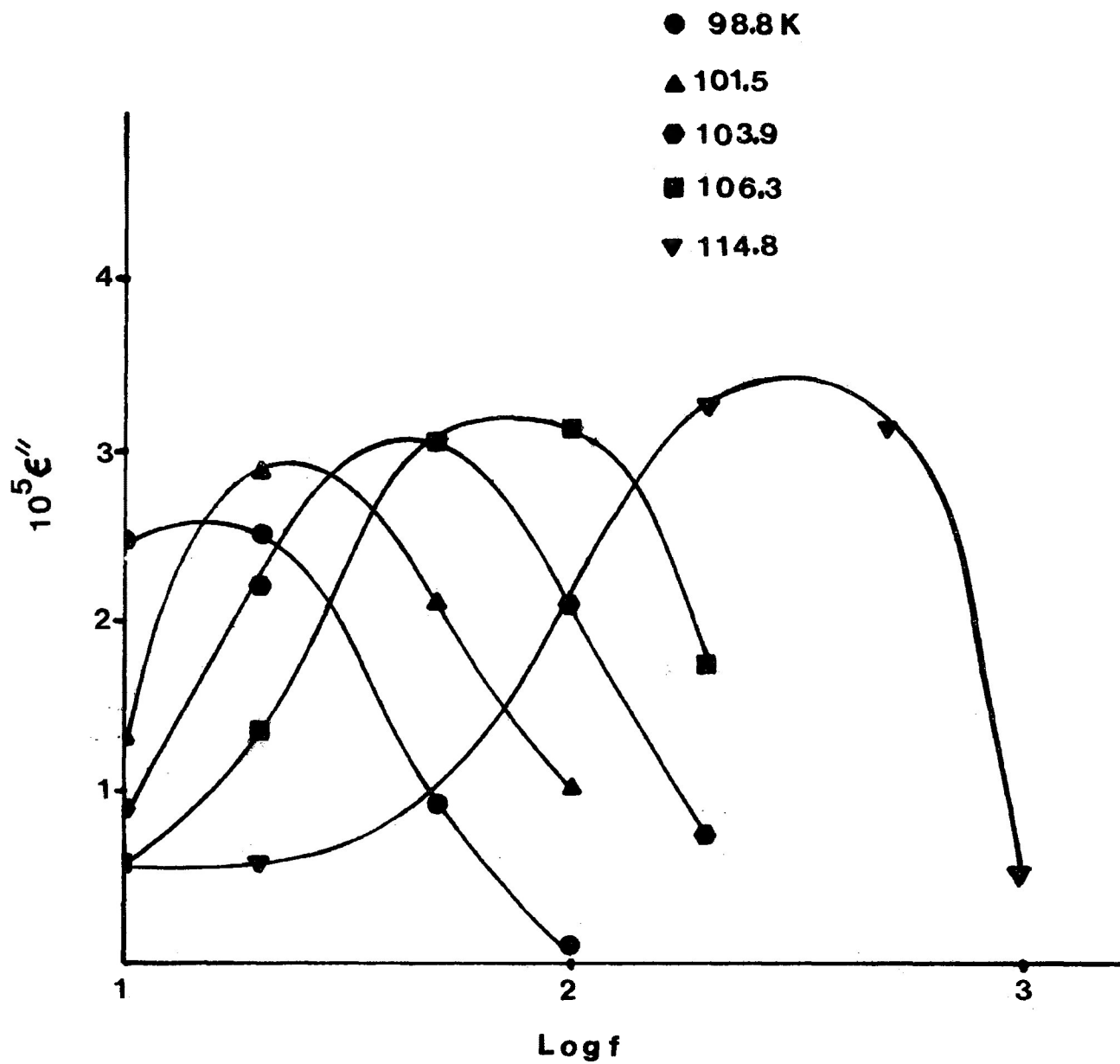


FIGURE 5.1: Dielectric loss factor ϵ'' versus log frequency for o-xylene.

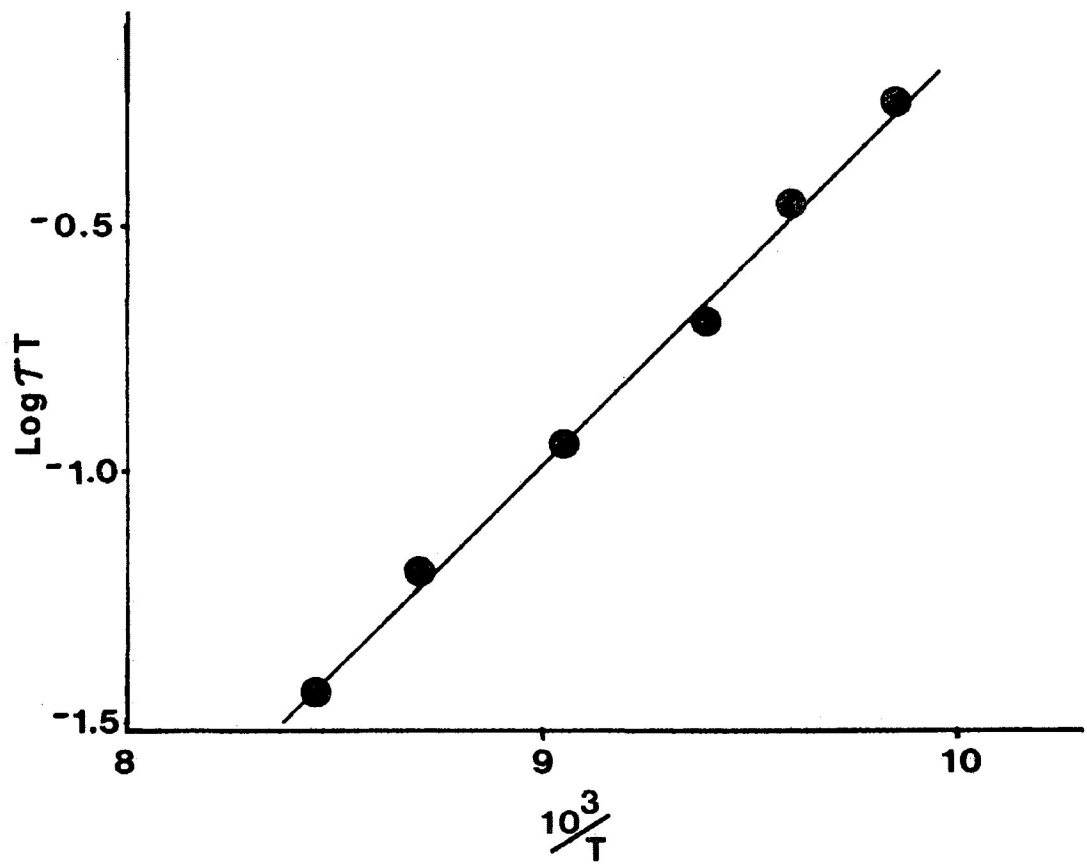


FIGURE 5.2: Eyring plot of $\log(\tau T)$ versus $\frac{1}{T}$ for o-xylene

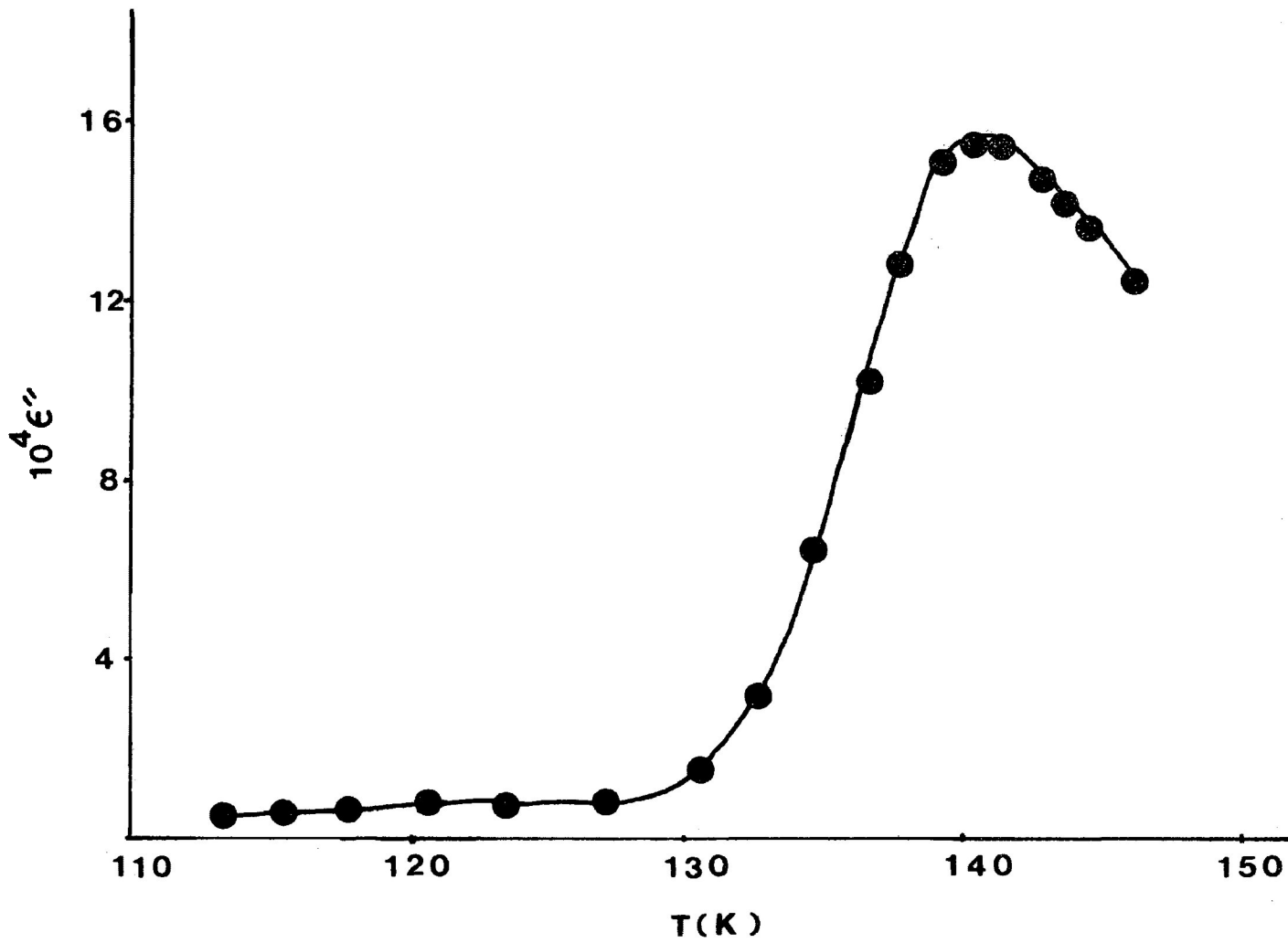


FIGURE 5.3: Dielectric loss factor ϵ'' versus temperature for mesitylene

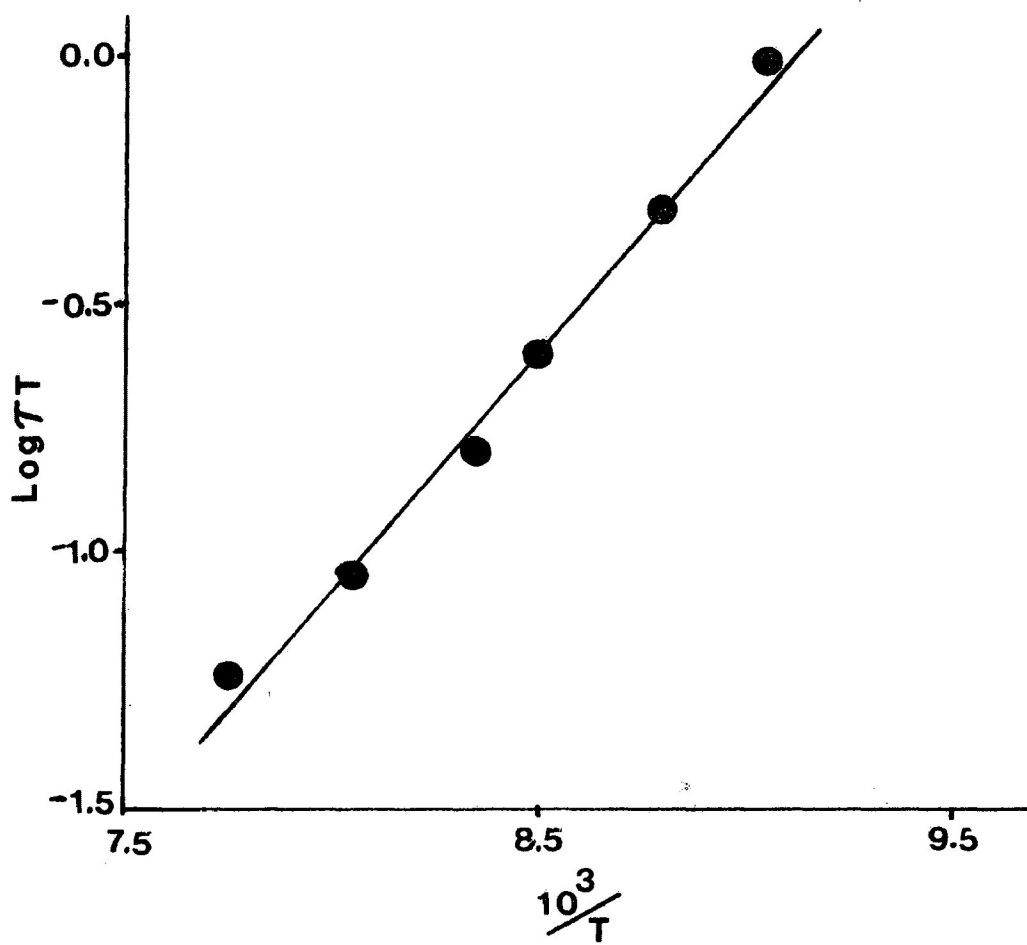


FIGURE 5.4: Eyring plot of $\log(\tau T)$ versus $\frac{1}{T}$ for p-diethylbenzene

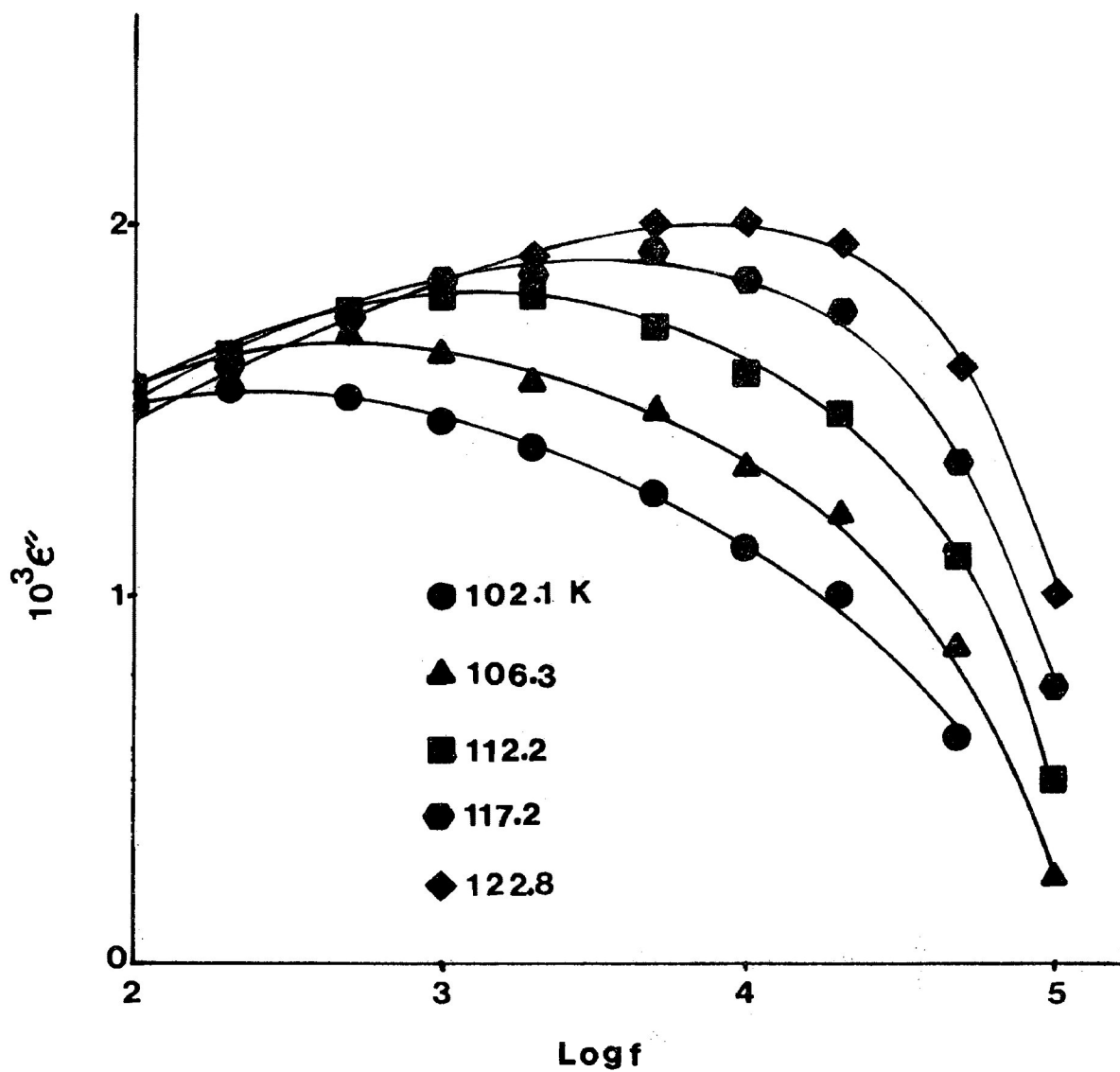


FIGURE 5.5: Dielectric loss factor ϵ'' versus log frequency for isopropylbenzene

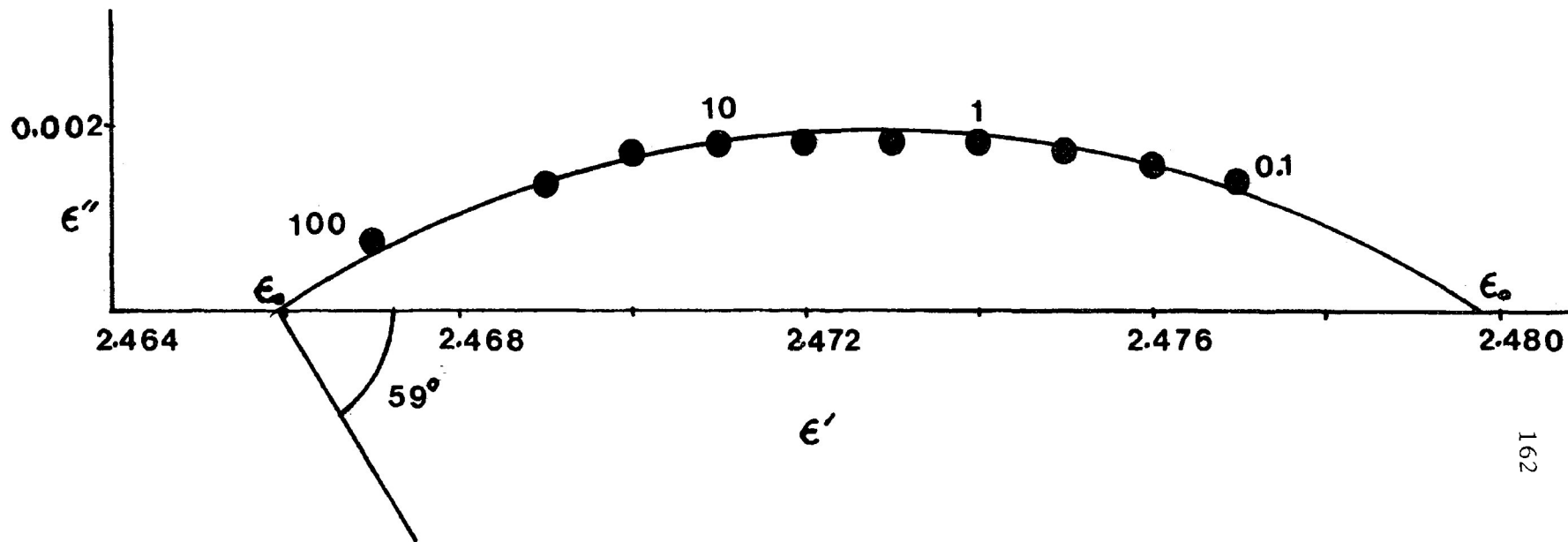


FIGURE 5.6: Cole-Cole plot for isopropylbenzene at 117.2 K.

Numbers beside points are frequencies in KHz

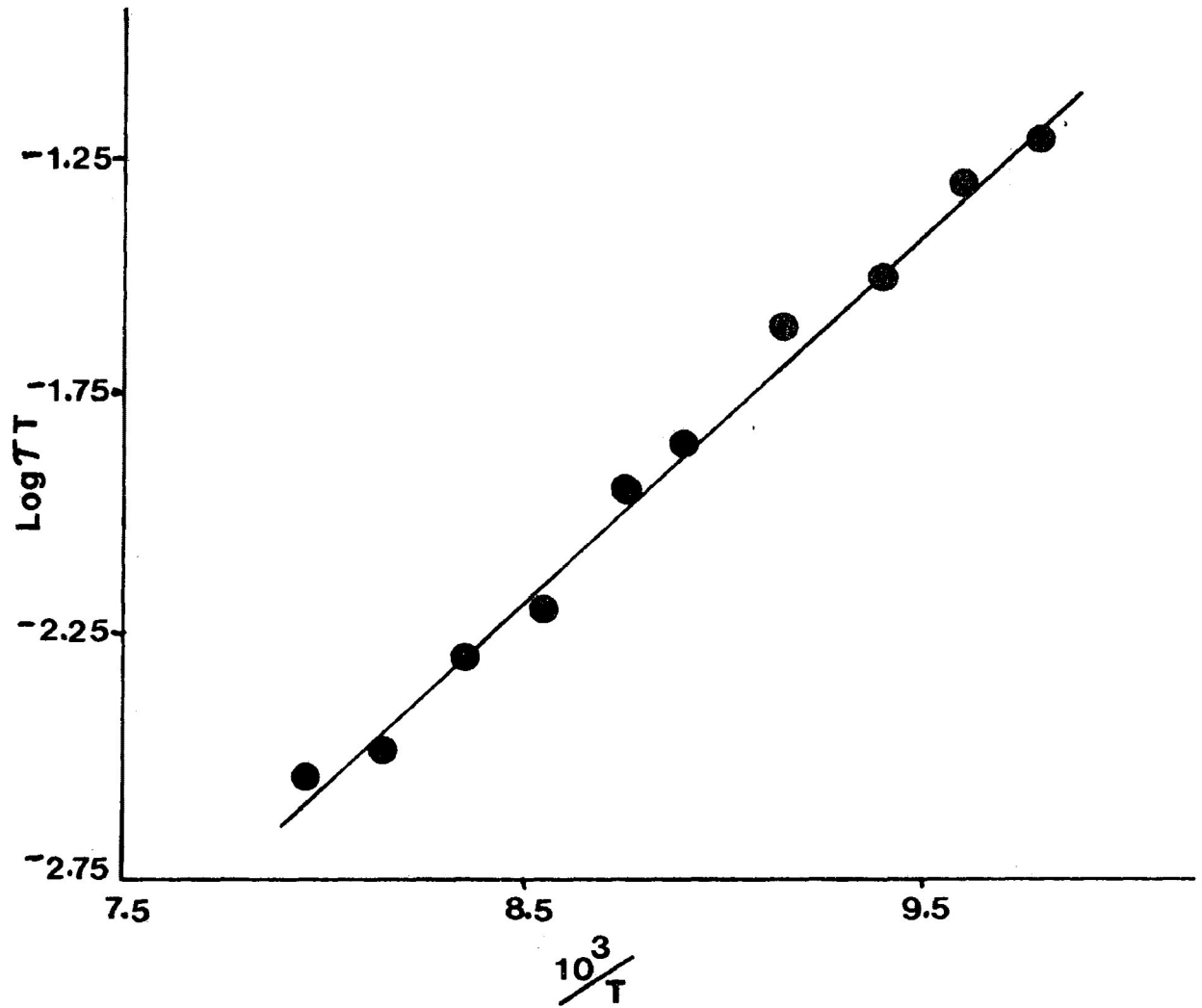


FIGURE 5.7: Eyring plot of $\log(\tau T)$ versus $\frac{1}{T}$ for isopropylbenzene

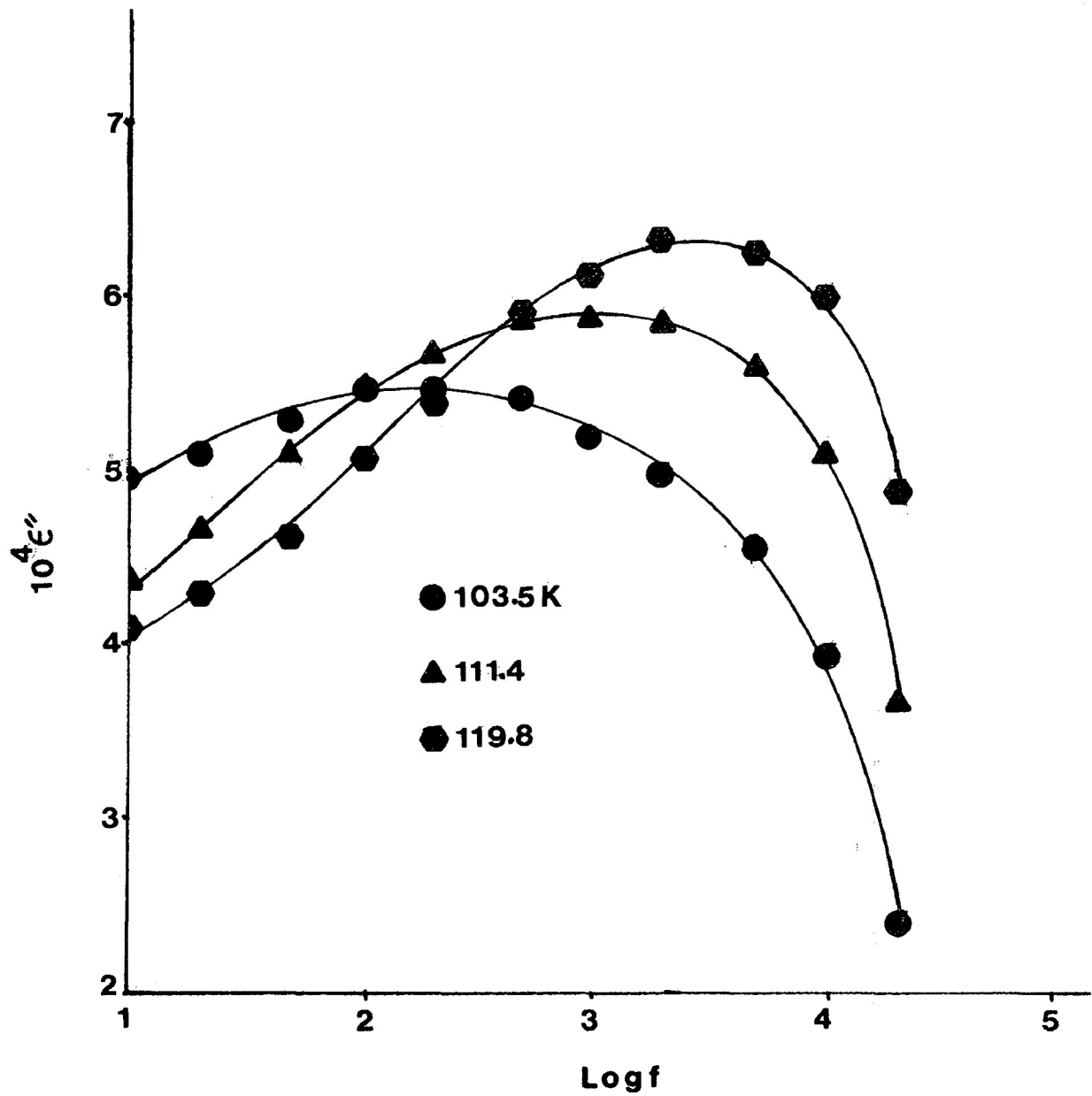


FIGURE 5.8: Dielectric loss factor ϵ'' versus log frequency for p-cymene

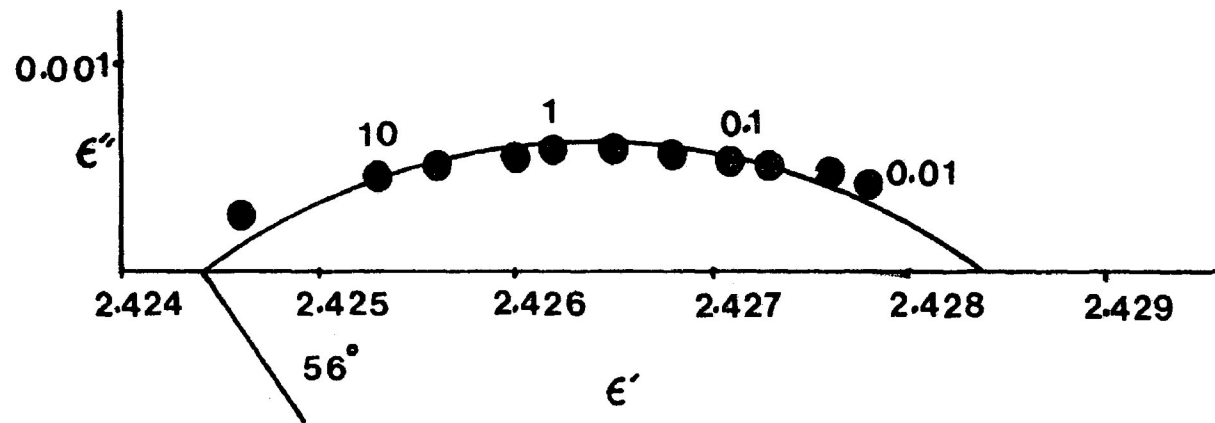


FIGURE 5.9: Cole-Cole plot for p-cymene at 107.2 K.
 Numbers beside points are frequencies in KHz

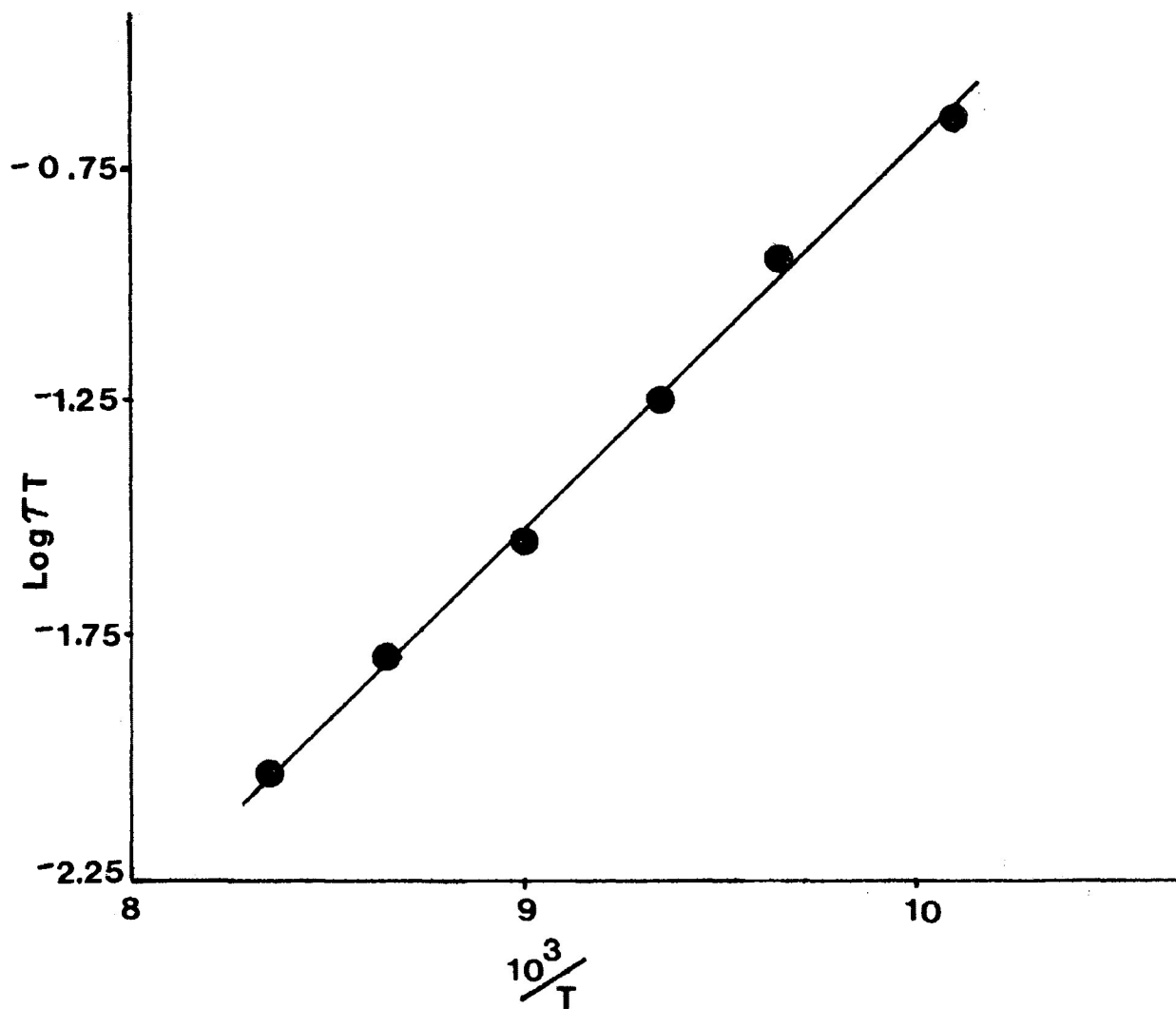


FIGURE 5.10: Eyring plot of $\log(\tau T)$ versus $\frac{1}{T}$ for p-cymene

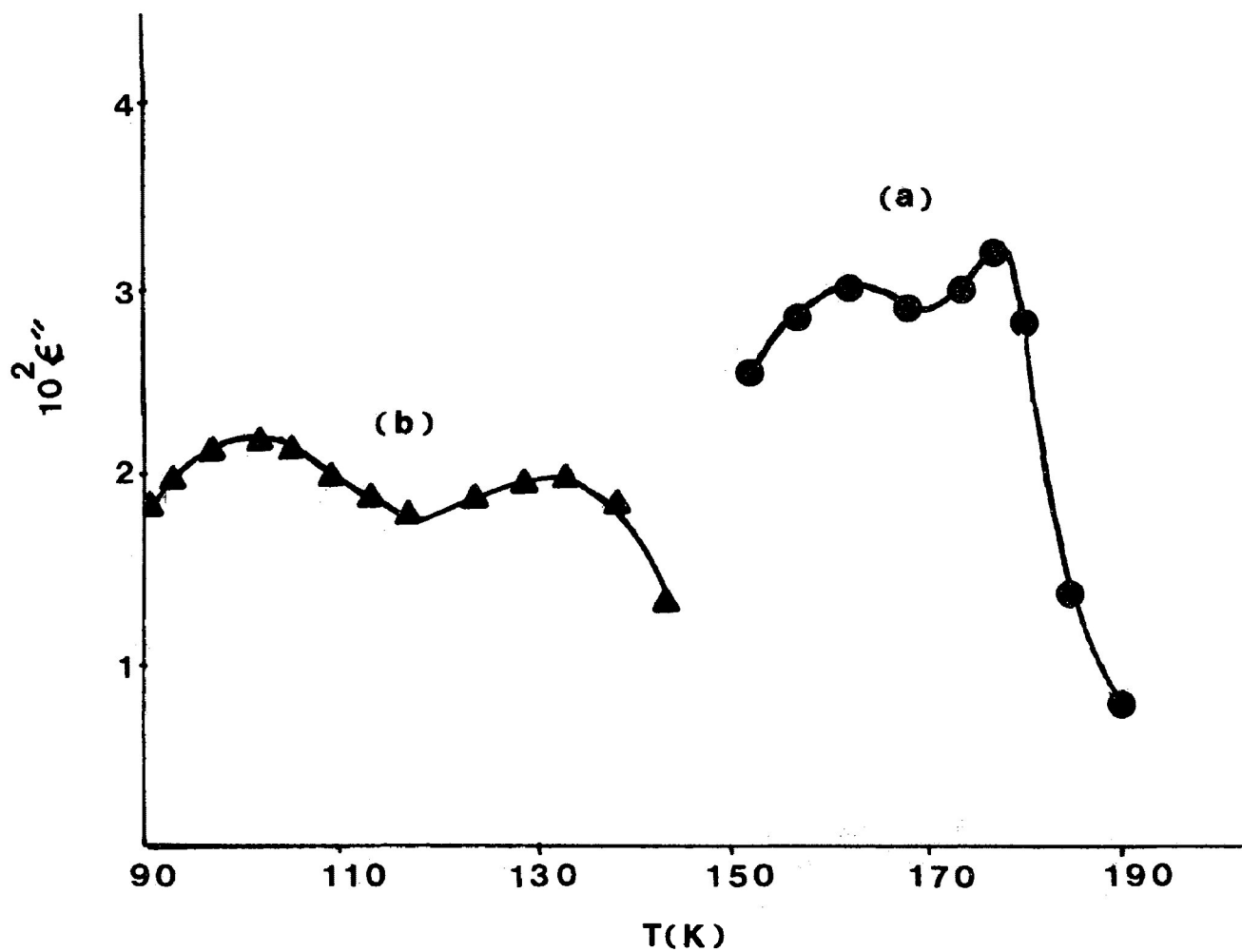


FIGURE 5.11: Dielectric loss factor ϵ'' versus temperature for (a) 1-methylnaphthalene, and (b) 1-chloronaphthalene, at 102 Hz.

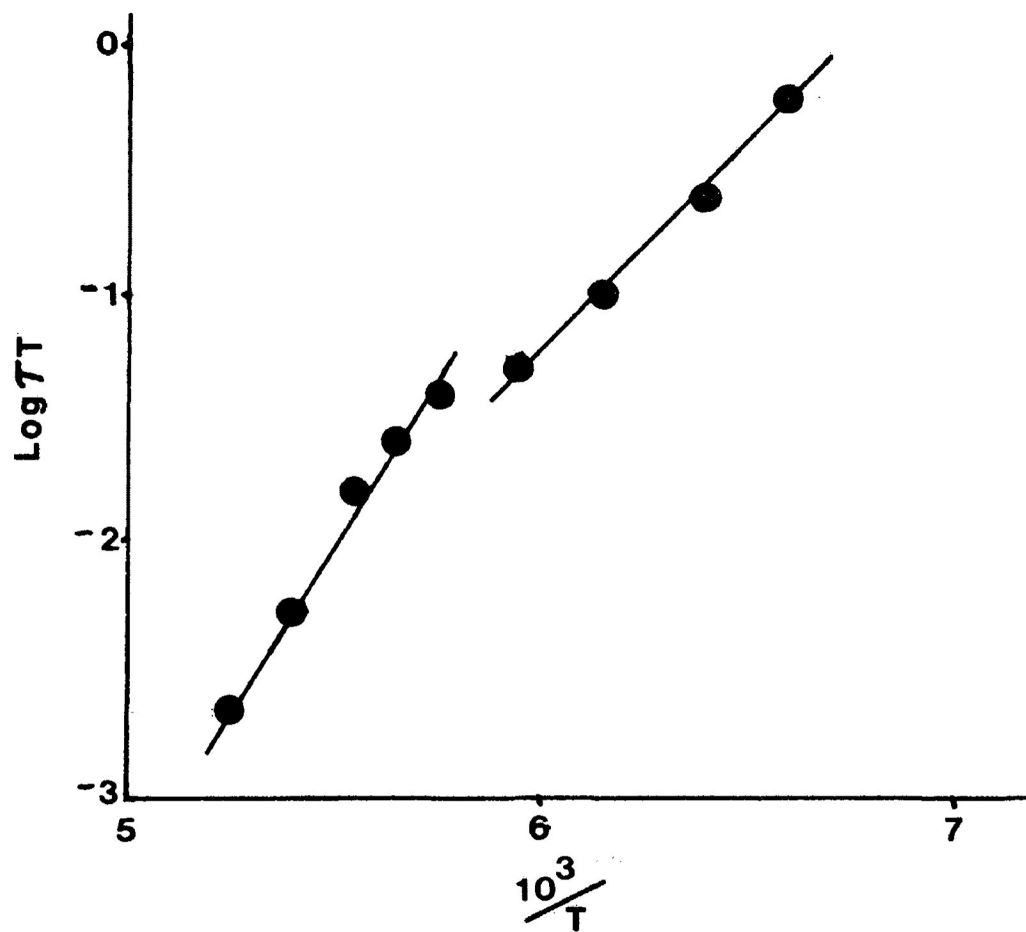


FIGURE 5.12: Eyring plot of $\log(\tau T)$ versus $\frac{1}{T}$ for 1-methylnaphthalene

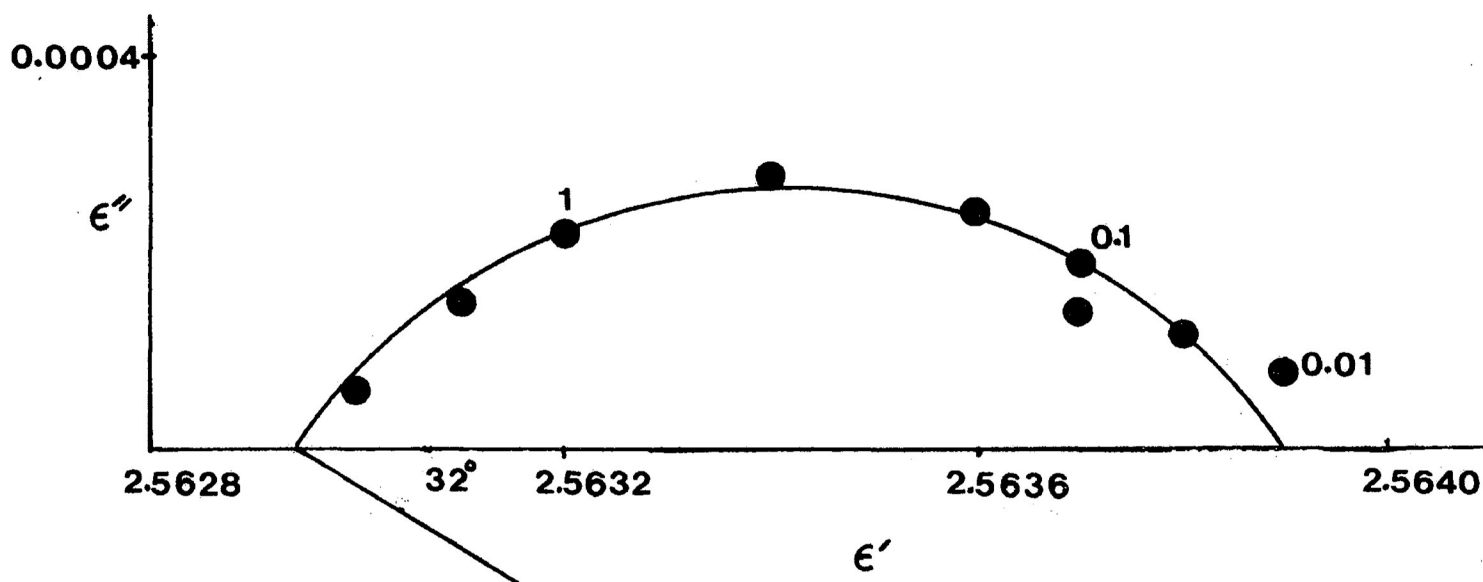


FIGURE 5.13: Cole-Cole plot for 1,5-dimethylnaphthalene at 115.6 K

Numbers beside points are frequencies in kHz.

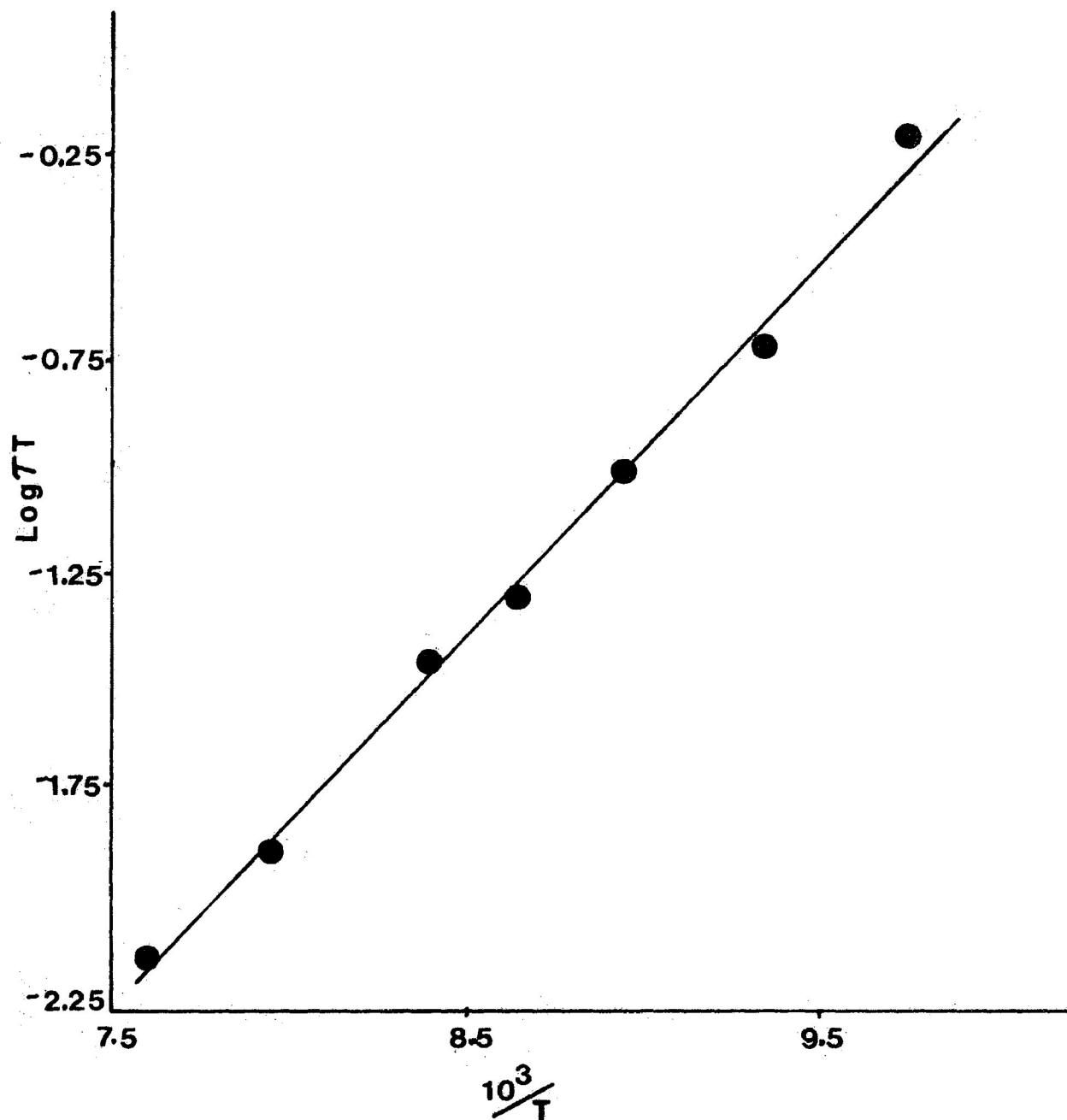


FIGURE 5.14: Eyring plot of $\log(\tau T)$ versus $\frac{1}{T}$ for 1,5-dimethylnaphthalene

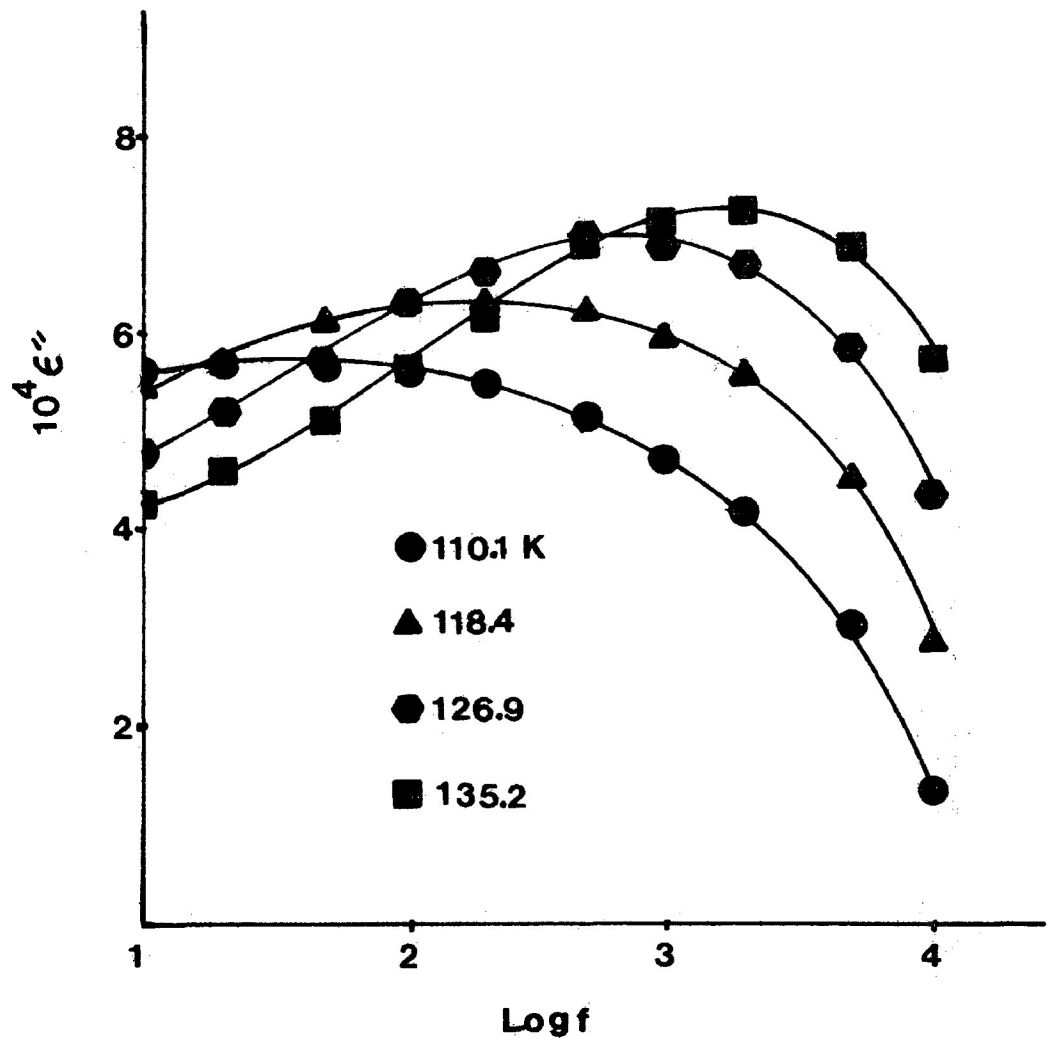


FIGURE 5.15: Dielectric loss factor ϵ'' versus log frequency for 2-methylnaphthalene

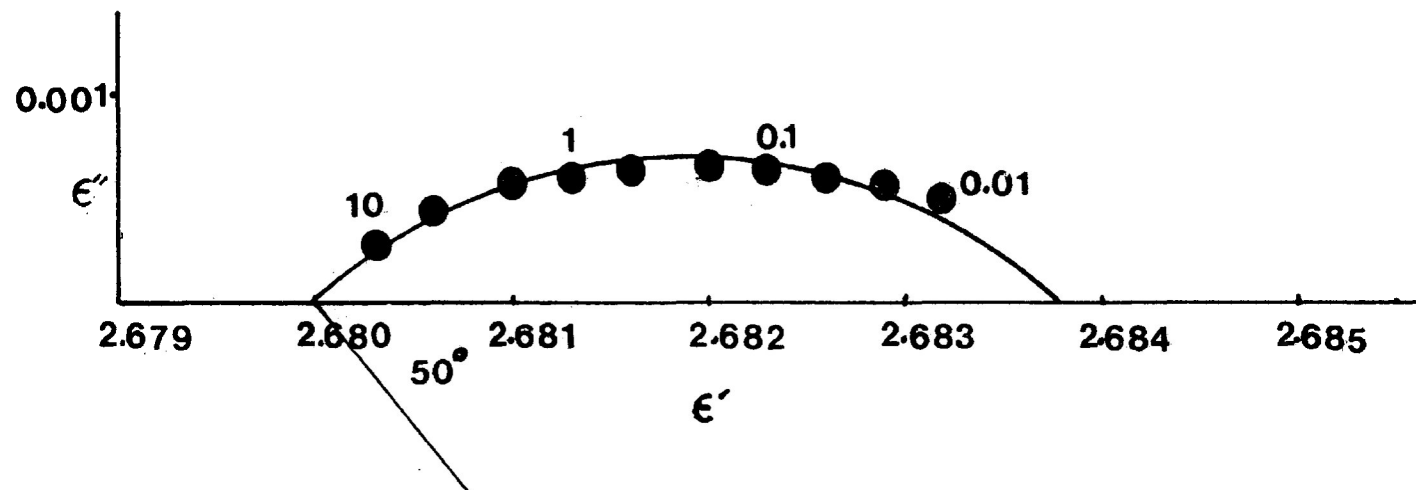


FIGURE 5.16: Cole-Cole plot for 2-methylnaphthalene at 118.4 K
Numbers beside points are frequencies in kHz.

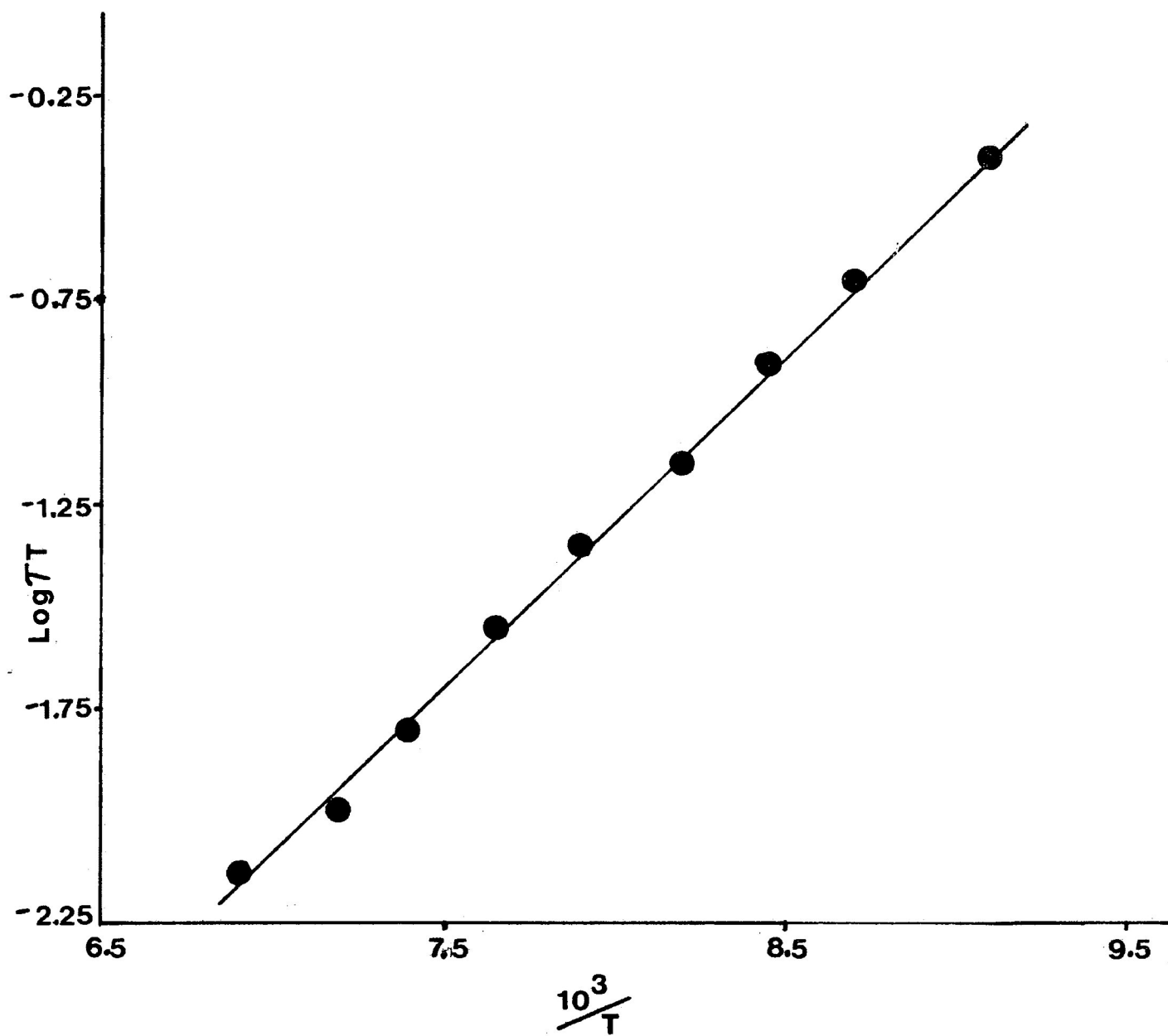


FIG URE

FIGURE 4.17: Eyring plot of $\log(\tau T)$ versus $\frac{1}{T}$ for 2-methylnaphthalene

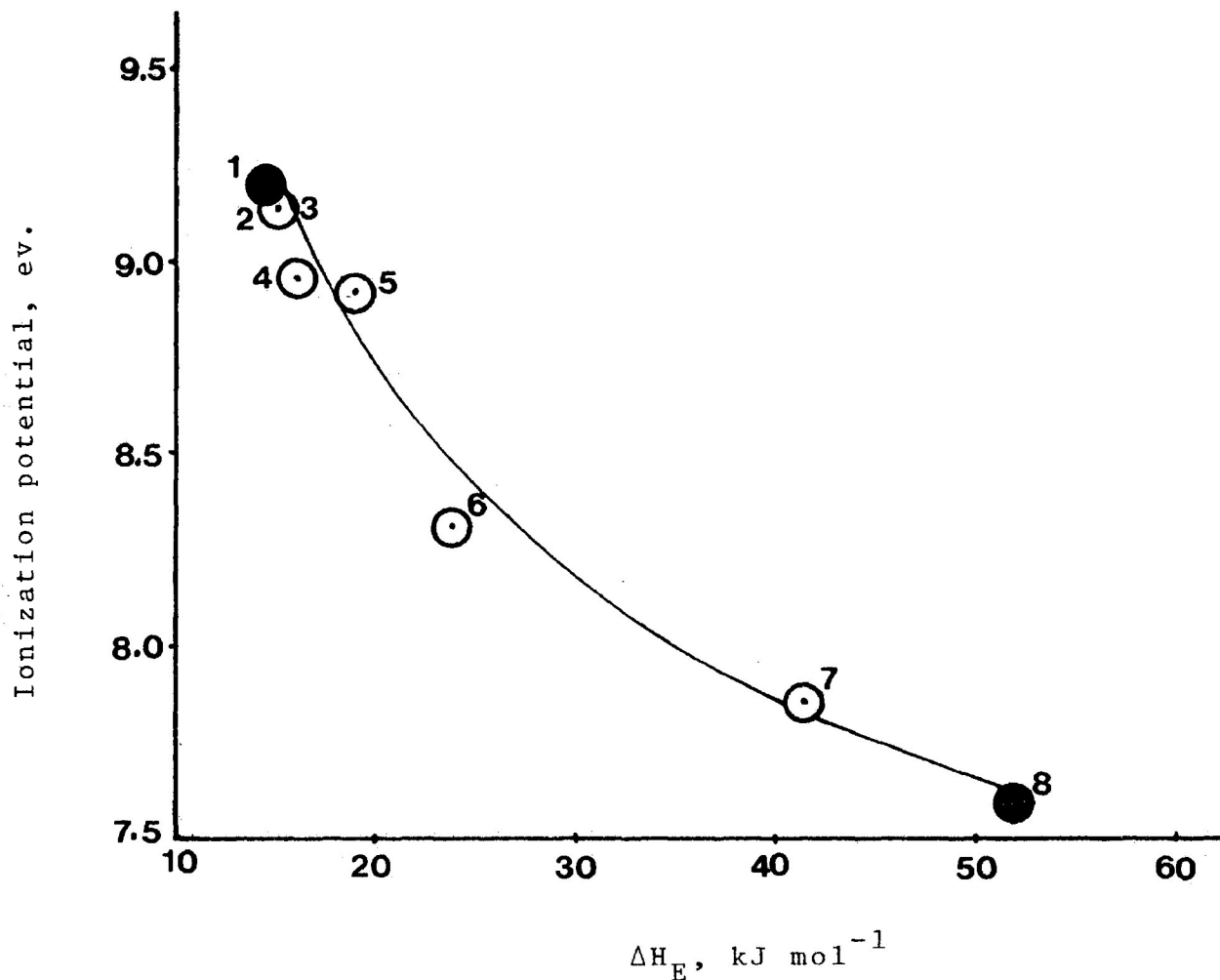


FIGURE 5.18: Plot of Eyring enthalpy of activation versus ionization potential of the following aromatic hydrocarbons:

1. Benzene (n.m.r. results) (ref. 25,26)
2. n-propylbenzene
3. Isopropylbenzene
4. o-xylene
5. p-diethylbenzene
6. durene
7. hexamethylbenzene
8. pyrene (n.m.r. result) (ref. 27)

C H A P T E R V I

CO-OPERATIVE RELAXATION PROCESSES OF
SOME HYDROCARBONS

INTRODUCTION

Two classes of organic liquids exhibit slow molecular reorientation: (i) alcohols and (ii) supercooled liquids (e.g. isomyl bromide or n-propylbenzene) or those nonassociated liquids which do not crystallize (e.g. di-n-butylphthalate) (1). There is a number of dielectric studies on alcohols (2-9) and the interpretation is complicated owing to the presence of hydrogen bonds in these molecules. For systems under (ii), the slow relaxations reflect the co-operative translational and rotational motions of "molecular aggregates". The present chapter is concerned with systems under (ii).

This co-operative motion is similar to the α -process observed in polymeric materials. This type of relaxation arises as a result of microBrownian motions of the dipolar molecules and is characterized (10) by (a) the low frequency (i.e. high temperature) at which this process occurs, (b) its rapid variation with temperature, (c) the breadth and asymmetric nature of the loss curves and (d) a large apparent activation energy.

One of the earlier dielectric works on supercooled isoamylbromide and isobutylbromide was given by Baker and Smyth (11) and noted the similarity to the relaxation of liquid glucose (12) and glycerol (13). Denney (14) made extensive measurements covering wide ranges of frequency and temperature on supercooled isoamylbromide, isobutylchloride, and isobutylbromide. Comprehensive studies were made by Mopsik and Cole (15) on n-octyliodide and by Berberian and Cole (16) on isoamylbromide. Berberian and Cole (16) noted that the various theories which had been proposed to account for the relaxation in such "cold" liquids have the common feature that they invoke co-operative interaction effects.

An important advance was made in this area by Johari and Smyth (17,18) and by Johari and Goldstein (19,20). These authors showed that if crystallization of a medium, made up of small molecules, could be suppressed, then low-frequency relaxations would be observed. They also showed that small rigid molecules could be made to reorient at low frequencies by placing them in a supercooled solvent, e.g. supercooled decalin (17,18,20).

Williams et al (21-25) reported low-frequency studies of a wide range of solutes in supercooled *o*-terphenyl. These studies characterize the dielectric α -process as a function of frequency, temperature, and concentration. The work of Williams and Hains (21,22) was restricted to low solute concentrations (<10%), and thus the co-operative process was dominated by the *o*-terphenyl solvent molecules. Later, Shears and Williams (23,24) studied fluorenone/*o*-terphenyl system up to ~25% concentration of solute and the di-*n*-butylphthalate/*o*-terphenyl system over the entire range from dilute solution to liquid di-*n*-butylphthalate, since the solute does not crystallize.

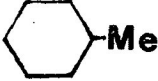
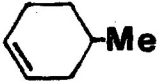

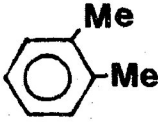
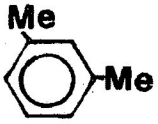
Higasi et al (26) made a dielectric study of a number of molecules in supercooled *o*-terphenyl over the temperature range 283-303 K. They observed relaxation processes with Eyring activation enthalpies ranging from 101 kJ mol⁻¹ for *m*-nitrophenol to 122 kJ mol⁻¹ for anthrone. Their dielectric data being represented by a Davidson-Cole skewed-arc function (27).


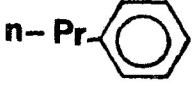
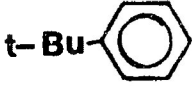
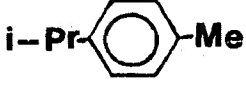
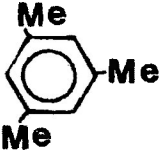


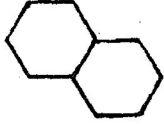
Viscosity studies by Barlow, Lamb, and Matheson

(28) indicated that most alkylbenzenes could be supercooled. Copeland and Denney (29) examined three alkylbenzenes (isopropylbenzene, n-butylbenzene and n-propylbenzene) and found that only the latter could be supercooled sufficiently. They observed the dielectric absorption of n-propylbenzene in the temperature range of 138.3-149.4 K - with an Eyring activation enthalpy of about 80 kJ mol^{-1} . This absorption was also adequately described by the asymmetric Davidson-Cole function. The authors suggested that the relaxation process involves co-operative intermolecular effects similar to those observed for isoamylbromide (16) and n-octyl iodide (15), which also show asymmetric dispersion but tend towards a single relaxation process with increased temperature. These results led the authors to suggest that the earlier microwave data (30,31) on liquid alkylbenzenes around room temperature might also be explained in terms of a co-operative phenomenon.

EXPERIMENTAL RESULTS

The compounds investigated in the present work are:

<u>Number</u>	<u>Name</u>	<u>Structure</u>
1.	2-methylpentane	$\begin{array}{c} \text{CH}_3\text{CH}-\text{CH}_2\text{CH}_2\text{CH}_3 \\ \\ \text{CH}_3 \end{array}$
2.	methylcyclohexane	
3.	4-methylcyclohexene-1	
4.	benzene	
5.	o-xylene	
6.	m-xylene	

7. p-xylene 
8. n-propylbenzene 
9. t-butylbenzene 
10. p-cymene 
11. mesitylene 
12. p-ethyltoluene 
13. p-diethylbenzene 
14. cis-decalin 

All these chemicals were commercially available with sufficient purity. Benzene was reagent-grade thio-

phene free. p-Xylene, p-diethylbenzene and p-cymene were distilled in a 30 theoretical plate spinning band column, and the middle fraction was collected. All the liquids were dried over sodium wire at least 48 hours prior to use. Pyrrole was distilled twice, and the middle fraction was collected. The $\nu_{\text{N-H}}$ frequencies of pyrrole in different hydrocarbons were measured with a Beckmann spectrophotometer IR 4250, and the experimental values were compared with the literature values as shown in Table 6.1.

Where the dielectric data were adequately represented by the Davidson-Cole skewed-arc function, the parameters ϵ_{∞} and β were estimated from such a plot as shown in Chapter II, Figure 2.6. The relaxation time τ_0 was calculated using the equation:

$$\tau_0 = \frac{1}{\omega_{\text{max}}} \tan \left(\frac{1}{1+\beta_{\text{av}}} \cdot \frac{\pi}{2} \right) \quad (6.1)$$

where $\omega_{\text{max}} = 2\pi f_{\text{max}}$, f_{max} is the frequency of maximum absorption obtained from Fuoss-Kirkwood analysis, and β_{av} is the average Davidson-Cole β -values.

In the case where dielectric data were not accurately

described by the asymmetry Davidson-Cole plot, Fuoss-Kirkwood analysis was done.

Table 6.2 summarizes the relaxation parameters, activation energy parameters, maximum loss factors (ϵ''_m) and glass transition temperatures (T_g) for all of the systems. Davidson-Cole and Fuoss-Kirkwood analysis parameters and dipole moments values are shown in Table 6.3.

DISCUSSION

2-Methylpentane is well known for being able to exist as a supercooled liquid (29). This compound exhibits dielectric absorption for a short range of temperature 91.2-95.3 K covering $\log f_m$ 2.541-3.859 with an Eyring enthalpy of activation 52 ± 4 kJ mol⁻¹ and entropy of activation 402 ± 47 J K⁻¹ mol⁻¹. The relaxation process occurs above the glass transition temperature ($T_g \sim 86$ K) of the compound.

Johari and Goldstein (7) observed dielectric relaxation peaks near liquid nitrogen temperature for 3-methylpentane. These authors concluded that the glass

transition temperature (T_g) of this compound was below 77 K and suggested that the observed relaxation behaviour of 3-methylpentane might be due to the co-operative microBrownian motion.

The co-operative motions of some hydrocarbons, e.g. 3-methylpentane ($T_g < 77$ K), n-propylbenzene (29) ($T_g \sim 123$ K), isopropylbenzene ($T_g \sim 127$ K) (20), and o-terphenyl ($T_g \sim 244$ K) (20), are found to occur above their glass transition temperatures (T_g) with high apparent enthalpies of activation (ΔH_E) and entropies of activation (ΔS_E) (in the case of n-propylbenzene, $\Delta H_E \approx 80$ kJ mol⁻¹, and $\Delta S_E \approx 410$ J K⁻¹ mol⁻¹). The present study of 2-methylpentane ($T_g \approx 86$ K), methylcyclohexane ($T_g \approx 93$ K) and 4-methylcyclohexene-1 ($T_g \approx 102$ K) reveals similar dielectric behaviour; in all three cases, the relaxation peaks were observed above the glass transition temperatures.

Dielectric data for co-operative relaxations may be interpreted by the Davidson-Cole skewed-arc function (27). Copeland and Denney (29) studied n-propylbenzene as a supercooled liquid in the temperature region 138.3-149.4 K and interpreted the observed relaxation as co-operative

intermolecular effects. Their dielectric data were adequately represented by the Davidson-Cole function. In this present work n-propylbenzene was also examined for a short temperature range 137.0-142.8 K, having an indication of glass transition temperature (T_g) around 123 K. The dielectric data for this compound agree extremely well with Copeland and Denney's data as is evident from the Eyring (Fig. 6.1) and Davidson-cole (Figure 6.2) plots. Representations of the Davidson-Cole function for co-operative motions are also found in the literature (16,26). Dielectric data for 2-methylpentane, methylcyclohexane, and 4-methylcyclohexene-1 can also be described accurately by the Davidson-Cole skewed-arc function (Fig. 6.3 for 2-methylpentane, Fig. 6.4 for methylcyclohexane, and Fig. 6.5 for 4-methylcyclohexene-1).

Johari and Goldstein (20) observed dielectric loss peaks for pure cis-decalin, a nonpolar hydrocarbon, around 142 K. These authors interpreted this loss as due to the presence of a small amount of impurities such as trans-decalin in their sample. However, pure cis-decalin was examined and dielectric absorption (Fig. 6.6) was observed in the temperature region 140.8-146.4 K,

covering $\log f_m$ 2.341-4.038 which yields an enthalpy of activation $119 \pm 9 \text{ kJ mol}^{-1}$ and an entropy of activation $665 \pm 59 \text{ J K}^{-1} \text{ mol}^{-1}$. The dipole moment of pure cis-decalin in the liquid state was measured and found to be indistinguishable from zero Debye. Trans-decalin was also measured and no loss peaks were discovered around 140 K. This dielectric dispersion observed in pure cis-decalin above the glass transition temperature ($T_g \sim 138 \text{ K}$) may be characterized by a microBrownian co-operative relaxation. Owing to the low loss ($\sim 1 \times 10^{-3}$), dielectric data cannot be accurately represented by the Davidson-Cole skewed-arc function.

In view of the distribution parameters, β , Davies and Edwards (32) pointed out that, since β values increased as the temperature increases, when the value of β is extrapolated beyond very high temperatures (well above T_g), its value will finally approach 1 as a certain temperature is reached, i.e. normal liquid behaviour is then anticipated. The attainment of that state will also be accompanied by a marked fall in the activation energy corresponding to the change in the character of the compound. In the present work, the β -values of 2-methylpentane increased from 0.32 to

0.56 as the temperature increased from 91.2 to 95.3 K. Similar consequences of high β values corresponding to high temperatures were observed in the other four molecules, namely, methylcyclohexane, 4-methylcyclohexene-1, n-propylbenzene and cis-decalin. The corresponding values obtained were in the ranges 0.37-0.62, 0.38-0.45, 0.61-0.72, and 0.25-0.40, respectively. Figure 6.7 shows the normalized complex plane loci of the normalized dielectric constant $(\epsilon^* - \epsilon_1) / (\epsilon_0 - \epsilon_1)$ for n-propylbenzene at 138.9 and 142.8 K. For n-propylbenzene, Copeland and Denney (29) observed an increase of β -values from 0.63₅ to 0.75 as the temperature increased from 138.3 to 149.4 K.

Davies et al (32) suggested that the dipole component responsible for the co-operative absorption decreases markedly with the increase of temperature. Chao (10) examined the co-operative relaxation behaviour of a number of rigid molecules in polystyrene matrices and observed a decrease of dipole moment with increase of temperature. In the present study of 2-methylpentane, methylcyclohexane, n-propylbenzene, cis-decalin, and 4-methylcyclohexene-1, a similar trend of a decrease of dipole moment with increase of temperature was observed for the first four molecules, but in the last one no definite trend was noted (see Table 6.3).

All of the characteristic features observed, strongly indicated that a co-operative process was present in 2-methylpentane, methylcyclohexane, 4-methylcyclohexene-1, n-propylbenzene, and cis-decalin. Such features included the high temperature (above T_g) at which the process occurred, broad asymmetric nature of the loss curves (but absent in cis-decalin) (Fig. 6.8 and Fig. 6.9 represent such curves for 2-methylpentane and methylcyclohexane, respectively), which varied rapidly with slight change of temperature, apparent large activation energy, representation of dielectric data by Davidson-Cole plot...etc.

Moreover, a nonlinear relationship existed in the Eyring analysis plot of $\log \tau_0 T$ against $\frac{1}{T}$. Fig. 6.10 and Fig. 6.11 show such plots for methylcyclohexane and cis-decalin, respectively. In terms of the Eyring transition state theory, as extended by Kauzmann (33), Smyth et al (18) indicated that various enthalpies of activation ranging from 105 kJ mol^{-1} to 293 kJ mol^{-1} were nonlinear with decreasing temperature for rigid molecules in supercooled decalin, i.e. the Arrhenius plots of the relaxation time.

The nine alkylbenzenes (n-propylbenzene

is not considered) studied here exhibit dielectric relaxation between 10^1 and 10^5 Hz over the temperature range 120-158 K with Eyring activation enthalpies ranging from 82 kJ mol^{-1} for benzene to 110 kJ mol^{-1} for p-ethyltoluene (see Table 6.2). These enthalpies of activation are comparable to those observed for 4-methylcyclohexene-1, n-propylbenzene, and cis-decalin above their glass transition temperatures for co-operative motions. Moreover, broad asymmetric nature of the loss curves which changed rapidly with slight variation of temperature were observed for benzene, m-xylene, p-xylene, t-butylbenzene and p-ethyltoluene. Figures 6.12 and 6.13 represent such curves for p-xylene and p-ethyltoluene, respectively. However, for o-xylene, mesitylene, p-cymene, and p-diethylbenzene, the nature of the loss-curves differ significantly (see Fig. 6.14 for mesitylene).

Co-operative relaxation is usually observed above the glass transition temperature (T_g) of a supercooled liquid. However, no T_g was found for any of the nine alkylbenzenes. Glass transition is a phase change phenomenon which is observed as a result of specific volume change with the change of temperature. Thus, determination of T_g mainly depends upon the sensitivity of the apparatus

with which the measurement is being carried out. If a very small fraction of volume change (due to phase change) which occurs, and this is beyond the sensitive limit of the apparatus. No indication of T_g will be found, but the occurrence of a co-operative relaxation above this transition cannot be ruled out.

The support of this view can be found from the experimental results of o-xylene, mesitylene, p-cymene, and p-diethylbenzene. These compounds exhibit β -peak (molecular relaxation) around 100 K (see Chapter V). A β -peak is usually expected around $0.75 T_g$ (34). Assuming this to be true, one would expect glass transition temperatures for these alkylbenzenes to be about 135 K. However, the present study shows high temperature high energy relaxation above 135 K for all these compounds.

Among nine alkylbenzenes, only the dielectric data for p-ethyltoluene can be represented accurately by the Davidson-Cole skewed-arc function (Fig. 6.15). Relaxation behaviour of o-xylene, p-cymene, mesitylene, and p-diethylbenzene could not be described adequately by such an asymmetric function (See Fig. 6.16 for mesitylene)

probably owing to the contribution from the low temperature molecular relaxation in these molecules (see Chapter V). For p-diethylbenzene, there is a clear indication of such overlapping (Fig. 6.17) which gives rise to a low enthalpy of activation ($\Delta H_E = 61 \pm 21 \text{ kJ mol}^{-1}$) and entropy of activation ($\Delta S_E = 256 \pm 147 \text{ J K}^{-1} \text{ mol}^{-1}$). For low loss compounds, such as benzene, m-xylene, p-xylene, and t-butylbenzene, Davidson-Cole plots are difficult to formulate owing to the errors involved in the dielectric constant values.

In co-operative relaxation, usually high β -values, which increase with temperature increases, are obtained as mentioned above. A similar trend of increase of β -value with temperature was observed for benzene (0.47-0.67), m-xylene (0.29-0.36), p-xylene (0.47-0.61), t-butylbenzene (0.40-0.58), p-ethyltoluene (0.37-0.50), and p-diethylbenzene (0.18-0.57). However, for o-xylene and mesitylene, a reverse trend was observed whereas for p-cymene, the β -value increases with the increase of temperature but remains in the range (0.15-0.22) of a typical molecular process.

It is noticeable from Table 6.3 that the dipole

moment values for t-butylbenzene, p-cymene, p-ethyltoluene, and p-diethylbenzene decrease as the temperature increases, which is usually the case for the co-operative relaxation process. However, mesitylene shows an increase of dipole moment with increase of temperature.

Non-Arrhenius behaviour is another characteristic feature for the co-operative relaxation process. Curved Eyring plots (non-Arrhenius behaviour) were obtained for m-xylene, p-xylene, t-butylbenzene, and p-ethyltoluene. Figure 6.18 represents such an Eyring plot for p-ethyltoluene. All other alkylbenzenes (except p-diethylbenzene) show linear relationships.

All factors considered, the observed relaxation behaviour of five alkylbenzenes, namely, benzene, m-xylene, p-xylene, t-butylbenzene, and p-ethyltoluene, may be assigned to a co-operative relaxation process. In o-xylene, mesitylene, p-cymene, and p-diethylbenzene, the molecular process associated with the co-operative motion may be overlapped in the region of investigation.

Levi (35) took values of ΔH_E and ΔS_E from various

sources and concluded that there is a linear relation between them and that the larger the ΔH_E , the more positive the ΔS_E becomes. He found the following equation for co-operative relaxation for polymers:

$$\Delta S_E \text{ (J K}^{-1} \text{ mol}^{-1}\text{)} = -67.5 + 2.49 \Delta H_E \text{ (kJ mol}^{-1}\text{)} \quad (6.2)$$

A linear regression analysis of 13 hydrocarbons (except p-diethylbenzene) recorded here yields an equation of:

$$\Delta S_E \text{ (J K}^{-1} \text{ mol}^{-1}\text{)} = 213.8 + 3.37 \Delta H_E \text{ (kJ mol}^{-1}\text{)} \quad (6.3)$$

for co-operative relaxation. Colepland's Denney's results for n-propylbenzene also fit this equation extremely well (see Fig. 6.19).

In the dielectric study of dilute solutions of small molecules in o-terphenyl in the supercooled liquid state, Williams and Hains (22) emphasized that the apparent activation energy near 260 kJ mol^{-1} should not be interpreted as the 'barrier' required to reorient a single

solute molecule, i.e. the dielectric process is significantly feasible for co-operative motions. Chao (10) examined a number of solute molecules in polystyrene at low concentration and obtained activation energy around 230 kJ mol^{-1} and activation entropy around $450 \text{ J K}^{-1} \text{ mol}^{-1}$ for co-operative motion. Baker and Smyth (36) investigated *i*-butylbromide and *i*-amylbromide in the supercooled liquid state and found enthalpies of activation for these molecules 96 and 74 kJ mol^{-1} with the corresponding entropies of activation 700 and $440 \text{ J K}^{-1} \text{ mol}^{-1}$. The present dielectric study of 14 hydrocarbons yields Eyring activation enthalpies and activation entropies ranging from 52 kJ mol^{-1} and $402 \text{ J K}^{-1} \text{ mol}^{-1}$ for 2-methylpentane to 119 kJ mol^{-1} and $665 \text{ J K}^{-1} \text{ mol}^{-1}$ for *cis*-decalin, respectively. On a comparison of the energy barrier values of low viscous liquids (e.g. *i*-butylbromide, *i*-amylbromide, and the hydrocarbons studied here) with those of high viscous molecules (e.g. *o*-terphenyl, polystyrene, etc.), it can be seen that for low viscous liquids, the enthalpies of activation for co-operative motions are comparatively lower than those for high viscous molecules - which is actually expected. The reverse case, however, is observed for entropies of activation. This is because in low

viscous liquids, molecules are not firmly fixed in the transition state and so are highly disordered, but in high viscous liquids such freedom is more or less hindered.

The dielectric loss factor (ϵ'') is directly proportional to the square of the dipole moment. The maximum absorption (ϵ''_{\max}) of each hydrocarbon at which the co-operative motions have been observed is shown in Table 6.2. It is noteworthy that nonpolar compounds, e.g. 2-methylpentane, methylcyclohexane, p-ethyltoluene, etc. show high dielectric loss in comparison to weakly polar compounds (e.g. o-xylene (0.50 D) and m-xylene (0.31 D). 3-Methylpentane (7) ($\mu = 0$), o-terphenyl (20) ($\mu = 0$), and isopropylbenzene (20) ($\mu = 0.39$ D) also show co-operative relaxation at which the $\tan\delta$ values are $\sim 2.8 \times 10^{-3}$, 2.9×10^{-3} , and 38×10^{-3} , respectively. This high loss may result from the random movement of dipoles, (either permanent or induced, see Chapters III and V) near the transition region. So, in addition to the dipole moment component, the extent to which the transition occurs also governs the loss factor in co-operative relaxation processes.

The interaction among molecules may be measured either with the relative change of stretching frequency ($\Delta\nu$) or with ionization potential (I). Here the pyrrole vapour was taken as standard, the stretching frequency of N-H bond of pyrrole, $\nu_{\text{N-H}}$, is 3530 cm^{-1} (37). When the stretching frequency of pyrrole, $\nu_{\text{N-H}}$, is measured using 2-methylpentane as solvent, $\nu_{\text{N-H}}$ shifted to 3507 cm^{-1} due to the donor-acceptor complex formation. So, the relative change of stretching frequency, $\Delta\nu = 3530 - 3507 = 23 \text{ cm}^{-1}$. The higher the relative change of stretching frequency or the lower the ionization potential, the stronger is the molecular interaction.

Table 6.1 shows the relative change of stretching frequencies of the N-H bond of pyrrole with some of the hydrocarbons studied here. Some literature values are also shown in the Table.

Figure 6.20 shows the plot of stretching frequency, $\Delta\nu$, against the enthalpy of activation, ΔH_E , for some of the hydrocarbons. It can be seen from the Figure 6.20 that, within the limits of experimental error, a linear correlation exists between the enthalpy of activation (ΔH_E) and the stretching frequency ($\Delta\nu$); the

TABLE 6.1 Stretching frequency of N-H bond of pyrrole with some hydrocarbons

Solvent	Experimental		Literature	
	$\nu_{\text{N-H}}, \text{cm}^{-1}$	$\Delta\nu, \text{cm}^{-1}$	$\nu_{\text{N-H}}, \text{cm}^{-1}$	$\Delta\nu, \text{cm}^{-1}$
pyrrole vapour			3530 ^(a)	
2-methylpentane	3507	23		
methylcyclohexane	3502	28		
4-methylcyclohexene-1	3484	46		
benzene	3456	74	3458 ^(b)	72
o-xylene	3446	84	3448 ^(b)	82
m-xylene	3447	83	3449 ^(b)	81
p-xylene	3446	84	3448 ^(b)	82
n-propylbenzene	3448	82		
t-butylbenzene	3444	86		
p-cymene	3439	91		
mesitylene	3435	95	3439 ^(a)	91

(a) M.L. Josien and N. Fuson, J. Chem. Phys., 22(1954)1169.

(b) L.J. Bellamy, H.E. Hallam and R.L. Williams, Trans. Faraday Soc., 54(1958)1120.

higher the ΔV value, the higher is the value of ΔH_E . This means that the higher the interaction among the molecules, the higher will be the energy barrier required for reorientation of molecules. A plot (Fig. 6.21) of ionization potential (I)(38) against enthalpy of activation (ΔH_E) also supports this view of the stronger molecular interaction the higher is the ΔH_E value.

REFERENCES

1. G. Williams in "Dielectric and Related Molecular Processes" edited by M. Davies (Specialist Periodical Reports), The Chemical Society, London, Vol. 2, 1975.
2. C.P.Smyth, "Dielectric Behaviour and Structure", McGraw-Hill, New York, 1955.
3. N.E. Hill, W. Vaughan, A.H. Price and M.Davies, "Dielectric Properties and Molecular Behaviour", Van Nostrand, New York, 1969.
4. F.X. Hassion and R.H. Cole, J. Chem. Phys., 23(1955)1756.
5. W. Dannhauser and R.H. Cole, J. Chem. Phys., 23(1955)1762.
6. G.P. Johari and W. Dannhauser, J. Chem. Phys., 50(1969)1862.
7. G.P. Johari and M. Goldstein, J. Chem. Phys., 55(1971)4245.
8. J. Crossley and G. Williams, J.C.S. Faraday II, 73(1977)1651.
9. J. Crossley and G. Williams, J.C.S. Faraday II, 73(1977)1906.
10. J.C.N. Chao, M.Sc. Thesis, Lakehead University, Thunder Bay, Canada, 1978.
11. W.O. Baker and C.P. Smyth, J. Am. Chem. Soc., 61(1939)2063.
12. S.B. Thomas, J. Phys. Chem., 35(1931)2103.
13. P.P. Kobeko and Co-workers, J. Techn. Phys. (U.S.S.R.), 8(1938)715.
14. D.J. Denney, J. Chem. Phys., 27(1957)259.
15. F.I. Mopsik and R.H. Cole, J. Chem. Phys., 44(1966)1015.

16. J. G. Berberian and R. H. Cole, J. Am. Chem. Soc., 90(1968)3100.
17. G.P. Johari and C.P. Smyth, J. Am. Chem. Soc., 91(1969)5168.
18. G.P. Johari and C.P. Smyth, J. Chem. Phys. 56(1972)4411.
19. G.P. Johari and M. Goldstein, J. Phys. Chem., 74(1970)2034.
20. G.P. Johari and M. Goldstein, J. Chem. Phys., 53(1970)2372.
21. G. Williams and P.J. Hains, Chem. Phys. Letters, 10(1971)585.
22. G. Williams and P.J. Hains, J.C. S. Faraday Symposia, 6(1972)14.
23. M.F. Shears and G. Williams, J.C.S. Faraday II, 69(1973)608.
24. M.F. Shears and G. Williams, J.C.S. Faraday II, 69(1973)1050.
25. M. Davies, P.J. Hains and G. Williams, J.C.S. Faraday II, 69(1973)1785.
26. M. Nakamura, H. Takahashi and K. Higasi, Bull. Chem. Soc., Jpn., 47(1974)1593.
27. D.W. Davidson and R.H. Cole, J. Chem. Phys., 19(1951)1484.
28. A.J. Barlow, J. Lamb and A.J. Matheson, Proc. R. Soc., London, A292(1966)322.
29. T.G. Copeland and D.J. Denney, J. Phys. Chem., 80(1976)210.
30. W.F. Hassell and S. Walker, Trans. Faraday Soc., 62(1966)861.
31. A.J. Petro and C.P. Smyth, J. Am. Chem. Soc., 79(1957)142.

32. M. Davies and D.A. Edwards, *Trans. Faraday Soc.*,
63(1967)2163.
33. W. Kauzmann, *Rev. Mod. Phys.*, 14(1942)12.
34. L. Hayler and M. Goldstein, *J. Chem. Phys.*,
66(1977)736.
35. D.L. Levi, *Trans. Faraday Soc.*, 42A(1946)152.
36. W.O. Baker and C.P. Smyth, *J. Chem. Phys.*,
7(1939)574.
37. M.L. Josien and N. Fuson, *J. Chem. Phys.*,
22(1954)1169.
38. V.I. Vedeneyev, L.V. Gurvich, V.N. Kondrat'yev,
V.A. Medvedev and Ye. L. Frankevich,
"Bond Energies, Ionization Potentials
and Electron Affinities", St. Martin's
Press, New York, 1966.

TABLE 6.2: RELAXATION TIMES, EYRING ANALYSIS RESULTS, MAXIMUM LOSS FACTOR AND GLASS TRANSITION TEMPERATURE FOR SOME HYDROCARBONS

Molecule	T(K)	Relaxation times τ (s)		ΔG_E in kJ mol^{-1}		ΔH_E (kJ mol^{-1})	ΔS_E ($\text{J K}^{-1} \text{mol}^{-1}$)	$\epsilon''_{\text{max}} 10^3$	T_g (K)	ν^* Lit. (D)
		100 K	150 K	100 K	150 K					
2-Methylpentane	91.2-95.3	8.7×10^{-7}	-	12.0	-	52 ± 4	402 ± 47	14.13	~86	0
Methyl cyclohexane	93.5-98.4	3.9×10^{-6}	-	13.2	-	57 ± 4	439 ± 39	9.59	93	0
4-Methyl-cyclohexene-1	108.4-114.8	4.6×10^{-1}	-	22.9	-	69 ± 3	457 ± 25	93.03	102	
Benzene	120.4-124.1	4.6×10^3	1.9×10^{-11}	30.6	5.1	82 ± 12	510 ± 97	0.17	-	0
o-Xylene	135.1-141.2	2.2×10^9	1.6×10^{-7}	41.5	16.3	92 ± 8	503 ± 57	0.34	-	0.50
m-Xylene	132.5-136.3	9.9×10^7	3.3×10^{-8}	38.9	14.4	88 ± 10	490 ± 78	0.29	-	0.31
p-Xylene	128.2-136.2	3.1×10^8	2.1×10^{-8}	39.8	13.8	92 ± 4	520 ± 32	0.49	-	0
n-Propylbenzene	137.0-142.8	5.6×10^9	7.5×10^{-7}	42.2	18.3	90 ± 6	479 ± 42	139.71	123	0.35
t-Butylbenzene	151.1-158.5		8.9×10^{-4}		27.1	93 ± 8	487 ± 50	1.24	-	0.36
p-Cymene	144.0-148.8	4.2×10^{12}	3.4×10^{-5}	47.8	23.2	97 ± 3	491 ± 22	5.10	-	0
Mesitylene	139.9-144.5	1.8×10^{13}	1.1×10^{-5}	48.9	21.7	103 ± 8	545 ± 53	1.59	-	0
p-Ethyltoluene	131.5-141.2	3.8×10^{11}	1.7×10^{-8}	45.7	13.5	110 ± 10	644 ± 74	7.01	-	0
p-Diethylbenzene	139.3-152.5	2.5×10^6	3.4×10^{-5}	35.8	23.0	61 ± 21	256 ± 147	2.01	-	0
cis-Decalin	140.8-146.4	8.0×10^{14}	1.2×10^{-6}	52.1	18.9	119 ± 9	665 ± 59	1.23	138	0

* A.L. McClellan, "Tables of Experimental Dipole Moments", W.H. Freeman and Company, San Francisco, 1963.

TABLE 6.3:

Davidson-Cole and Fuoss-Kirkwood Analysis
Parameters and Apparent Dipole Moments for
Some Hydrocarbons in the Solid State

T(K)	$10^6 \tau$ (s)	$\log f_{\max}$	β	$10^3 \epsilon''_{\max}$	ϵ_{∞}	μ (D)
<u>2-Methylpentane</u>						
91.2	896.2	2.541	0.32	13.15	2.06	0.161
92.2	660.4	2.940	0.36	13.28	2.06	0.163
92.7	246.0	3.103	0.39	13.41	2.06	0.158
93.7	111.8	3.445	0.46	14.00	2.06	0.149
94.3	83.1	3.574	0.50	14.08	2.06	0.144
95.3	43.1	3.860	0.56	14.13	2.06	0.137
<u>Methylcyclohexane</u>						
93.5	955.3	2.467	0.37	9.53	2.26	0.129
94.3	455.3	2.789	0.40	9.53	2.26	0.124
94.9	291.1	2.984	0.44	0.59	2.26	0.119
96.1	101.1	3.443	0.49	9.47	2.26	0.113
96.6	74.7	3.574	0.52	8.92	2.26	0.107
97.5	38.8	3.858	0.58	7.91	2.26	0.096
98.4	24.6	4.056	0.62	6.68	2.26	0.086
<u>4-Methylcyclohexene-1</u>						
108.4	1579.3	2.303	0.38	84.62	2.44	0.371
109.8	480.3	2.820	0.40	86.60	2.44	0.368
110.5	311.8	3.008	0.41	86.55	2.44	0.365
111.4	183.2	3.239	0.42	87.56	2.44	0.364
112.6	78.7	3.606	0.42	90.07	2.44	0.372
113.7	38.5	3.916	0.44	91.19	2.44	0.367
114.8	20.2	4.196	0.45	93.03	2.43	0.369

TABLE 6.3: continued...

T(K)	$10^6 \tau$ (s)	$\log f_{\max}$	β	$10^3 \epsilon''_{\max}$	ϵ_{∞}	μ (D)
<u>Benzene</u>						
120.4	236.9	2.827	0.47	0.16	2.35	-
120.8	190.8	2.921	0.51	0.16	2.35	-
121.8	103.5	3.187	0.57	0.17	2.35	-
122.5	47.1	3.528	0.61	0.16	2.35	-
123.3	29.4	3.734	0.64	0.14	2.35	-
124.1	22.4	3.852	0.67	0.14	2.35	-
<u>o-Xylene</u>						
135.1	556.9	2.456	0.39	0.32	2.42	-
136.2	296.9	2.729	0.35	0.32	2.42	-
137.0	202.5	2.895	0.30	0.32	2.42	-
138.8	56.5	3.450	0.29	0.33	2.42	-
139.8	37.1	3.633	0.27	0.33	2.42	-
141.2	9.6	4.222	0.23	0.34	2.42	-
<u>m-Xylene</u>						
132.5	416.8	2.582	0.29	0.29	2.52	-
133.2	282.0	2.752	0.31	0.28	2.52	-
133.8	187.5	2.929	0.32	0.29	2.52	-
135.1	78.7	3.306	0.33	0.28	2.52	-
135.9	59.8	3.426	0.34	0.29	2.52	-
136.3	50.0	3.503	0.36	0.29	2.52	-
<u>p-Xylene</u>						
128.2	7334.1	1.337	0.47	0.45	2.33	-
130.0	1885.0	1.927	0.53	0.46	2.33	-
132.2	470.5	2.529	0.58	0.49	2.33	-
133.6	179.3	2.948	0.61	0.45	2.33	-
134.8	92.1	3.238	0.61	0.39	2.33	-
136.2	44.5	3.553	0.59	0.24	2.33	-

TABLE 6.3: continued...

T(K)	$10^6 \tau$ (s)	$\log f_{\max}$	β	$10^3 \epsilon''_{\max}$	ϵ_{∞}	μ (D)
<u>n-Propylbenzene</u>						
137.0	1131.7	2.285	0.61	138.14	2.51	0.446
138.9	346.1	2.800	0.64	139.62	2.50	0.442
139.9	195.3	3.048	0.66	139.71	2.50	0.437
141.0	104.1	3.322	0.70	138.41	2.50	0.425
142.8	44.2	3.694	0.72	137.54	2.50	0.421
<u>tert-Butylbenzene</u>						
151.1	605.3	2.420	0.40	1.20	2.42	0.059
152.2	301.9	2.722	0.42	1.20	2.42	0.058
153.1	176.8	2.954	0.45	1.20	2.42	0.056
154.3	93.1	3.233	0.49	1.22	2.42	0.055
155.7	52.9	3.478	0.52	1.24	2.42	0.054
157.6	22.8	3.844	0.55	1.15	2.42	0.051
158.5	18.1	3.944	0.58	1.12	2.42	0.049
<u>p-Cymene</u>						
144.0	1026.8	2.190	0.15	4.39	2.49	0.18
145.8	377.2	2.625	0.16	4.60	2.49	0.18
147.0	202.1	2.896	0.19	4.77	2.50	0.17
147.9	115.9	3.138	0.20	4.91	2.50	0.16
148.8	73.9	3.333	0.22	5.10	2.50	0.16
<u>Mesitylene</u>						
139.9	4559.5	1.543	0.31	1.59	2.49	0.070
141.2	2287.3	1.843	0.27	1.57	2.49	0.075
142.1	1276.6	2.096	0.24	1.55	2.49	0.079
143.5	520.9	2.485	0.21	1.55	2.49	0.085
144.5	265.7	2.777	0.18	1.52	2.49	0.091

TABLE 6.3: continued...

T(K)	$10^6 \tau$ (s)	$\log f_{\max}$	β	$10^3 \epsilon''_{\max}$	ϵ_{∞}	μ (D)
<u>p-Ethyltoluene</u>						
131.5	11835.4	1.404	0.37	6.86	2.52	0.128
132.5	4493.6	1.825	0.40	6.89	2.52	0.124
133.8	1187.6	2.403	0.45	7.00	2.52	0.118
135.2	453.9	2.821	0.47	7.01	2.52	0.116
137.2	115.7	3.414	0.50	6.87	2.52	0.112
138.9	43.6	3.838	0.50	6.63	2.52	0.111
141.2	9.4	4.503	0.49	6.35	2.52	0.111
<u>p-Diethylbenzene</u>						
139.3	4398.9	1.559	0.18	1.84	2.30	0.109
141.1	789.4	2.304	0.21	1.91	2.30	0.103
142.6	273.3	2.765	0.25	1.92	2.30	0.095
143.8	157.7	3.004	0.32	1.95	2.30	0.085
145.6	106.0	3.196	0.45	1.97	2.31	0.073
147.9	55.9	3.454	0.54	2.01	2.31	0.067
150.7	29.7	3.729	0.55	1.88	2.31	0.065
152.5	26.5	3.778	0.57	1.68	2.31	0.061
<u>cis-Decalin</u>						
140.8	726.6	2.341	0.25	1.07	2.37	0.072
141.2	462.8	2.536	0.29	1.09	2.37	0.065
142.5	173.0	2.964	0.30	1.15	2.37	0.066
143.5	91.1	3.242	0.31	1.19	2.37	0.066
144.7	38.4	3.618	0.34	1.22	2.37	0.064
145.4	23.5	3.831	0.36	1.23	2.37	0.063
146.4	114.6	4.038	0.40	1.23	2.37	0.060

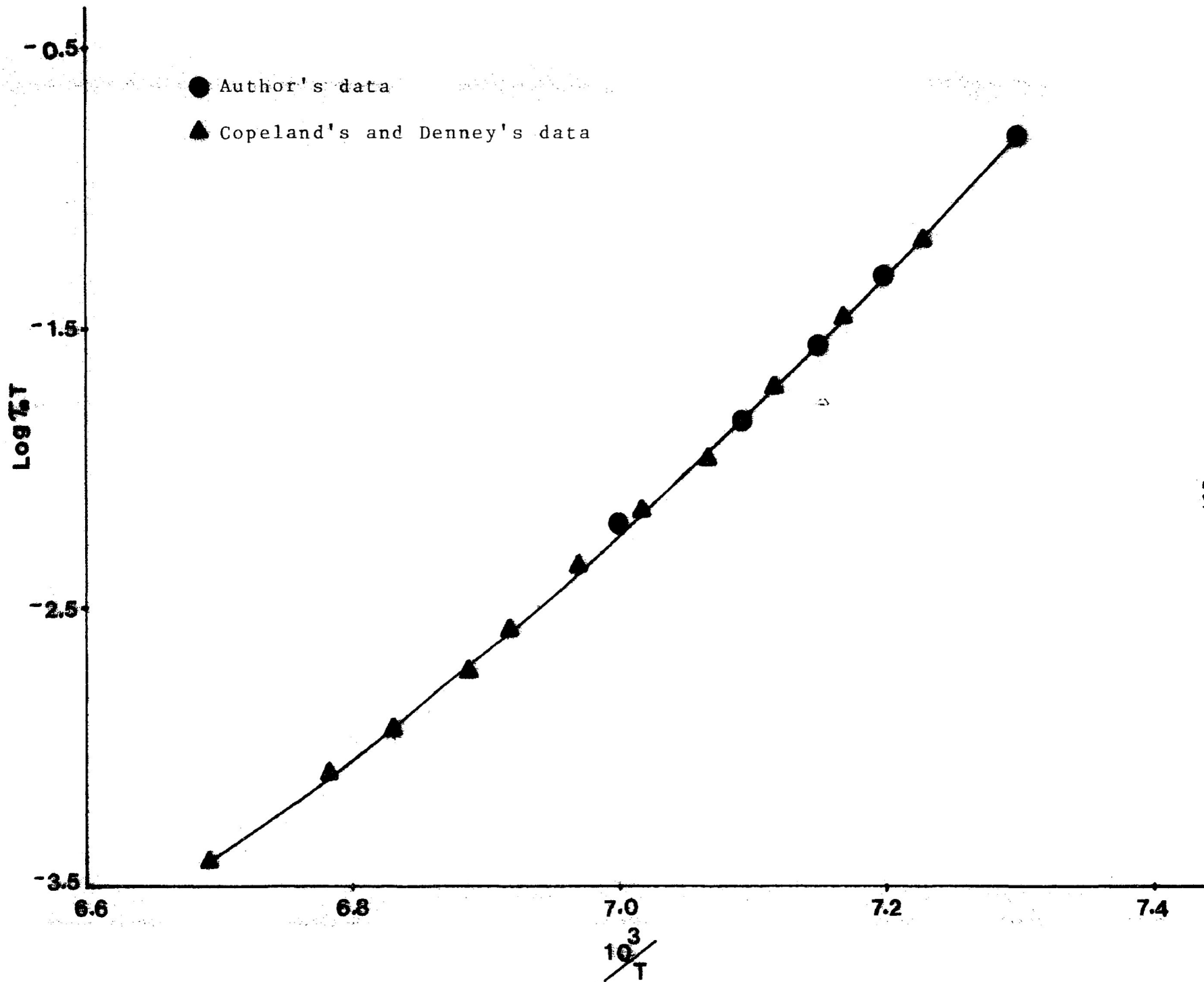


FIGURE 6.1: Eyring rate plot of $\log(\tau_0 T)$ versus $\frac{1}{T}$ for n-propylbenzene

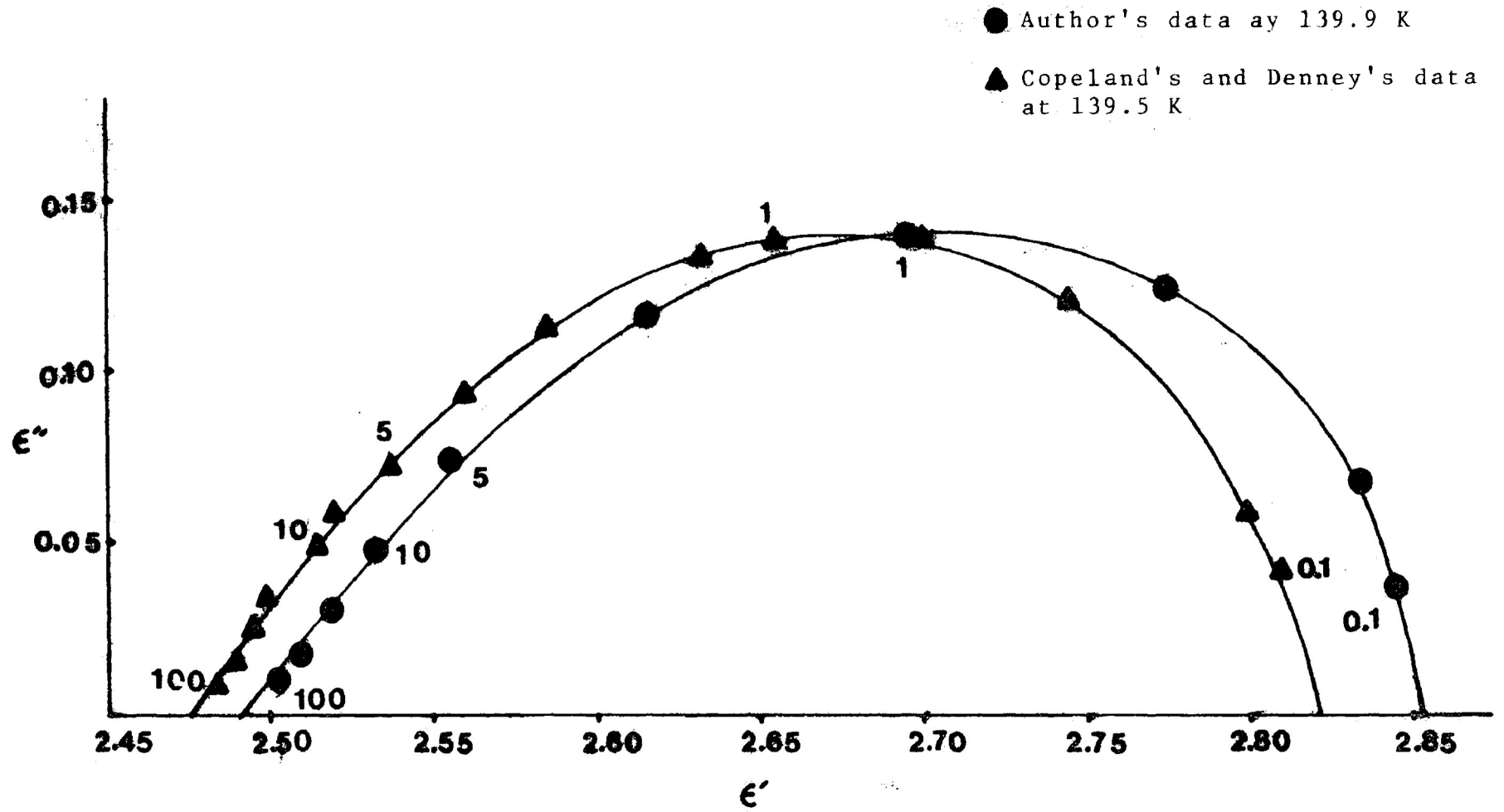


FIGURE 6.2: Complex plane diagram for n-propylbenzene
 Numbers beside points are frequencies in kHz

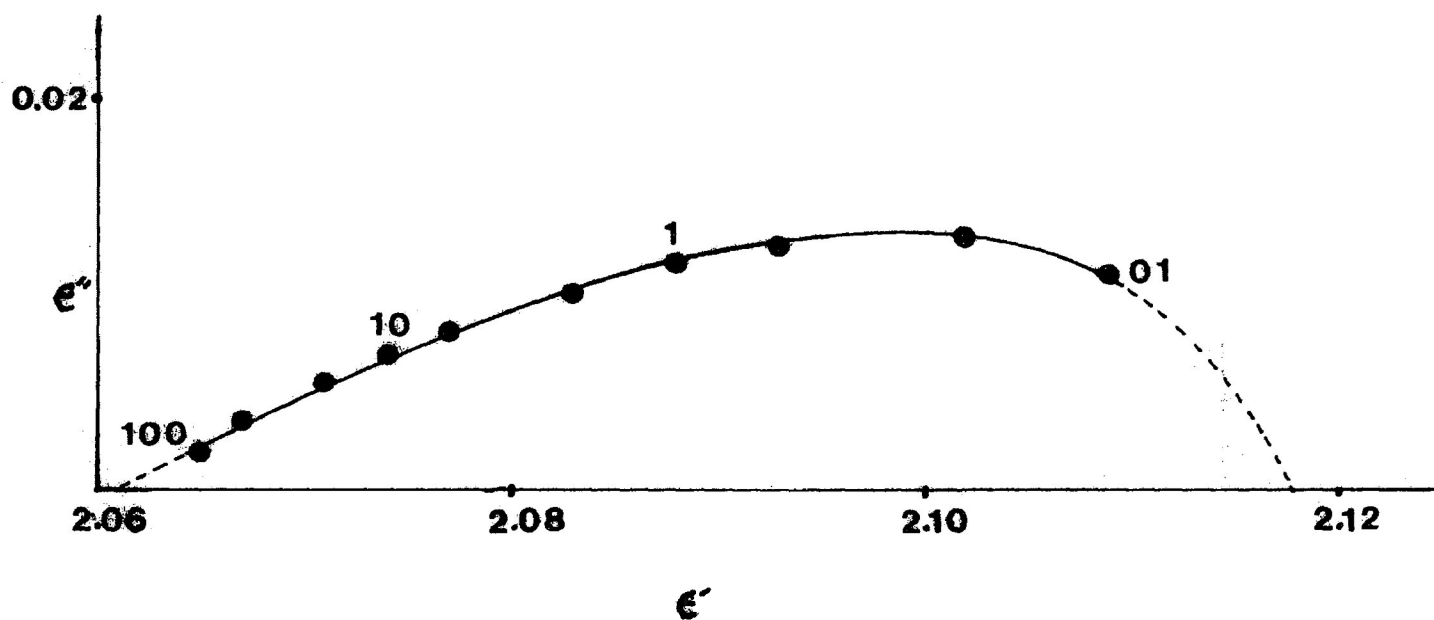


FIGURE 6.3: Complex plane diagram for 2-methylpentane at 91.2 K

Numbers beside points are frequencies in kHz

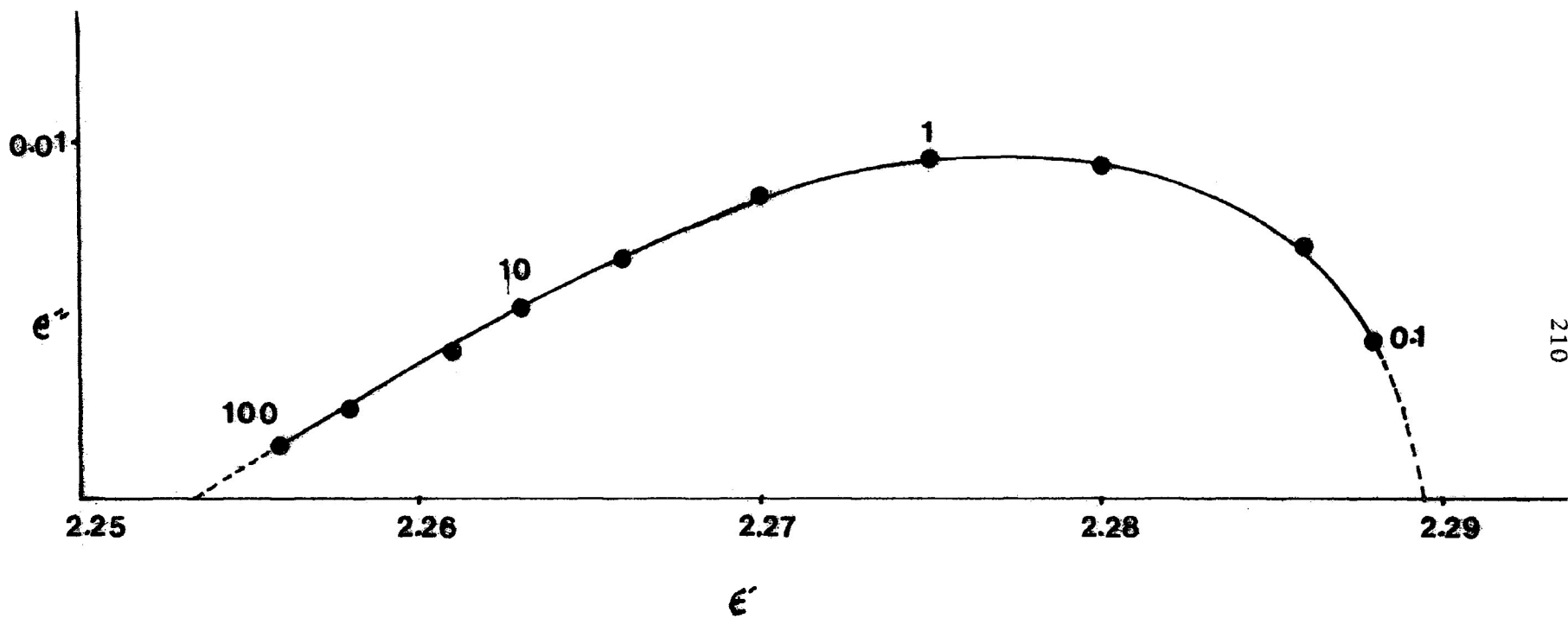


FIGURE 6.4: Complex plane diagram for methylcyclohexane at 94.9 K
 Numbers beside points are frequencies in kHz

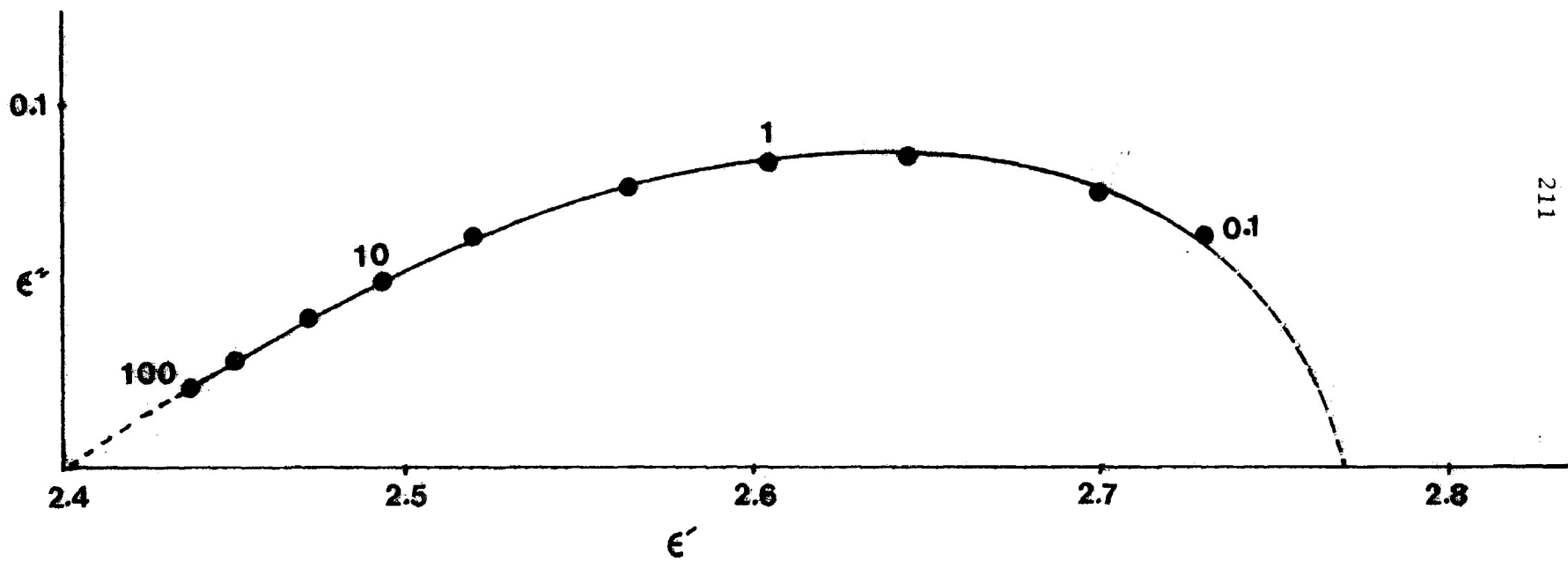


FIGURE 6.5: Complex plane diagram for 4-methylcyclohexene-1 at 109.8 K
 Numbers beside points are frequencies in kHz

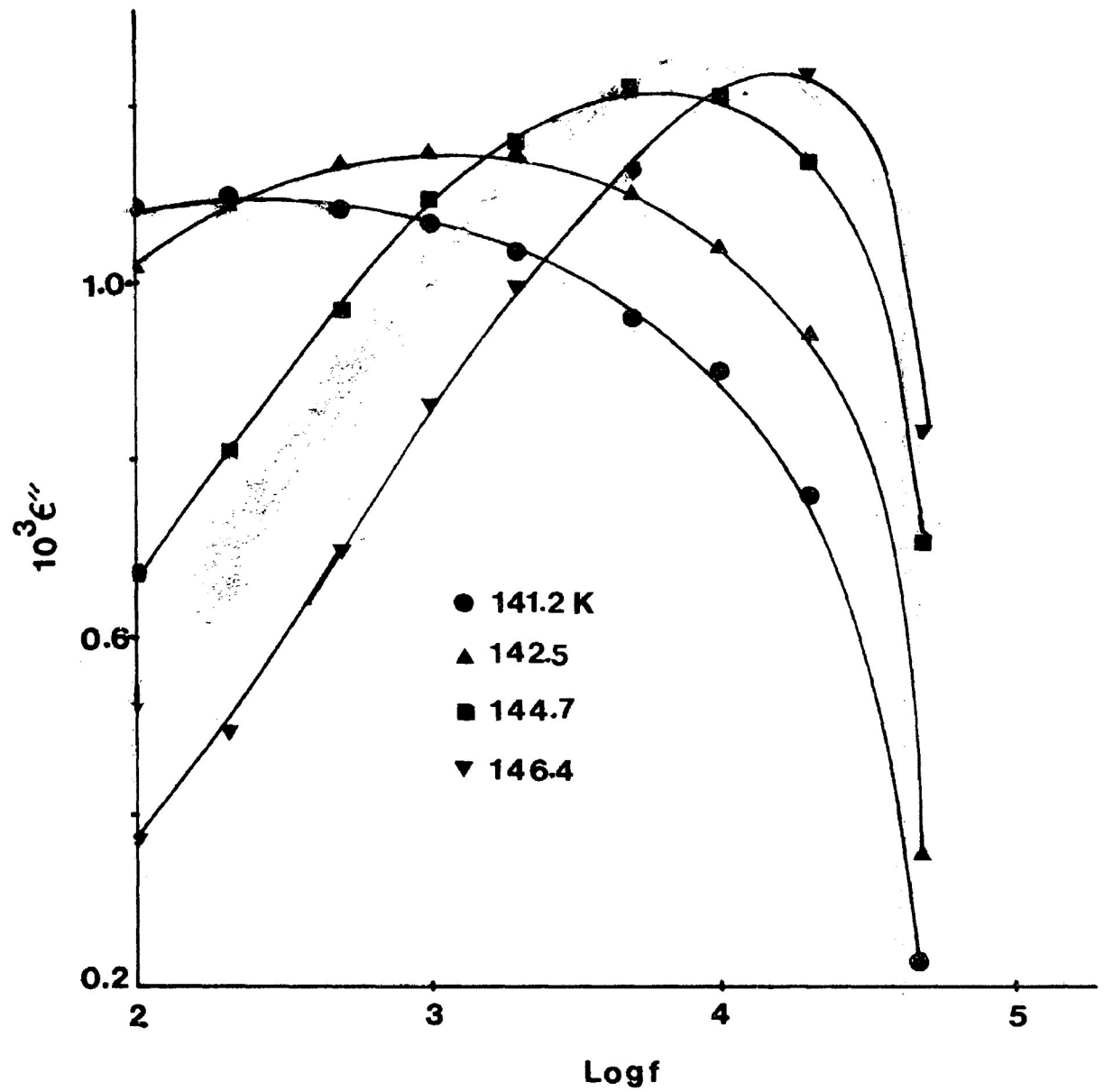


FIGURE 6.6: Dielectric loss factor ϵ'' versus log frequency for cis-decalin

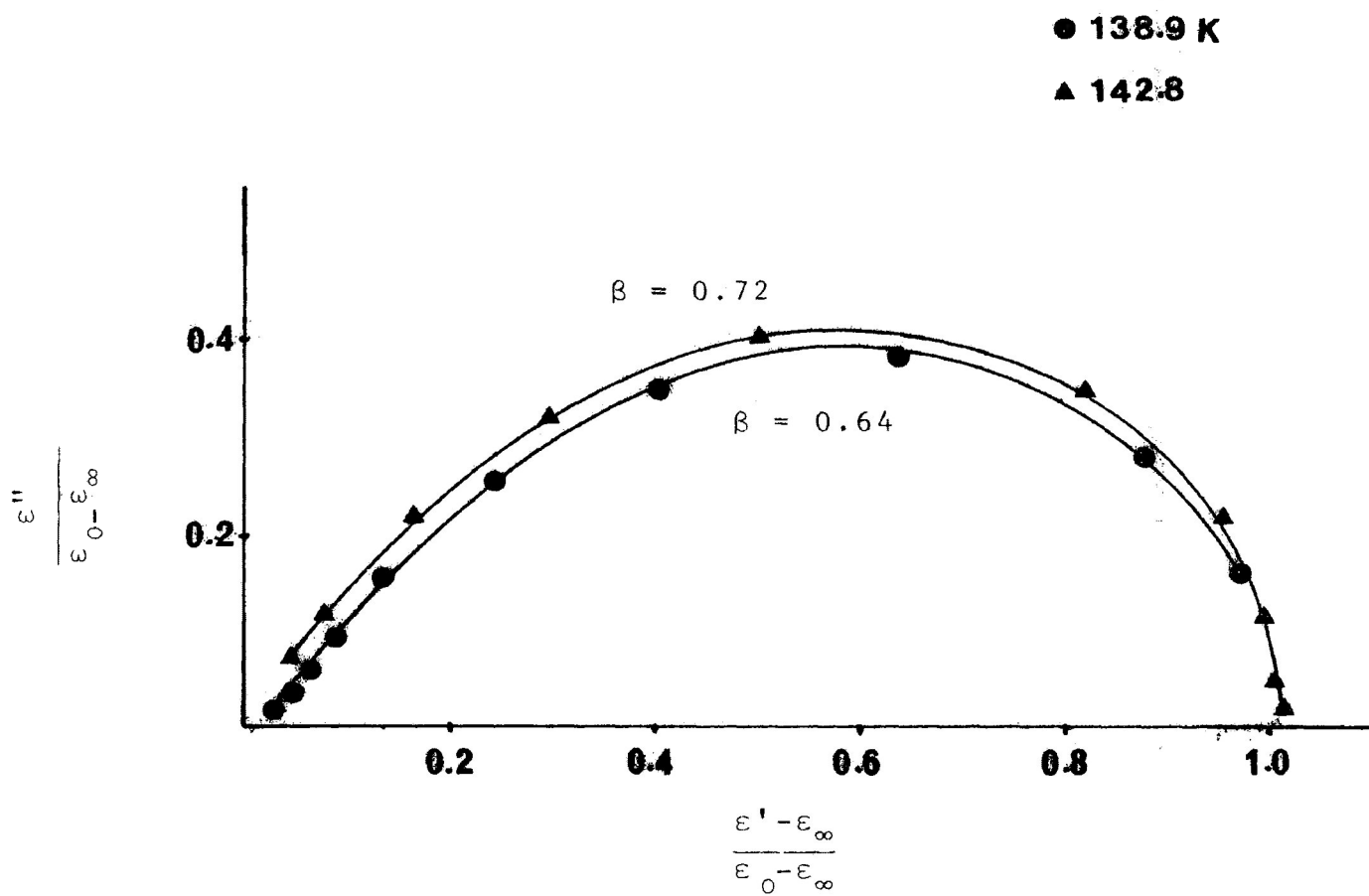


FIGURE 6.7: Complex plane loci of the normalized dielectric constant $(\epsilon^* - \epsilon') / (\epsilon_0 - \epsilon_\infty)$ for n-propylbenzene at 138.9 and 142.8 K.

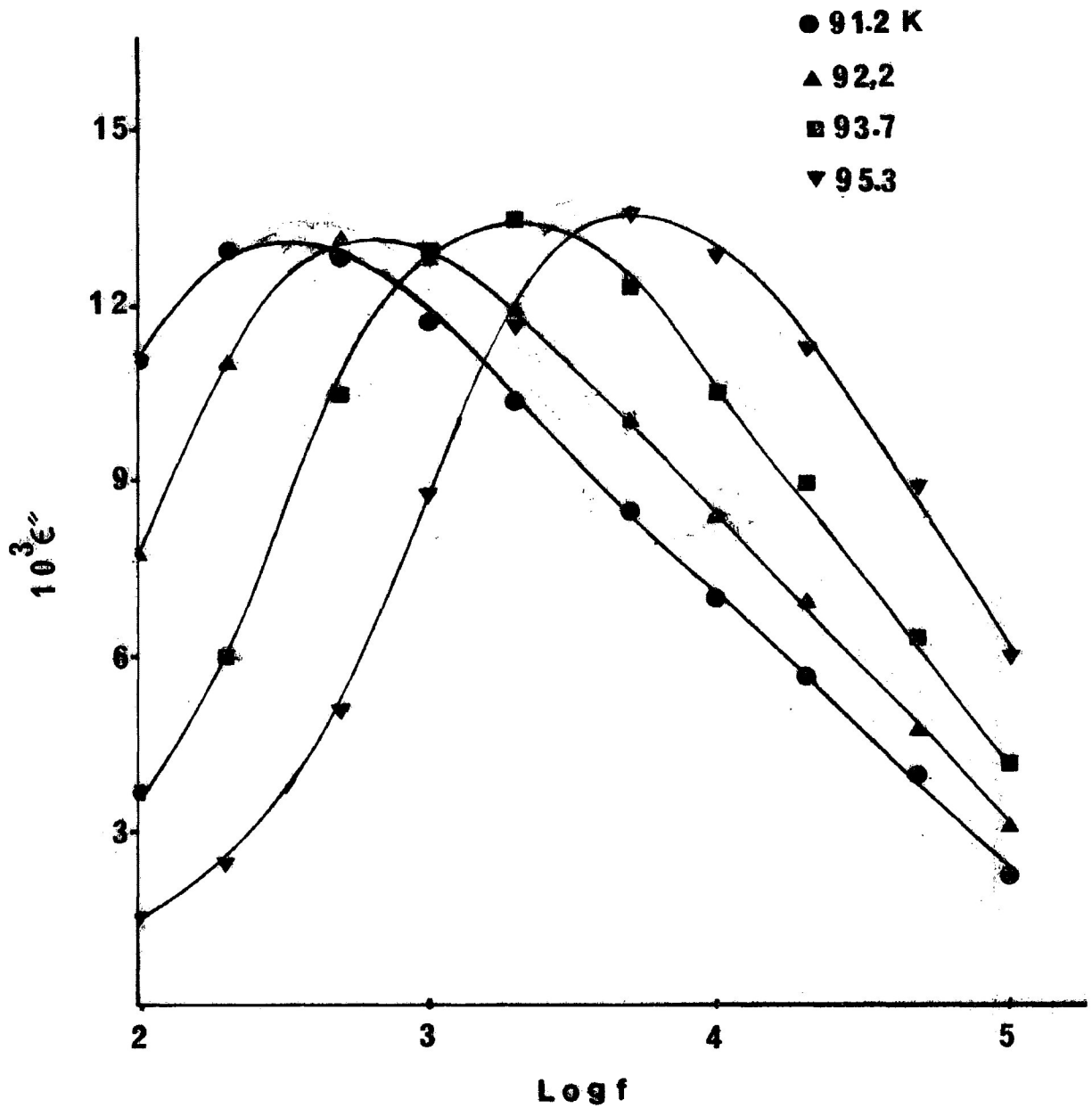


FIGURE 6.8: Dielectric loss factor ϵ'' versus log frequency for 2-methylpentane

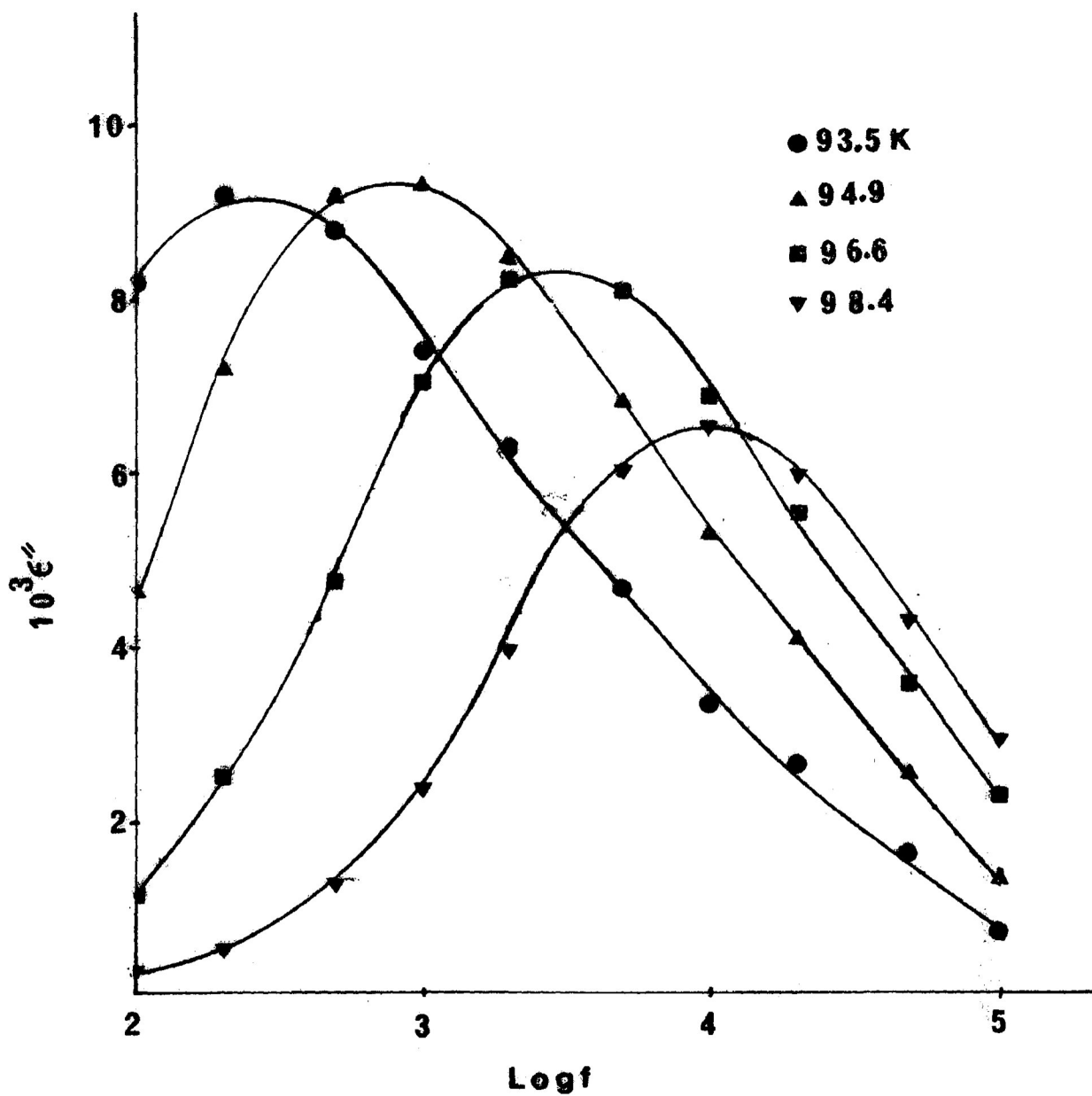


FIGURE 6.9: Dielectric loss factor ϵ'' versus log frequency for methylcyclohexane

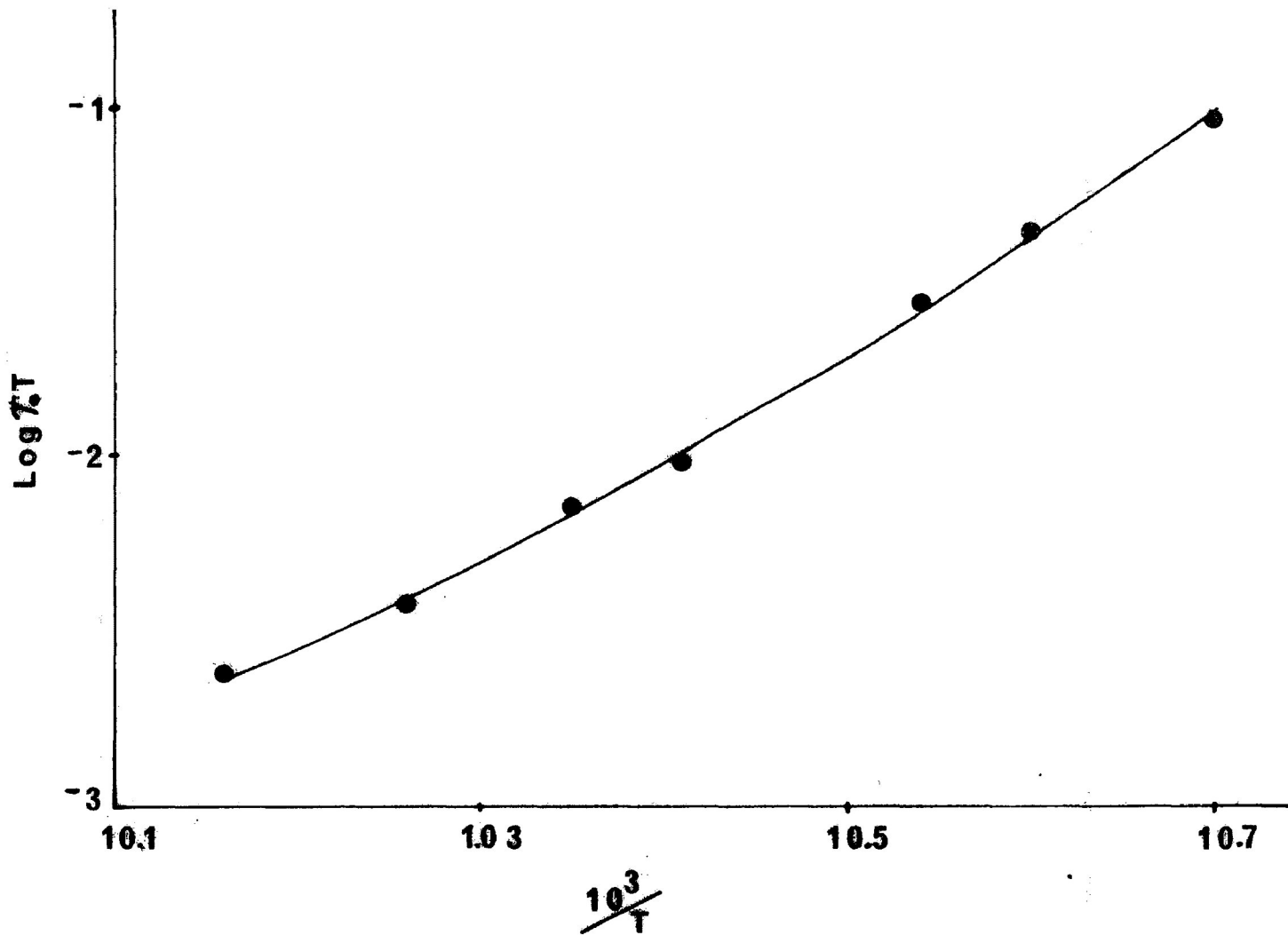


FIGURE 6.10: Eyring plot of $\log(\tau_0 T)$ versus $\frac{1}{T}$ for methylcyclohexane

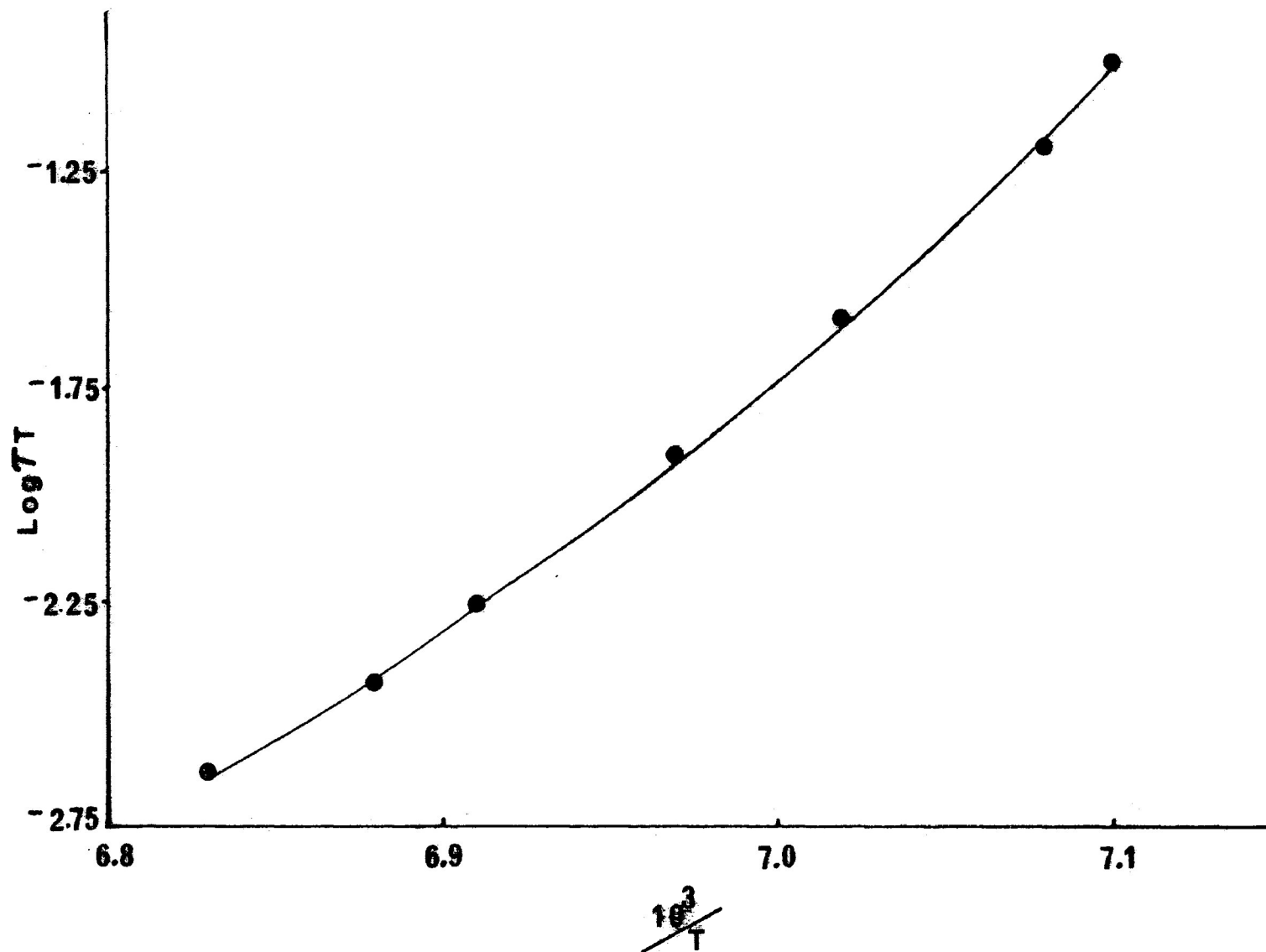


FIGURE 6.11: Eyring plot of $\log(\tau T)$ versus $\frac{1}{T}$ for cis-decalin

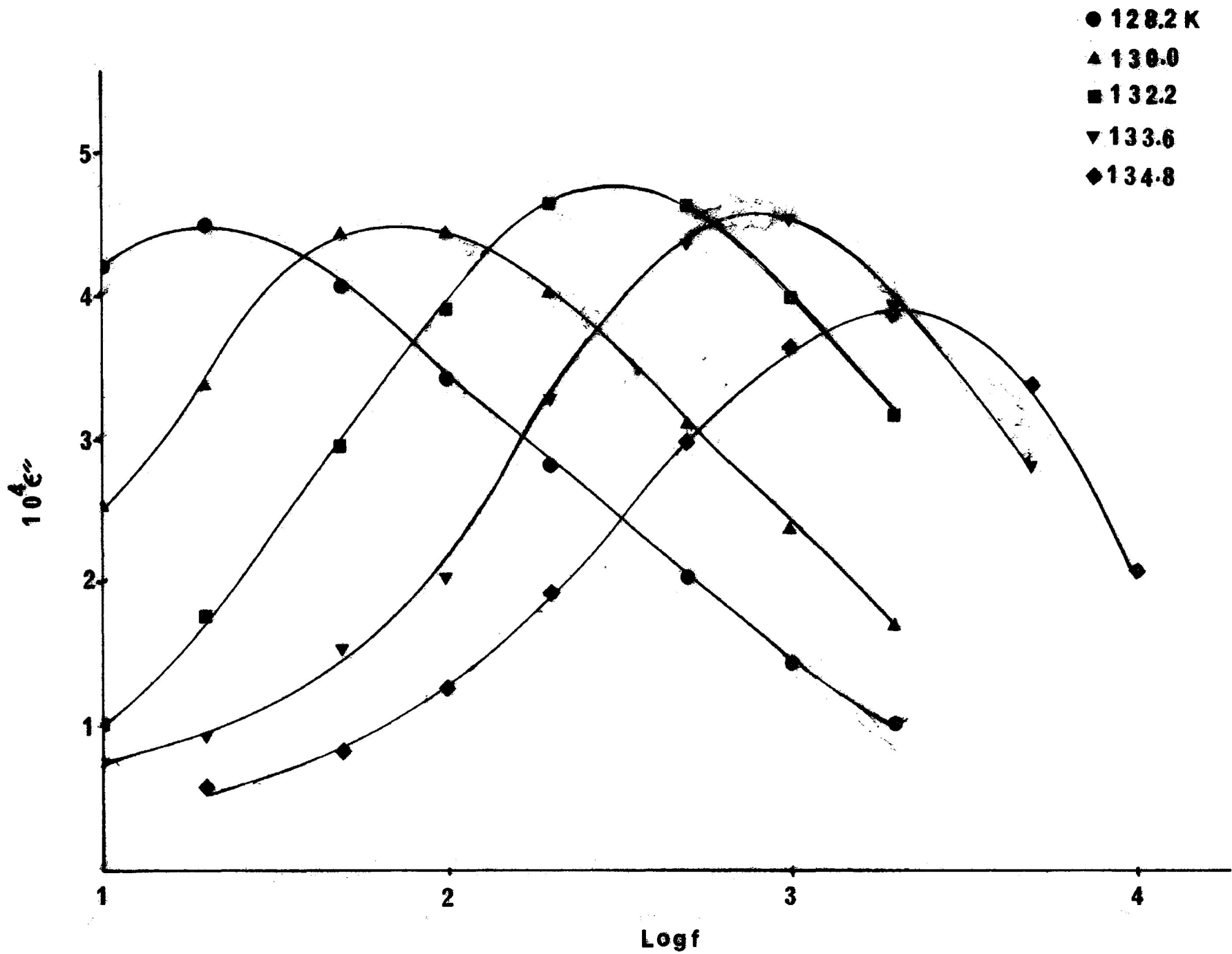


FIGURE 6.12: Dielectric loss factor ϵ'' versus log frequency for p-xylene

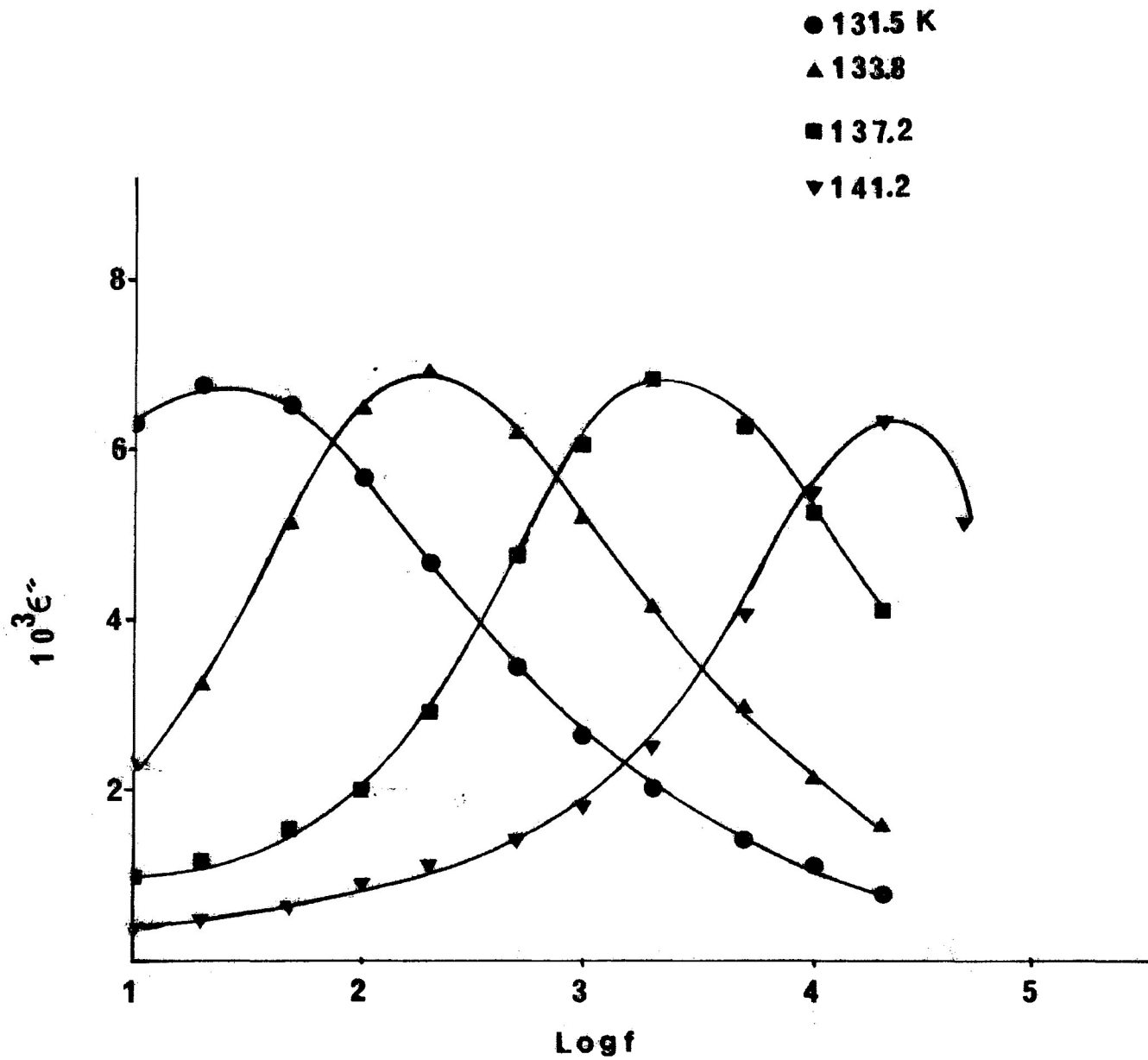


FIGURE 6.13: Dielectric loss factor ϵ'' versus log frequency for p-ethyltoluene

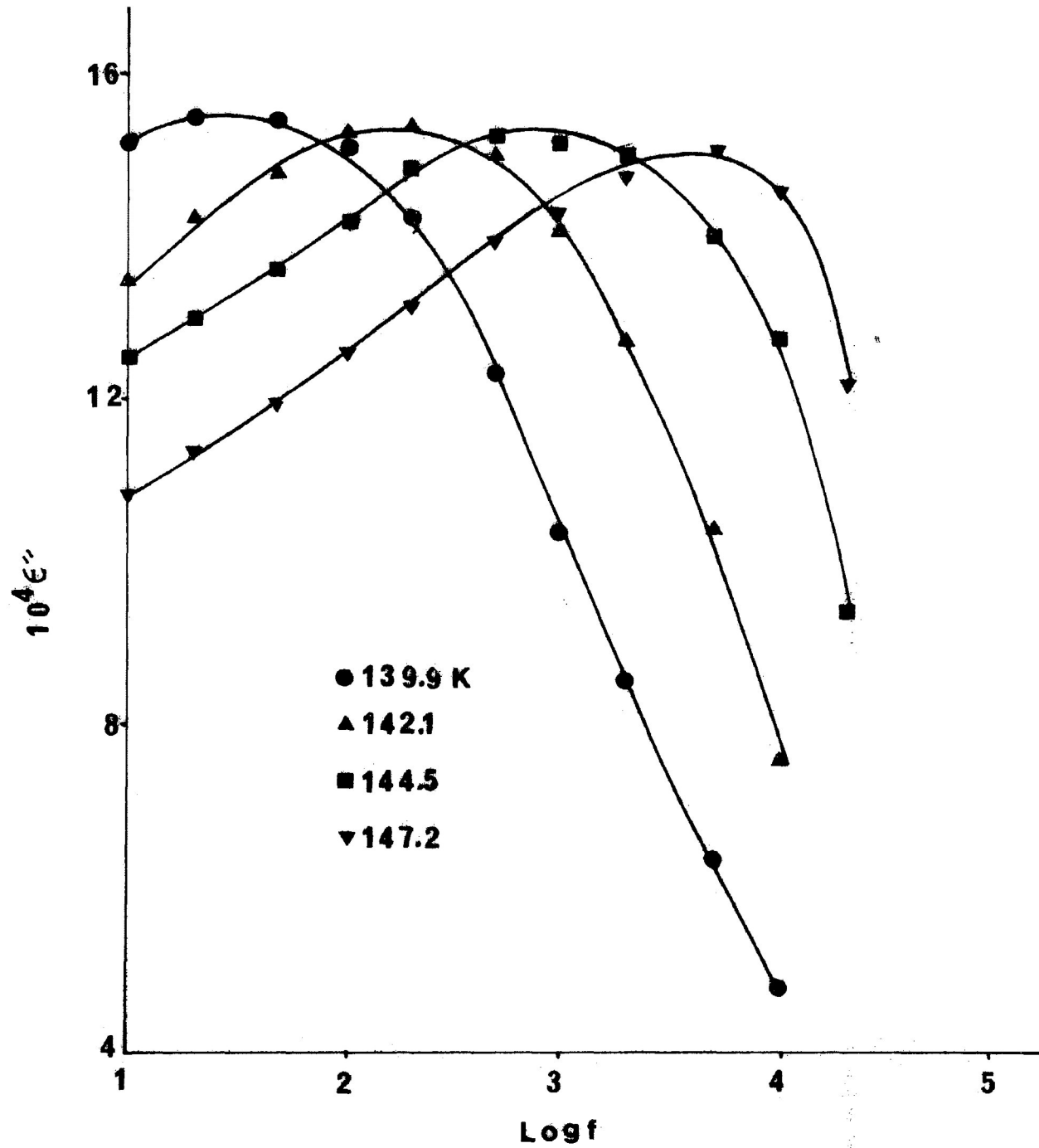


FIGURE 6.14: Dielectric loss factor ϵ'' versus log frequency for mesitylene

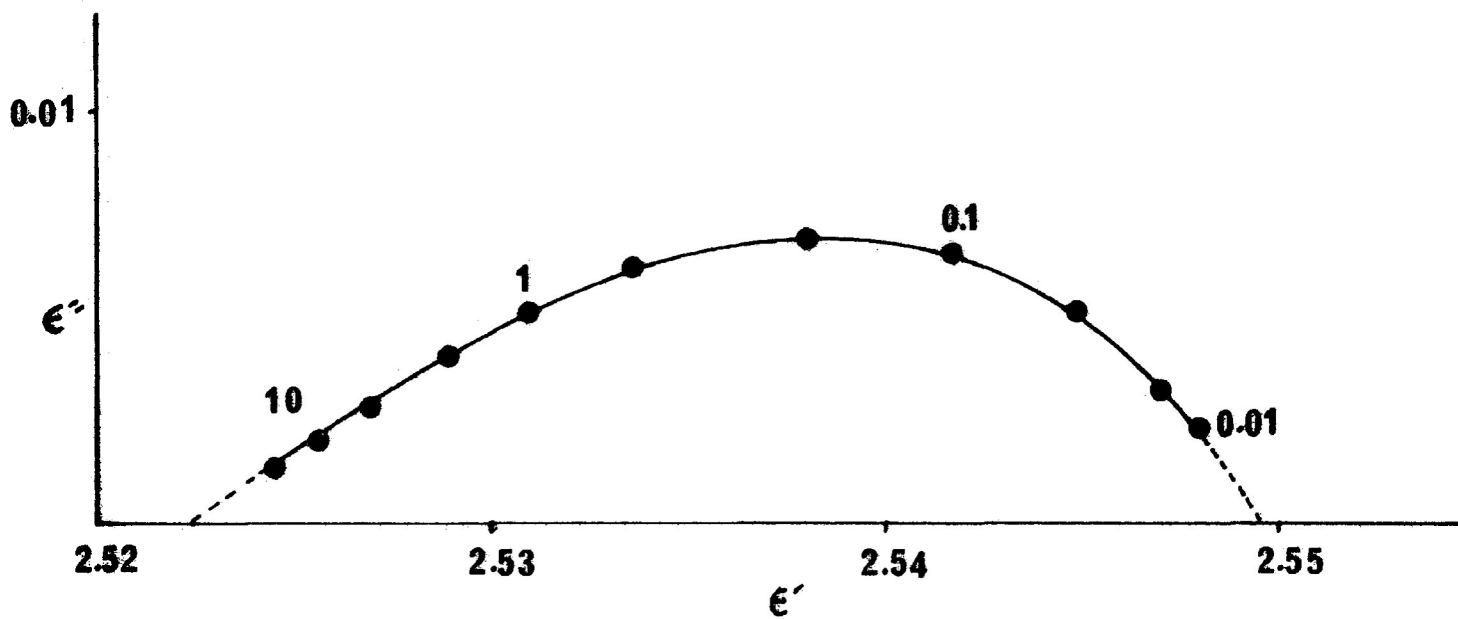


FIGURE 6.15: Complex plane diagram for p-ethyltoluene at 133.8 K
 Numbers beside points are frequencies in kHz

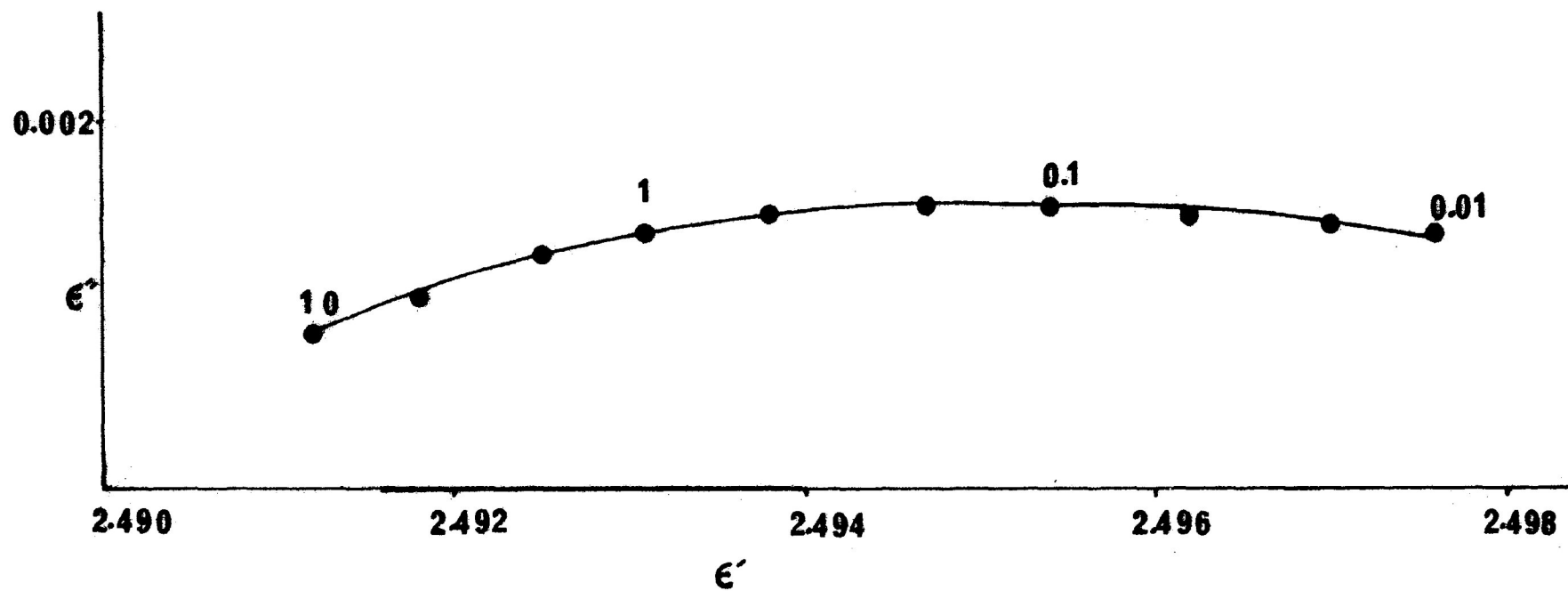


FIGURE 6.16: Complex plane diagram for mesitylene at 142.1 K
Numbers beside points are frequencies in kHz

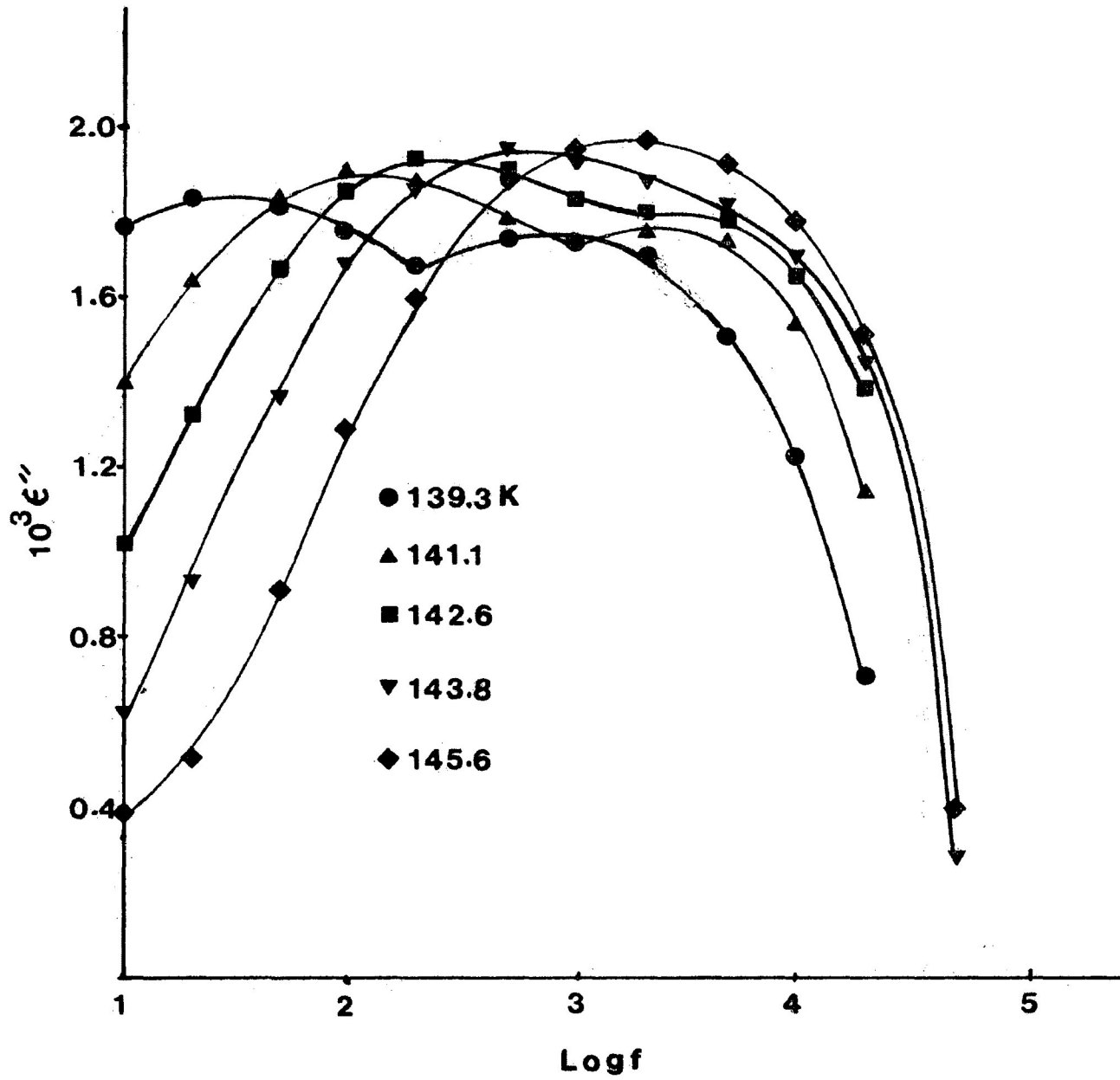


FIGURE 6.17: Dielectric loss factor ϵ'' versus log frequency for p-diethylbenzene

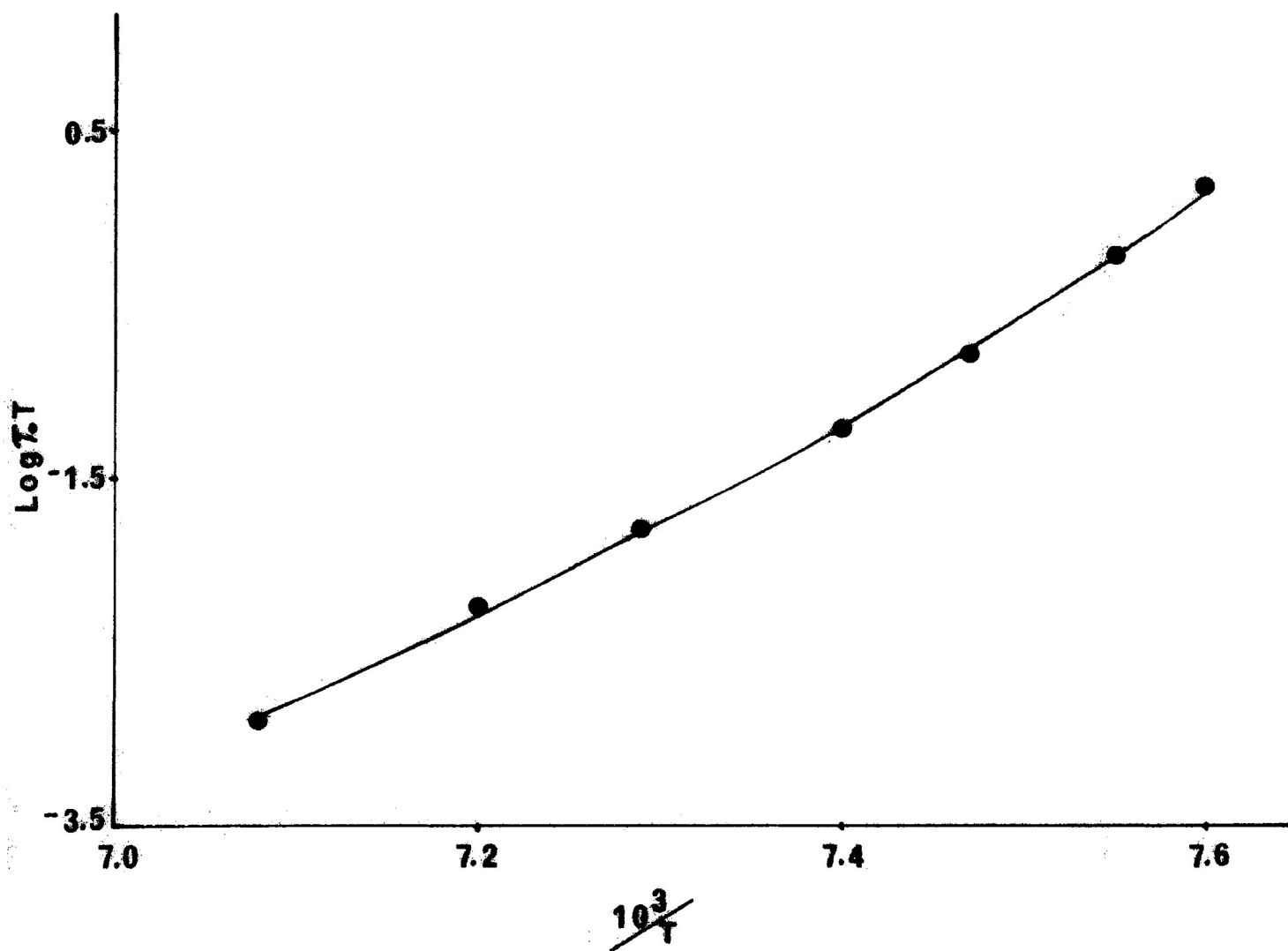


FIGURE 6.18: Eyring plot of $\log(\tau_0 T)$ versus $\frac{1}{T}$ for p-ethyltoluene

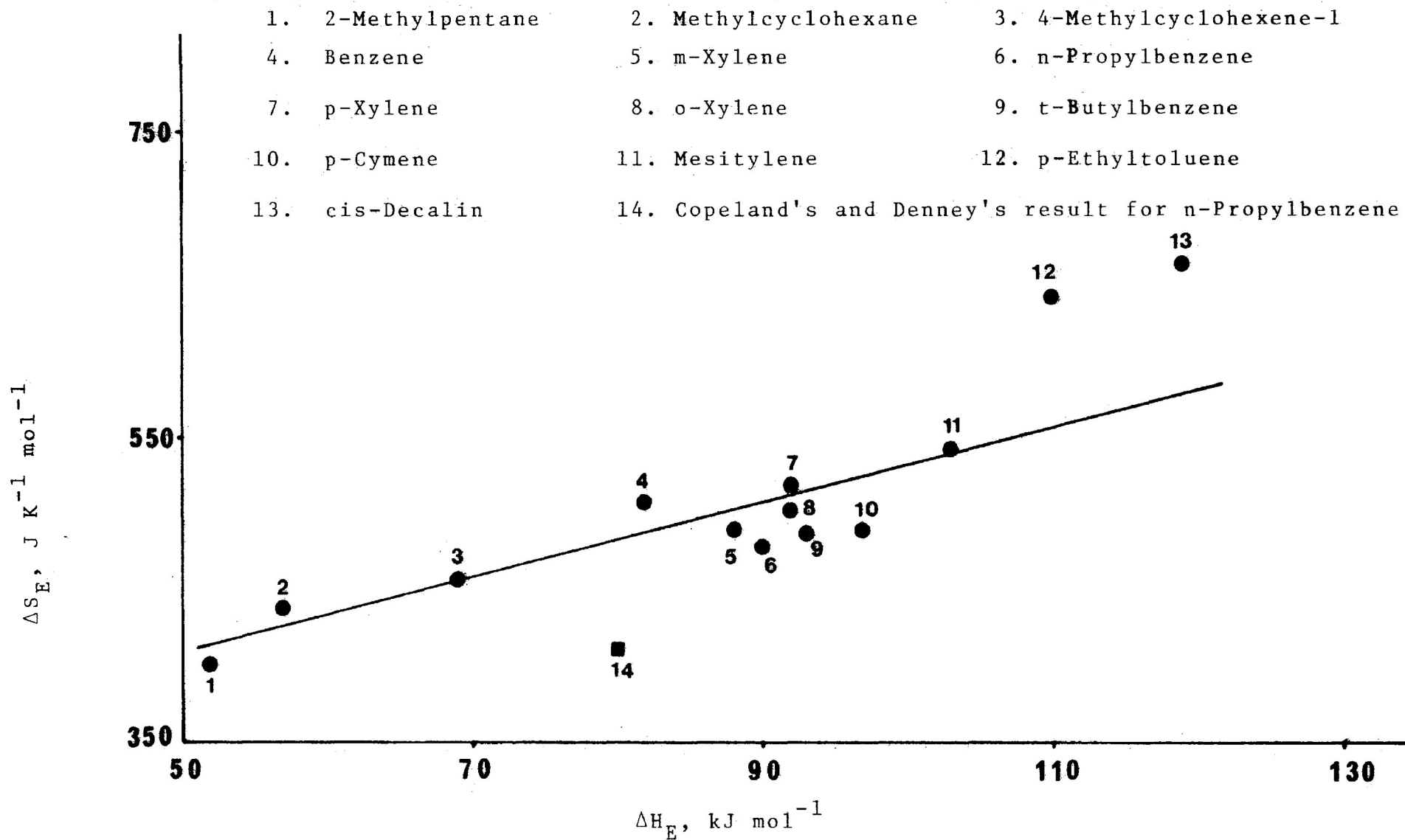


FIGURE 6.19: Plot of ΔH_E versus ΔS_E for some hydrocarbons

1. 2-Methylpentane 2. methylcyclohexane 3. 4-Methylcyclohexene-1
 4. Benzene 5. m-Xylene 6. n-Propylbenzene 7. o-Xylene 8. p-Xylene
 9. t-Butylbenzene 10. p-Cymene 11. Mesitylene

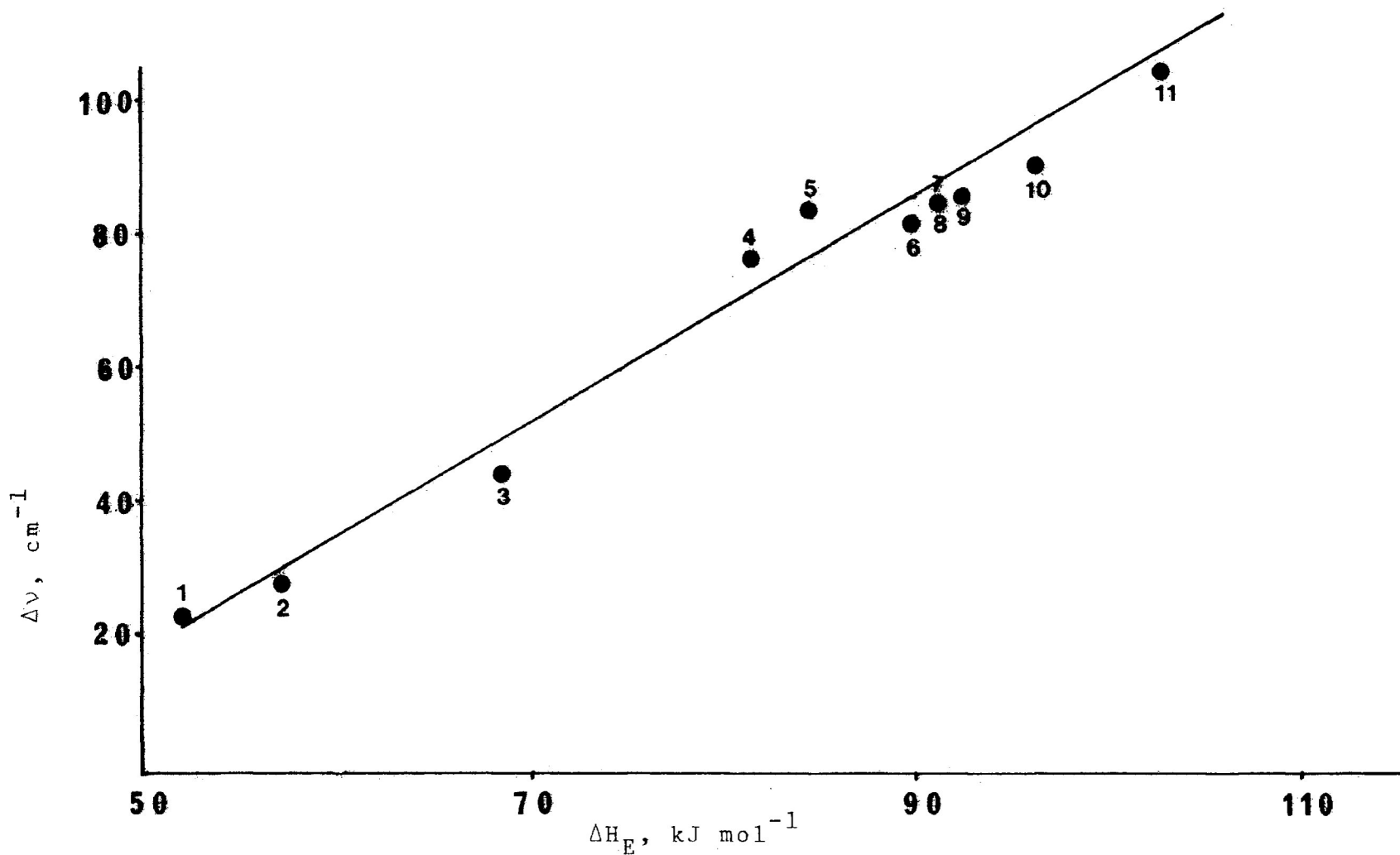


FIGURE 6.20: Stretching frequency, $\Delta \nu$, versus Eyring enthalpy of activation, ΔH_E , for some hydrocarbons

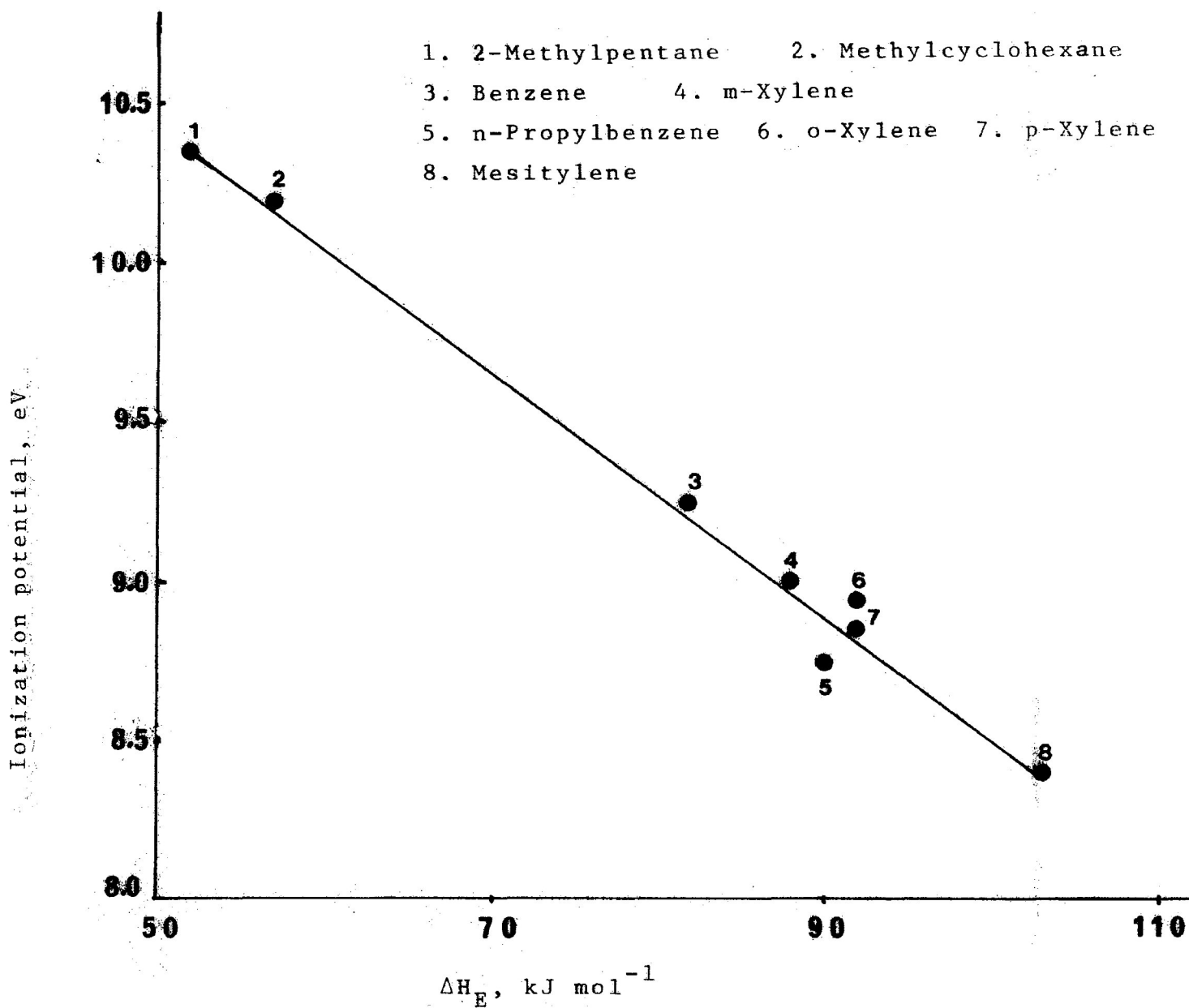


FIGURE 6.21: Eyring enthalpy of activation versus ionization potential for some hydrocarbons

C H A P T E R V I I

SOME RIGID DIPOLAR MOLECULES

INTRODUCTION

A variety of rigid polar molecules has been investigated as pure liquids using microwave techniques. Pure liquids consisting of rigid molecules show a single relaxation time (1-9) or a narrow distribution of relaxation times (5,8,9,10), in many cases described with the help of the Cole-Cole equation with a low value of distribution parameter, α .

The dielectric relaxation behaviour of compounds with rigid molecules has also been investigated extensively in solution in nonpolar, non-viscous solvents such as carbon tetrachloride (1,11-14), cyclohexane (3, 12-17), benzene (3,11,13, 18-20), and p-xylene (13,17,21, 22). The results show the same picture as for these compounds in the pure liquid state; with a few exception single relaxation time or narrow distribution of relaxation times, often described with the help of the Cole-Cole equations are obtained.

The dielectric relaxation behaviour of rigid polar molecules in viscous or vitreous nonpolar solvents

differs distinctly from the behaviour in non-viscous solvents treated above. Whereas solutions in non-viscous solvents are as a rule reported to have a single relaxation times or narrow distributions, solution in viscous or viterous solvents, e.g. supercooled cis-decalin (23-25) or o-terphenyl (26-29), generally show two distinct relaxation ranges, each showing a broad distribution of relaxation times, whether symmetric or asymmetric. Similar phenomena have been observed in solutions in polymeric solvents, e.g. polystyrene (30-32).

When the measurements are carried out at audio- or radio-frequencies, one of the relaxation ranges, denoted as the α -relaxation range, is observed above the glass transition temperature (T_g), and the other, the β -relaxation range, normally below that temperature (23).

In the description of the α -relaxation range for rigid molecules in supercooled cis-decalin or o-terphenyl, use can be made of the Cole-Davidson equation (33), Havriliak-Negami equation (34) or the Williams-Watts equation (35), and that for the description of both α - and β -relaxation ranges in polystyrene use can be made of the Fuoss-Kirkwood equation (36).

Very few rigid molecules have been investigated in the solid state. Among these, the substituted methanes (7,37) and benzenes (38-41) are noteworthy. It is worthwhile, therefore, to examine a few more rigid polar molecules in the solid state which were not studied earlier.

EXPERIMENTAL RESULTS

The following compounds were included in the present study:

1. fluorobenzene
2. chlorobenzene
3. bromobenzene
4. o-dichlorobenzene

5. m-dichlorobenzene
6. 1-chloronaphthalene
7. N-methylpyrrole
8. pyridine
9. 4-methylpyridine
10. quinoline
11. isoquinoline

All of these chemicals were commercially available with sufficient purity. All of these were dried over

activated molecular sieve prior to use.

In the discussion, emphasis has been given on the Eyring enthalpy of activation values. This parameter (ΔH_E) does not vary appreciably whether the analysis is made from Fuoss-Kirkwood, Cole-Davidson, Williams-Watts or Havriliak-Negami equations. The analyses were made using Fuoss-Kirkwood equation.

Table 7.1 lists the values of ΔH_E , ΔS_E , along with ΔG_E and τ values at 100 K, 150 K and 200 K for each system where appropriate.

Experimental values of τ , $\log f_{\max}$, β , ϵ''_{\max} , ϵ_{∞} and μ at various temperatures obtained for these compounds are listed in Table 7.2.

DISCUSSION

Fluorobenzene

This compound was studied previously in polystyrene matrices by Khwaja (42) and recently in o-terphenyl by Gourlay(43). In polystyrene, the dielectric absorption

was observed in the temperature range 95-118 K with an Eyring enthalpy of activation (ΔH_E) 9 kJ mol⁻¹. In o-terphenyl, the temperature range was 79-97 K and the observed ΔH_E was 12 ± 3 kJ mol⁻¹. This dielectric absorption of fluorobenzene in polystyrene and o-terphenyl was attributed to the relaxation of the whole molecule.

Present dielectric studies of this compound in the pure solid state show two distinct relaxation processes (Fig. 7.1), one in the temperature range 83-120 K, which, from a good straight line of Eyring plot (Fig. 7.2), yields an enthalpy of activation (ΔH_E) 12.5 ± 0.9 kJ mol⁻¹ and entropy of activation -41 ± 9 J K⁻¹ mol⁻¹, and the other in the 161.1-177.8 K region with an apparent enthalpy of activation 106 ± 2 kJ mol⁻¹ and entropy of activation 463 ± 14 J K⁻¹ mol⁻¹.

Dielectric data for the lower temperature relaxation may be represented by Cole-Cole plot (Fig. 7.3). The value of enthalpy of activation (ΔH_E) for this relaxation, within experimental error, agrees extremely well with those observed in polystyrene and in o-terphenyl for molecular rotation and may, therefore, be assigned to molecular relaxation. It is also to be noted that the temperature and frequency ranges for molecular relaxation of this molecule in two different media, polystyrene and

o-terphenyl, and in the pure solid state are almost the same.

The higher temperature relaxation of fluoro-benzene may be suspected to co-operative motion. Dielectric data for this relaxation may be adequately represented by Havriliak-Negami equation (Fig. 7.4). The Havriliak-Negami equation is usually applicable for the α -relaxation range of many polymers in the amorphous state (44).

Figure 7.5 shows the dielectric loss factor, ϵ'' , versus log frequency plot of this high temperature relaxation. It can be seen that the maxima of the asymmetric loss curves change rapidly with slight variation of temperature, which is one of the characteristic features of a co-operative relaxation process.

It is noticeable from Table 7.2 that the distribution parameter, β , value increases whereas the dipole moment, μ , value decreases with the increase of temperature.

Considering all the characteristic features observed, such as (i) high temperature relaxation with apparent large

ΔH_E and ΔS_E values, (ii) change of asymmetric loss curves with slight variation of temperature, (iii) representation of dielectric data by Havriliak-Negami equation...etc. strongly indicated that a co-operative relaxation process was found in fluorobenzene in the temperature range 161-178 K.

Chlorobenzene

Earlier this compound was studied in cis-decalin by Johari and Goldstein (23) and later by Khwaja (42) and Mazid (45) independently in polystyrene matrices. Johari and Goldstein (23) observed a β -relaxation in the temperature region 112-133 K. Khwaja (42) and Mazid (45) both observed low temperature (~ 80 -125 K) relaxation with an enthalpy of activation around 10 kJ mol^{-1} for molecular rotation. Recently, Kashem (46) has examined this compound in two different media, o-terphenyl and polyphenylether (Santovac). He observed dielectric relaxation in the temperature region 99-140 K in o-terphenyl ($\Delta H_E = 14.4 \text{ kJ mol}^{-1}$) and in the 104-139 K region in polyphenylether ($\Delta H_E = 16.0 \text{ kJ mol}^{-1}$).

The present dielectric study of chlorobenzene in

the pure solid state shows two relaxation processes (Fig. 7.7). The lower temperature relaxation is not well-defined probably due to overlap with the higher temperature process. The results reported here are for a short temperature range (94-100 K) and hence are not free from considerable errors. However, the observed enthalpy of activation ($\Delta H_E \approx 14 \text{ kJ mol}^{-1}$) is comparable to those found in o-terphenyl ($\Delta H_E \approx 14 \text{ kJ mol}^{-1}$) and in polyphenylether ($\Delta H_E \approx 16 \text{ kJ mol}^{-1}$) for molecular rotation.

The higher temperature (115.5-119.6 K) relaxation, which yields an apparent enthalpy of activation (ΔH_E) $116 \pm 10 \text{ kJ mol}^{-1}$ and entropy of activation $798 \pm 81 \text{ J K}^{-1} \text{ mol}^{-1}$, may be assigned to co-operative microBrownian motion. Dielectric data may be represented by Havriliak-Negami equation.

Bromobenzene

Johari and Goldstein (23) studied bromobenzene in cis-decalin and found no β -relaxation. Khwaja (42) and Mazid (45) examined this compound in polystyrene matrices and observed molecular motion in the same temperature

region 100-135 K but with a slightly different enthalpy of activation 13 and 16 kJ mol⁻¹ respectively. Recently Kashem (46) observed dielectric relaxation for this compound in o-terphenyl and in polyphenylether in the temperature regions 115-164 K and 113-160 K with ΔH_E values of 17.4 and 18.1 kJ mol⁻¹, respectively.

In the pure solid state, bromobenzene shows an ill-defined relaxation around 110 K (Fig. 7.8). A distinct peak is resolved only at the lowest measuring frequency (10 Hz). For this reason, no attempt was made to calculate the activation energy for this low temperature relaxation. However, the observed free energy of activation at 110 K ($\Delta G_E \approx 19$ kJ mol⁻¹) is comparable to those found in polystyrene ($\Delta G_E = 17$ kJ mol⁻¹), o-terphenyl ($\Delta G_E = 21$ kJ mol⁻¹) and polyphenylether ($\Delta G_E = 20$ kJ mol⁻¹) at 100 K for molecular relaxation.

The higher temperature relaxation of bromobenzene which was observed in the temperature region 140.0-147.0 K covering $\log f_m$ 1.575-3.531, yields an apparent enthalpy of activation 112 ± 3 kJ mol⁻¹ and entropy of activation 607 ± 22 J K⁻¹ mol⁻¹ and may be assigned to co-operative

relaxation. This view is supported from the other observed characteristic features, such as representation of dielectric data by Havriliak-Negami equation (Fig. 7.9) and rapid change of asymmetric loss curves with slight variation of temperature.

o-Dichlorobenzene

Earlier o-dichlorobenzene was studied by Davies and Swain (31) in polystyrene and observed molecular relaxation in the temperature region 88-122 K with enthalpy of activation (ΔH_E) 16.3 kJ mol and ΔS_E 1.4 J K⁻¹ mol⁻¹. A β -relaxation was observed in cis-decalin (23) around 90 K. Recently, Kashem (46) from a careful study at 80-103 K, 81-114 K and 81-115 K temperature regions has observed dielectric absorption for o-dichlorobenzene in three viscous media, polystyrene, ($\Delta H_E = 11$ kJ mol⁻¹), o-terphenyl ($\Delta H_E \approx 11$ kJ mol⁻¹) and polyphenylether ($\Delta H_E = 13$ kJ mol⁻¹), respectively.

Three distinct relaxation processes were observed for o-dichlorobenzene in the solid state (Fig. 7.10). The

observed relaxation in the temperature region 79-101 K yields $\Delta H_E = 10.7 \pm 0.6 \text{ kJ mol}^{-1}$ and $\Delta S_E = -42 \pm 7 \text{ J K}^{-1} \text{ mol}^{-1}$. The temperature and frequency region as well as ΔH_E are in excellent agreement with those found for this molecule in different media for molecular relaxation.

The higher temperature relaxations in the 123-153 K and 158-182 K regions may be accounted for molecular relaxation of this molecule in two different solid phases.

m-Dichlorobenzene

In polystyrene (45), dielectric absorption was found in the temperature region 115-146 K with ΔH_E of 16 kJ mol^{-1} and ΔS_E of $-30 \text{ J K}^{-1} \text{ mol}^{-1}$ for molecular relaxation.

Present dielectric study of m-dichlorobenzene in the pure solid state shows two relaxation processes, one around 90 K and the other in the 125-152 K ranges. The lower temperature one is not well-defined due to the influence of the higher temperature one. The results reported here are for a short temperature range (88-97 K)

and hence are subject to considerable errors. However, within the limit of experimental error, the enthalpy of activation ($\Delta H_E = 17.8 \pm 2.2 \text{ kJ mol}^{-1}$) for this low temperature relaxation agrees extremely well with that found in polystyrene.

It is notable that both m- and o-dichlorobenzene show dielectric absorptions in a similar temperature range (125-153 K) with a similar magnitude of enthalpy of activation ($\Delta H_E = 24 \text{ kJ mol}^{-1}$).

The two relaxation processes observed in m-dichlorobenzene may be accounted for molecular relaxations in two different solid phases.

1-Chloronaphthalene

Present dielectric study of this molecule shows two relaxation processes in the temperature regions 91-139 K and 128-158 K (Fig. 7.11). The lower temperature relaxation yields enthalpy of activation $16.5 \pm 0.6 \text{ kJ mol}^{-1}$ and for higher temperature it is $25.3 \pm 1.4 \text{ kJ mol}^{-1}$. This compound was studied earlier by Tay and Walker (32) in

polystyrene matrices and found molecular relaxation in the temperature region 103-133 K with ΔH_E value of $14.7 \pm 0.7 \text{ kJ mol}^{-1}$. Recently, Kashem (46) has examined this molecule in o-terphenyl and also in polyphenylether, and dielectric relaxation behaviour in the temperature range 100-146 K in o-terphenyl ($\Delta H_E = 14.8 \pm 0.8 \text{ kJ mol}^{-1}$) and 103-145 K in polyphenylether ($\Delta H_E = 17.0 \pm 0.8 \text{ kJ mol}^{-1}$). It is notable that both temperature region and ΔH_E values observed for this compound in three different media for molecular relaxation agrees extremely well with the lower temperature process in the pure solid state.

The higher temperature process may be assigned to molecular relaxation process in different solid phase.

N-Methylpyrrole

This compound was not studied earlier. Present study shows a dielectric absorption in the temperature region 83-121 K which, from a good straight line of Eyring plot (Fig. 7.12), yields ΔH_E of $5.6 \pm 0.2 \text{ kJ mol}^{-1}$ and ΔS_E of $-110 \pm 2 \text{ J K}^{-1} \text{ mol}^{-1}$. Dielectric data for this relaxation may be represented by Cole-Cole plot (Fig. 7.13). This low temperature relaxation having the dis-

tribution parameter 0.20-0.34 and the relaxation time $\tau_{100\text{ K}} = 2.5 \times 10^{-4}$ s, may be assigned to molecular process.

Pyridine

Previous dielectric study (47) of this compound in polystyrene showed molecular relaxation around 80 K with ΔH_E of 3 kJ mol⁻¹ and ΔS_E of -92 J K⁻¹ mol⁻¹. Recent dielectric studies in o-terphenyl (46) and in cis-decalin (48) yield ΔH_E of 8.4 and 14.2 kJ mol⁻¹ and ΔS_E of -44 and -3 J K⁻¹ mol⁻¹, respectively.

In the pure solid no low temperature low energy relaxation was found. A process was found to occur in the temperature range 164.0-175.2 K covering $\log f_m$ 2.46-4.33. This process may be characterized by (i) high enthalpy ($\Delta H_E = 90$ kJ mol⁻¹) and entropy of activation ($\Delta S_E = 373$ J K⁻¹ mol⁻¹), (ii) rapid change of absorption curves (Fig. 7.14) with slight variation of temperature, (iii) representation of dielectric data by Williams-Watts equation (Fig. 7.15), (iv) high β -value which increases with increase of temperature and (v) decrease of dipole moment with increase of temperature. All of these observed facts suggest that this relaxation might be due to co-operative intermolecular effects.

4-Methylpyridine

The dielectric absorption was found for this compound in polystyrene matrices in the temperature region 88-124 K with ΔH_E of 14 kJ mol⁻¹ and ΔS_E of -19 J K⁻¹ mol⁻¹ which was interpreted as molecular relaxation process (45). Recently, Kashem (46) and Ahmed (48) have studied this molecule in o-terphenyl (46), polyphenylether (46) and cis-decalin (48). Their ΔH_E and ΔS_E values are 16 kJ mol⁻¹ and -33 J K⁻¹ mol⁻¹ in o-terphenyl, 17 kJ mol⁻¹ and -26 J K⁻¹ mol⁻¹ in polyphenylether and 16 kJ mol⁻¹ and 1 J K⁻¹ mol⁻¹ in cis-decalin respectively.

Present study in the solid state shows no low temperature low energy relaxation. However, a process is found to occur in the temperature range 181.4-189.8 K which yields ΔH_E of 120 kJ mol⁻¹ and ΔS_E of 486 J K⁻¹ mol⁻¹. This high energy barrier as well as adequate representation of dielectric data by Davidson-Cole skewed are function (Fig. 7.17), high β -value (0.50-0.72) which increases with the increase of temperature and decrease of dipole moment with temperature suggest that the observed relaxation might be due to microBrownian cooperative motion.

Quinoline and Isoquinoline

Both the compounds were studied in polystyrene by Walker et al (47) and observed molecular relaxation for quinoline in the temperature region 139-174 K and for isoquinoline in the 129-153 K region with a similar ΔH_E value of 24 kJ mol^{-1} . Neither quinoline nor isoquinoline shows such low temperature relaxation in pure solid state. However, these two compounds show high temperature relaxations (for quinoline, 197.6-206.2 K and for isoquinoline, 202.5-210.3 K). The ΔH_E and ΔS_E values for this relaxation of quinoline are 151 kJ mol^{-1} and $587 \text{ J K}^{-1} \text{ mol}^{-1}$ and for isoquinoline these are 130 kJ mol^{-1} and $464 \text{ J K}^{-1} \text{ mol}^{-1}$, respectively. Dielectric data for both quinoline and isoquinoline may be represented by Havriliak-Negami equation (Fig. 7.20 for quinoline and Fig. 7.21 for isoquinoline). In both cases, the distribution parameter (0.30-0.36 for quinoline and 0.29-0.38 for isoquinoline) increases and dipole moment decreases with the increase of temperature. All these facts suggest that the observed high temperature relaxation for quinoline and isoquinoline might be due to co-operative motion.

From the above results, it is seen that all the

arylhalides in the pure solid state show molecular relaxations almost in the same temperature and frequency region as those observed in different viscous media as mentioned above (the slight difference may be due to the difference in viscosity of the solvents). Moreover, a similar magnitude of ΔH_E values are found in all cases.

But when we consider nitrogen containing heterocyclic rigid molecules, the situation is different: only N-methylpyrrole shows molecular relaxation in the solid state. No molecular relaxation was found for pyridine, 4-methylpyridine, quinoline and isoquinoline, in the pure solid state though these molecules show such relaxation in different viscous media. This is probably because of the crystal packing and lack of free volume in these molecules.

It can be seen from the results of o-dichlorobenzene, m-dichlorobenzene and 1-chloronaphthalene that more than one molecular relaxation may be present in different solid phases. But in a viscous medium, at low temperature the solute molecules are in a definite phase of solvent molecules until the glass transition temperature of the solvent is reached. So, more than one molecular relaxation

below T_g is unlikely in the case of a molecule measured in a viscous medium.

The distribution parameter, β , values for molecular relaxation are always greater when a molecule is measured in the pure solid state than when it is measured in a viscous medium. For example, pure o-dichlorobenzene has a β -value of 0.45-0.71; but in polystyrene, o-terphenyl and polyphenylether (46), the β -values are 0.17-0.21, 0.15-0.24 and 0.17-0.24, respectively. The high β -values for pure o-dichlorobenzene are of the same order of those observed by Davies and Swain (31) for the intramolecular ring inversion of cyclohexyl derivatives in polystyrene. These authors commented that "the increase in β would be expected for an intramolecular dipolar motion as this would be appreciably less dependent upon the co-operative movement of the adjacent polystyrene units than is the whole molecule rotation". A wide range of local environments are generally encountered by the polar solutes dispersed in viscous media as is reflected in typically low β -values. In the pure solid state a large number of molecules are in the same environments and hence, a large β value would be expected.

It is apparent from Figures 7.4 and 7.9 that

dielectric data for co-operative motion of arylhalides (e.g. fluorobenzene, chlorobenzene and bromobenzene) may be represented by Havriliak-Negami equation. But no single equation can represent the dielectric data for the co-operative motion of the heterocyclic molecules. It is not apparent from the present work why the dielectric loss data fit different types of equations. Further, it should be noted that the mean or most probable relaxation time is different from the reciprocal of the angular frequency at which the loss peak takes place in the Havriliak-Nagami and the Williams-Watts equations.

REFERENCES

1. R.C. Miller and C.P. Smyth, J. Chem. Phys.,
24(1956)814.
2. W.E. Vaughan and C.P. Smyth, J. Phys. Chem.,
65(1961)89.
3. A.A. Antony and C.P. Smyth, J. Am. Chem. Soc.,
86(1964)152.
4. S.K. Garg and C.P. Smyth, J. Chem. Phys.,
42(1965)1397.
5. S. Mallikurjan and N.E. Hill, Trans. Faraday
Soc., 61(1965)1397.
6. T.V. Gopalan and P.K. Kadaba, J. Phys. Chem.,
72(1968)3676.
7. C. Clemett and M. Davies, Trans. Faraday Soc.,
58(1962)1705.
8. J.H. Calderwood and C.P. Smyth, J. Am. Chem. Soc.,
78(1956)1295.
9. A. Mansingh and D.B. McLay, J. Chem. Phys.,
54(1971)3322.
10. S. Chandra and D. Nath, J. Chem. Phys.,
51(1969)5299.
11. J.K. Eloranta and P.K. Kadaba, Chem. Phys. Letters,
11(1971)251.
12. W.F. Hassell and S. Walker, Trans. Faraday Soc.,
62(1965)861.
13. J. Crossley, W.F. Hassell and S. Walker, Can. J.
Chem., 46(1968)2181.
14. G.D. Martin and S. Walker, Can. J. Chem.,
50(1972)707.
15. J. Crossley and S. Walker, J. Chem. Phys.,
45(1966)4773.

16. J. Crossley, W.F. Hassell and S. Walker, J. Chem. Phys., 48(1968)1261.
17. J. Crossley and S. Walker, Can. J. Chem., 46(1968)2369.
18. D.B. Farmer, A. Holt and S. Walker, J. Chem. Phys., 44(1966)4116.
19. E. Forest and C.P. Smyth, J. Phys. Chem., 69(1965)1302.
20. A. Mansingh, J. Chem. Phys., 51(1969)2762.
21. W.F. Hassell and S. Walker, Trans. Faraday Soc., 62(1965)2690.
22. J. Crossley and S. Walker, J. Chem. Phys., 48(1968)4742.
23. G.P. Johari and M. Goldstein, J. Chem. Phys., 53(1970)2372.
24. G.P. Johari and C.P. Smyth, J. Am. Chem. Soc., 91(1969)5168.
25. G.P. Johari and C.P. Smyth, J. Chem. Phys., 56(1972)4411.
26. G. Williams and P.J. Hains, Chem. Phys. Letters, 10(1971)585.
27. G. Williams and P.J. Hains, Faraday Symp. Chem. Soc., 6(1972)14.
28. M.F. Shears and G. Williams, J. Chem. Soc. Faraday II, 69(1973)608.
29. M. Nakamura, H. Takahashi and K. Higasi, Bull. Chem. Soc. Japan, 47(1974)1593.
30. M. Davies and A. Edwards, Trans. Faraday Soc., 63(1967)2163.
31. M. Davies and J. Swain, Trans. Faraday Soc., 67(1971)1637.

32. S.P. Tay and S. Walker, J. Chem. Phys.,
63(1975)1634.
33. D.W. Davidson and R.H. Cole, J. Chem. Phys.,
19(1951)1484.
34. S. Havriliak and S. Negami, J. Polymer Sci.,
C14(1966)99.
35. G. Williams and D.C. Watts, Trans. Faraday Soc.,
66(1970)80.
36. J.G. Kirkwood and R.M. Fuoss, J. Chem. Phys.,
9(1941)329.
37. W. van Dahl and R.H. Cole, J. Chem. Phys.,
45(1966)1849.
38. C. Brot and I. Darmon, J. Chem. Phys.,
53(1970)2271.
39. A. Aihara, C. Kitazowa, and A. Nahara, Bull. Chem.
Soc., Japan, 43(1970)3750.
40. P.G. Hall and G.S. Horsfall, J. Chem. Soc.
Faraday II, 69(1973)1071.
41. P.G. Hall and G.S. Horsfall, J. Chem. Soc.
Faraday II, 69(1973)1515.
42. H.A. Khwaja, M.Sc. Thesis, Lakehead University,
Thunder Bay, Canada, 1977.
43. D.L. Gourlay, M.Sc. Thesis, Lakehead University,
Thunder Bay, Canada, 1982.
44. C.J.F. Böttcher and P. Bordewijk, "The Theory of
Electric Polarization", Vol. II, Elsevier
Scientific Publishing Company, Amsterdam,
1978.
45. M.A. Mazid, M.Sc. Thesis, Lakehead University,
Thunder Bay, Canada, 1977.
46. M.A. Kashem, Private Communication, This Laboratory.
47. J.P. Shukla, S.Walker and J. Warren, J. Chem.
Soc. Faraday I, 74(1978)2045.
48. S. Ahmed, Private Communication, This laboratory.

TABLE 7.1:

EYRING ANALYSIS RESULTS FOR SOME RIGID POLAR MOLECULES IN THE SOLID STATE

MOLECULE	T(K)	τ (s)			ΔG_E (kJ mol ⁻¹)			ΔH_E	ΔS_E
		100 K	150 K	200 K	100 K	150 K	200 K	(kJ mol ⁻¹)	(J K ⁻¹ mol ⁻¹)
Fluorobenzene	83-120	2.3×10^{-4}	1.0×10^{-6}		16.6	18.7		12.5 ± 0.9	-41 ± 9
	161.1-177.8		2.3	9.3×10^{-10}		13.8	-32.6	106 ± 2	463 ± 14
Chlorobenzene	94-100	5.2×10^{-3}			19.2			14.2 ± 2.9	-50 ± 30
	115.5-119.6	2.3×10^6	1.2×10^{-14}		35.8	-4.1		116 ± 10	798 ± 81
Bromobenzene	108-112				~19				
	140-147		6.7×10^{-6}		21.0			112 ± 3	606 ± 22
o-Dichlorobenzene	79-101	3.2×10^{-5}			15.0			10.7 ± 0.6	-42 ± 7
	123-153	2.9	1.8×10^{-7}		24.5	23.5		26.4 ± 1.1	19 ± 8
	158-182		3.4×10^{-2}	6.5×10^{-7}		31.7	28.5	41.3 ± 2.1	64 ± 12
m-Dichlorobenzene	88-97	1.0×10^{-3}			17.9			17.8	-1 ± 16
	125-152	2.5	1.6×10^{-4}		24.3	25.7		23.0 ± 3.0	-14 ± 22

TABLE 7.1: continued...

MOLECULE	T (K)	τ (s)			ΔG_E (kJ mol ⁻¹)			ΔH_E	ΔS_E
		100 K	150 K	200 K	100 K	150 K	200 K	(kJ mol ⁻¹)	(J K ⁻¹ mol ⁻¹)
1-Chloro-naphthalene	91-139	7.4×10^{-4}	6.7×10^{-7}		17.6	18.2		16.5 ± 0.6	-11 ± 5
	128-158		3.4×10^{-5}			23.0		25.3 ± 1.4	15 ± 10
N-Methylpyrrole	83-121	2.5×10^{-4}			16.7			5.6 ± 0.2	-110 ± 2
Pyridine	164.0-175.2		2.6×10^{-1}	2.7×10^{-9}		34.2	15.5	90 ± 5	373 ± 31
4-Methylpyridine	181.4-189.4			1.6×10^{-7}		22.3		120 ± 4	486 ± 22
Quinoline	197.6-206.2						33.1	151	587
Isoquinoline	202.5-210.3						37.0	130	464

TABLE 7.2: Fuoss-Kirkwood Analysis Parameters, Cole-Cole ϵ_∞ and Experimental Apparent Dipole Moments for Some Rigid Molecules in the Solid State

T(K)	$10^6 \tau$ (s)	$\log f_{\max}$	β	$10^3 \epsilon''_{\max}$	ϵ_∞	μ (D)
<u>Fluorobenzene</u>						
<u>Lower Temperature Process</u>						
83.3	6842.8	1.367	0.51	0.42	2.48	-
85.3	3878.2	1.613	0.61	0.43	2.48	-
87.0	1977.7	1.906	0.40	0.41	2.48	-
89.3	1366.3	2.066	0.39	0.42	2.48	-
93.8	678.4	2.370	0.47	0.42	2.48	-
98.5	266.8	2.776	0.43	0.43	2.48	-
103.0	200.0	2.901	0.49	0.45	2.48	-
108.1	88.3	3.256	0.46	0.48	2.48	-
113.2	36.4	3.641	0.44	0.54	2.48	-
119.9	12.2	4.117	0.52	0.67	2.48	-
<u>Fluorobenzene</u>						
<u>Higher Temperature Process</u>						
161.1	5829.4	1.436	0.30	1.91	2.56	0.067
162.1	3694.2	1.634	0.30	1.90	2.56	0.067
163.2	2060.1	1.888	0.30	1.91	2.57	0.068
164.0	1492.9	2.028	0.31	1.89	2.57	0.067
165.7	637.3	2.398	0.32	1.88	2.57	0.066
167.5	267.3	2.775	0.32	1.86	2.57	0.068
169.3	117.9	3.130	0.33	1.85	2.57	0.065
171.1	47.6	3.524	0.34	1.87	2.58	0.064
173.9	16.9	3.975	0.40	1.82	2.58	0.059
175.8	8.8	4.258	0.43	1.70	2.59	0.055
177.8	2.7	4.778	0.42	1.63	2.59	0.055
<u>Chlorobenzene</u>						
93.5	18520.0	0.934	0.36	0.056	2.84	-
97.4	8313.6	1.282	0.41	0.058	2.84	-
99.6	5716.6	1.445	0.45	0.060	2.84	-
102.5	4205.0	1.578	0.45	0.062	2.84	-
115.5	17274.0	0.964	0.23	0.41	2.85	-
116.5	5318.2	1.476	0.23	0.41	2.85	-
117.6	1794.2	1.948	0.36	0.45	2.85	-
118.5	650.2	2.389	0.39	0.45	2.85	-
119.6	278.2	2.758	0.33	0.49	2.85	-

TABLE 7.2: continued...

T(K)	$10^6 \tau$ (s)	$\log f_{\max}$	β	$10^3 \epsilon''_{\max}$	ϵ_{∞}	μ (D)
<u>Bromobenzene</u>						
140.0	4331.3	1.565	0.40	1.04	2.66	0.042
140.8	2497.9	1.804	0.32	0.97	2.66	0.045
141.8	1209.4	2.119	0.36	0.99	2.66	0.043
142.8	699.8	2.357	0.32	0.95	2.66	0.045
143.8	354.2	2.653	0.31	0.92	2.66	0.045
145.0	142.3	3.049	0.30	0.88	2.66	0.045
146.0	75.3	3.325	0.30	0.87	2.66	0.045
147.0	44.7	3.551	0.33	0.84	2.66	0.042
<u>o-Dichlorobenzene</u>						
79.2	1112.4	2.156	0.51	0.62	2.82	-
80.9	808.5	2.294	0.49	0.62	2.82	-
83.6	561.9	2.452	0.48	0.64	2.82	-
86.1	288.5	2.742	0.45	0.63	2.82	-
89.8	134.4	3.073	0.45	0.64	2.82	-
93.0	99.6	3.204	0.71	0.70	2.82	-
97.4	46.2	3.537	0.61	0.63	2.82	-
100.8	27.4	3.764	0.51	0.56	2.82	-
<u>o-Dichlorobenzene</u>						
123.2	7262.6	1.341	0.40	2.79	2.82	0.064
126.4	3042.3	1.719	0.39	2.85	2.82	0.066
129.1	1459.6	2.038	0.43	2.89	2.82	0.064
133.2	685.1	2.366	0.46	2.94	2.82	0.064
137.3	356.0	2.650	0.47	2.96	2.82	0.064
141.2	192.9	2.916	0.48	2.99	2.82 ⁵	0.065
145.0	104.6	3.182	0.50	3.02	2.83	0.064
149.3	56.8	3.447	0.49	3.05	2.83	0.066
153.2	32.5	3.690	0.51	3.11	2.83	0.067
157.8	25.4	3.798	0.68	3.26	2.83	0.060
163.0	14.0	4.056	0.63	3.10	2.83 ⁵	0.062
167.4	10.2	4.191	0.65	2.92	2.84 ⁵	0.060

TABLE 7.2: continued...

T(K)	$10^6 \tau$ (s)	$\log f_{\max}$	β	$10^3 \epsilon''_{\max}$	ϵ_{∞}	μ (D)
<u>o-Dichlorobenzene</u>						
157.8	6217.0	1.408	0.44	2.64	2.84	0.067
163.0	2069.5	1.886	0.47	2.79	2.84	0.068
167.4	1056.2	2.178	0.45	2.88	2.84	0.071
172.1	469.4	2.530	0.40	2.77	2.84 ⁵	0.075
177.3	175.4	2.958	0.41	2.80	2.85 ⁵	0.075
182.4	72.9	3.339	0.44	2.88	2.85	0.075
<u>m-Dichlorobenzene</u>						
<u>Lower Temperature Process</u>						
88.2	19834.0	0.904	0.44	0.043	2.82	-
91.3	9062.4	1.245	0.52	0.048	2.82	-
93.8	4595.2	1.540	0.83	0.064	2.82	-
96.5	2263.3	1.847	0.73	0.055	2.82	-
<u>Higher Temperature Process</u>						
124.5	11551.0	1.139	0.55	1.83	2.83	0.045
126.1	7833.0	1.308	0.52	1.92	2.83	0.047
129.1	3015.7	1.722	0.48	1.90	2.83	0.050
133.2	1287.6	2.092	0.63	1.72	2.83	0.042
137.1	807.4	2.295	0.63	1.62	2.83	0.041
142.2	480.1	2.520	0.89	1.75	2.83	-
147.7	277.7	2.758	0.90	2.05	2.83	0.040
152.4	128.9	3.092	0.89	2.19	2.83	0.042

TABLE 7.2: continued...

T(K)	$10^6 \tau$ (s)	$\log f_{\max}$	β	$10^3 \epsilon''_{\max}$	ϵ_{∞}	μ (D)
<u>1-Chloronaphthalene</u>						
<u>Lower Temperature Process</u>						
90.5	5624.3	1.452	0.29	20.0	2.87	0.186
92.8	3745.0	1.628	0.28	20.6	2.87	0.195
97.0	1376.8	2.063	0.28	21.7	2.87	0.204
100.7	643.2	2.394	0.33	23.6	2.88	0.200
104.9	301.0	2.723	0.26	23.8	2.86	0.231
109.1	156.2	3.008	0.27	25.1	2.86	0.237
113.3	76.4	3.319	0.25	26.1	2.85	0.257
117.1	37.1	3.632	0.27	27.0	2.86	0.255
122.9	11.4	4.145	0.29	28.4	2.86	0.222
128.4	5.9	4.430	0.26	29.7	2.85	0.286
133.2	3.7	4.634	0.28	30.8	2.86	0.285
138.5	2.6	4.790	0.28	31.2	2.87	0.292
<u>1-Chloronaphthalene</u>						
<u>Higher Temperature Process</u>						
128.1	1148.5	2.142	0.25	24.9	3.10	0.254
133.1	484.7	2.516	0.28	26.5	3.11	0.252
138.1	243.7	2.815	0.31	27.9	3.12	0.250
143.5	99.0	3.206	0.32	29.8	3.12	0.259
148.6	37.6	3.626	0.32	32.5	3.11	0.276
153.4	22.0	3.860	0.34	33.9	3.11	0.278
158.3	10.3	4.19	0.34	36.3	3.11	0.292
<u>N-Methylpyrrole</u>						
83.1	1208.0	2.120	0.34	0.25	2.59	-
85.9	858.0	2.268	0.34	0.26	2.59	-
89.2	634.3	2.400	0.31	0.27	2.59	-
93.5	424.3	2.574	0.32	0.28	2.59	-
99.5	248.6	2.806	0.26	0.28	2.59	-
105.4	148.2	3.031	0.27	0.28	2.59	-
110.3	116.8	3.134	0.28	0.28	2.59	-
115.7	92.4	3.236	0.27	0.28	2.59	-
120.5	65.3	3.387	0.24	0.26	2.60	-

TABLE 7.2: continued...

T(K)	$10^6 \tau$ (s)	$\log f_{\max}$	β	$10^3 \epsilon''_{\max}$	ϵ_{∞}	μ (D)
<u>Pyridine</u>						
164.0	549.8	2.462	0.43	16.21	2.84	0.144
165.4	286.1	2.745	0.46	16.18	2.84	0.140
166.3	188.0	2.928	0.48	16.29	2.84	0.137
167.3	122.8	3.113	0.53	16.26	2.84	0.131
168.8	65.4	3.387	0.55	15.70	2.85	0.127
170.5	34.7	3.662	0.57	15.02	2.85	0.123
172.4	18.7	3.929	0.57	14.59	2.85	0.121
175.2	7.4	4.331	0.57	12.33	2.86	0.112
<u>4-Methylpyridine</u>						
181.4	424.3	2.574	0.50	300.03	2.70	0.651
182.7	214.5	2.871	0.54	306.56	2.71	0.635
184.7	68.6	3.366	0.58	303.98	2.72	0.615
186.7	28.3	3.750	0.67	308.76	2.78	0.574
187.6	20.4	3.891	0.70	309.02	2.82	0.560
188.9	11.6	4.137	0.71	316.03	2.82	0.560
189.8	8.23	4.287	0.72	315.00	2.83	0.560
<u>Quinoline</u>						
197.6	298.8	2.727	0.30	37.27	2.92	0.330
198.6	201.2	2.898	0.31	36.91	2.92	0.325
199.5	133.5	3.077	0.32	36.51	2.92 ⁵	0.322
200.4	92.1	3.238	0.33	36.24	2.93	0.317
201.3	63.3	3.400	0.35	35.78	2.94	0.310
202.5	37.9	3.624	0.35	35.30	2.94	0.309
203.7	21.7	3.865	0.36	34.60	2.94	0.308
205.0	10.9	4.165	0.36	34.17	2.94	0.307
206.2	6.3	4.405	0.36	33.37	2.94	0.305

TABLE 7.2: continued...

$T(K)$	$10^6 \tau(s)$	$\log f_{\max}$	β	$10^3 \epsilon''_{\max}$	ϵ_{∞}	$\mu(D)$
<u>Isoquinoline</u>						
202.5	436.7	2.562	0.29	24.31	2.98	0.279
203.9	223.2	2.853	0.31	23.67	2.98	0.267
205.4	140.6	3.054	0.32	22.76	2.98	0.259
207.3	66.0	3.382	0.33	22.50	2.98	0.255
208.5	43.2	3.567	0.36	22.43	2.98	0.250
209.5	30.5	3.718	0.37	22.54	2.98	0.242
210.3	23.3	3.834	0.38	22.71	2.98	0.240

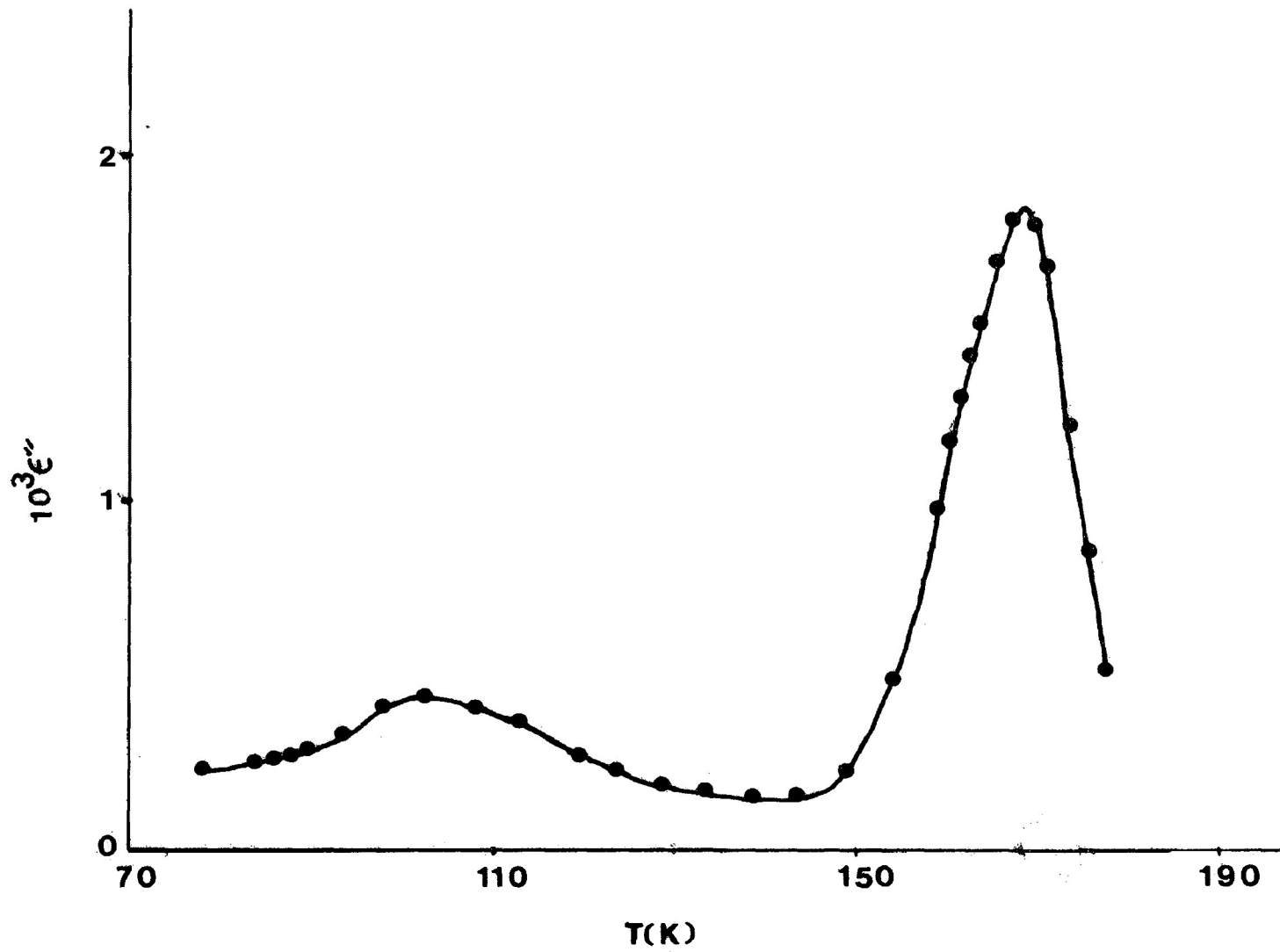


FIGURE 7.1: Dielectric loss factor ϵ'' versus temperature $T(K)$ for fluorobenzene at 1 kHz.

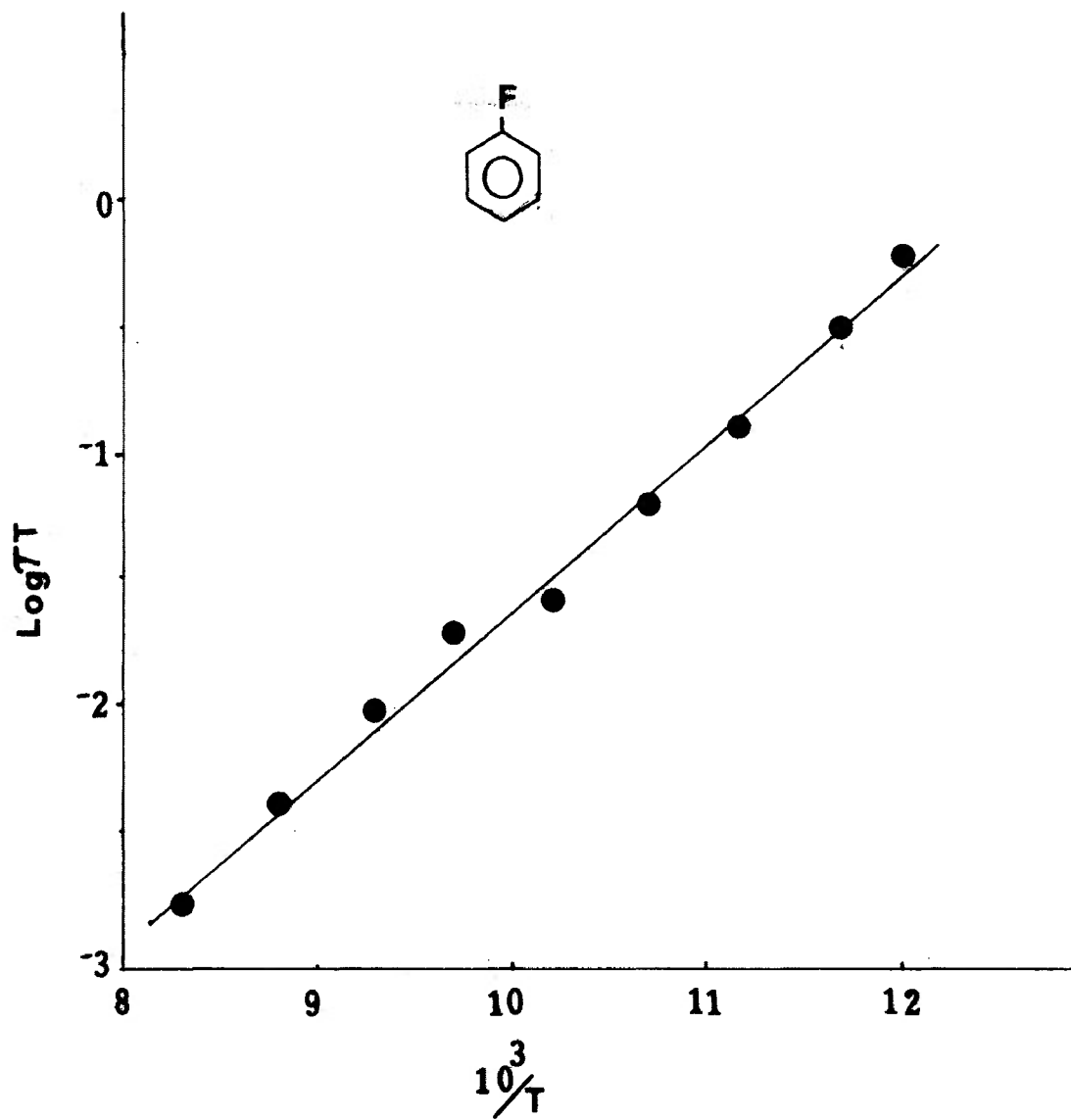


FIGURE 7.2: Eyring plot of $\log(\tau T)$ versus $\frac{1}{T}$ for fluorobenzene

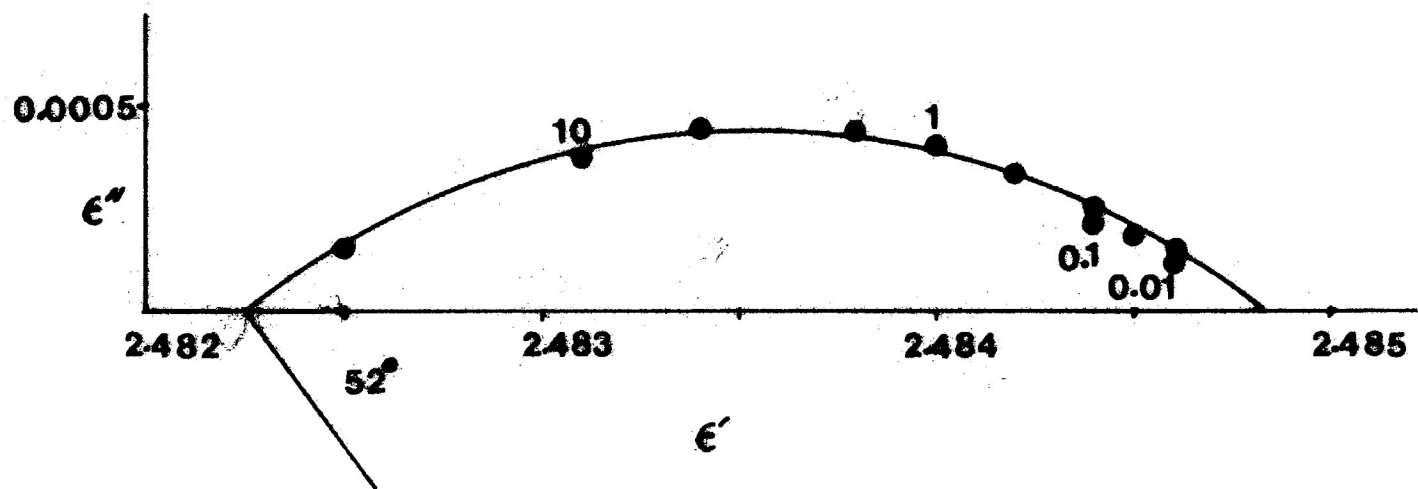


FIGURE 7.3: Cole-Cole plot for fluorobenzene at 108.1 K
 Numbers beside points are frequencies in kHz

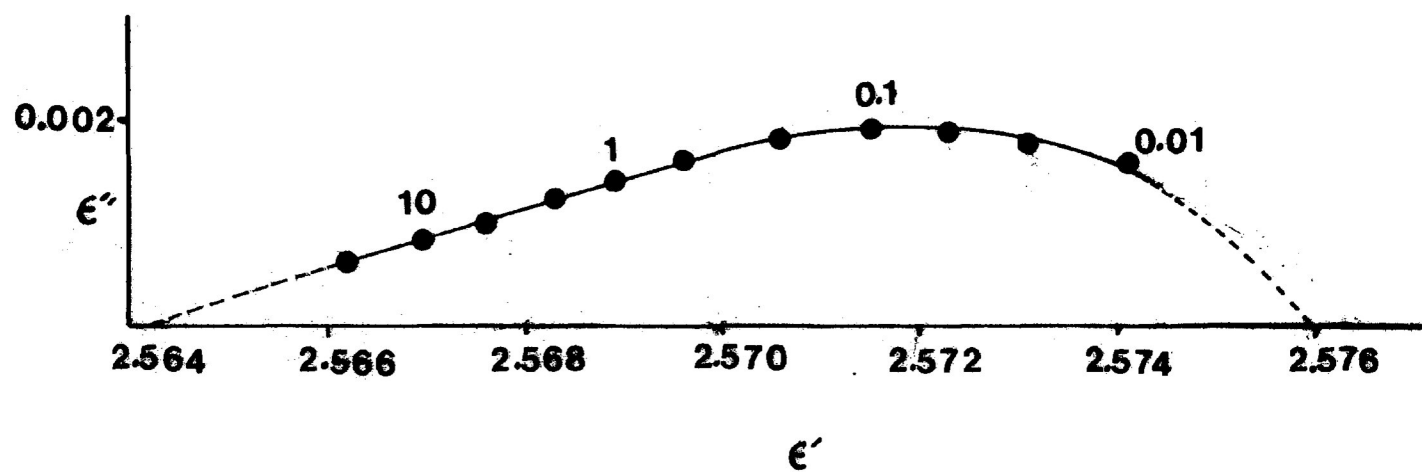
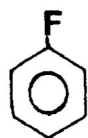
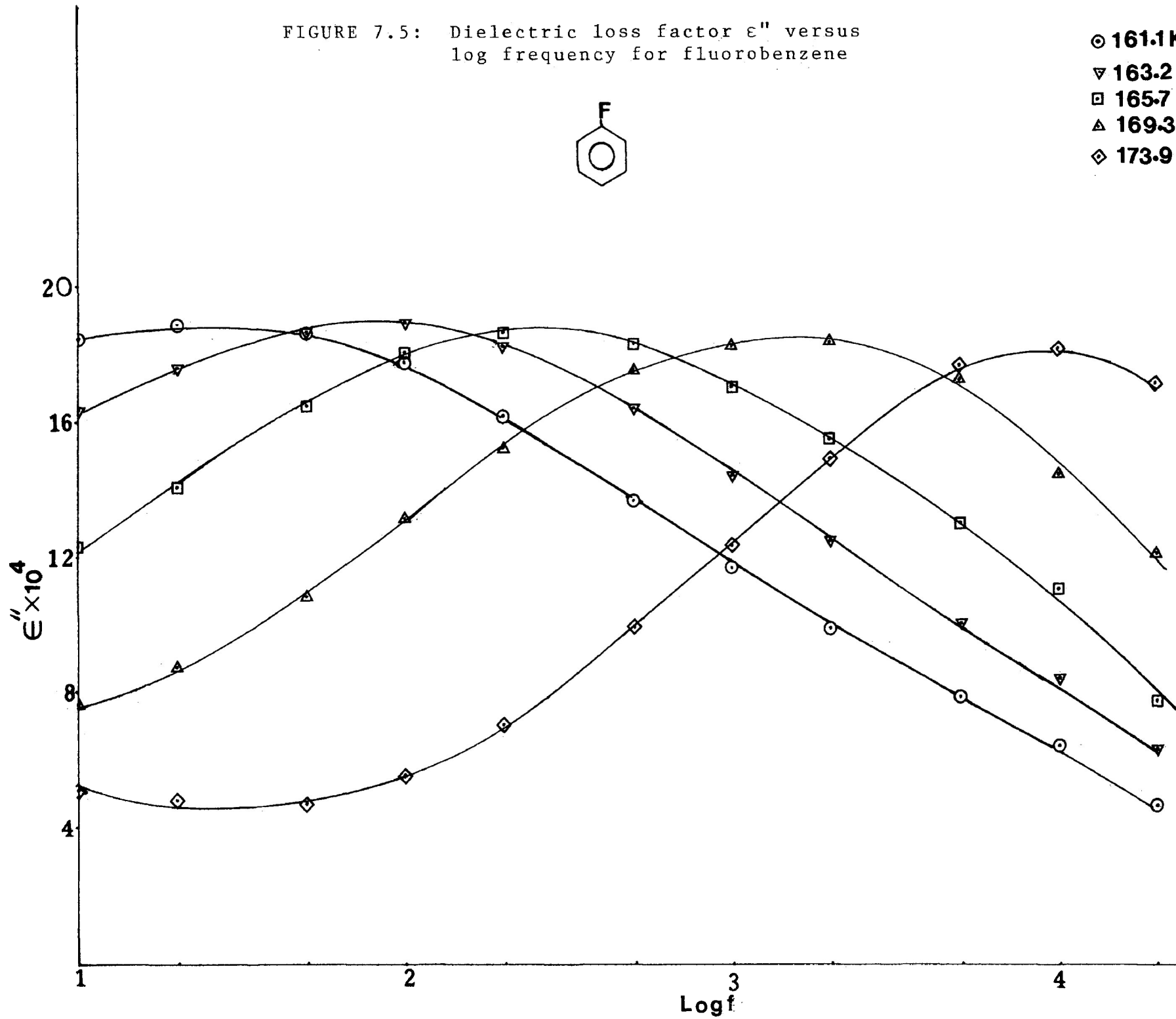


FIGURE 7.4: Complex plane diagram for fluorobenzene at 163.2 K
 Numbers beside points are frequencies in kHz

FIGURE 7.5: Dielectric loss factor ϵ'' versus log frequency for fluorobenzene



- 161.1K
- ▽ 163.2
- 165.7
- △ 169.3
- ◇ 173.9



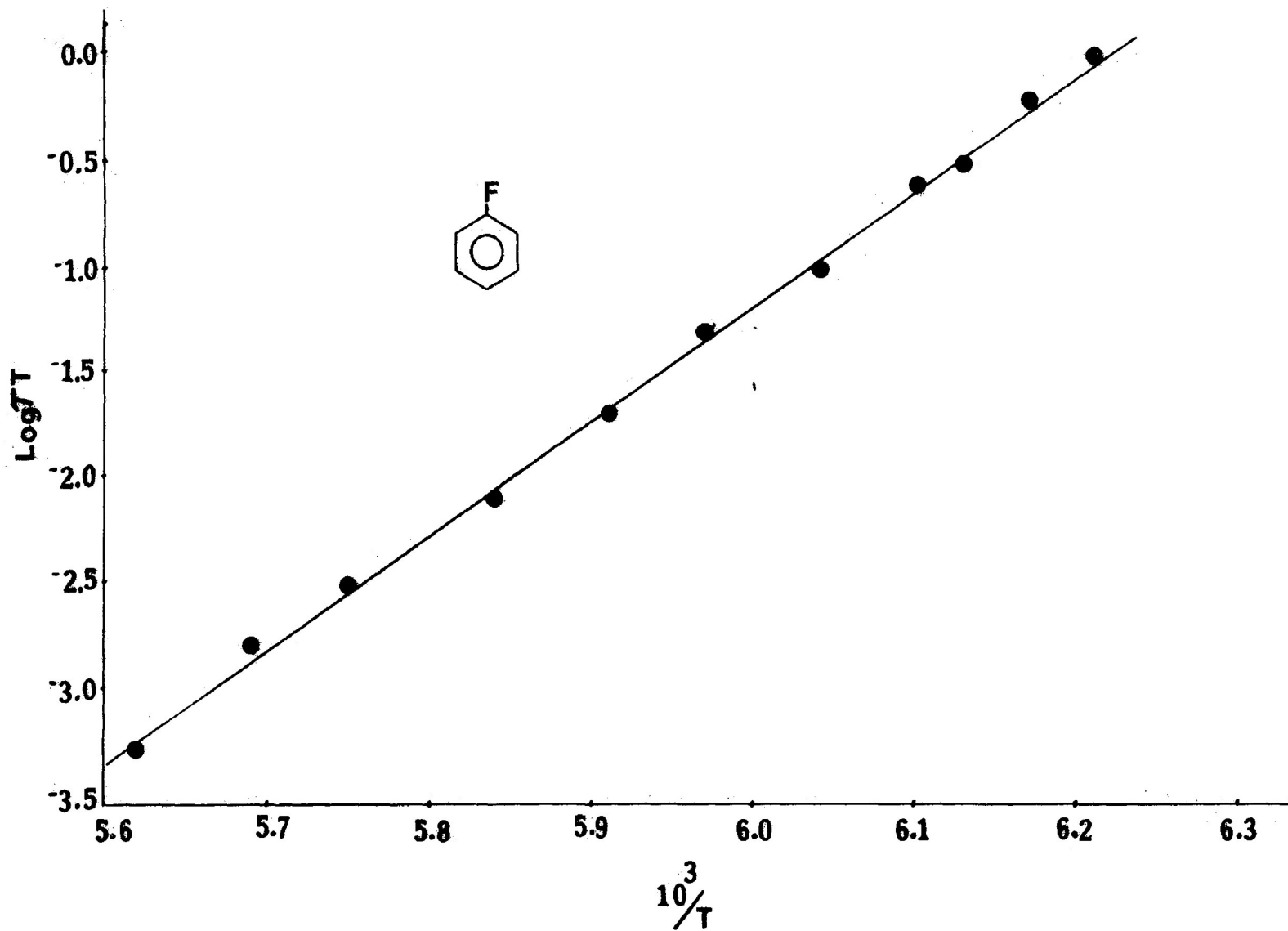


FIGURE 7.6: Eyring plot of $\log(\tau T)$ versus $\frac{1}{T}$ for fluorobenzene.

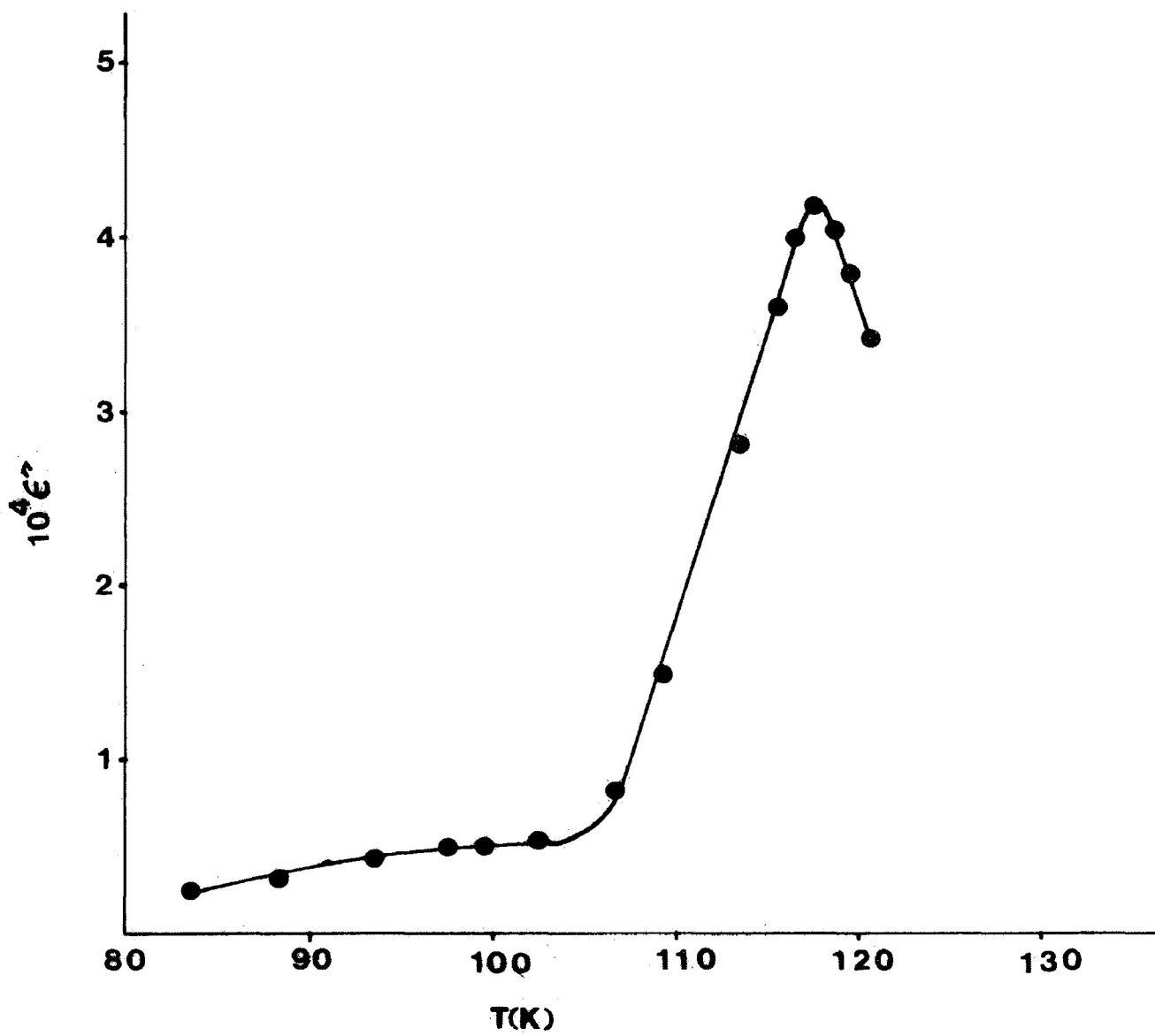


FIGURE 7.7: Dielectric loss factor ϵ'' versus temperature $T(K)$ for chlorobenzene at 102 Hz

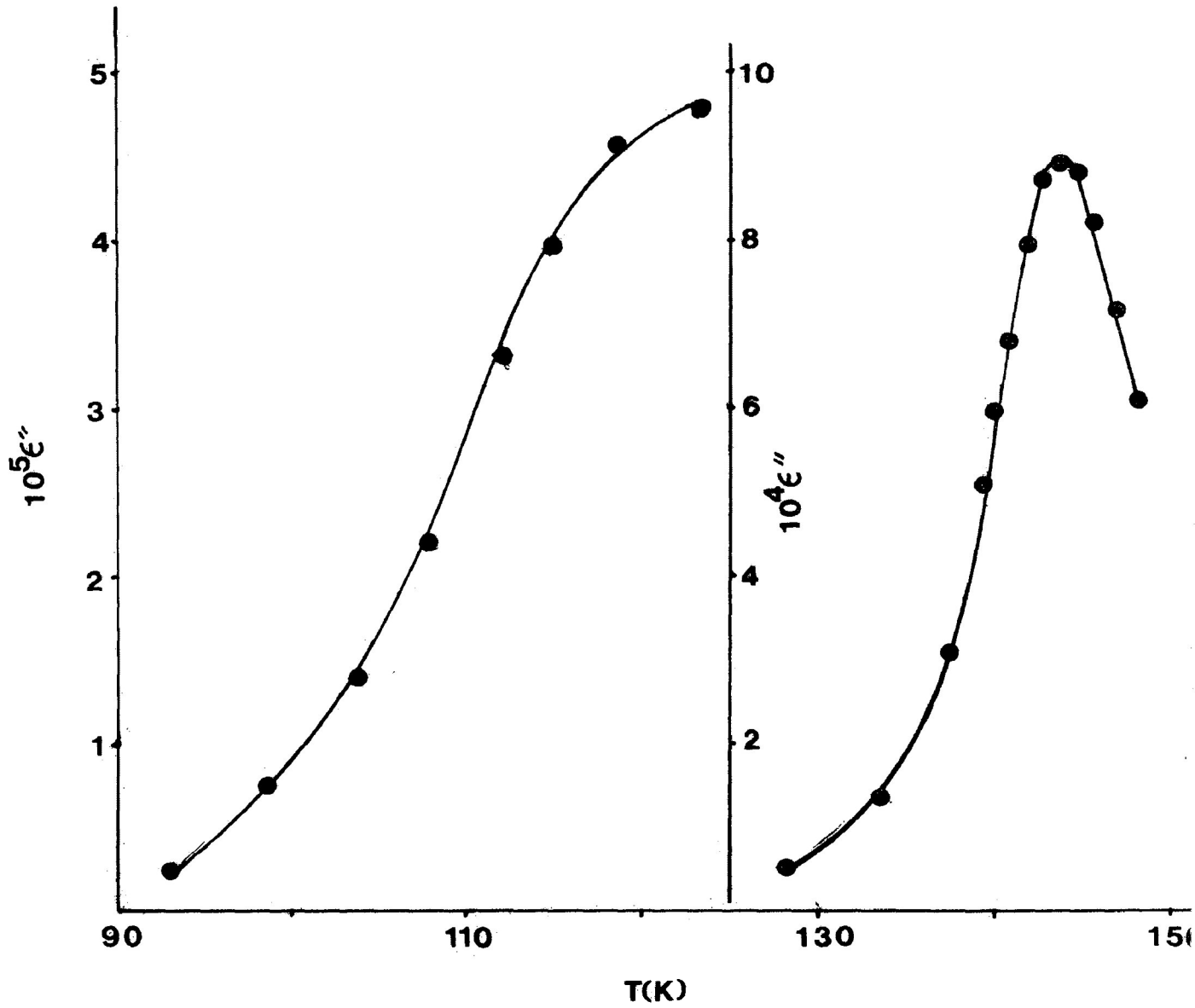


FIGURE 7.8: Dielectric loss factor ϵ'' versus temperature $T(K)$ for bromobenzene at 1 kHz.

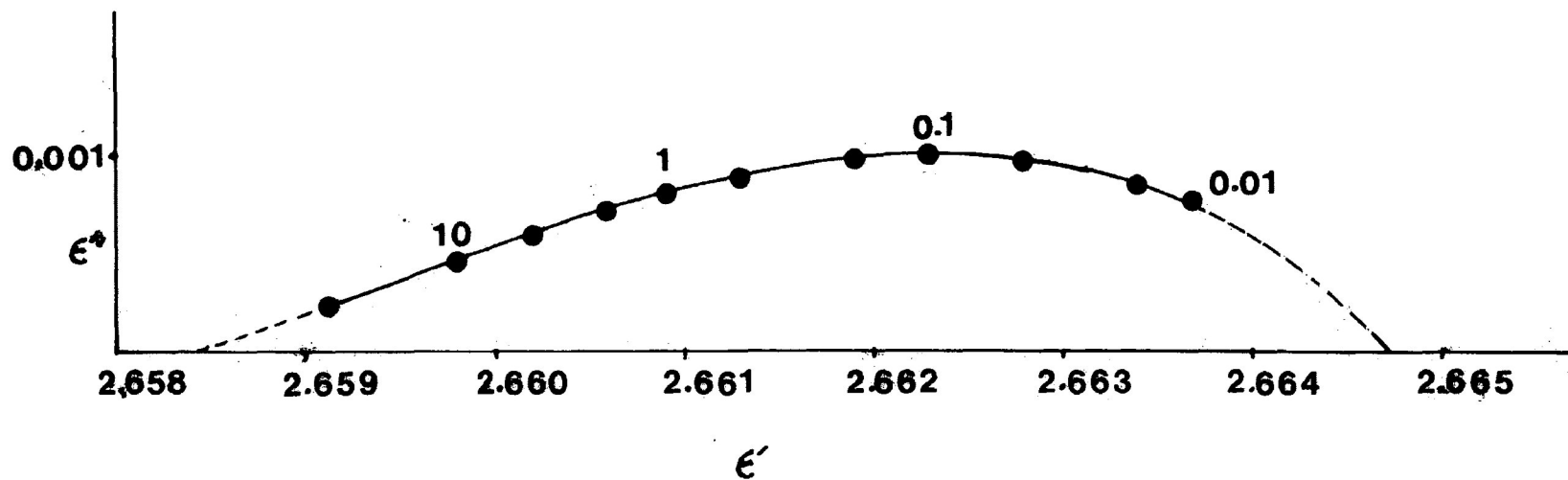


FIGURE 7.9: Complex plane diagram for bromobenzene at 141.8 K
Numbers beside points are frequencies in kHz

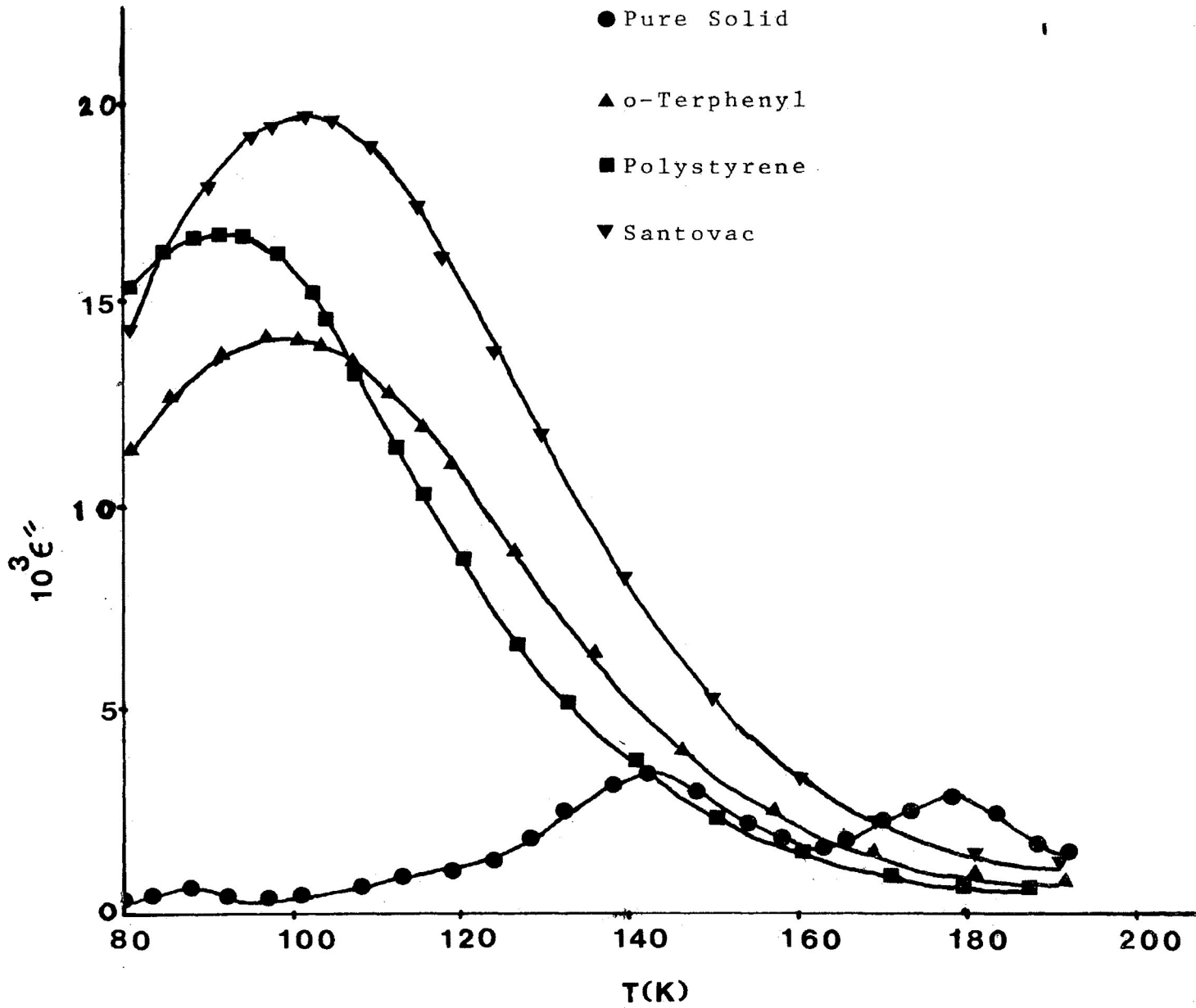


FIGURE 7.10: Dielectric loss factor ϵ'' versus temperature (K) for o-dichlorobenzene at 1 kHz

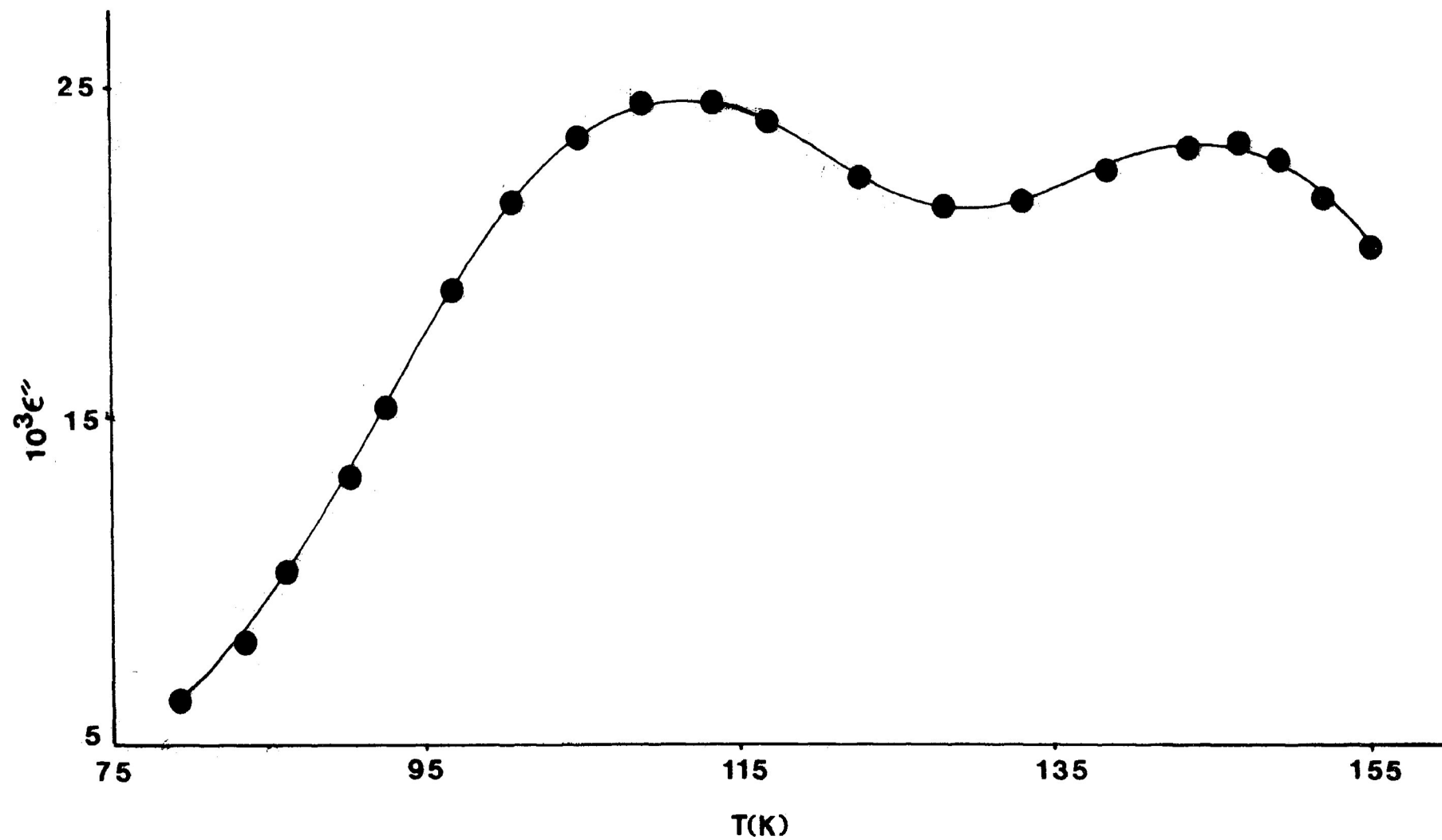


FIGURE 7.11: Dielectric loss factor ϵ'' versus temperature $T(K)$ for 1-chloronaphthalene at 1 kHz

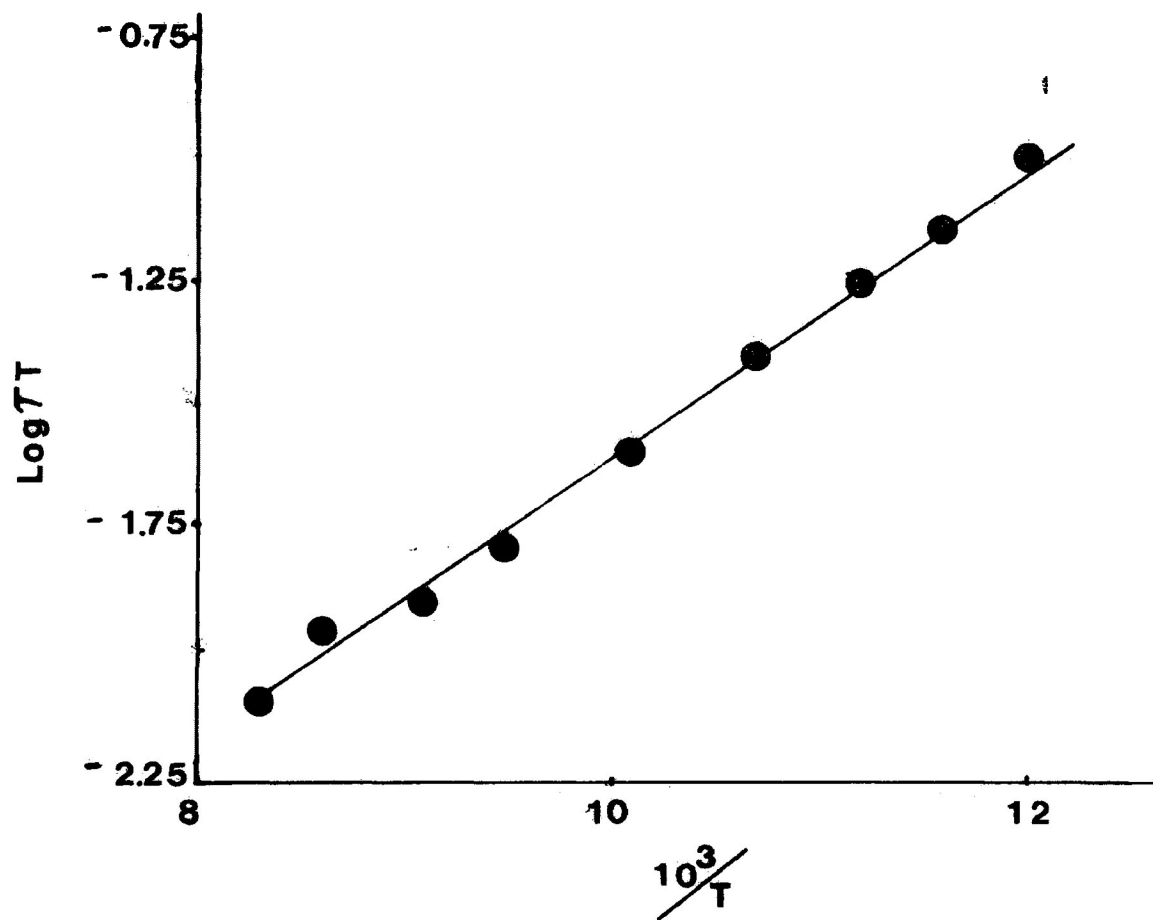


FIGURE 7.12:

Eyring rate plot of $\log(\tau T)$ versus $\frac{1}{T}$
for N-methylpyrrole

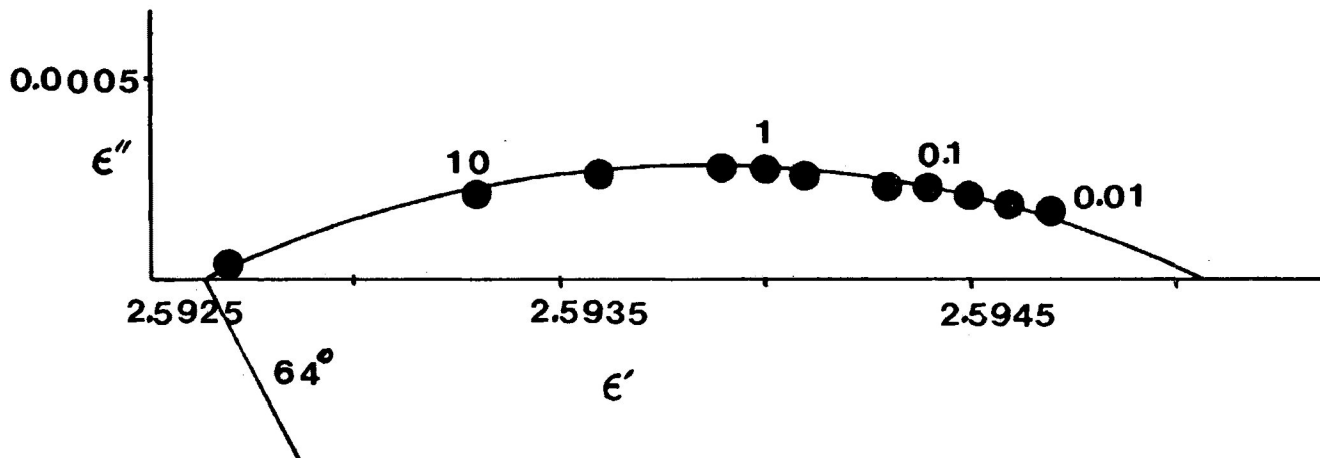


FIGURE 7.13: Cole-Cole plot for N-methylpyrrole at 110.3 K
Numbers beside points are frequencies in kHz

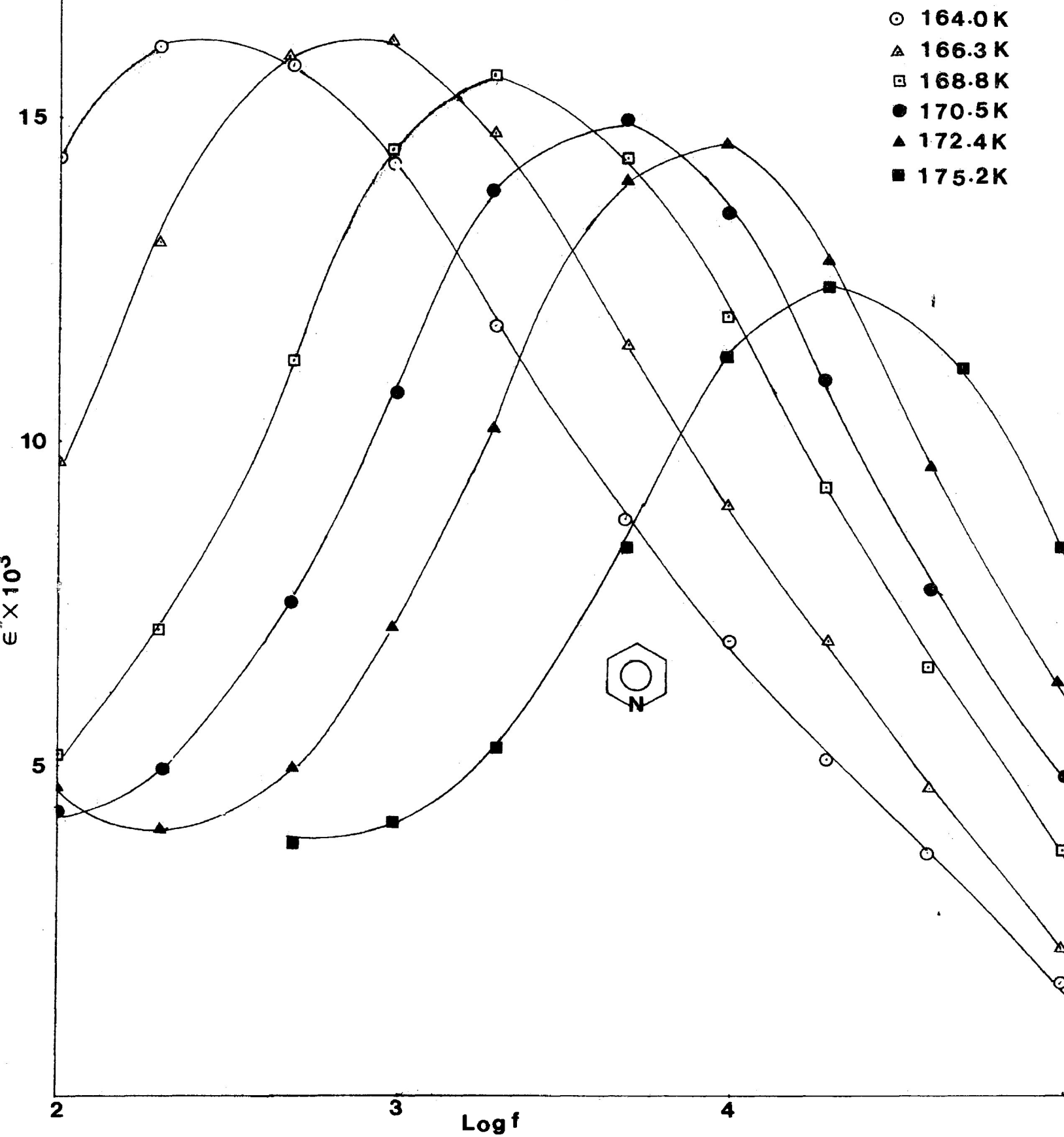


FIGURE 7.14: Dielectric loss factor ϵ'' versus log frequency for pyridine

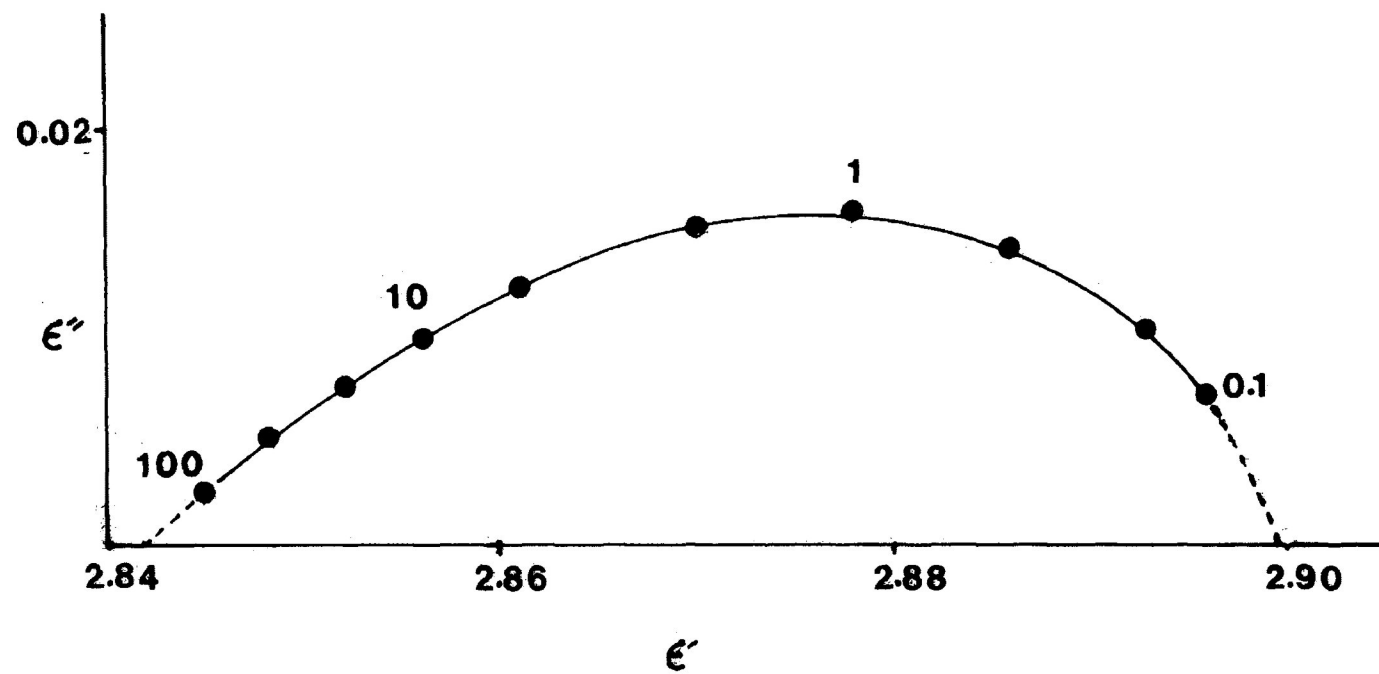


FIGURE 7.15: Complex plane diagram for pyridine at 167.3 K
 Numbers beside points are frequencies in kHz

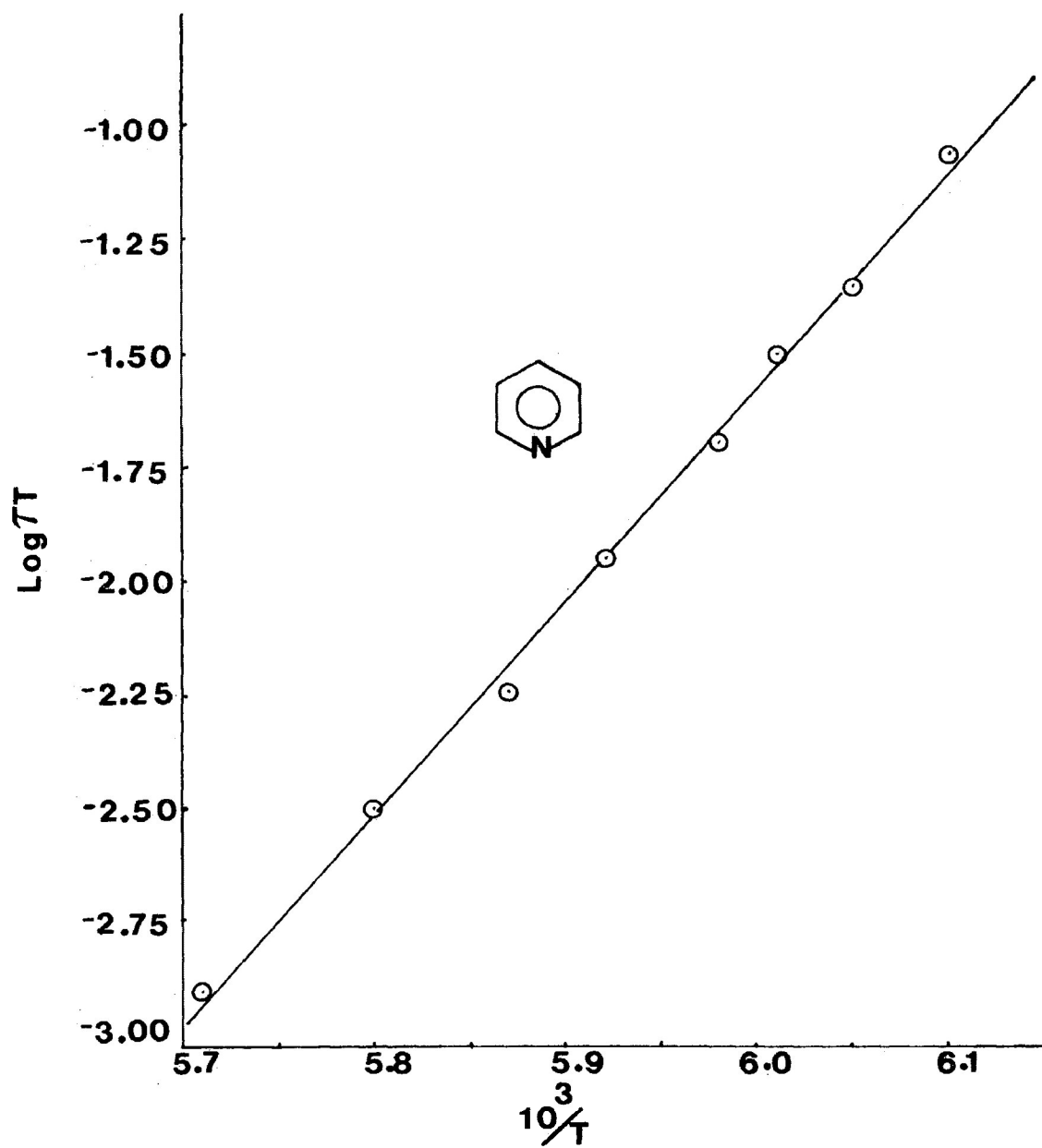


FIGURE 7.16: Eyring plot of $\log(\tau T)$ versus $\frac{1}{T}$ for pyridine

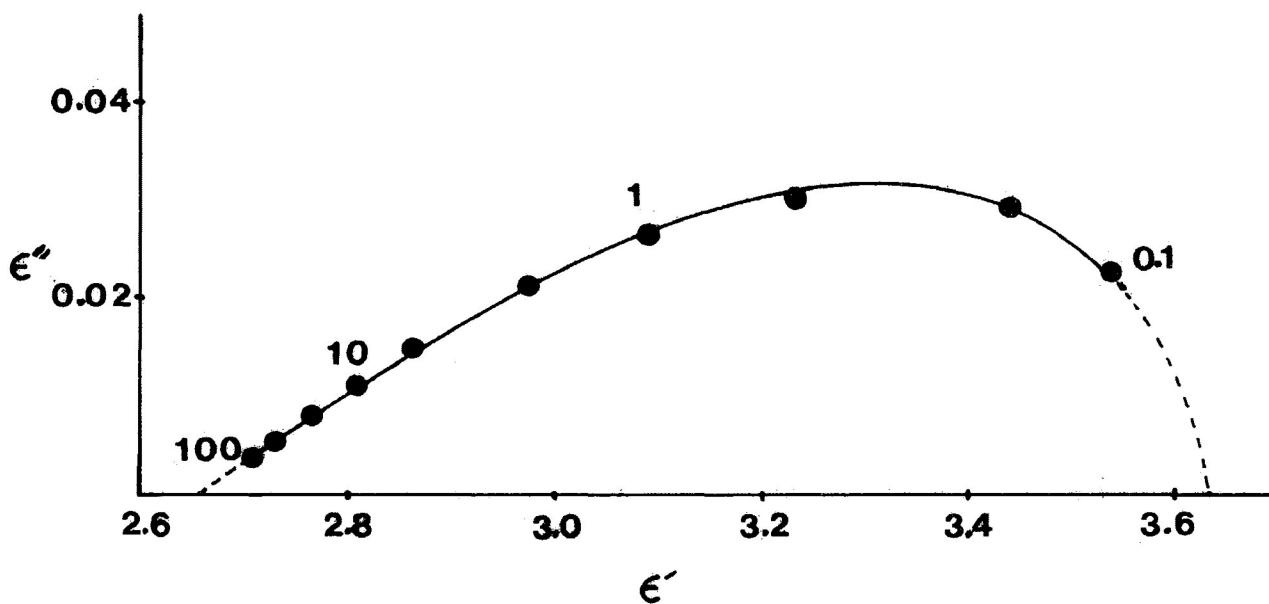
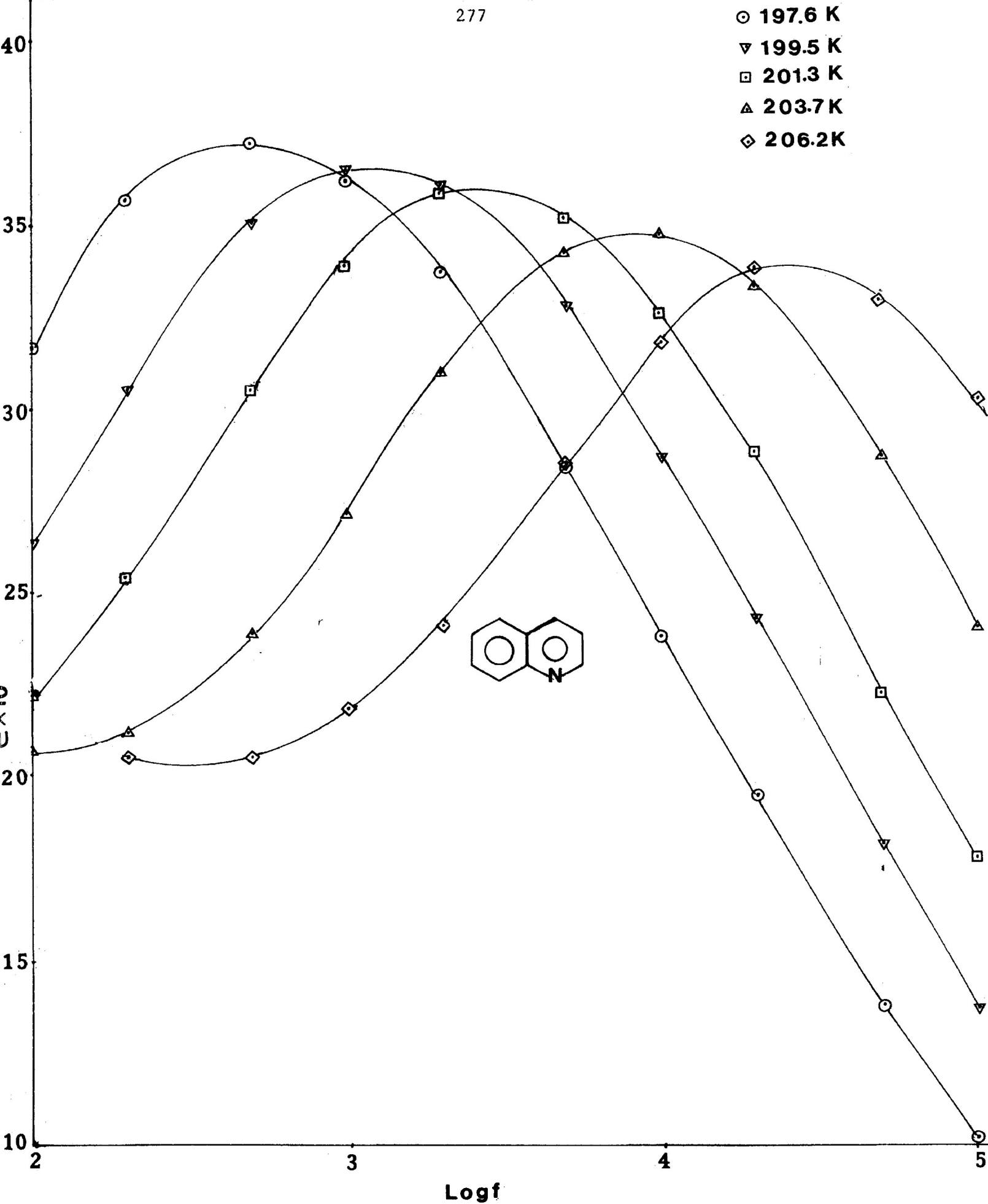


FIGURE 7.17: Complex plane diagram for 4-methylpyridine at 181.4 K

Numbers beside points are frequencies in kHz

FIGURE 7.18: Dielectric loss factor ϵ'' versus log frequency for quinoline

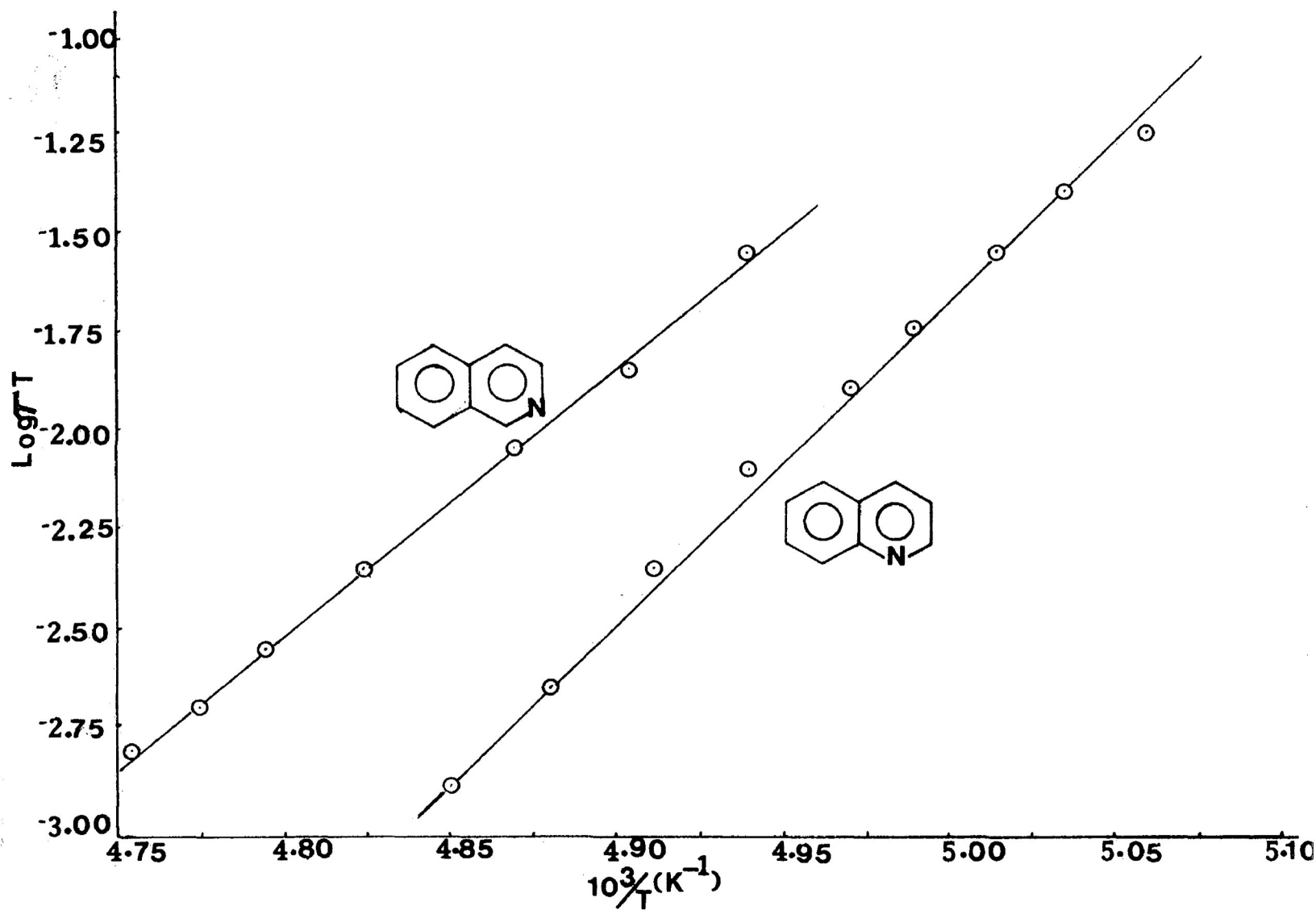


FIGURE 7.19: Eyring plot of $\log(\tau T)$ versus $\frac{1}{T}$ for quinoline and isoquinoline

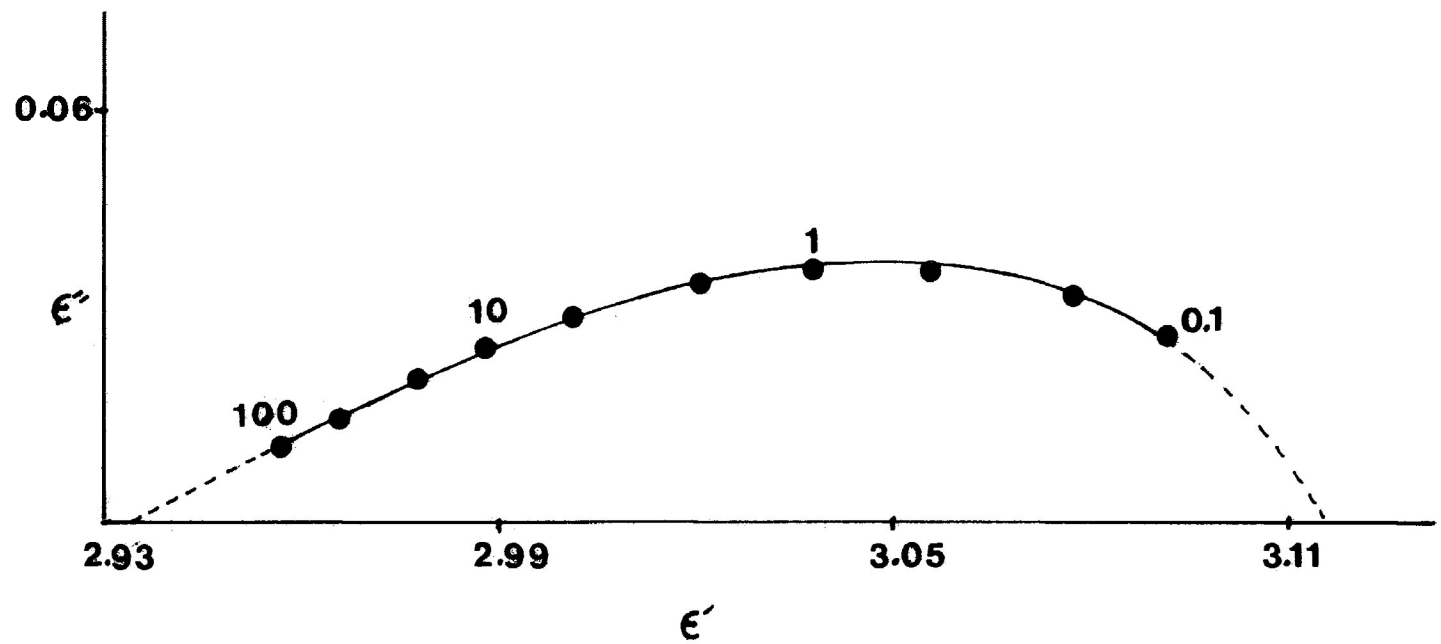


FIGURE 7.20: Complex plane diagram for quinoline at 198.6 K

Numbers beside points are frequencies in kHz

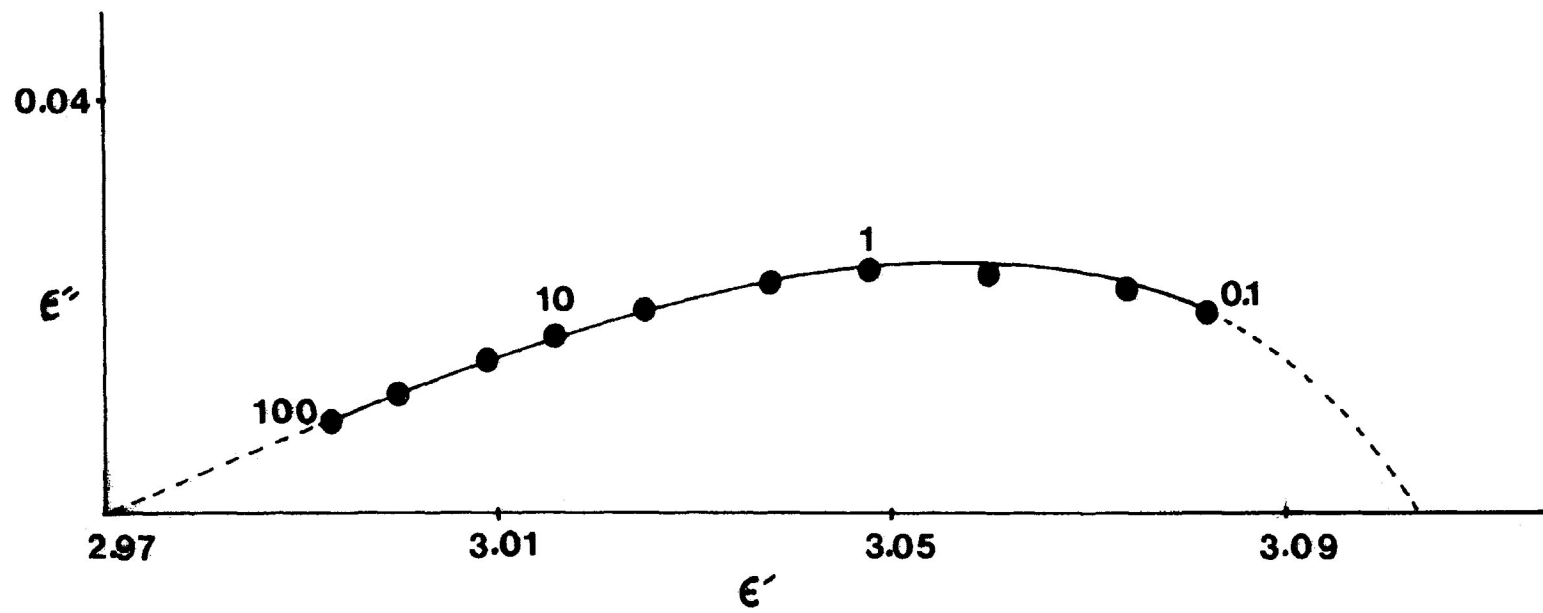


FIGURE 7.21: Complex plane diagram for isoquinoline at 203.9 K
 Numbers beside points are frequencies in kHz